

# 中華民國核醫學學會 2021年會暨國際學術研討會


2021 Annual Meeting and International  
Symposium of The Society of Nuclear  
Medicine, Taiwan (R.O.C)  
(Virtual)



11月20日(星期六) (視訊會議)

主辦單位  中華民國核醫學學會

協辦單位  台中榮民總醫院

 行政院原子能委員會核能研究所

 經濟部技術處





蔡世傳 會長

## 歡迎詞

中華民國核醫學學會 (The Society of Nuclear Medicine ROC) 將於 2021 年 11 月 20 日舉辦 2021 年會暨國際學術研討會。承蒙學會顏理事長暨理監事們的委任，本人忝為本次年會會長，深感榮幸。謹代表中華民國核醫學學會及臺中榮民總醫院向各位嘉賓及先進致上最誠摯的邀請及歡迎。

臺中榮民總醫院首度承辦核醫學學會年會暨國際學術研討會，也是台中市三十年來首次舉辦核醫學學會這項年度盛會。無奈卻因面臨 COVID19 疫情的重大威脅，被迫改為全視訊會議，因此無緣親自招待各位嘉賓及先進於當天蒞臨敝院參觀及指教，不便之處敬請見諒。也希望將來臺中榮民總醫院還有機會舉辦這項年度盛會的實體會議，以再度邀請各位蒞臨指導。

儘管正在經歷 COVID19 疫情流行的艱困時期，但核醫學在診斷和治療方面的進步並未停下腳步，仍再繼續往上發展。借用敝院陳適安院長的勉勵「Never stop growing」，相信藉由年會的股份與討論，讓國內核醫界持續與國際接軌，提供臨床與病人所需，造就核醫榮景。

最後，再度誠摯及歡迎邀請各位嘉賓及先進共襄盛舉，也預祝大會成功圓滿。

蔡世傳

臺中榮民總醫院核子醫學科

中華民國 110 年 11 月 20 日



陳長盈 所長

## 行政院原子能委員會核能研究所陳長盈所長致詞

首先感謝核醫學會顏若芳理事長誠摯的邀約，核能研究所非常榮幸能參與每年一次的核醫盛會，尤其今年核醫學會年會首度移師台中，特別感謝台中榮民總醫院主辦本次年會暨國際學術研討會。長期以來，藉由國內外核醫專家、學者與臨床醫師的先知卓見，對於核研所核醫藥物新藥開發的研發方向，甚至於 70 MeV 中型迴旋加速器建置，均提供許多懇切與精闢的經驗分享及指導，特致謝忱。

因應美中貿易戰及新冠肺炎疫情導致的全球經濟與供應鏈板塊快速變動，總統於去 (109) 年 5 月 20 日就職演說宣示推動 6 大核心戰略產業，其中「台灣精準健康」醫療為國家發展的重點；精準醫療並為現今全球醫療發展趨勢，伴隨著大數據及 AI 技術的大躍進，已揭開精準醫療嶄新的時代。

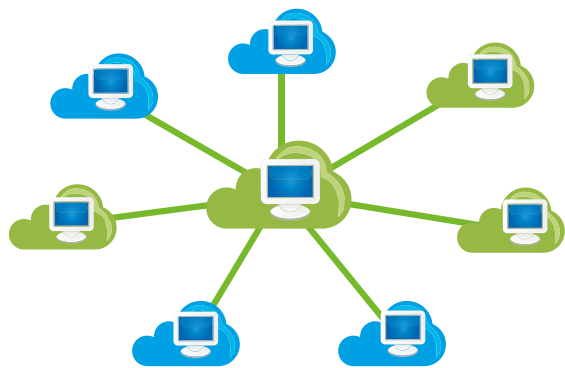
核研所以增進國人健康福祉為重要目的，除積極穩定核醫藥物生產供應外，更同時肩負核醫藥物創新開發的使命。具體作為包括：1. 在穩定核醫藥物生產部份：為因應全球疫情影響所造成國外輸入核醫藥物短缺，核研所緊急投入專業人力加班輪值，增加核研氯化亞鉈 [鉈 -201] 注射劑及核研檸檬酸銻 [銻 -67] 注射劑生產作業，以滿足臨床之迫切需求，本年核研所核醫藥物的供應已自去年的二成提升至今年約五成。2. 在核醫藥物創新開發部份：(1) 核研心交碘 -123 注射劑 (I-123-MIBG injection) 已於 108 年獲得藥品許可證，為符合放射性針劑藥品生產工廠登記，目前已規劃於 112 年完成新 PIC/SGMP 無菌充填生產線。另，現階段已完成碘 -123 MIBG 三批次製程確效與安定性試驗，開始供應學術臨床試驗用藥。(2) 核研多雷克銻肝功能造影劑具絕佳的肝標靶特性，可評估肝功能並靈敏偵測出肝病病程的變化。今年度並獲衛生福利部食品藥物管理署 (TFDA) 核准二期臨床試驗，預定 12 月底前於林口長庚醫院執行第一例二期臨床試驗。

此外，核研所積極爭取「國家中子與質子科學應用研究：70 MeV 中型迴旋加速器建置計畫」，以擴展迴旋加速器應用範疇，很榮幸已有長足的進程；目前本計畫甫於上個月 (110 年 10 月 21 日) 獲行政院核定，並將自 112 年起至 115 年共四年完成建置。

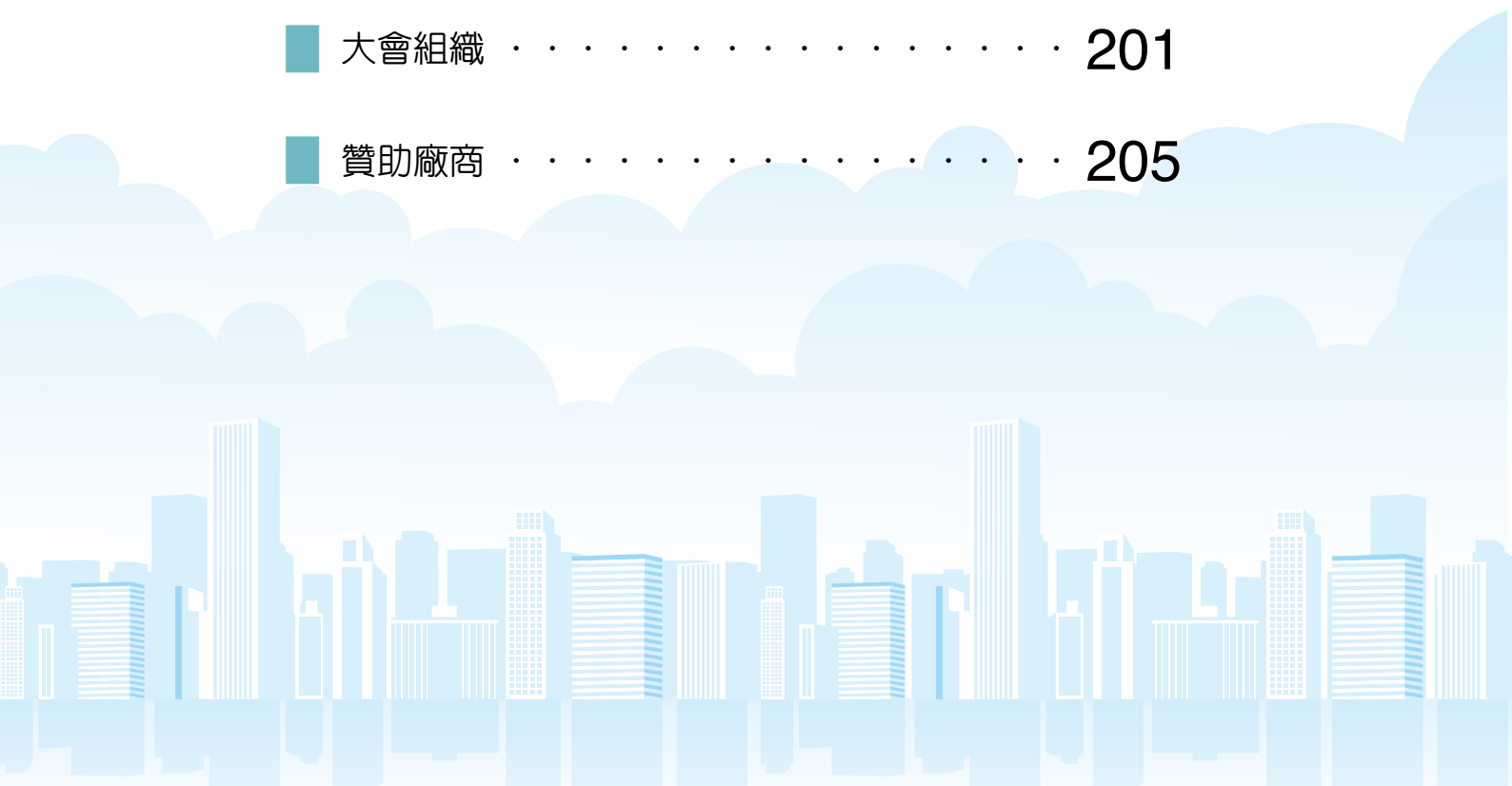
核研所期待持續與國內外產、學、醫研界組成緊密合作聯盟，共同開發具潛力與價值之核醫新藥，促進核醫藥物市場蓬勃發展。持續提供國人在臨床上之高品質藥物，以落實原子能應用於民生用途，促進民生福祉達成照護國民健康之目標。最後，感謝諸位先進們對核研所的支持與協助，預祝大會圓滿成功，與會先進們身體健康，平安喜樂！

核能研究所所長 陳長盈

# 目次



■ 大會致詞 . . . . .	2
■ 大會議程表 . . . . .	5
■ 講師及演講摘要 . . . . .	6
■ 口頭論文發表摘要 - 基礎組 . . . . .	18
■ 口頭論文發表摘要 - 臨床組 . . . . .	22
■ 壁報論文發表摘要 - 基礎組 . . . . .	35
■ 壁報論文發表摘要 - 臨床組 . . . . .	66
■ 大會組織 . . . . .	201
■ 贊助廠商 . . . . .	205



## 中華民國核醫學學會 2021 年會暨國際學術研討會議程

日期：2021 年 11 月 20 日(六)

地點：線上視訊會議，報名獲取連結

大會  
議程  
表

08:50~09:00		主席致詞 (核研所執秘、理事長、年會會長)	
09:00~10:00	01	Living with COVID-19 - our new reality 主講：陳宜君 教授 座長：彭南靖 主任	口頭論文發表
	02	New Era in Alzheimer disease: Next generation of AD clinical management 主講：Dr. Donna Masterman (USA) 座長：林昆儒 教授	口頭論文基礎 (10:00~10:40)
10:45~10:55		Break	
10:55~11:40	03	Guideline on Diagnosis and Treatment of Cardiac Amyloidosis in Japan 主講：Prof. Yasuhiro Izumiya (Japan) 座長：吳彥雯 教授	口頭論文臨床 (非醫師)
	04	COVID-19 對台灣核醫的影響及因應 主講：蔡世傳 主任 主講：林宜瀟 醫師	(11:00~11:50)
12:00~12:15		會員大會	
12:15~13:00		Lunch Break	
13:00~13:45	05	Clinical Experience of Peptide Receptor Radionuclide Therapy for Neuroendocrine Tumor in Korea 主講：Prof. Keon-wook, Kang (Korea) 座長：鄭媚方 主任	口頭論文臨床 (醫師) (13:30~15:00)
	06	PSMA based RLT: Global vision and local experience 主講：Prof. Sean Yan (Singapore) 座長：黃玉儀 主任	
14:30~14:40		Break	
14:40~15:20	07	Prescription of <sup>90</sup> Y glass microsphere radioembolization ( <sup>90</sup> Y-GMRE) for treatment of HCC: - role of dual-tracer PET/CT in differentiating metabolic heterogeneity 主講：何志禮 教授 (Hong Kong) 座長：李潤川 主任	
15:20~16:00	08	The Evolving Treatment Landscape of mCRPC 主講：洪健華 醫師 座長：闕士傑 教授	
16:00~16:20		Ra-223 新書發表《骨轉移標靶治療輻射安全衛教建議手冊》 主講：譚鴻遠 主任 座長：顏若芳 理事長	
16:20~17:00	09	Developing re-differentiation therapy for advanced thyroid cancer 主講：譚鴻遠 主任 座長：曾芬郁 理事長	
17:00~		閉幕	



Name: 陳宜君  
Title: 教授  
Institute: 台大醫學院內科

---

## Living with COVID-19 – Our New Reality

因為 SARS CoV-2 病毒的特性，以及全球防疫的積極度、疫苗接種的涵蓋率差距很大，病毒持續變異，疫情持續在各國社區散播。而國際的交流勢必要恢復，因此這 60 分鐘演講讓我們回顧 COVID-19 全球延燒近兩年之疫情，一起前瞻思考在生活及職場如何面對與 COVID-19 共存的新常態 (new normal)。



Name: **Donna Masterman**  
Title: Executive Medical Director  
Institute: Biogen, Inc  
Global Medical Affairs, AD Lead Intercontinental Region

---

## New Era in Alzheimer Disease: Next Generation of AD Clinical Management

Alzheimer's disease (AD) is a disorder that causes degeneration of the brain and it is the main cause of dementia, which is characterized by a decline in cognition and independence in patients' daily activities. Alzheimer disease became a growing public health concern affecting millions of patients worldwide and it is projected to have a devastating impact by 2050 with 130 million affected.

To address the critical challenges around the world, the development of effective therapeutics and preventative strategies is being accelerated.

In last decades, the researchers were focusing on understanding AD pathology by variable potential mechanisms, such as abnormal metabolism of tau protein,  $\beta$ -amyloid, inflammatory response, cholinergic and free radical damage, devoting to develop treatments that could modify the course of the disease.

It is now widely acknowledged that biomarker changes precede clinically relevant changes in cognition in patients with Alzheimer's disease. Furthermore, biomarkers are defined as measurable substances that serve as indicators of the severity, particular biomarkers can be used to track the pathophysiological processes in Alzheimer's disease, such as amyloid or tau protein.

Further exploring the role of biomarkers in Alzheimer disease, how to early diagnosis, early intervention, new treatment approaches to patients are critical issues to be addressed.



Name: **Yasuhiro Izumiya**

Title: Professor

Institute: Department of Cardiovascular Medicine, Osaka City University

## Guideline on Diagnosis and Treatment of Cardiac Amyloidosis in Japan

Amyloidosis is defined as organ dysfunction due to deposition of  $\beta$ -sheet structured amyloid fibril in multiple organs. Cardiac involvement is the most significant predictor for poor prognosis in patients with systemic amyloidosis. Cardiac amyloidosis has been believed as a rare disease for a long time, but recent sophisticated imaging modalities demonstrate that considerable number of CA patients are hidden in heart failure. In the clinical setting, cardiologists mainly encounter 2 types of amyloidosis including, (1) amyloid light-chain (AL) amyloidosis and (2) transthyretin amyloidosis (ATTR). Recent progress in disease-modifying therapeutic interventions, such as transthyretin stabilizers, has resulted in ATTR cardiomyopathy changing from an incurable disease to a curable disease. These interventions are particularly effective in patients with mild symptoms of heart failure, indicating that early detection and precise diagnosis are important for improving the prognosis. Bone scintigraphy is extremely effective for detecting ATTR. However, it should be noted that cardiac uptake of bone scintigraphy does not reflect amyloid fibril itself. Therefore, tissue biopsy is necessary to diagnose cardiac amyloidosis, even if bone scintigraphy indicate high possibility of ATTR in Japan. In this lecture, I will summarize recent findings of early screening of ATTR cardiomyopathy and talk about important points of a precise diagnosis according to the JCS 2020 Guideline on Diagnosis and Treatment of Cardiac Amyloidosis.





Name: 蔡世傳

Title: 主任

Institute: 臺中榮民總醫院核子醫學科

## COVID-19 對台灣核醫的影響及因應

新冠肺炎病毒 (COVID-19) 於 2019 年底首次在中國被發現，隨後引起世界疫情大流行。COVID-19 疫情影響了各行業，包括核子醫學也因為放射性同位素供應明顯減少以及病人就醫受疫情衝擊而受到顯著影響。與其他國家不同，台灣於 2020 年疫情受到相對良好的控制，但直到 2021 年 5 月出現群聚感染，並迅速蔓延至全島。因此台灣核醫學部門受疫情的影響狀況與大部分國家在 2020 年爆發疫情的情形也略顯不同。因此，我們透過學會合作問卷的方式，收集分享這次 COVID-19 對台灣核醫影響的相關資訊。



Name: 林宜瀾  
Title: 主治醫師  
Institute: 臺中榮民總醫院核子醫學科

## 新冠肺炎對台灣核子醫學的影響

冠狀病毒 (COVID-19) 於 2019 年底首次在中國被發現，並於 2020 年初迅速傳播到附近的亞洲國家。由於核藥供給模式的特殊，雖然每個國家的爆發情況不同，有些國家在本地 COVID-19 大流行之前，就已因為供藥國家受疫情影響藥品製造與運送，進而顯著影響了核醫臨床業務。與其他亞洲國家不同，台灣嚴格的旅遊禁令使得整個 2020 年，台灣在國內保持最低限度的社區爆發。國內因此並沒有受到疫情影響，而改變生活模式。醫療體系也因此而無大變動。不幸的是，台灣幾乎完全依賴海外供應 Tc-99m/Mo-99 孳生器和 I-131 的供應，而在這期間，供應鏈因為封鎖和航班取消而中斷，是非常常見的。可想而知，此階段因此有受供藥影響而產生的醫療業務調整。直到 2021 年 5 月中旬，在其他一些國家開始放鬆措施的同時，台北才出現集群性疫情，並迅速蔓延至全島。雖全國配合三級疫情防範措施，但由於疾病主要流行在北部縣市，中南部僅有零星個案，各地醫療衝擊勢必有所不同。而由於此時國際間已處於逐漸放寬防疫措施、加速復甦各項產業的情況，藥物供給穩定，與其他國家同時受到疫情與供藥雙重打擊的情形也略顯不同。本次演講的內容，將透過文獻與國內核醫科部的問卷資料分析結果，從地域上、醫療機構層級、核醫臨床業務、同位素病房使用率、放射性同位素的供應、核醫從業人員職務調動、健保點數等相關議題進行討論。提供針對疫情的緊急應變，可能面臨的問題，包含業務變動、人員調度、藥物供給、物資安排等方面等相關資訊，能有更深的認識。不僅可運用在尚為平息的新冠肺炎疫情，更能拋磚引玉，對以後可能發生的傳染性疾病有更具體的準備。



Name: **Keon Wook Kang**

Title: Professor

Institute: Seoul National University College of Medicine

講師及演講摘要

## Clinical Experience of Peptide Receptor Radionuclide Therapy for Neuroendocrine Tumor in Korea

Peptide receptor radionuclide therapy (PRRT) is an emerging radionuclide therapy targeting peptide receptors overexpressed in cancer. Neuroendocrine tumors (NET) are rare tumors expressing somatostatin receptors. Eligible patients to be effective to PRRT using Lu-177 DOTATATE can be pre-screened by confirming the expression of somatostatin receptor on tumors using Octreoscan or Ga-68 DOTATOC PET/CT prior to treatment. This pair of molecular targeted treatment and companion diagnostics, so called molecular theranostics makes PRRT a good example for a precision medicine. However, PRRT for NET had been performed only in some countries where the compassionate use of unapproved drugs is allowed. Advanced Accelerator Applications (AAA) conducted a multinational clinical trial with the Lu-177 DOTATATE treatment and Lutathera (Lu-177 DOTATATE) was approved as an orphan drug in Europe and the US since 2018. Lutathera is available as an emergency drug which can be purchased through Korea Orphan & Essential Drug Center in Korea since 2019. On the other hand, Kai Biotech, a Korean radiopharmaceutical company is also performing a clinical trial using Lu-177 DOTATATE for NET patients. I will present clinical cases of PRRT in the patients with gastroenteropancreatic neuroendocrine tumor and discuss remained issues to be solved.



Name: **Sean Yan Xuexian**

Title: Senior Consultant; Professor

Institute: Singapore General Hospital; Duke-NUS Medical School

## PSMA Based RLT: Global Vision and Local Experience

Prostate cancer is the number one common malignancy for men. PSMA targeted radionuclide therapy has emerged recently as a promising treatment option for selected patients. There are variable forms of PSMA based radio ligand therapy for prostate cancer based on the types of ligand from antibody to small peptide, labelled radionuclide from beta emitter to alpha emitter etc. Major results of recently completed or currently ongoing clinical trials for example Vision and Therap will be discussed. Research and development in multiple continents including America, Europe and Australia and commercialization efforts by notable pharmaceutical manufacturers will be outlined. Local experience since 2018 with 100 plus patients and 300 treatment cycles will be summarized and presented. And our protocol with underlying reasoning and logistics will be presented for discussion and critiques.



Name: **HO, Chi Lai Garrett 何志禮**

Title: Head of Department of Nuclear Medicine & PET

Institute: Hong Kong Sanatorium & Hospital

講師及演講摘要

## Prescription of $^{90}\text{Y}$ Glass Microsphere Radioembolization ( $^{90}\text{Y}$ -GMRE) for Treatment of HCC: – Role of Dual-tracer PET/CT in Differentiating Metabolic Heterogeneity

The prescription of  $^{90}\text{Y}$  glass microsphere radioembolization ( $^{90}\text{Y}$ -GMRE) for treatment of inoperable HCC aims at optimizing the treatment dose to the tumors while minimizing the bystander damage to normal liver and shunting to other organs. Patient's injected dose calculation can be individually adjusted based on a dosimetry algorithm that takes into consideration the cytokinetic information obtained from pretreatment dual-tracer ( $^{11}\text{C}$ -acetate and  $^{18}\text{F}$ -FDG) PET/CT. The algorithm specifies 2 prerequisite technical validations and 2 dose limit boundary conditions. The first technical validation is to investigate the reliability of  $^{90}\text{Y}$  PET/CT to provide accurate dosimetry for  $^{90}\text{Y}$ -GMRE. The second technical validation is to evaluate the degree of linearity correlation between the tumor-to-nontumor partition ratios of pretreatment  $^{99\text{m}}\text{Tc}$ -MAA SPECT/CT and posttreatment  $^{90}\text{Y}$  PET/CT. The 2 dosimetry boundary conditions used in  $^{90}\text{Y}$ -GMRE calculation are designated as 30 Gy in lung and 70 Gy in normal liver parenchyma, which are empirically recommended by international criteria as the toxicity limits of radiation exposure to these organs, respectively. HCC is well known to be a highly heterogeneous tumor, but much of the reported data in the literature on  $^{90}\text{Y}$ -GMRE treatment did not have a common consensus to take into consideration the metabolic heterogeneity factor or cytokinetic properties of HCC. Our data showed that by resolving the metabolic heterogeneity and including the cytokinetic information obtained from dual-tracer PET/CT into the dosimetry calculation of individual patients, both treatment response and overall survival could be significantly improved.



Name: 洪健華  
Title: 主治醫師  
Institute: 台大醫院泌尿部

---

## The Evolving Treatment Landscape of mCRPC

轉移性攝護腺癌的治療基礎需要透過賀爾蒙治療以控制病人體內男性賀爾蒙或阻斷其受器結合，但終究癌細胞會發展出抗藥機轉而進入轉移性賀爾蒙抗性攝護腺癌 (mCRPC) 的階段。本次主題將探討 mCRPC 最新治療進展，包括新一代賀爾蒙用藥、化學治療、鐳 -223、精準治療等內容。



Name: 謹鴻遠

Title: 主任

Institute: 高雄榮民總醫院核子醫學科

## Developing Re-differentiation Therapy for Advanced Thyroid Cancer

De-differentiation occurs to well-differentiated thyroid cancer (WDTC) and results in so-called “dedifferentiated thyroid cancer (DeTC)”, an entity of follicular-derived thyroid cancers with enhanced FDG avidity but lack of radioiodide uptake. In contrast to WDTC, DeTC is often incurable mostly because of poor response to radioiodine therapy. Similarly advanced WDTC might develop to radioiodine-refractory differentiated thyroid cancer (RAI-R DTC) when lesional RAI uptake is lost or disease progression despite adequate RAI treatment. Thus a feeling of déjà vu might be sensed between these two entities and to restore RAI uptake becomes an important issue to solve both problems. Indeed re-differentiation therapy has been issued to resume dysfunctioning sodium iodide symporter (NIS). It is known that aberrant activation of mitogen-activated protein kinase (MAPK) pathway is the key event lead to oncogenesis as well as NIS dysfunction in thyroid cancers. Recent studies show that some specific mutated gene-directed targeted therapies might be used for advanced thyroid cancers to re-gain RAI uptake, allowing for I-131 treatment in these cases. These molecular-targeted therapies include inhibitors to target MEK, bRAF, neurotrophic receptor kinase (NTRK) fusion and RET fusion. These reagents are promising to serve as re-differentiation therapy, by which NIS function can be restored in order to render RAI treatment effective to achieve tumoricidal effects. Furthermore, whether combination of these mutated gene-directed target therapies and RAI treatment can augment RAI effectiveness warrants for further clinical investigation.



Name: 莊智淵  
Title: Technical Sales Specialist  
Institute: Randox Laboratories Ltd

---

## The Importance of Proficiency Testing in Laboratory Quality Assurance

以實務經驗分享導入符合 ISO17043 認證規範的外部能力試驗及品管系統，提供持續性的品質監控以  
提升檢驗系統準確性和實驗室品質管理。





Name: 吳欣榮  
Title: 資深產品專員  
Institute: 美商伯瑞股份有限公司台灣分公司

## 醫學實驗室品質管制的建立

“品管”對實驗室來說到底是什麼？為什麼實驗室必須要做品管？怎樣的品管規則是適合我們實驗室的？藉由這堂課，希望讓大家對於品管的意義與價值有所了解，並對於如何建立實驗室的品管規則有初步的概念。

OB-001

## Tc-99m 標誌藥物之 SPECT/CT 造影術 與碳十四藥物之全身自動放射顯影術 共同應用於複合劑型藥物傳遞路徑推估

王世民<sup>1</sup> 官孝勳<sup>1</sup> 鄭淑珍<sup>2</sup> 杜佳穆<sup>2</sup> 羅瑋霖<sup>1</sup> 翁茂琦<sup>1</sup> 樊修秀<sup>1</sup>

<sup>1</sup>核能研究所同位素組

<sup>2</sup>工業技術研究院生醫與醫材研究所

**背景介紹：**此研發是工研院開發眼藥劑型，在猴子身上進行試驗，有初步藥效，獲得 4 年將近 2 億元之研發經費。但利用質譜與其他影像技術，無法得到影像，以評估其路徑。因而委託本所，以 Tc-99m 標誌技術與碳十四藥物確認其路徑。本眼藥劑型係屬於藥物複合劑型，利用環糊精等多種親水性賦形劑組合作為載體。將親脂性的 VEGF 抑制藥物包覆其中，大幅提升其水溶性，改善藥物組織滲透能力，將藥物遞送至眼底視網膜治療黃斑部病變，因此環糊精與 VEGF 抑制藥物之傳遞路徑最為重要。

**方法：**考慮藥物結構大小與代表性，無法同時獲得環糊精 (HP $\beta$ CD) 與 VEGF 抑制藥物之影像，因此必須將兩者分開標誌。其中 VEGF 抑制藥物分子較小，經由碳十四標誌，加入其他配方，形成原有眼藥劑型，於大鼠眼球表面給藥，分別於 30 及 60 分鐘後，犧牲動物進行 VEGF 抑制藥物 (標誌碳十四) 之全身自動放射顯影術。環糊精則以 Tc-99m 加上氯化亞錫還原劑標誌原有眼藥劑型，確認標誌藥物安定性後，於大鼠眼球表面給藥，分別於 15 及 75 分鐘後，進行 nanoSPECT/CT 動態造影。

**結果：**標誌碳十四之 VEGF 抑制藥物的實驗結果說明，在 30 分鐘已經有部分藥物，從眼球表面穿過角膜，進入晶體，60 分鐘後也有看到透過結膜到達玻璃體。Tc-99m 標誌環糊精藥物實驗結果說明，在 15 分鐘已經有部分藥物，從眼球表面進入眼睛內部，75 分鐘後有更多藥物進入眼睛內部。

**結論：**根據標誌碳十四之 VEGF 抑制藥物的分布顯示，推測藥物是經由結膜、角膜、晶體與玻璃體到達眼球內部，與工研院之猴子試驗結果相符合。Tc-99m 標誌環糊精藥物結果顯示，載體也會由眼球表面進入到眼球內部，顯示該載體可以協助藥物進入眼球內部。由於該眼藥劑型攜帶藥物效果獲得證實，經濟部同意給予本所 600 萬委託案額度，協助工研院進行新型態藥物開發。目標是測試高組織滲透的劑型平台除了眼用外，是否能由鼻腔達成腦部傳輸，後續可包覆低腦組織穿透的 ALK 抑制劑進行驗證。

OB-002

## Computer Simulation Novel CXCR4 Molecular Imaging for Atherosclerotic Diagnosis

Chien-Chung Hsia, Chung-Hsin Yeh, Chun-Tang Chen, Cheng-Liang Peng

*Institute of Nuclear Energy Research, Taoyuan, Taiwan*

**Introduction:** C-X-C motif chemokine receptor 4 (CXCR4) plays a prominent role in inflammation, atherosclerosis, and cancer biology. This research design novel small molecular CXCR4 antagonist APD based on the structure of Tetrahydro-isoquinoline- Based CXCR4 antagonists TIQ-15 by computer simulation for the purpose to increase the sensitivity and specificity on binding CXCR4. After being labeled with [<sup>68</sup>Ga]-GaCl<sub>3</sub> and confirmed the radiochemical purity, the biological characteristics of [<sup>68</sup>Ga]-APD were evaluated by atherosclerotic apolipoprotein E deficiency (ApoE<sup>-/-</sup>) mice model and compared with [<sup>18</sup>F]-FDG and [<sup>18</sup>F]-NaF.

**Methods:** Novel CXCR4 antagonist APD was simulated by the software of BIOVIA Discovery Studio with the screen from binding energy and CDocker. The structure, molecular weight and purity of the synthesized APD were analyzed by NMR, Mass spectra and HPLC. After being labeled with [<sup>68</sup>Ga]-GaCl<sub>3</sub>, the radiochemical purity (RCP) was double analyzed by iTLC and HPLC. Biological characteristics of [<sup>68</sup>Ga]-APD were evaluated from the atherosclerotic ApoE<sup>-/-</sup> mice model and compared with other tracers.

**Results:** Mass, NMR and HPLC spectrum were proved that the identification and quality of APD needed our requirement. After being labeled with [<sup>68</sup>Ga]-GaCl<sub>3</sub> under acetate buffer (pH ≈ 5.5), radiochemical purity was over 90% by the analysis of TLC and HPLC. Biodistribution and receptor blocking studies were performed on ApoE<sup>-/-</sup> mice. After being injected into the tail vein, [<sup>68</sup>Ga]-APD could quickly eliminate from the kidney and accumulate in the atherosclerosis site. The highest target/background ratio (TBR) of atherosclerosis mice was 17.68 ± 0.71 (n = 3) after the high-fat diet for 3 months. CXCR4 antagonist AMD3465 could effectively block the uptake of [<sup>68</sup>Ga]-APD on the atherosclerotic site and liver. However, [<sup>18</sup>F]-FDG and [<sup>18</sup>F]-NaF could not show good sensitivity and specificity on the imaging of atherosclerosis.

**Conclusion:** This study represented that novel CXCR4 antagonist PET tracer [<sup>68</sup>Ga]-APD by computer simulation technology could efficiently increase the targeting effect and suitable for preclinical research in ApoE<sup>-/-</sup> mice models.

OB-003

## Deep Learning-enhanced Ultra-low-dose [<sup>18</sup>F]-PI-2620 Tau PET/MRI: A Reader Study

Kevin T. Chen<sup>1,2</sup>, Robel Tesfay<sup>3</sup>, Mary Ellen I. Koran<sup>2</sup>, Jiahong Ouyang<sup>4</sup>, Sara Shams<sup>2</sup>, Tie Liang<sup>2</sup>, Mehdi Khalighi<sup>2</sup>, Elizabeth Mormino<sup>5</sup>, Greg Zaharchuk<sup>2</sup>

<sup>1</sup>Department of Biomedical Engineering, National Taiwan University, Taipei, Taiwan

<sup>2</sup>Department of Radiology, Stanford University, Stanford, CA, USA

<sup>3</sup>Meharry Medical College, Nashville, TN, USA

<sup>4</sup>Department of Electrical Engineering, Stanford University, Stanford, CA, USA

<sup>5</sup>Department of Neurology, Stanford University, Stanford, CA, USA

**Introduction:** Deep learning (DL) methods have been applied widely in the medical imaging field and have shown great promise in image enhancement. In this project, we aim to investigate whether a DL network can generalize to ultra-low-dose tau PET image enhancement and whether the generated images are of diagnostic quality.

**Methods:** 44 participants (18 female, 70.2 ± 7.5 years) were recruited; 221 ± 61 MBq of the tau radiotracer <sup>18</sup>F-PI-2620 was injected. T1-weighted and T2-FLAIR MRI and PET data (60-90 minutes post-injection) were simultaneously acquired. The raw list-mode PET data were randomly undersampled by a factor of 20 and then reconstructed to produce an ultra-low-dose PET image. A generative adversarial network was trained and 4-fold cross-validation was used for image enhancement. The enhanced PET and the ultra-low-dose PET images were compared using paired t-tests to the original full-dose image on the metrics peak signal-to-noise ratio (PSNR), structural similarity (SSIM), and root-mean-squared error (RMSE). Three readers rated the subjective image quality as well as the tracer uptake (positive vs. negative) in relevant ROIs; agreement of the readers was evaluated using Gwet's AC.

**Results:** The three metrics all improved significantly after enhancement ( $p < 0.05/3$ ). Non-inferiority tests for subjective image quality showed that the full-dose images were scored higher than the low-dose and enhanced images. The readers also had high agreement in evaluating the status of tau uptake in the regions (Gwet's AC > 0.65); the uptake in the low-dose and enhanced images were read accurately (accuracy > 0.84 for all relevant regions) compared to their full-dose counterparts.

**Conclusions:** The deep learning-enhanced images were able to be read clinically for regional uptake patterns of tau accumulation similarly as the full-dose images.

OB-004

## Development of INER-PP-F11N as the Radionuclide Theranostic Agent Against Cholecystinin B Receptor-overexpressed Tumors

Chun-Tang Chen, Ming-Cheng Chang, Ping-Fang Chiang, Yu-Jen Kuo,  
Cheng-Liang Peng, I-Chung Tang

*Institute of Nuclear Energy Research, Taoyuan, Taiwan*

**Introduction:** The cholecystinin B receptor also known as CCK2R is an attractive target in nuclear medicine due to its overexpression by different tumors (such as medullary thyroid cancer and small cell lung cancer). PP-F11N, a CCK2R-targeting minigastrin analog, has been currently used in clinical trials; however, a major drawback observed with this radiolabeled peptide is its high uptake by the kidneys. In this study, we developed novel minigastrin analogs INER-PP-F11N 1 & 2, and evaluated for their applications as theranostic agent against CCK2R-overexpressed tumors.

**Methods:** INER-PP-F11N-1 & 2 radiolabeled with Lutetium-177, and then were subjected to preclinical evaluation *in vitro* (stability test and cell uptake analysis in A431-CCK2R cells) and *in vivo* (SPECT/CT imaging and anti-tumor activity in nude mice bearing A431-CCK2R tumor xenografts), including a side-by-side comparison with Lu-177-PP-F11N.

**Results:** INER-PP-F11N-1 & 2 radiolabeled with Lutetium-177 were successful with a radiochemical purity of up to 95% by radio-TLC analysis. *In vitro* study suggested that Lu-177-INER-PP-F11N-1 & 2 were highly stable for at least 48 hours at 37°C. Lu-177-INER-PP-F11N-1 & 2 showed a better cell surface binding and internalization in A431-CCK2R cells than Lu-177-PP-F11N. SPECT/CT images of Lu-177-INER-PP-F11N-1 & 2 in nude mice bearing A431-CCK2R tumor xenografts demonstrated higher tumor accumulation and low amounts of radioactivity in the kidneys as compared with Lu-177-PP-F11N. And lastly, the anti-tumor activity of Lu-177-INER-PP-F11N-1 & 2 were also investigated in nude mice bearing A431-CCK2R tumor xenografts. Mice treated with Lu-177-INER-PP-F11N-1 & 2 slowed tumor growth, compared with the control group (normal saline).

**Conclusions:** We have successfully developed minigastrin analogs INER-PP-F11N-1 & 2, in an effort to improve its performance in molecular imaging and peptide receptor radionuclide therapy (PRRT). INER-PP-F11N 1 & 2 have the potential for clinical application in nuclear medicine for the diagnosis and therapy of CCK2R-overexpressed tumors.

OC-001

## AI-assisted Quantitative Analysis of FDG-PET in Medial Temporal Lobe Epilepsy

Syu-Jyun Peng<sup>1</sup>, Yen-Cheng Shih<sup>2,3,4</sup>, Tse-Hao Lee<sup>5</sup>, Hsiang-Yu Yu<sup>2,3,4</sup>

<sup>1</sup>Professional Master Program in Artificial Intelligence in Medicine, College of Medicine,  
Taipei Medical University, Taipei, Taiwan

<sup>2</sup>Department of Neurology, Neurological Institute, Taipei Veterans General Hospital, Taipei, Taiwan

<sup>3</sup>Faculty of Medicine, National Yang Ming Chiao Tung University, Taipei, Taiwan

<sup>4</sup>Brain Research Center, National Yang Ming Chiao Tung University, Taipei, Taiwan

<sup>5</sup>Department of Nuclear Medicine, Taipei Veterans General Hospital, Taipei, Taiwan

**Introduction:** Fluorodeoxyglucose-positron emission tomography (<sup>18</sup>F-FDG-PET) was widely used in epilepsy surgery. In patients with medial temporal lobe epilepsy (MTLE), the lateralization value of FDG-PET varied by visual analysis. We conducted this study to establish a robust quantitative method for lateralization epileptogenic foci and examine the value of machine-assisted analysis of PET in MTLE.

**Methods:** We retrospectively reviewed patients who underwent epilepsy surgery for MTLE with high resolution brain MRI and <sup>18</sup>F-FDG-PET. Three clinicians who were blind to the side of surgery identified the side of MTLE by visual inspection. The side of surgery was set as a standard in this study. Two segmentation methods and corresponding atlases (AAL atlas for DARTEL, aparc+aseg atlas for freesurfer) were used to extract the normalized PET uptake of the interested regions. The two atlases were applied to automatically delineate MTLE associated regions in either hemisphere, respectively. The lateralization index of each MTLE associated regions were submitted for machine learning to establish MTLE side classification model.

**Results:** A total of 95 patients were enrolled in this study (47 left, 48 right). The hit rate of lateralization by visual analysis was 74.7%. In DARTEL segmentation method, the accuracy of lateralization according to 11 ROIs achieved 95.8% with Cosine KNN model, and the area under the ROC curve (AUC) is 0.99. When we limited the ROI to amygdala and hippocampus only, the accuracy decreased to 92.6%. When compared the freesurfer and the DARTEL method, there is no significant differences (accuracy 96.8%, AUC 0.99).

**Conclusions:** Visual analysis of FDG-PET to lateralize MTLE showed inter-rater difference and a lower hit rate compared to the results of machine-assisted interpretation. While reviewing the PET in MTLE, taking the information of the regions of MTLE associates into consideration showed a better performance than analyzing the regions limited to amygdala and hippocampus.

OC-002

## Interpretation of Basal Nuclei in Brain Dopamine Transporter Scans Using a Deep Convolutional Neural Network

Syu-Jyun Peng<sup>1</sup>, Ya-Ju Tsai<sup>2</sup>, Hsin-Yung Chen<sup>1,2</sup>

<sup>1</sup>*Professional Master Program in Artificial Intelligence in Medicine, College of Medicine,  
Taipei Medical University, Taipei, Taiwan*

<sup>2</sup>*Department of Nuclear Medicine, Taipei Medical University Hospital, Taipei, Taiwan*

**Introduction:** Parkinson's disease (PD) is the second most common neurodegenerative disorder after Alzheimer's disease. Parkinsonian motor symptoms can be attributed to a loss of nigrostriatal dopaminergic neurons. Functional imaging using the dopamine transporter (DAT) as a biomarker has proven effective in assessing dopaminergic neuron loss in the stratum, even in early-stage PD. In assessing the severity of dopaminergic neuron loss, visual and semi-quantitative methods are used to interpret DAT single photon emission tomography (SPECT) scans based on striatal to background activity, striatal shape, and symmetry. However, visual analysis is subjective and reviewer-dependent whereas semi-quantitative methods are operator-dependent.

**Methods:** In the current study, deep learning was used to estimate the degree of dopaminergic neuron loss in the caudate and putamen for use in the classification of images according to stage. Grades were indicated by dopaminergic neuron loss as follows: grade 0 (0-19%), grade 1 (20-39%), grade 2 (40-59%), and grade 3 (> 60%). Transfer learning was used to train a deep convolutional neural network, based on scans retrospectively obtained from 430 patients who underwent DAT SPECT imaging.

**Results:** Classification performance was evaluated by generating confusion matrices showing the actual and predicted distributions, the overall accuracy, macro F1-score, Cohen's Kappa coefficient, and other multi-class classification indicators. Accuracy in the identification of dopaminergic neuron loss respectively reached 90.7% and 92.0% in the caudate and putamen.

**Conclusions:** The proposed deep convolutional neural network provided a good model by which to interpret DAT SPECT images of the basal nuclei.

OC-003

## 評估利用 Centiloid scale 方法標準定量化 β 類澱粉蛋白 C-11 PIB 正子影像

楊邦宏<sup>1,2</sup> 吳承翰<sup>3</sup> 劉仁賢<sup>2,4</sup>

<sup>1</sup> 臺北榮民總醫院核醫部暨國家多目標醫用迴旋加速中心

<sup>2</sup> 國立陽明交通大學生物醫學影像暨放射科學系

<sup>3</sup> 衛生福利部雙和醫院影像醫學部 (委託台北醫學大學經營)

<sup>4</sup> 振興醫療財團法人振興醫院核醫部

**背景介紹：**正子 β 類澱粉蛋白影像 (β-Amyloid Protein PET Imaging) 常作為阿茲海默症診斷的一項重要 biomarker，藉由將影像進行量化 (quantification) 後，根據其數值的高低即可對阿茲海默症進行評估。然而影像量化的指標有很多種 (如 SUVR 或 DVR 等)，同一種指標間甚至可能會因為不同的造影或影像重建參數條件不同而有所差異，無法斷定數值的差異為疾病所造成或是影像處理方法所造成。因此本研究提出將定量指標皆能轉換至統一的量表，如此可以讓量化指標更加適用於疾病的診斷。

**方法：**Centiloid scale (CL) 為正子 β 類澱粉蛋白最常使用的量表之一，目的在於為正子 β 類澱粉蛋白影像量化提供統一的標準，CL 為 0 至 100 分的量表，以年輕正常人訂為 0，典型阿茲海默症患者訂為 100。使用標準資料庫中的 34 名小於 45 歲年輕正常受試者及 45 名阿茲海默症患者的 C-11 PIB 影像與 T1-MRI 影像，並依照 GAAIN 所提出的標準影像處理流程對影像進行前處理來計算出 SUVR 定量指標，並比較我們計算出來之 SUVR 與標準資料庫提供之 SUVR 的差異，若誤差小於 2% 則將 SUVR 利用公式轉換為 CL，最後計算出之 CL 與資料庫的 CL 做線性回歸。

**結果：**R-square 值大於 0.98 且回歸直線的斜率與截距分別介於 0.98~1.02 與 -2~2 之間，完成 1st-Level Analysis。2nd-Level Analysis 主要將自己收集的 C-11-PIB 影像資料進行 CL 轉換，得到 R-square 值大於 0.7。

**結論：**本研究定量化指標可以順利轉換至 CL 為統一的標準，將可以使用於 β 類澱粉蛋白 C-11 PIB 正子影像輔助量化分析診斷。



OC-004

## COVID-19 疫情下核醫檢查之經驗分享

陳薇璇<sup>1</sup> 許幼青<sup>1</sup> 張秀瑛<sup>1</sup> 莊紫翎<sup>1,2</sup> 王昱豐<sup>1,2,3</sup>

<sup>1</sup> 慈濟醫療財團法人大林慈濟醫院核子醫學科

<sup>2</sup> 慈濟學校財團法人慈濟大學醫學系放射線學科

<sup>3</sup> 慈濟學校財團法人大林慈濟醫院預防醫學中心

**背景介紹：**2020 年至今，嚴重特殊傳染性肺炎 (COVID-19) 肆虐全球，呼吸道的冠狀病毒傳播讓疫情一直難以恢復平靜，而台灣在 2021 年 5 月間，社區的傳播導致疫情不斷蔓延，面對有檢查需求的病患，各醫院對住院病患皆採 PCR 檢驗，陰性才得以住院，因此病房的病患是相對安全的，但是門診病患各家醫院的方法不同，在無法確定病患為陰性的前提下，可能會使工作人員暴露在感染的風險，本次分享則是以過往需去除口罩執行造影的檢查為主以及其消毒方式。在面對 COVID-19 疫情的考驗之下，放射師要如何安全的完成檢查，這絕對是需要探討的部分。

**經驗分享：**一、唾液腺檢查：此檢查採動態造影的檢查方式，病患需躺在檢查台上不動，共 50 分鐘，在第 40 分鐘時會由口給予檸檬酸刺激，以往請病人將口罩移除，以利做檢查；今年因為疫情的影響，因此本科採用讓病人戴上口罩，但事先將口罩上的鐵絲移除，以免出現冷區影像而影響分析結果，在第 40 分時用滴管吸取檸檬酸，稍微拉起病患口罩側邊，以滴管滴入口中，縮短病患口鼻暴露的時間，並在檢查完成時立即以紫外線滅菌燈進行消毒，結束之後再以酒精進行細部消毒。

二、胃排空檢查：此檢查病患需在 3 分鐘內吃完含有 Tc-99m DTPA 的三明治，加上 150 ml 的水，之後立即進行造影。但病患在進食期間會移除口罩，因此我們讓病患進入單獨的休息室，裡面有監視器以及對講機，讓我們能以遠端的方式確認病患有完成檢查步驟，並在病患上檢查台造影時，將休息室以紫外線滅菌燈進行消毒，結束之後再以酒精進行細部消毒。

**結論：**在 COVID-19 疫情下，既要維持原本的影像品質，也要兼顧病患及工作人員的健康安全，在兩者間需達成平衡，本科採取應變的方式依接觸的空間、時間、方法，這三點去做微調過往的檢查方式與程序，給予病患獨立空間，透過科技設備來達到遠距溝通減少接觸染疫風險，接觸病人時人員穿著隔離衣、手套、面罩，減少與病人相處時間，檢查後透過紫外線滅菌給予下個病人安全且乾淨的環境，在這疫情時代依然能夠給予病人最高的醫療品質，以及提供醫護人員安全的作業環境，是本科至本院全體同仁一致目標。

OC-005

## The Value of Taiwanese Normal Database in the Quantification of Thallium-201 Myocardial Perfusion Using the CZT Camera

Yi-Chieh Chen, Cheng Hsu, Mei-Feng Cheng, Chi-Lun Ko

*Department of Nuclear Medicine, National Taiwan University Hospital  
and National Taiwan University College of Medicine, Taipei, Taiwan*

**Introduction:** Quantitative myocardial perfusion imaging (MPI) relies on normal databases to compare patients' scans against reference normal limits. The original equipment manufacturer (OEM)-provided normal database was created from North Americans with conventional SPECT, which could be inappropriate to be applied on Taiwanese population with CZT camera. This study aims to evaluate the benefit of creating Taiwanese normal limits specific to the local population and acquisition system.

**Methods:** Images of 968 patients who underwent Thallium-201 stress/rest MPI using CZT SPECT and subsequent coronary angiography (CAG) were enrolled. All CAGs were performed within 90 days of MPI, and 70% or more luminal stenosis of epicardial vessels was considered obstructive CAD. Taiwanese normal database was generated from 53 men and 45 women who had CAG-documented patent coronary arteries and no modifiable risk factors of CAD. The gender-matched stress total perfusion deficit (TPD) was automatically derived from the MPI through the Quantitative Perfusion SPECT (QPS) software with Taiwanese (TPD-Taiwan) and manufacturer-provided (TPD-OEM) normal databases. Receiver operator characteristic (ROC) was used to assess the difference of diagnostic performance between TPD-Taiwan and TPD-OEM in detecting obstructive CAD.

**Results:** TPD-Taiwan showed excellent correlation ( $r = 0.96, p < 0.001$ ) with TPD-OEM and did not reveal a systemic bias. The area under ROC curve of TPD-Taiwan was significantly greater than TPD-OEM in detecting CAD (0.785 vs. 0.750,  $p < 0.001$ ). With an empirical TPD threshold of  $> 5\%$ , the TPD-Taiwan had a sensitivity of 62% and a specificity of 84%, compared with that of TPD-OEM of 77% and 52%, respectively.

**Conclusions:** Using the normal database created from Taiwanese low-risk and patent-artery cohort improved the diagnostic performance of quantitative TPD in detecting CAD for Taiwanese population using the CZT camera.

OC-006

## $^{123}\text{I}$ -MIBG SPECT/CT Versus $^{18}\text{F}$ -FDG PET/CT in Advanced Neuroblastoma of Paediatric Patients

Chin-Ho Tsao<sup>1,3,5</sup>, Bing-Fu Shih<sup>1</sup>, Ting-Chi Yeh<sup>2</sup>, Ren-Shyan Liu<sup>4,5</sup>

<sup>1</sup>Department of Nuclear Medicine, Mackay Memorial Hospital Taipei, Taiwan

<sup>2</sup>Department of Pediatrics, Mackay Memorial Hospital Taipei, Taiwan

<sup>3</sup>Department of Medicine, Mackay Medical College, New Taipei City, Taiwan

<sup>4</sup>Department of Nuclear Medicine, Cheng-Hsin General Hospital Taipei, Taiwan

<sup>5</sup>Institute of Clinical Medicine, School of Medicine, National Yang Ming Chiao Tung University Taipei, Taiwan

**Introduction:** Neuroblastoma is a common malignant tumor in children. Our purpose is to evaluate and compare uptake patterns of  $^{123}\text{I}$ -MIBG SPECT/CT and  $^{18}\text{F}$ -FDG PET/CT in advanced neuroblastoma patients

**Materials and Methods:** A total 25 people from 9 patients with advanced neuroblastoma have underwent both  $^{123}\text{I}$ -MIBG SPECT/CT scans and  $^{18}\text{F}$ -FDG PET/CT scans (2 stage III neuroblastoma, 5 stage IV neuroblastoma and 2 stage IVS neuroblastoma). SPECT imaging of the abdomen was available in all patients. All lesions were confirmed by histology and clinical follow-up.

**Result:** For detecting bone metastatic lesions, the sensitivity of  $^{123}\text{I}$ -MIBG SPECT/CT and  $^{18}\text{F}$ -FDG PET/CT were 70.3% and 97.3%, respectively. False-positive results of extraosseous lesions in one  $^{123}\text{I}$ -MIBG SPECT/CT scans were a retroperitoneal lesion due to posttherapy changes. False-negative results of extraosseous lesions in one  $^{18}\text{F}$ -FDG PET/CT scan were meningeal and liver metastasis due to physiological background activity. In addition, false-negative results of extraosseous lesions in one  $^{123}\text{I}$ -MIBG SPECT/CT were lymph nodes metastasis involving abdominopelvic region, mediastinum and neck.

**Conclusion:**  $^{18}\text{F}$ -FDG PET/CT shows more sensitivity than  $^{123}\text{I}$ -MIBG SPECT/CT in detecting bone metastasis of advanced neuroblastoma. However, in extraosseous lesions, these two imaging scans are complementary. Therefore, our findings suggest that both  $^{123}\text{I}$ -MIBG SPECT/CT and  $^{18}\text{F}$ -FDG PET/CT should be performed in advanced neuroblastoma.

OC-007

## Left Ventricle Function Assessment by Using First-pass Radionuclide Angiography: Validation Against Best-septal-view Equilibrium Radionuclide Angiocardiography

Yu Kuo<sup>1</sup>, Chien-Ying Lee<sup>1</sup>, Chi-Fen Lin<sup>1</sup>, Liang-Chi Wu<sup>1</sup>,  
Nan-Jing Peng<sup>1,2</sup>, Lien-Hsin Hu<sup>1,2</sup>

<sup>1</sup>Department of Nuclear Medicine, Taipei Veterans General Hospital, Taipei, Taiwan

<sup>2</sup>School of Medicine, National Yang Ming Chiao Tung University, Taiwan

**Introduction:** First-pass radionuclide angiography (FPRNA) is a classic exam to evaluate both left and right heart function in one study. With bolus injection of radiotracer, initial central circulation data was collected and analyzed. It is a safe and time efficient examination in which image acquisition takes only 40-60 seconds. Equilibrium radionuclide angiocardiography (MUGA), on the other hand, is considered as the gold standard of left ventricle ejection fraction (LVEF). Traditionally, during image acquisition in MUGA, there is an empirical 45 degree left anterior oblique angle (LAO) for separation of left ventricle from right ventricle. In our institution, this step is improved by selecting personalized angles best suited to the patients from SPECT images before data acquisition. In our site, both FPRNA and MUGA are routine clinical services with high throughput. In this study, we aim to evaluate the correlation and consistency of LVEF of FPRNA and personalized best-septal-view MUGA.

**Methods:** Patients who underwent both FPRNA and personalized MUGA studies at an interval less than 45 days from Jan. 2014 to Jun. 2021 were retrospectively selected. In order to minimize confounding factors, those who had clinical events possibly affecting patients' LVEF during this 45-day interval are excluded. LVEF values in FPRNA and personalized MUGA examination were analyzed (n = 33) with linear regression and Bland-Altman plot.

**Results:** We find a strong positive linear relationship between LVEF values in FPRNA and personalized MUGA. The equation for the line fitting the relationship is  $LVEF_{MUGA} = 0.90 (LVEF_{FPRNA}) + 7.24$  ( $r = 0.93$ ,  $R^2 = 0.861$ , p-value for F-test < 0.001, standard error of estimate = 5.5). There was no violation to the assumptions of normal distribution and independency of residuals. The Bland-Altman analysis revealed no systemic bias of LVEF between the two methods and the SD = 5.53.

**Conclusions:** LVEF of FPRNA shows excellent correlation and consistency with LVEF from a personalized best-septal-view MUGA study.

OC-008

## Radioactive Iodine Treatment and the Risk of Long-term Cardio-vascular Morbidity and Mortality in Thyroid Cancer Patients: A Nationwide Cohort Study

Chun-Hao Kao<sup>1</sup>, Chi-Hsiang Chung<sup>2</sup>, Wu-Chien Chien<sup>2</sup>,  
Daniel Hueng-Yuan Shen<sup>1</sup>, Li-Fan Lin<sup>1</sup>, Chuang-Hsin Chiu<sup>1</sup>, Cheng-Yi Cheng<sup>1</sup>,  
Chien-An Sun<sup>3</sup>, Ping-Ying Chang<sup>4</sup>

<sup>1</sup>*Department of Nuclear Medicine, Tri-Service General Hospital and National Defense Medical Center, Taipei City, Taiwan*

<sup>2</sup>*Department of Medical Research, Tri-Service General Hospital and National Defense Medical Center, Taipei City, Taiwan*

<sup>3</sup>*Big Data Research Center, College of Medicine, Fu-Jen Catholic University, New Taipei City, Taiwan*

<sup>4</sup>*Division of Hematology/Oncology, Department of Internal Medicine, Tri-Service General Hospital and National Defense Medical Center, Taipei City, Taiwan*

**Introduction:** This study aimed to investigate the association between radioactive iodine (RAI) and long-term cardiovascular disease (CVD) morbidity/mortality in thyroid cancer.

**Methods:** The study was conducted using data from the Taiwan National Health Insurance Database during 2000-2015. Thyroid cancer patients aged  $\geq 20$  years were categorized into RAI (thyroidectomy with RAI) and non-RAI (thyroidectomy only) groups. Cox proportional hazard regression model and Kaplan-Meier method were used for analysis.

**Results:** Total 13,310 patients were included. Kaplan-Meier analysis demonstrated the two groups had similar cumulative risks of CVD (log-rank  $P = 0.72$ ) and CVD-specific mortality (log-rank  $P = 0.62$ ). On Cox regression analysis of different RAI doses, the risk of CVD was higher in the cumulative dosage  $> 3.7$  GBq (hazard ratio = 1.69, 95% confidence interval = 1.24-2.40,  $P < 0.001$ ).

**Conclusions:** RAI was not associated with an increased risk of CVD in thyroid cancer. However, CVD surveillance is indicated in the patients receiving the cumulative RAI dosage above 3.7 GBq.

OC-009

## Detecting Relation of Myocardial Glucose Metabolism Change in Hodgkin's Lymphoma Patients after Anthracycline-based Chemotherapy

Tzu-Shan Tseng<sup>1</sup>, Shan-Ying Wang<sup>1</sup>, Yu-Chien Shiau<sup>1</sup>, Yen-Wen Wu<sup>1,2</sup>

<sup>1</sup>Department of Nuclear Medicine, Far Eastern Memorial Hospital, New Taipei City, Taiwan

<sup>2</sup>Division of Cardiology, Cardiovascular Medical Center, Far Eastern Memorial Hospital, New Taipei City, Taiwan

**Background:** Anthracycline-based chemotherapy for Hodgkin lymphoma (HL) creates outstanding disease-free survival, but with risk of left ventricular (LV) dysfunction and heart failure, featured with delayed onset. Previous studies suggested that myocardial metabolic alteration after anti-cancer therapy might lead to LV dysfunction. We investigated the glucose uptake on <sup>18</sup>F-FDG positron emission tomography-computed tomography (PET/CT) in HL patients using visual and quantitative analyses.

**Methods:** Myocardial <sup>18</sup>F-FDG uptake pattern and utilization were assessed in patients undergoing oncologic whole-body <sup>18</sup>F-FDG-PET/CT, this pilot study compared 5 HL patients treated with doxorubicin-based chemotherapy in both the pre- and post-therapy setting; and 5 cancer patients followed by FDG PET twice with doxorubicin intervention as the control group. Myocardial uptake pattern was visually evaluated, and assessed the SUVmax in the LV wall, ratio of LV wall/ longissimus, and the change of SUV ( $\Delta$ SUV) or SUV ratios between baseline and follow-up studies.

**Results:** In HL patients treated with doxorubicin-based chemotherapy group, post-therapy PET disclosed widely variation without significantly change of SUV of LV wall/longissimus muscle ratios in comparison to the baseline ( $p = n.s$ ), same as in the control group. We also tried to estimate the myocardial glucose utilization using a commercially available PMOD version 4.2 software. However, it failed to analyze automatically in patients with none, minimal or focal <sup>18</sup>F-FDG uptake patterns, which are the predominantly observed on oncologic patients underwent <sup>18</sup>F-FDG PET/CT.

**Conclusions:** In this study, the method to examine  $\Delta$ SUV ratios was feasible and the study revealed neutral results which were not like the previous studies published. There are some limitations in this study and can be improved in future series study. First of all, probable small sample size, the variation of SUV max was obvious. Second, we did not correlate with post-therapy LV ejection fraction. In addition, the <sup>18</sup>F-FDG myocardial uptake could be influenced by various physiologic conditions and a strict prolonged fasting protocol should be considered. Low and heterogeneous <sup>18</sup>F-FDG uptake of LV wall, combined visual assessment and manual SUV measurement is more feasible than automatical analysis using the PMOD software. Obtaining and taking this information into account might help to understand the cardio-toxicity of anti-cancer therapy and stratify patients according to risk and might reduce unnecessary cardiovascular complications in cancer patients.

OC-010

## Semi-quantification of Tc-99m TRODAT SPECT: Comparison between DaTQUANT and MRI-based ROI

Chun-Pang Huang, Yen-Hsiang Chang, Pei-Wen Wang, Shu-Hua Huang,  
Yung-Cheng Huang, Hong-Jie Chen, Chien-Chin Hsu

*Department of Nuclear Medicine, Kaohsiung Chang Gung Memorial Hospital,  
Chang Gung University College of Medicine, Kaohsiung, Taiwan*

**Introduction:** Dopamine transporter (DAT) brain single photon emission computed tomography (SPECT) is widely used to evaluate parkinsonian disorders. DaTQUANT (GE Healthcare) is a commercial software and has been validated for I-123 Ioflupane SPECT automatic semi-quantification. The feasibility of DaTQUANT for Tc-99m TRODAT SPECT semi-quantification is unknown. To assess the feasibility, we compared semi-quantitative data between DaTQUANT and magnetic resonance imaging (MRI)-guided region of interest (ROI) method in Tc-99m TRODAT SPECT.

**Methods:** From May 2021 to July 2021, 45 patients who underwent Tc-99m TRODAT-1 brain SPECT/CT and brain MRI within six months were enrolled in this retrospective study. DaTQUANT used a predefined voxel of interest template to calculate the specific binding ratios (SBRs) of striatum, putamen, and caudate nucleus. MRI-based method used manually delineated ROIs of the striatum, putamen, caudate nucleus, and occipital cortex on MRI, and transfer them to SPECT images to calculate the SBRs of striatum, putamen, and caudate nucleus.

**Results:** The SBRs of striatum, putamen, and caudate nucleus were  $0.51 \pm 0.30$ ,  $0.47 \pm 0.31$ , and  $0.58 \pm 0.32$  from DaTQUANT;  $0.55 \pm 0.31$ ,  $0.55 \pm 0.31$ , and  $0.54 \pm 0.32$  from MRI-based method, respectively. The concordance correlation coefficients were 0.919, 0.869, and 0.901, respectively. Striatal and putaminal SBRs from DaTQUANT were significantly lower than those from MRI-based method ( $P = 0.004$ ,  $P < 0.001$ , respectively), while caudate SBR from DaTQUANT was significantly higher than that from MRI-based method ( $P = 0.011$ ). The systemic biases of striatal, putaminal, and caudate SBRs from DaTQUANT were  $-0.037$ ,  $-0.077$ , and  $0.038$  as compared to MRI-based method.

**Conclusion:** The semi-quantitative data of DaTQUANT correlate well with those of MRI-based method in Tc-99m TRODAT SPECT. However, biases between them are significant so that they cannot be used interchangeably.

OC-011

## Predictive Factors and Practical Solutions to Halo Artifacts in $^{18}\text{F}$ -FDG PET/CT

Chih-Yi Lin, Chi-Lun Ko, Ruoh-Fang Yen, Mei-Fang Cheng,  
Ching-Chu Lu, Jei-Yie Huang, Chia-Ju Liu

*Department of Nuclear Medicine, National Taiwan University Hospital, Taipei, Taiwan*

**Background:** Halo artifact is commonly noted in  $^{68}\text{Ga}$ -PSMA imaging. However, we observed that similar effect is seen in  $^{18}\text{F}$ -FDG PET/CT image in our daily work. To some degree, this artifact has impact on clinical practice. The goal of this study is to investigate the occurrence and try to find some way to eliminate this artifact.

**Methods:** In total 80 patients received PET/CT scan, 34 of these PET data were constructed twice using standard correction (SC) and scatter limitation correction (SLC). We chose another 46 cases without significant halo artifact in visual presence and the PET data only constructed by SC. We categorized halo artifact into three types by visual judgment. The first one is a stripe of severe photopenic region. The second one is decreased tracer activity in pelvis or upper thigh. The third one is recognized as photopenic region, near non-FDG uptake at soft tissue, in abdomen. Semiquantitative measurements are performed with standardised uptake value (SUV). We also recorded body weight, body height, BMI of patients, whether peripheral venous catheter is out of the CT field-of-view (FOV) and the residual tracer activity in venous catheter, kidney and urinary bladder SUV of each person and visual degree of arm truncation.

**Results:** SLC is able to visually eliminate halo artifact in  $^{18}\text{F}$ -FDG PET/CT scan. The difference of lesions in the abdomen and pelvis reaches statistical significance between PET data constructed by SLC and SC, but lesions in chest does not. For type 1 of halo artifact, peripheral venous catheter out of the CT FOV yielded an odds ratio (OR) of 6.41, with a 95% confidence interval (CI) of 2.11 to 19.44. Increased SUVmax of urinary bladder resulted in a small but statistically significant increase in the second type halo artifact ( $p < 0.05$ ), and the same result is found between BMI value of patient and the occurrence of third type halo artifact.

**Conclusions:** Halo artifact in FDG PET/CT may result from mismatch between PET and CT, higher BMI, and high urinary bladder activity. The most severe artifact is caused by mismatch between PET and CT with intense activity outside the FOV of CT. To ensure that peripheral venous catheter is in the FOV of CT may reduce the occurrence and effect of halo artifact. Otherwise, reduction urinary bladder activity by hydration and voiding scan is also recommended. If halo artifact is inevitable, reconstructed by SLC may be an acceptable solution.



OC-012

## Value of $^{18}\text{F}$ -FDG PET Derived Parameter in Predicting Survival and Prognosis of Early Staged Esophageal Cancer: A Single-center Retrospective Study

Fu-Ren Tsai, Hung-Pin Chan, Chin Hu, Daniel Hueng-Yuan Shen

*Department of Nuclear Medicine, Kaohsiung Veterans General Hospital, Kaohsiung, Taiwan*

**Introduction:**  $^{18}\text{F}$ - FDG PET/CT has been utilized in multiple cancer work-ups, and has already taken a place in staging and post-treatment response evaluation of esophageal cancer. However, there's limited literature described the use of  $^{18}\text{F}$ - FDG PET/CT imaging in prognosis prediction of esophageal cancer. This study aim to compare the power of multiple  $^{18}\text{F}$ - FDG PET/CT-derived parameter, including SUV, MTV and TLG, in predicting prognosis of esophageal cancer.

**Methods:** Twenty patients with pathological or clinical stage II esophageal cancer with at least five year of follow-up duration were enrolled for retrospective review. Semi- quantitative analysis of FDG tumor uptake was performed with PET VCAR application. SUVmean and MTV were calculated using SUV threshold of 41% of SUVmax; the total lesion glycolysis (TLG) was calculated as the product of SUVmean and MTV. Correlation of these PET derived metabolic parameters was evaluated using Spearman correlation coefficient. Maximally selected rank statistics was performed to detect the optimal cutoff used for dichotomizing each PET derived parameter.

**Results:** Both MTV and TLG showed significant relationship with recurrence-free survival in stage II esophageal cancer, while SUVmean and SUVmax failed to proof their prognostic value. TLG has the greatest accuracy in recurrence prediction. We run the maximally selected rank statistics to provide the classification of observations in 2 groups by a continuous predictor parameter; the free from recurrence rate was significantly greater in patients lower MTV and TLG.

**Conclusions:** This research supports our hypothesis that PET derived metabolic parameters are well correlated with recurrence-free survival of stage II esophageal cancer. The results also suggest these parameters are good prognostic predictors.

OC-013

## Potential Pitfall of Axillary Lymphadenopathy on $^{18}\text{F}$ -FDG PET/CT after COVID-19 Vaccination

Dallas Yew (Shun-Yu), Gu-Hong Lin

*Taipei Mackay Memorial Hospital*

**Introduction:** Due to the global pandemic, COVID-19 vaccinations have been administered to the public, with a high priority for high-risk groups such as cancer patients. However, recent studies have shown that vaccinations may cause inflammation in ipsilateral axillary lymph nodes. This is a potential pitfall during PET scans for staging and follow-up.

**Methods:** One hundred eighty five  $^{18}\text{F}$ -FDG PET/CT scans were performed at Taipei Mackay Memorial hospital during August to September of 2021. Of the 185 patients, 35 received a COVID-19 vaccination prior to PET/CT scan and were included in this study. Date of vaccination, which vaccine, and which arm received the injection were noted before the scan. After PET/CT scan, lymph nodes in the ipsilateral axillary region with visible tracer uptake, and their SUVmax value, were recorded.

**Results:** Out of 35 patients who received a vaccination prior to PET/CT scan, 24 cases (68.6%) showed focally increased tracer uptake in ipsilateral axillary region. PET/CT scans for 22 cases showed primary tumor and metastasis far away from axillary region. Two cases, one breast cancer and the other advanced esophageal cancer both showed multiple sites of metastatic lymphadenopathy in and around axillary regions. The longest duration between vaccination and visible reactive axillary lymph node during PET scan was 51 days for Moderna vaccine with SUVmax: 4.3; and 81 days for Astra-Zeneca vaccine with SUVmax: 2.1.

**Conclusion:** COVID-19 vaccinations may cause inflammation in axillary lymph nodes ipsilateral to injection site. Reactive lymph nodes may be seen for as long as 51 days after Moderna vaccine and 81 days after Astra-Zeneca vaccine. Cancer patients with tumor origin and spread far away from axillary regions makes diagnosing reactive lymph nodes easier; however, cases such as breast and esophageal cancer may make differentiating between reactive and metastatic lymph nodes difficult.

PB-001

## Using Animal PET with [<sup>18</sup>F] T-807 to Investigate the Anti-tauopathy and Neuroprotection Effects of Bezafibrate, A Pan-PPAR Agonist, in an STZ-icv Tauopathy Rat Model

Li-Fan Lin<sup>1,2</sup>, Yun-Ting Jhao<sup>3</sup>, Ta-Kai Chou<sup>1</sup>, Cheng-Yi Cheng<sup>1</sup>,  
Chuang-Hsin Chiu<sup>1</sup>, Kuo-Hsing Ma<sup>2,3</sup>

<sup>1</sup>Department of Nuclear Medicine and PET center, Tri-Service General Hospital,  
National Defense Medical Center, Taiwan

<sup>2</sup>Graduate Institute of Medical Sciences, National Defense Medical Center, Taiwan

<sup>3</sup>Department and Graduate Institute of Biology and Anatomy, National Defense Medical Center, Taiwan

**Introduction:** Tauopathy, caused by hyperphosphorylated tau protein (pTau), may have an important role in many neurodegenerative diseases, especially the Alzheimer's disease (AD). Previous studies demonstrated that “peroxisome proliferator-activated receptor (PPAR)” agonists could ameliorate the tauopathy associated neurodegenerative impairment in animal models, which seem to be a promising treatment for AD. To in vivo evaluate the neuroprotective effects of bezafibrate (BEZA; a pan-PPAR agonist), animal behavior tests as well as animal PET with a pTau-specific tracer, [<sup>18</sup>F] T-807, were applied in a tauopathy rat model.

**Methods:** Small animal-PET with [<sup>18</sup>F] T-807, a PET tracer specifically binding to insoluble neurofibrillary tangles formed by pTau, was applied to evaluate the tauopathy in a streptozotocin intracerebroventricularly injection (STZ-ICV) induced tauopathy rat model. Sprague Dawley rats (280-320 g) were randomly divided into three groups (n = 6 for each group). The STZ and STZ + BEZA groups underwent STZ ICV injection (3 mg/Kg, on D1 & D3) while the sham group was only ICV injected with artificial CSF. The STZ + BEZA group was co-treated with BEZA for 4 weeks (50 mg/kg/day, intraperitoneal injection, D1-D28). Radial arm maze (RAM) tests were used to assess the cognitive function before, and 1, 2 and 3 months after STZ ICV. [<sup>18</sup>F] T807 PET studies were performed at the same time-points to evaluate the pTau deposition in the brain. The rats were sacrificed at the third month. Immunohistochemistry (IHC) stains of brain were done with anti-pS396 antibody (a marker for pTau). pS396 + cell counts (for cortex) or optical density (OD) ratio of pS396 (for hippocampus) were analyzed to evaluate the pTau deposition.

**Results:** In comparison with the sham group, the STZ group showed significantly higher error rates in RAM tests (3M error rate: 31.11% vs 13.83%,  $p < 0.01$ ) as well as gradually increased [<sup>18</sup>F] T807 uptake in cortex (SUR: 1M, 0.30 vs 0.19,  $p < 0.01$ ; 3M, 0.47 vs 0.23,  $p < 0.001$ ) and hippocampus (SUR: 1M, 0.29 vs 0.19,  $p < 0.01$ ; 3M, 0.45 vs 0.23,  $p < 0.001$ ). With the bezafibrate co-treatment, the STZ + BEZA group demonstrated no statistical difference in the error rates and [<sup>18</sup>F] T807 uptake as compared with those in the sham group (3M error rate: 18.17% vs 13.83%,  $p > 0.05$ ; 3M SUR: 0.29 vs 0.23 [cortex], 0.28 vs 0.23 [hippocampus],  $p > 0.05$ ). In IHC studies, the STZ group showed significantly increased pTau deposition (cortex pS396+ cells: 230.93/mm<sup>2</sup> vs 52.79/mm<sup>2</sup>,  $p < 0.001$ ; hippocampus OD ratio of pS396: 4.55 vs 1.36,  $p < 0.001$ ) while the STZ + BEZA showed no statistical difference as compared with the sham group.

**Conclusion:** Our study demonstrated that bezafibrate, a pan-PPAR agonist, could ameliorate the cognitive impairment and cerebral pTau deposition in the STZ-icv tauopathy rat model. Due to the crucial role of tauopathy in AD, we suggest that bezafibrate could be applied in the regimen of AD treatment. Furthermore, our results also suggested that small animal PET with the pTau-specific tracer, [ $^{18}\text{F}$ ] T-807, could be useful to dynamically evaluate the cerebral pTau deposition in vivo, leading to precise estimation of the therapeutic response in the animal models.

PB-002

## Comparison of $^{18}\text{F}$ -T807 and $^{18}\text{F}$ -MK6240 PET Imaging in the Mouse Model of Tauopathy

Chuang-Hsin Chiu<sup>1</sup>, Kuo-Hsing Ma<sup>2</sup>, Ta-Kai Chou<sup>1</sup>, Ing-Jou Chen<sup>1</sup>,  
Cheng-Yi Cheng<sup>1</sup>, Chyng-Yann Shiue<sup>1</sup>

<sup>1</sup>Department of Nuclear Medicine, Tri-Service General Hospital, National Defense Medical Center, Taipei, Taiwan

<sup>2</sup>Department of Biology and Anatomy, National Defense Medical Center, Taipei, Taiwan

**Introduction:** PET imaging of tauopathy has facilitated development of anti-tau therapy.  $^{18}\text{F}$ -T807 tracks neurodegenerative progression.  $^{18}\text{F}$ -MK-6240 is a novel PET tracer for tau protein imaging, which is implicated in neurologic disorders. In this study, we conducted the head-to-head comparison of  $^{18}\text{F}$ -T807 and  $^{18}\text{F}$ -MK-6240 PET imaging in mouse model of tauopathy.

**Methods:** PET imaging were obtained in groups of P301S (N = 3) and wild-type (N = 3) at 6 and 11 months of age. Dynamic PET scan were performed with a small animal PET scanner (BIOPET 105, BIOSCAN, Santa Clara, CA, USA) for up to 120 min after bolus injection of  $^{18}\text{F}$ -T807 and  $^{18}\text{F}$ -MK-6240. PET imaging data were spatially normalized into mouse MRI brain template, and VOIs (striatum, cortex, hippocampus, thalamus, hypothalamus, amygdala, brainstem and cerebellum) in the template were applied for quantitative analysis. Reference region method analysis were performed using cerebellum as reference region including distribution volume ratio (DVR) and standard uptake ratio (SUVR).

**Results:** The comparison of the time activity curves (TACs) showed the faster tracer washout of  $^{18}\text{F}$ -T807 than  $^{18}\text{F}$ -MK-6240 in the brain. Relative to the average peak activity, 90% remained at 5 min and 70% remained at 60 min after  $^{18}\text{F}$ -MK-6240 injection, while 87% remained at 5 min and 18% at 60 min after  $^{18}\text{F}$ -T807 injection. SUVRs at 40-60min were consistency to DVR.

**Conclusion:** The result indicated dynamic imaging capability of tau tracer, and the characteristics of two tracers were similarity.

PB-003

## Investigate the Important Features of Diagnosis in Different Types of Dementia Using Neurobehavioral Assessments and the Cortical Volumes of MRI

Chen-Han Cheng<sup>1</sup>, Ming-Chyi Pai<sup>2,3</sup>, Ya-Ting Chang<sup>4</sup>, Yu-Ching Ni<sup>1</sup>, Fan-Pin Tseng<sup>1</sup>

<sup>1</sup>Health Physics Division, Institute of Nuclear Energy Research, Atomic Energy Council, 1000 Wenhua Rd.  
Jiaan Village, Longtan, Taoyuan City 325, Taiwan

<sup>2</sup>Division of Behavioral Neurology, Department of Neurology, National Cheng Kung University,  
138, Sheng Li Road, North District, Tainan 704, Taiwan

<sup>3</sup>Alzheimer's Disease Research Center, National Cheng Kung University Hospital, Tainan, Taiwan

<sup>4</sup>Division of Neurology, Institute of Translational Research in Biomedicine, Kaohsiung Cheng Gung Memorial Hospital,  
Cheng Gung University College of Medicine, Kaohsiung, Taiwan

**Introduction:** It is difficult to determine the exact type of dementia because different dementias' symptoms and brain changes may overlap. In this study, we investigated the neurobehavioral assessments and cortical volume of various regions associated with three types of dementia.

**Methods:** The patients in this study included Alzheimer's disease (AD, n = 60), dementia with Lewy bodies (DLB, n = 49), and vascular dementia (VD, n = 60). Each patient was evaluated on seven neurobehavioral assessments and Magnetic Resonance Imaging (MRI). The twenty-two cortical volumes were calculated by MRI images for each patient. One-way ANOVA, F-test, and Scheffe post-hoc tests were used to find the important features of differentiating three types of dementia ( $P < 0.05$ ). Also, a logistic regression model was built to differentiate three types of dementia.

**Results:** In F-test, Clinical Dementia Rating (CDR), Neuropsychiatry Inventory (NPI), Barthel index (BA), amygdala, middle frontal cortex, caudate, putamen, and thalamus were significant differences between AD, DLB, and VD. In Scheffe post-hoc test, NPI, IADL, BA, caudate, and putamen were shown the significant differences between AD and DLB; CDR, NPI, IADL, BA, amygdala, middle frontal cortical volume, putamen volume, and thalamus volume were shown the significant differences between AD and VD. Only caudate volume was shown the significant difference between DLB and VD. The accuracy of model using neurobehavioral assessments with cortex information (74.75%) was higher than without cortex information (64.39%).

**Conclusions:** Our study indicated that the volume of putamen might contribute to the diagnosis of AD/DLB and AD/VD. Patients with DLB or VD often had the decreased motor function, which was associated with caudate and putamen. Caudate was the only feature that contributed to the diagnosis of DLB/VD. The results implied that caudate and putamen could be the biomarkers for the diagnosis of these three dementia types.

PB-004

## Using z-score Analysis to Improve the Diagnosis of Tau PET Imaging

Shao-Yi Huang<sup>1</sup>, Kun-Ju Lin<sup>2</sup>, Ing-Tsung Hsiao<sup>1,2</sup>

<sup>1</sup>Department of Medical Imaging and Radiological Sciences, Chang-Gung University, Taoyuan, Taiwan

<sup>2</sup>Department of Nuclear Medicine, Lin-Kou Chang-Gung Memorial Hospital, Taoyuan, Taiwan

**Introduction:** The development of Positron Emission Tomography (PET) tau tracers (tau-PET) in Alzheimer's disease (AD) is able to evaluate the deposition and distribution of neurofibrillary tangles (NFTs) in the human brain for clinical diagnosis of AD. Among them, the tau-PET tracer F-18-AV1451 has high selectivity between tau protein and A $\beta$  but with off-target binding in the basal ganglia, choroid plexus, and thalamus regions, and which interferes with image diagnosis. In this research, we utilized z-score analysis to reduce the influence of background signal due to nonspecific binding by comparing AD/MCI to healthy subject, and then improve the detection of tau protein in the cerebral cortex.

**Methods:** There were total 278 participants in this study (150 normal control, 78 Mild cognitive impairment, 50 AD) downloaded from the Alzheimer's Disease Neuroimaging Initiative (ADNI). They all underwent MRI, F-18-AV45, F-18-AV1451 and neuropsychological testing. We used PMOD 3.7 software for image processing, selecting ROIs (region of interests) based on the Braak stages, and calculating the standard uptake value ratio (SUVR) with the inferior cerebellar gray matter as the reference region. Then, we obtained a brain norm by processing the NC (A $\beta$  negative) SUVR image for calculating the z-score individually as a z-map. Finally, z scores within different ROIs and off-target binding regions were analyzed and discussed.

**Results:** For regional analysis, there is a relationship between tau deposition and the disease severity: the more serious, the higher the SUVR. We also found that participants with early-onset AD have higher tau protein deposition. Under the z-score calculation, disease severity of AD is related to higher z-score, and that indicates the more significant difference between normal control and AD. Within the off-target regions including the basal ganglia, choroid plexus, and thalamus regions the z-scores all approach to zero. For the typical regions with higher tau-burden for AD such as temporal lobe and entorhinal cortex, as expected, higher z-scores were observed.

**Conclusions:** The presentation of z-map resolved the signal interference of these off-target regions on the image. From the preliminary result, the z-score analysis is more sensitive to the detection of tau protein, and can improve the diagnosis power of tau-PET imaging with off-target binding.

PB-005

## The Radiosynthesis of [ $^{18}\text{F}$ ]THK5351 by Eckert-Ziegler Modular-Lab System

Chi-Wei Chang, Chun-Tse Hung, Geng-Ying Li, Shih-Pei Chen,  
Wen-Yi Chang, Nan-Jing Peng

*Department of Nuclear Medicine, National PET/Cyclotron Center, Veterans General Hospital, Taipei, Taiwan*

**Introduction:** [ $^{18}\text{F}$ ]THK5351 is a highly sensitive and specific radiotracer for tau protein fibrils in the human brain. [ $^{18}\text{F}$ ]THK5351 was used for AD animal model imaging by using  $\mu\text{PET}/\text{MR}$  in our center. Reliable procedure of [ $^{18}\text{F}$ ]THK5351 in cGMP conditions was developed by Modular-Lab system.

**Methods:** For the radiosynthesis, [ $^{18}\text{F}$ ]fluoride was transferred to the Modular-Lab system and fixed on a QMA cartridge. The activity was eluted from the cartridge with 1.1 mL of a potassium carbonate and Kryptofix solution in water/acetonitrile (1/4) and transferred to the reactor by nitrogen. The complex was azeotropically dried at 120°C by addition of 1.6 mL of acetonitrile. After complete drying, 5 mg of the THK5351 tosylate precursor in 0.6 mL of DMSO was added to the activated and dried [ $^{18}\text{F}$ ]fluoride/ $\text{K}2.2.2$  complex and the reaction vessel was heated at 100°C for 10 min. Then, the hydrolysis was performed by adding HCl (1 M, 0.5 mL) to the reaction solution at 110°C for 3 min. The reaction was quenched with AcOK (0.8 M, 0.5 mL) and the crude product was purified by a semi-preparative HPLC column (YMC-Actus Triart C18 250 x 20 mm I.D S-5  $\mu\text{m}$ , 12 nm) and eluted with a solution of HPLC M.P. ( $\text{CH}_3\text{CN}/20 \text{ mM NaH}_2\text{PO}_4$  in  $\text{H}_2\text{O}$  (13/7) (flow at 6 mL/min). The fraction containing the product was collected and mixed with 40 mL of water. Subsequently, [ $^{18}\text{F}$ ]THK5351 was trapped on a pre-conditioned (10 mL ethanol and 20 mL water) tC18plus SepPak cartridge and acetonitrile was washed off by rinsing tC18plus SepPak cartridge with water. The product ([ $^{18}\text{F}$ ]THK5351) was eluted with ethanol (0.9 mL) and formulated with normal saline (9 mL).

**Results:** The sterile [ $^{18}\text{F}$ ]THK5351 was produced in 100 min with greater than 99% radiochemical purity. The quality control was performed in accordance to the guidelines of the literature with a mean 10~15% EOS yield and 130 GBq/ $\mu\text{mol}$  ( $n = 2$ ) The findings of  $\mu\text{PETMR}$  images suggest that [ $^{18}\text{F}$ ]THK5351 provides useful information on Tau-protein pathology in living subjects.

**Conclusions:** The routine production of [ $^{18}\text{F}$ ]THK5351 proved to be reliable and stable. [ $^{18}\text{F}$ ]THK5351 of the cGMP quality could be used for imaging neurofibrillary pathology in Alzheimer disease by using PET/MR in the future.



PB-006

## Difference of the $^{18}\text{F}$ -FDG Brain PET Images Reconstructed with Bayesian Penalized Likelihood and Ordered Subset Expectation Maximization Algorithms- Comparison of the Z-score

Tse-Hao Lee, Hsiao-Ling Chiang, Rong-Hong Jhou, Nan-Jing Peng

*Department of Nuclear Medicine, Taipei Veterans General Hospital, Taipei, Taiwan*

**Introduction:**  $^{18}\text{F}$ -FDG Brain PET image is a major pre-surgical evaluation for patients with epilepsy. In interictal phase, the epileptogenic lesion is usually glucose hypometabolic and presented relatively low  $^{18}\text{F}$ -FDG uptake. Conventionally, the hypometabolic lesion was visually evaluated and compared with the contralateral mirrored brain region. In addition to visually qualitative evaluation, quantitative evaluation of  $^{18}\text{F}$ -FDG uptake in patient's brain could be achieved by comparing with the  $^{18}\text{F}$ -FDG uptake in a group of healthy subjects. Different algorithms for brain PET image reconstruction might result in different image quality and influence the epileptogenic lesion detection. In this study, we compared the difference between  $^{18}\text{F}$ -FDG brain PET from two reconstruction algorithms- Bayesian penalized likelihood (BPL) and Ordered Subset Expectation Maximization (OSEM).

**Methods:** Seven patients with epilepsy who received  $^{18}\text{F}$ -FDG brain PET were included. The scanner was GE Healthcare MI DR PET/CT. PET acquisition started 30-60 minutes after  $^{18}\text{F}$ -FDG injection. Every patient's image was reconstructed by OSEM and BPL ( $\beta$ -value: 400), respectively. The  $^{18}\text{F}$ -FDG uptake ratio in different brain regions was compared to that in the corresponding regions from normal subjects (the data of normal subjects were built in the PET scanner suit), in which Z-score was calculated. For every brain region, we compared the difference of Z-score between PET reconstructed by OSEM and BPL.

**Results:** There were 26 brain regions for comparison. In bilateral lateral prefrontal, right sensorimotor, left precuneus, bilateral parietal, bilateral lateral occipital, bilateral primary visual cortex and bilateral lateral temporal regions, the Z-score of PET reconstructed with OSEM was less than that of PET reconstructed with BPL. In bilateral mesial temporal regions and cerebellum, the Z-score of PET reconstructed with BPL was less than that of PET reconstructed with OSEM.

**Conclusions:** Brain PET reconstruction by different algorithms might result in different image presentation and quantitative value, in which the influence of image interpretation and diagnosis needs further study evaluation.

PB-007

## Image Quality of Bone Scintigraphy in Semi-conductor SPECT Maintained with Half Scanning Time

Yu-Tzu Chang, Chun-Che Lo

*Department of nuclear medicine, Chung-Shan Medicine University Hospital, Taichung, Taiwan*

**Introduction:** In this study, we aim to show planar Bone scintigraphy in semi-conductor SPECT with half scanning time also remain diagnostic value.

**Methods:** Thirty patients was enrolled in this study, they were injected 20-25 mCi  $^{99m}\text{Tc}$ -MDP. The total body conventional bone scintigraphy protocol were 100 seconds per bed (step and shoot mode) with symmetric energy window of 140 keV  $\pm$  7.5%, and all list mode data were all collected. Sequentially, planar images with half scanning time (50 seconds) were reconstructed. Both readers blinded compared the two image sets and give 5-grade scores (ranging from 1 = conventional better to 5 = half scanning time better). A p-value < 0.05 was statistically significant.

**Results:** There was no significant difference between both planar images sets. Two readers scores were  $2.4 \pm 0.8$  and  $2.8 \pm 1.6$  ( $p > 0.05$ ).

**Conclusions:** Our result shows that if we reduce the scanning time, the diagnostic values were not loss. Moreover, in the future, if we reduce the  $^{99m}\text{Tc}$ -MDP dose but standard protocol used, this data shows that kept diagnostic values.

PB-008

## 核醫骨骼掃描骶髂關節 SUV 定量分析一致性評估

龔瑞英<sup>1,2</sup> 許峻豪<sup>2</sup> 林秣蓁<sup>2,3</sup> 林宜瀟<sup>1,2</sup> 鄭凱元<sup>2</sup> 蔡世傳<sup>1,2\*</sup> 張振榮<sup>2\*</sup>

<sup>1</sup> 臺中榮民總醫院核子醫學科

<sup>2</sup> 中臺科技大學醫學影像暨放射科學系

<sup>3</sup> 東元醫療社團法人東元綜合醫院放射科

**背景介紹：**近幾年新型單光子斷層掃描 / 斷層掃描 (SPECT/CT) 多已提供標準攝取值 (Standard Uptake Value; SUV) 計算功能，國內外相關定量化數據陸續發表，為穩定分析模式及數據分析，本研究嘗試建立不同分析模式，並探討不同分析模式之觀察者內部及外部一致性。

**方法：**使用單光子斷層掃描 / 斷層掃描儀 (Discover NM/CT 670 Pro, GE Healthcare, Waukehsa, WI, USA) 收取 30 位正常受試者 (20 位男性，10 位女性，年齡  $49.17 \pm 8.45$  歲) 骨盆 SPECT/CT 影像，以 Q. Matrix 軟體進行影像 SUV 分析，使用冠狀法以及橫切法針對骶髂關節部位進行手動圈選以計算其最大 SUV 數值 (SUV<sub>max</sub>)。其中冠狀法取用骨盆冠狀切面，於骶髂關節中線進行繪製感興趣區 (ROI)，橫切法則取用骨盆橫切面，於骶髂關節中線進行繪製 ROI。本研究由兩位觀察者進行影像分析，資深觀察者已執行 SUV 分析兩年，資淺觀察者從未執行過 SUV 分析，每種模式圈選兩次，每次分析至少間隔一週以上，所有分析數據以組內相關係數 (Intraclass Correlation Coefficient, ICC) 評估相同觀者之再現性 (Intra-observer reproducibility) 和不同觀察者之間之再現性 (Inter-observer reproducibility)。(IRB 編號 TCVGCRC-1081122010)

**結果：**不論使用冠狀法或是橫切法，資深觀察者與資淺觀察者在完整訓練後，分析結果皆顯現出良好、具顯著意義的一致性。資深觀察者使用冠狀法分析之 SUV<sub>max</sub> 為  $1.720 \pm 0.435$ ，一致性為 0.982，使用橫切法分析之 SUV<sub>max</sub> 為  $1.605 \pm 0.385$ ，ICC 為 0.997；資淺觀察者使用冠狀法分析之 SUV<sub>max</sub> 為  $1.704 \pm 0.426$ ，ICC 為 0.969，使用橫切法分析之 SUV<sub>max</sub> 為  $1.566 \pm 0.326$ ，ICC 為 0.999；不同觀察者使用冠狀法分析之 ICC 為 0.976，不同觀察者使用橫切法分析之 ICC 為 0.984。

**結論：**本研究完成骶髂骨關節 SUV 定量方法之內部一致性及外部一致性分析，不論使用何種分析方法，資深觀察者與資淺觀察者在完整訓練後，皆有良好一致性。

PB-009

## 製造符合國際標準 PICs/GMP 品質的 <sup>177</sup>Lu-PSMA I&T 產品及其有效性動物實驗

高志浩<sup>1</sup> 黃弘杰<sup>2</sup> 朱培君<sup>2</sup> 陳繼光<sup>2</sup> 黃永睿<sup>3</sup> 陳亮丞<sup>3</sup> 陳明偉<sup>3</sup>

<sup>1</sup> 美國南加州大學醫學院

<sup>2</sup> 士宣生技股份有限公司

<sup>3</sup> 核能研究所

**背景介紹：**以符合國際藥品製造最高標準 PICs/GMP 規範完成製造攝護腺癌治療性核藥 <sup>177</sup>Lu-PSMA I&T (本產品)，並以動物腫瘤模式實驗證明其有效性符合已發表論文之同等效果。

**方法：**本產品于士宣生技公司的 PICs/GMP 核藥廠進行連續三批次製造，所使用的主要原料於進貨後先經過獨立檢驗公司抽樣檢驗合格，操作車間環境監控及其他使用物料的微生物檢驗合格，產品放射合成步驟和品質分析系參考已發表文獻。製造所使用的主要成分含量：PSMA I&T 前驅物 250 微克、<sup>177</sup>LuCl<sub>3</sub> 46-232 毫居禮。所得產品注射至皮下 LNCaP 攝護腺腫瘤免疫缺陷小鼠，進行 SPECT/CT 生物體造影以及療效追蹤試驗，分析 48 小時內產品在腫瘤及其他器官的蓄積情形，並觀察 4 周內腫瘤大小及動物存活，並與對照組比較。

**結果：**產品製造：PICs/GMP 規範對於核藥製造的要求極高，尤其是對於無菌操作環境、原物料控管檢驗、製造過程的風險等都需要對特定產品有獨特的做法。本公司連續三批次製造穩定取得合格產品，產品放射化學產率為  $93.1 \pm 0.6\%$ ，放射化學純度為  $98.7 \pm 0.6\%$ ，其他檢驗項目都符合品質標準，起始的 <sup>177</sup>Lu 放射活度的大小並無影響產品產率及品質。

**動物實驗：**腫瘤蓄積量在給藥後 4 小時最高 ( $4.9 \pm 1.7\%ID/g$ , N = 3)，給藥後 48 小時則仍有  $2.2 \pm 0.9\%ID/g$ 。腫瘤和肌肉的比值在 1 小時為  $14.8 \pm 7.5$ ，最高點則在 48 小時 ( $176.0 \pm 89.9$ )。治療組 (N = 5) 腫瘤出現明顯的初步縮小，對照組 (N = 5) 腫瘤則持續變大；治療組的 4 周存活率為 8 成，對照組則是 4 成。

**結論：**士宣生技公司為 PICs/GMP 合格的核藥製造廠，其生產的 <sup>177</sup>Lu-PSMA I&T 符合最高製造品質標準並在攝護腺腫瘤動物實驗中呈現明顯療效，符合文獻紀載結論。

PB-010

## Radiomic Analysis of NPC for Treatment, Prognosis Correlation, and Prediction

Chia Ni Lee<sup>1,3</sup>, Yuan Yuan Chen<sup>1</sup>, Jui Yin Kung<sup>2</sup>,  
Shih-Chuan Tsai<sup>2</sup>, Jyh-Cheng Chen<sup>1</sup>

<sup>1</sup>*Department of Biomedical Imaging and Radiological Sciences, National Yang Ming Chiao Tung University, Taipei Taiwan*

<sup>2</sup>*Department of Nuclear Medicine, Taichung Veterans General Hospital, Taiwan*

<sup>3</sup>*Philips Health System, Taiwan*

**Introduction:** The incidence of nasopharyngeal carcinoma in men in Taiwan is about 8.8 per 100,000. The patient undergoes clinical examinations in the ENT department, including blood examinations, and the use of nasopharyngoscopy biopsy, with imaging examinations such as computed tomography (CT), magnetic resonance imaging (MRI), and positron emission tomography/computed tomography (PET/CT) to assist in diagnosis. Nasopharyngeal carcinoma cannot be treated with surgery due to its special location. Radiotherapy or chemotherapy must be used to achieve the best therapeutic effect, reduce the chance of metastasis, and prolong the survival of patients. This study continues the collection of PET images of NPC patients from the previous year, and conducts radiomic analysis, to combine pathology, treatment methods, metastasis and survival rates, and hope to provide more than traditional SUVs (standard uptake value), MTV (metabolic tumor volume), and TLG (total lesion glycolysis) data analysis can do.

**Methods:** We collected the NPC patients who underwent the PET/CT examination during 99.01.01 to 109.12.31, with baseline (pre-treatment), post-treatment (after radiotherapy or radiotherapy combined with chemotherapy) and follow up (finished treatment). Those patients were examined using traditional PET/CT protocol. The preparation of the patients should be fasting at least 6 hours, injected FDG using unidose around 10 mCi, and did the imaging collection. The CT images were reconstructed using FBP, and the PET images were reconstructed using OSEM.

**Results:** Compared the radiomic feature with SUV, the radiomic features were showed with high relationship in shape, flatness and first order. These results might be due to the original tumor size of NPC, so that radiomic features showed high correlation with tumor morphology. But high order radiomic features did not have good results in this study.

**Conclusions:** Using radiomic features selection in PET images to add the benefit for prediction prognosis in the different diseases becomes popular in recently years and also can increase the clinical value, including staging or improvement of the treatment process. In our future work, we would try to create the prediction model for nasopharyngeal carcinoma and do the validation in our clinical patients.

PB-011

## The Study of Analysis of the Precursor of Lu-177-AB-56 by Mass Spectrometry

Po-Chih Chang, Shiou-Shiow Farn

*Isotope Application Division, Institute of Nuclear Energy Research, Tao-Yuan, Taiwan*

**Introduction:** AB-56 is one of the inhibitors targeting prostate-specific membrane antigen (PSMA) that overexpresses on the surface all prostate cancers. AB-56 was labeled with radiometal Lu-177 here for targeted radionuclide therapies and imaging of prostate carcinoma. The study aims to apply HPLC coupled with mass spectrometry to analyze AB-56 and metal-labeled AB-56.

**Method:** HPLC-ESI-MS was conducted on an Agilent 1100 HPLC system interfaced with a Sciex 4000 QTRAP triple-quadrupole mass spectrometer. AB-56 was monitored in positive and negative ionization mode; The metal-labeled AB-56 was monitored in negative ionization mode.

**Results:** The MS1 spectra revealed the abundant double-charged signal and the single-charged signal of AB-56. The MS2 spectra were high characteristic for compound identification when the CID energy was 25. The fragmentation signal at  $m/z$  320 comprises the urea-based binding motif that involves specific binding to PSMA (prostate-specific membrane antigen). An unknown compound with a mass difference of +14 Da compared with AB-56 was noted. The fragmentation signal of the urea-based binding motif at  $m/z$  334 also has a mass difference of +14 Da compared with AB-56. These spectra estimate that the unknown compound and AB-56 have a similar structure and a mass difference of 14 Da was assigned in the urea-based binding motif. Lu-175-AB-56 was also analyzed to confirm the formation of metal-labeled AB-56 products.

**Conclusions:** The method is capable of identification of AB-56 and the radiometal labeled product Lu-177-AB-56. An unknown compound was identified that is similar to AB-56 in structure and its interference should be noted in the evaluation of targeted radionuclide therapy with prostate cancer.

PB-012

## Investigation of a Newly Developed Bifunctional PROTAC Molecule on Human Prostate Cancer Therapy by SPECT/CT Imaging

Mao-Chi Weng<sup>1</sup>, Kai-Hung Cheng<sup>1</sup>, Yu-Chin Lin<sup>2</sup>, Chiu-Lien Hung<sup>2</sup>, Chang Ya-Jane<sup>1</sup>,  
Chung-Li Ho<sup>1</sup>, Lin Min-Xuan<sup>1</sup>, Lin Yun-Sheng<sup>1</sup>, Wei-Chuan Hsu<sup>1</sup>,  
Shih-Min Wang<sup>1</sup>, Shiou-Shiow Farn<sup>1</sup>

<sup>1</sup>Institute of Nuclear Energy Research, Taoyuan, Taiwan

<sup>2</sup>Preclinical Drug Discovery Technology Department, Industrial Technology Research Institute, Hsinchu, Taiwan

**Introduction:** Proteolysis-targeting chimera (PROTAC) has been reported to be a useful technology for targeted protein degradation in cancer therapy. In this research, a bifunctional PROTAC molecule, protacAr, was newly designed and subjected to prostate cancer therapy; after it was successfully radiolabeled, we have further investigated the possible advantages *in vitro* and *in vivo* by preclinical molecular imaging on prostate tumor-bearing mice.

**Materials and Methods:** The protacAr was provided from Industrial Technology Research Institute. After it was iodinated with Iodine-123, Iodine-125 and Iodine-131 and purification by C-18 cartridges, the radiochemical purity (R.C.P.) was analyzed by a radio-TLC system; the stability of <sup>125</sup>I-protacAr was also evaluated for 6 d. After <sup>131</sup>I-protacAr were added to LNCap cells for 2 h, the *in vitro* cellular uptake efficiency was calculated. CWR22RV1 cells were subcutaneously inoculated on SCID mice. After intravenous (i.v.) injection of <sup>123</sup>I-protacAr, the prostate tumor-bearing mice were anesthetized and imaged at 6 and 24 h by SPECT/CT, respectively; mice were sacrificed and organs/tissues were then analyzed after bio-distribution evaluation.

**Results:** The R.C.P. of <sup>123</sup>I-protacAr, <sup>125</sup>I-protacAr and <sup>131</sup>I-protacAr were all determined > 90% by radio-TLC, respectively. The stability of <sup>125</sup>I-protacAr evaluated as > 80% within 6 d. The cellular uptake efficiency in LNCap cells showed higher uptake than block and control groups at 2 h. The protacAr products were then dissolved with DMSO and Cremophor EL for injection. SPECT/CT images showed there were high uptake of <sup>123</sup>I-protacAr in livers, intestines and CWR22RV1 tumors at 6 h; at 24 h, it revealed clearance in tumors. In results of bio-distribution test at 24 h, we found high activities in blood and livers; the tumor-to-muscle count ratio was 1.925 and tumor-to-brain ratio was 12.506.

**Conclusions:** In our research, the radiolabeled bifunctional PROTAC molecule, \*I-protacAr, was successfully developed; <sup>123</sup>I-protacAr also showed specific characteristics in *in vivo* SPECT/CT evaluation on human prostate tumor-bearing model. We suggested that protacAr for further research and it may also provide innovative information for development of treatment strategies of prostate cancer in the future in Taiwan.

PB-013

## Radiopharmaceutical Stability Testing of [<sup>18</sup>F]PSMA-1007 Injection Manufactured by the PET Center of Taipei Veterans General Hospital

Shih-Pei Chen<sup>1,2</sup>, Chi-Wei Chang<sup>1,2</sup>, Wen-Yi Chang<sup>1,2</sup>, Chun-Tse Hung<sup>1,2</sup>,  
Geng-Ying Li<sup>1,2</sup>, Chih-Yung Chang<sup>1,2</sup>, Nan-Jing Peng<sup>1,2</sup>

<sup>1</sup>Department of Nuclear Medicine, Taipei Veterans General Hospital, Taipei, Taiwan

<sup>2</sup>National PET/Cyclotron Center of Taipei Veterans General Hospital, Taipei, Taiwan

**Introduction:** Prostate specific membrane antigen (PSMA) was a transmembrane protein observed by virtually all prostate cancers. [<sup>18</sup>F]PSMA-1007 was a radio pharmaceutical for showing the distribution of PSMA by positron emission tomography (PET) imaging. [<sup>18</sup>F]PSMA-1007 injection would not be used until all quality control (QC) tests had passed excepted for sterility test. It should be promised that the quality of [<sup>18</sup>F]PSMA-1007 would keep stable until finishing the injection of the last patient.

**Methods:** QC tests of [<sup>18</sup>F]PSMA-1007 and their acceptance criteria were compliant with European Pharmacopoeia (Ph. Eur.) Supplement (10.5) standards such as appearance, radio nuclidic purity, half-life, radiochemical purity, chemical impurity, pH, ethanol concentration, residual solvent, bacterial endotoxins, filter integrity, and sterility. They were accomplished by visual, multi-channel analyzer, dose calibrator, high performance liquid chromatography (HPLC), thin layer chromatography (TLC), pH paper, gas chromatography, recombinant Factor C assay, bubble point test, and medium. All QC items excepted for sterility test would start at the end of synthesis (EOS). Appearance, radiochemical purity, pH, and chemical impurity would be checked again for stable each hour after EOS, last for 8 hours.

**Results:** It had been verified that [<sup>18</sup>F]PSMA-1007 injection manufactured by the PET Center of Taipei Veterans General Hospital would pass all QC items excepted for sterility test, and keep both stable and available in 8 hours after EOS.

**Conclusions:** The cGMP-compliant production and QC of [<sup>18</sup>F]PSMA-1007 injection had been established in Taipei Veterans General Hospital. Patients with prostate cancer would have a new choice for diagnosis here.



PB-014

## Synthesis and Biological Evaluation of Radiofluorinated Fibroblast Associated Protein Inhibitors as Novel PET Imaging Probes

Pei-Wen Wu, Wei-Min Zheng, Chuan-Lin Chen

*Department of Biomedical Imaging and Radiological Sciences of National Yang Ming Chiao Tung University, Taipei, Taiwan*

**Introduction:** Fibroblast activation protein (fibroblast-associated protein; FAP) is abundantly expressed on cancer associated fibroblast. In this study, we designed and synthesized novel radioactive fluorine-labeled probes based on the structure of fibroblast associated protein inhibitor (FAPI). Using genetically engineered FAP expression cell line to perform radiopharmaceutical experiments to evaluate the feasibility of fluorine-labeled probe.

**Methods:** New type of radioactive fluorine-labeled positron contrast agents were synthesized, including [<sup>18</sup>F]-FE-FAPI and authentic compounds F-FE-FAPI. After purification and drug quality control, cellular uptake of this drug was conducted. Nude mice bearing FAP-GFP<sup>+</sup>-HT-1080 in the right flank and wild type-HT-1080 cells on the left flank were enrolled for animal studies. The biodistribution study and microPET imaging of [<sup>18</sup>F]-FE-FAPI was performed in animals bearing both FAP (+) and FAP (-) tumors.

**Results:** [<sup>18</sup>F]-FE-FAPI was synthesized with a  $42 \pm 8\%$  radiochemical conversion rate and a high radiochemical purity of  $> 95\%$ . In FAP-GFP<sup>+</sup>-HT-1080 cells, [<sup>18</sup>F]-FE-FAPI showed high specific uptake. PET imaging at 2 hours demonstrated that the ratio of ROI value in two cell lines (FAP-GFP<sup>+</sup>-HT-1080 and wild type-HT-1080) of [<sup>18</sup>F]-FE-FAPI was  $2.25 \pm 0.69$ . The results of the competition experiment in animal also showed high specificity.

**Conclusions:** This study successfully developed new fluorine-labeled FAP inhibitor [<sup>18</sup>F]-FE-FAPI which has high specificity and in vitro radiochemical stability. Fluorine-18-labeled FAP inhibitor will be a potential candidate for PET imaging and be more suitable for translation to the clinic application with the longer physical half life and imaging properties. Additionally, it can also be applied to FAP-related disease such as myocardial infarction (MI), or recurrent inflammation-related diseases.

PB-015

## 因應 COVID-19 疫情之簡易式電子排程系統

張志維 龔瑞英 陳耀文 蔡世傳\*

臺中榮民總醫院核子醫學科

**背景介紹：**許多醫院核醫科執行檢查時使用紙本檢查單傳遞。今年五月中台灣 COVID-19 疫情爆發，衝擊日常醫療工作型態，根據 IAEA 公布之核醫指引建議，因應 COVID-19 疫情，單位應進行分艙分流，調整人員及檢查流程以避免工作人員接觸。為達到有效疫情控制，減少人員接觸頻率，應避免使用紙本檢查單，改採電子排程系統，但完整排程系統建置耗時費力，且礙於疫情，醫院進行人員管制，廠商無法順利建置。本研究探討如何使用現有電腦系統，以低成本方式快速建置簡易式電子排程系統。

**方法：**分析探討病患報到至報告發出階段，各環節使用排程及紙本檢查單，以及人員接觸之狀態，進行簡易式電子排程系統建置。為達到快速無紙化系統建置，第一階段使用“EXCEL 表單共享”，建置後執行一周觀察使用情況，並依照回饋進行即時滾動式調整，第二階段使用“ACCESS 資料庫”進行完整資料庫建置。

**結果：**“EXCEL 表單共享”建置容易，執行一周後，初步可完全取代紙本表單。原記載於檢查單之資訊可即時記錄於電子系統中並自動儲存，各檢查站可即時取得並輸入資訊。唯當病患資訊於各站傳遞時，偶需搭配使用電話進行額外溝通。另外，電腦當機時，需提撥人力進行線上調整。“ACCESS 資料庫”建置較複雜，建置時須於各欄位進行重複確認，需耗費較多人力及時間進行建置，建置完成後使用較為便利。

**結論：**完整電子排程系統建置耗時費力。疫情期間，緊急建置之簡易式電子排程系統可有效滿足大部分使用需求。唯其為簡易版本，各步驟串聯有時需藉由電話訊息傳達，需視臨床使用狀況再調整。但採用這項緊急建置之簡易式“EXCEL 表單共享”系統能達到避免因為使用紙本檢查單造成工作人員接觸的機會。

PB-016

## 運用 Intego 自動注射系統於 正子藥物實驗室分裝流程之效益評估與經驗分享

簡御庭 溫湘萍 邱晉宏 郭維華

國立台灣大學醫學院附設醫院核子醫學部

**背景介紹：**因應核子醫學正子檢查人數逐年增加，本院核子醫學部正子製藥實驗室每日所需產出正子檢查藥劑也日漸增加。在 2020 年 1 月之前本實驗室 18F-FDG 藥劑皆為人工以單次單支藥劑以半自動分裝機的方式產出。為了改善正子製藥實驗室在 18F-FDG 藥劑產出時的分裝流程與降低核醫工作人員的輻射暴露劑量，於 2020 年 2 月啓用一台 Intego 自動注射系統 (MEDRAD® Intego PET Infusion System)，以本實驗室為例，作為經驗分享。

**方法：**為了比較使用 Intego 自動注射系統前後之分裝流程差異，本實驗室依據每位放射化學師與藥師之分裝經驗不同紀錄每次人工分裝藥劑所需時間與調查在分裝藥劑時可能發生的意外事件，總體評估完成臨床所需的 18F-FDG 藥劑的所需時間與人力配置。另外，依據國際放射防護委員會 (ICRP) 建議，輻射作業應根據合理抑低 (ALARA) 之輻射防護原則進行，因使用 Intego 自動注射系統需將單日臨床 18F-FDG 藥劑全數劑量一次性取出並安裝到機器內與以往單支單次人工分裝所需劑量不同，故也會以校正完成的蓋格計數器持續監測使用 Intego 自動注射系統分裝流程中所參與的工作人員所收到的輻射暴露劑量率作為之後調整人員配置與最佳化分裝流程的參考依據。

**結果：**使用 Intego 自動注射系統前每個工作人員平均人工分裝單支藥劑時間為 5 分鐘，測量距離 1 公尺之輻射劑量率為 0.4  $\mu\text{Sv/hr}$ ，運送藥物分為 4 批次，每批次耗時 2 分鐘，運送藥物單趟以 5 支 10 mCi 針劑測量距離 1 公尺之輻射劑量率為 8.2  $\mu\text{Sv/hr}$ ，以本部單日平均 18F-FDG 檢查人次為 20 人計算，共需耗時 108 分鐘。而使用 Intego 自動注射系統為人員分裝 1 瓶 18F-FDG 藥劑耗時 7 分鐘，測量距離 1 公尺之輻射劑量率為 0.5  $\mu\text{Sv/hr}$ ，放入 1 瓶 18F-FDG 藥劑安裝完成耗時 1 分鐘，測量距離 1 公尺之輻射劑量率為 50  $\mu\text{Sv/hr}$ ，設定系統完成推送至存放區耗時 10 分鐘，測量距離 1 公尺之輻射劑量率為 0.4  $\mu\text{Sv/hr}$ ，共需耗時 18 分鐘。依測量結果計算未使用 Intego 自動注射系統人員暴露劑量為 1.763  $\mu\text{Sv}$ ，使用 Intego 自動注射系統人員暴露劑量為 0.955  $\mu\text{Sv}$ 。

**結論：**依據本實驗室的經驗，使用 Intego 自動注射系統不僅可以縮短 18F-FDG 藥劑分裝時間亦能降低人員輻射暴露劑量，另外使用該系統儀器可降低人工分裝藥物的意外發生機率，對藥物產出的品質穩定性有一定程度上的提升。

PB-017

## 簡介美國 USP 825 法規 與台灣放射性藥品調劑法規現況探討

張文議 彭南靖

臺北榮民總醫院核子醫學部

**背景介紹：**美國於 2020 年 12 月 1 日公告了 USP<825>，其為放射性藥品調劑(製)之專章，其歷史沿革為美國於 2004 年公告之 USP<797> 無菌製劑中將放射性藥品調劑(製)歸類於無菌調劑(製)的一種，但同屬放射性藥品之正子藥物調劑因其與藥品製造較為類似，從而另設 USP<823> 專章給予規範。美國 FDA 從 2015 年至 2020 年經過多次討論會議，將放射性藥品調劑(製)由 USP<797> 移出，另設 USP<825> 專章加以規範，其用意並非指放射性藥品調劑(製)不屬於無菌調劑(製)，而是 USP<797> 中對於輻射防護之描述太少，因而設立 USP<825> 使得更適用於放射性藥品調劑(製)。簡言之美國現行狀況為正子藥物調劑(製)屬 USP<823>，而非正子藥物調劑(製)則屬 USP<825>。

台灣對於放射性藥品之正式法規僅出現於行政院衛生署於民國 74 年公告〔核醫藥局管理要點〕，該要點所稱核醫藥局，係指從事醫用放射性藥品服務，包括配方、調劑、標示、儲存、運輸等項目之藥局，但此法規至今未有更新，難以符合現今國際趨勢。

**討論：**國內與藥品調劑相關的法規為 1995 年公告之〔優良藥品調劑作業規範〕，其於 2004 年變更為〔藥品優良調劑作業準則〕，但條文中未有針對放射性藥品調劑(製)之相關描述與規定。反觀在正子藥物調劑(製)在 2003 年即依據美國正子藥物之規範訂定了〔斷層掃描用正子放射同位素調製作業要點〕，且近年來不斷更新，2021 年更依據 PIC/S GMP 修訂了〔斷層掃描用正子放射同位素優良條製作業準則〕將於 2022 年執行。台灣衛生福利部食品藥物管理署於 2021 年八月公告了〔藥品優良調劑作業準則〕修正草案，其中包含了首次將放射性藥品調劑(製)納入描述與管理，但就其內容未有無菌調劑(製)放射性藥品之描述也與美國 USP<825> 內容明顯不同，未來衛生主管機關是否會再次修正內容，國內核醫的軟硬體設備與人員又該如何因應未來法規的變化，藉由本次年會整理 USP<825> 內容與國內先進報告與討論。

PB-018

## Effects of Crystal Size on the Imaging Performance Using Two Collimator Series of Siemens Symbia and GE NM/CT 800: A Monte Carlo Study

Sin-Di Lee<sup>1</sup>, Hsin-Hon Lin<sup>2,3</sup>, Nan-Jing Peng<sup>4</sup>

<sup>1</sup>Department of Nuclear Medicine, Kaohsiung Veterans General Hospital, Kaohsiung, Taiwan

<sup>2</sup>Department of Medical imaging & Radiological Sciences, Chang Gung University, Taoyuan, Taiwan

<sup>3</sup>Department of Nuclear Medicine, Keelung Chang Gung Memorial Hospital, Taoyuan, Taiwan

<sup>4</sup>Department of Nuclear Medicine, Taipei Veterans General Hospital, Taipei,

Taiwan National Yang-Ming University, Taipei, Taiwan

**Introduction:** The collimator and crystal size are crucial factors for imaging performance and manages the tradeoff between the sensitivity and system resolution. The aim of this study is to evaluate the effect of crystal size on the imaging performance for the two series of collimators from different vendors (Siemens Symbia series and GE NM/CT 800 series) on the basis of the same scintillator detector array.

**Methods:** The simulation model of the gamma camera comprises a removable collimator, a NaI crystal (59.1-cm long, 44.5-cm wide), a 6.5-cm thick back-compartment, a 0.95-cm thick back lead shielding, and a 1.27-cm side shielding. We use two different settings of crystal thickness (3/8-inch and 5/8-inch), and variable models of the collimator, including GE-ELEGP, GE-LEHR, GE-LEHRS, GE-LEHS, GE-LEUHR, GE-Medium, Siemens-LEAP, and Siemens-Medium. A point source is 38.505 cm away from the outer surface of the crystal, in the center of a 30-cm diameter sphere filled with water or air. For each realization,  $2.22 \times 10^8$  particles were simulated. The system sensitivity was obtained. The spatial resolution was obtained as the full width at half maximum (FWHM) along the x-axis and the y-axis.

**Results:** For <sup>99m</sup>Tc imaging, GE-ELEGP collimator among the GE collimators have equivalent system sensitivity with Siemens-LEAP collimator but has a better spatial resolution. For <sup>67</sup>Ga and <sup>131</sup>I imaging, Siemens-Medium collimator provides better sensitivity and inferior resolution compared to GE-Medium collimator. For the use of a thicker crystal, the sensitivity increased by 9.2% for <sup>99m</sup>Tc, 8.9% for <sup>67</sup>Ga, and 35.7% for <sup>131</sup>I, while no significant degradation of spatial resolution was observed.

**Conclusions:** The imaging performance of a gamma camera, including sensitivity and spatial resolution, is strongly determined by the collimator design for the camera. For <sup>131</sup>I imaging, the use of the thicker crystal can significantly increase the sensitivity of a gamma camera without sacrificing system resolution.

PB-019

## Automated Production of [ $^{18}\text{F}$ ]fallypride as a Dopamine D2/3 Receptors Imaging Agent

Ching-Hung Chiu<sup>1</sup>, Wei-Hua Kuo<sup>1</sup>, Hsiang-Ping Wen<sup>1</sup>, Yu-Ning Chang<sup>1</sup>,  
Chyng-Yann Shiue<sup>1,2</sup>, Ruoh-Fang Yen<sup>1,2</sup>

<sup>1</sup>*PET Center, Department of Nuclear Medicine, National Taiwan University Hospital*

<sup>2</sup>*Molecular Imaging Center, National Taiwan University*

**Introduction:** [ $^{18}\text{F}$ ]fallypride is a potent dopamine D2/3 receptors imaging agent and has been widely used in neuroscience. In order to fulfill the demand of this tracer for clinical studies, we have developed a GMP-compliant automated production of this tracer using a GE TRACERlab FX<sub>FN</sub> module and reported herein of our preliminary results.

**Methods:** In this study, [ $^{18}\text{F}$ ]fallypride was fully automatic radiosynthesized with a commercial cassette and synthesizer (GE TRACERlab FX<sub>FN</sub>). Briefly, 400  $\mu\text{L}$  Kryptofix 2.2.2 (K2.2.2) / K<sub>2</sub>CO<sub>3</sub> solution (in H<sub>2</sub>O/MeCN) was eluted into the reaction vessel. After the drying process, the precursor solved in DMSO were added to the reaction vessel for fluorination. When the reaction ended, the mixture was transferred to the semi-preparative HPLC (column: Phenomenex Luna C18 (2), 250 x 10 mm ; mobile phase: MeCN/HCOOHNH<sub>4</sub> (aq, 25 mM) 65:45 v/v; flow rate: 4 mL/min) for purification. Finally, the product was eluted with EtOH solution into the product vial, passed through a sterile Millex-MP 0.22- $\mu\text{m}$  filter and was diluted with 10 mL sterile saline.

**Results:** The fully automated syntheses of [ $^{18}\text{F}$ ]fallypride were successfully validated, resulting in radiochemical yield of  $11 \pm 1\%$  (EOS) within 70 min ( $n = 3$ ). Radiochemical purity and specific activity of each batch were  $\geq 95\%$  and  $44 \pm 27$  GBq/ $\mu\text{mol}$  (EOS,  $n = 3$ ), respectively.

**Conclusions:** [ $^{18}\text{F}$ ]fallypride has been automatically manufactured in the NTUH cleanroom lab for research projects. The manufacture of [ $^{18}\text{F}$ ]fallypride on the GE Tracerlab FXFN consistently fit the defined acceptance criteria. The standard operating procedures and related documentation developed in-house describe all aspects of [ $^{18}\text{F}$ ]fallypride production. Each batch of [ $^{18}\text{F}$ ]fallypride will produce sufficient product activity for clinical demand. The validation process will provide a study support for its the clinical usage at NTUH.

PB-020

## 利用 MATLAB 分析病人接受 NaF-18 之 PET/CT 檢查時的體內動力學定量模式

陳俊吉<sup>1</sup> 潘榕光<sup>2\*</sup>

<sup>1</sup> 中山醫學大學附設醫院核子醫學科

<sup>2</sup> 中臺科技大學醫學影像暨放射科學研究所

**背景介紹：**本研究使用申請經過人體試驗委員會 (IRB) NaF-18 之 PET/CT 檢查健康受試者的核子醫影像，將所收集數據進一步分析健康受試者的體內動力學模式。從自主開發的 MATLAB 程式，其中規定人體分為六個相互關聯的區域，針對每一個健康受試者各別計算出隨時間變化的最佳體內動力學分析結果，進行驗證並與臨床資料證實理論模擬的評估值與實際測量值吻合。

**方法：**按照常規 NaF-18 核子醫學檢查的代謝機制，將體內動力學模式於人體中分為六個主要的部分，分別為體液、骨體，腎臟、其餘器官、肝臟以及排出，每一部分皆有其獨特的生物半衰期。使用 PHILIPS 廠牌的 PET/CT，量測 11 位接受 NaF-18 的健康受試者。於健康受試者的 NaF-18 影像，對腎臟，股骨頭，肝臟，膀胱進行感興趣區 (ROI) 圈選，記錄各部位隨著時間變化之計數值及面積。將數據做進一步的正規化後，帶入體內動力學模式。

**結果：**利用 MATLAB 程式，模擬設定核種於各部位之衰變常數來逐一回推、導出與實際測得數據相近的代謝分佈。而這是項複雜的循環過程，因此各部位衰變常數的設定最好每次的變動為一個參數，經過數次便可知其變化的大小，再來做更多的參數調整。最後再以 AT 值檢定本研究實驗與理論值的一致性，AT 值公式如下：

$$A T = \sqrt{\frac{\sum_{i=1}^n \left[ \frac{Y_i(\text{MATLAB}) - Y_i(\text{Normalize item})}{Y_i(\text{Normalize item})} \right]^2}{N}} \times 100$$

利用 MATLAB 程式軟體做回歸計算，可針對每一個病患各別計算出隨時間變化的最佳體內動力學分析結果，其符合度 (AT) 針對骨頭、腎臟、肝臟平均百分比分別為  $15.0 \pm 3.28$ ； $52.5 \pm 29.4$ ； $52.6 \pm 11.9$ 。

**結論：**藉由 MATLAB 的輔助計算與分析，將可針對此特定核種在人體中所造成的劑量，以及在各個主要器官中的分布作非常精準的定量分析，此種分析也將重新修正通用型體內動力學模式，對骨體模式也能做更精準的修正，以提供後續相關研究的參考。

PB-021

## 實驗室長期使用微量吸管 是否對人體手臂肌肉骨骼造成影響

陳宜伶 蕭莉茹 林秋美 陳素英 古琴鳳  
陳怡如 曾翠芬 劉怡慶 林家揚 張晉銓

高雄醫學大學附設中和紀念醫院核醫部

**目的：**PIPETTE 中文名稱—微量吸管，在一般實驗室是非常基本而且也是最常見，使用度最頻繁的器材。重量輕操作簡易使用手心握住微量吸管，利用姆指按壓做吸、排動作。長期重複性的動作會造成肌腱、腱鞘、韌帶、神經及肌肉的磨損或拉傷。主要想探討職業工作者或研究員在長時間的使用微量吸管，是否會對肩頸、手臂及骨骼肌肉產生影響。

**材料與方法：**研究對象主要為職業工作者或研究室人員有使用微量吸管。受試者均接受問券調查的自我評估。

**結果與結論：**工作時數與肌肉疼痛無關 ( $p = 0.7355$ )，這是我們須要再檢討為甚麼結果會這樣。年齡層與肌肉疼痛有關 ( $p = 0.0103$ )，年齡越大有肌肉疼痛的越增加。服務年資與肌肉疼痛有關 ( $p = 0.0239$ )，這與上面的結果非常一致。年齡層與疼痛程度有關 ( $p = 0.0103$ )，隨著年齡上升疼痛程度也增加。



PB-022

## 預防性除汙減少輻射汙染之功效研究 – 以南部某醫院放射免疫分析組為例 — 以南部某醫院為例

陳素英<sup>1</sup> 卓世傑<sup>2</sup> 陳宜伶<sup>1</sup> 蕭莉茹<sup>1</sup> 林秋美<sup>1</sup> 古琴鳳<sup>1</sup>  
陳怡如<sup>1</sup> 曾翠芬<sup>1</sup> 劉怡慶<sup>1</sup> 林家揚<sup>1</sup> 張晉銓<sup>1</sup>

<sup>1</sup> 高雄醫學大學附設中和紀念醫院核子醫學科

<sup>2</sup> 奇美醫院核子醫學科

### 一、前言：

依據現行法規的規定，使用非密封射源進行作業，必須定期於每週或每次進行汙染偵測。當發現汙染後即必須進行除汙，以降低輻射汙染值並避免汙染擴散。本研究即是以南部某醫院核子醫學部放射免疫分析組為例，探討預防性除汙減少輻射汙染功效之研究。

### 二、方法：

收集 RIA 實驗室 2020 年 1 月至 2021 年 8 月，計 86 週，每週分別對（實驗室一至三及計測室）等四個區域 28 個偵測，以 Packard COBRA-II 儀器偵測汙染數值，共 2408 筆之擦拭偵測數據。偵測值超過 80 CPM 之數據即定義為汙染數值，分別擷取、統計並整理成結果，再據以提出結論。

### 三、結果：

1. 資料顯示自 2020.1.2 至 2021.8.25 止，發生汙染之偵測點共 14 處，其中實驗室三之 7 個偵測點即佔了 10 次汙染紀錄，另 4 次則發生於實驗室二。
2. 實驗室三之 7 個偵測點，發生汙染之偵測點分別為：第 1 點（放置實驗架處）1 次，第 2~4 點（廢水槽周邊）9 次。實驗室二之 5 個偵測點，發生汙染之偵測點分別為：第 1、2 點（Aspirator 操作實驗桌面）4 次。
3. 於 2020 年 7 月開始，依據之前紀錄數據，於易發生汙染之偵測點，經每週進行 2 次預防性除汙後，僅於 2020 年 9 月、11 月及 2021 年 3 月分別出現零星之汙染紀錄。

### 四、結論：

依據 RIA 實驗室之資料顯示：

1. 發生汙染之偵測點集中於實驗室三之（放置實驗架處）1 次，（廢水槽周邊）9 次，實驗室二之（Aspirator 操作實驗桌面）4 次等區域，表示這些區域是較可能發生汙染的地區。
2. 自 2020 年 7 月開始，於易發生汙染之偵測點，每週進行 2 次之預防性除汙後，僅放置實驗架處於 2020 年 9、11 月與 2021 年 3 月再出現零星之汙染紀錄，表示預防性除汙應可有效防止汙染之殘留與擴散。

PB-023

## 建立 F-18 pentixather 合成方法 以作為趨化因子受體 CXCR4 之腫瘤造影劑

詹啓仁<sup>1</sup> 孟凡傑<sup>1</sup> 李銘忻<sup>2</sup> 邱創新<sup>3</sup> 林立凡<sup>1</sup> 薛晴彥<sup>1</sup>

<sup>1</sup> 三軍總醫院正子中心

<sup>2</sup> 核能研究所同位素應用組

<sup>3</sup> 三軍總醫院核子醫學部

**背景：**研究顯示腫瘤的生成、發展、轉移以及不良預後與趨化因子受體 CXCR4 的過量表現相關，因此，利用 Ga-68 pentixafor 正子影像對 CXCR4 進行定量分析在臨床上已獲得高度興趣。F-18 核種相較於 Ga-68 有較好的正子影像解析度，結合 pentixafor 對於 CXCR4 有良好的標靶特性，目前已發展出以 Al<sup>18</sup>F 標誌的類似物 NOTA-pentixather。本研究建立 [<sup>18</sup>F]AlF-NOTA-pentixather 的標誌方法並進行純化、分析。

**方法：**先將從 QMA 沖提下來的 <sup>18</sup>F- 與 AlCl<sub>3</sub> 溶液於室溫下反應 5 分鐘生成 Al<sup>18</sup>F。接著將 NOTA-pentixather 溶液 (50 μg 溶於 50% DMSO 水溶液) 加入前一步驟的 Al<sup>18</sup>F 溶液中，105°C 反應 15 分鐘。反應結束後，以 C18 管柱進行純化，將樣品載入管柱後，先以去離子水沖提管柱，接著以乙醇沖提出最終產物。

**結果：**以高效能液相層析儀進行放射化學純度分析，結果顯示已能得到高純度的 [<sup>18</sup>F]AlF-NOTA-pentixather。

PB-024

## AV-133 系列前驅物與標準品合成及相關標誌反應研究

吳文卿 于鴻文 李青雲 劉秀雯 陳誼芝 徐成芳 丁澤錚 陳威希 張瑜

核能研究所

**背景介紹：**巴金森症為老年人嚴重的中樞神經疾病，由核研所成功研製的商品化產品，Tc-99m-TRODAT-1 多巴胺轉運體造影劑，為臨床診斷巴金森症重要的核醫藥物，並於 104 年成為國內第一個成功技轉的核醫藥物；近年來另一積極發展中的 F-18 正子巴金森症診斷用核醫藥物為 F-18-AV-133，核研所亦規劃開發 F-18-AV-133 類似物，兩者不同的是，F-18-AV-133 之 F-18 標幟於側鏈，核研所新開發之類似物，則是先合成出將硼氧環接上 AV-133 芳香環的標誌前驅物，再將 F-18 標幟於芳香環上，期能研發出更多元 F-18-AV-133 系列物，成為具潛力之新型 F-18 正子巴金森症診斷用核醫藥物。

**方法：**以 9-desmethyl-(+)DTBZ (或稱 (+)-9-OH- $\alpha$ -DTBZ)，即 AV-133 系列物的共同合成起始物，經側鏈丙烷基化、芳香環上氯化，再於鉬金屬催化下，將硼氧環部分連接於 AV-133 之芳香環上，研製此硼氧芳香環 AV-133 類似物，作為標誌前驅物，進行 F-18 標幟實驗。至於標幟實驗部分，首先將 [ $^{18}$ F]F<sup>-</sup> 以負離子交換管柱進行純化，再將標幟前驅物加入含銅的催化劑 Cu (OTf)<sub>2</sub> (py)<sub>4</sub>，活化 [ $^{18}$ F]F<sup>-</sup> 之 KF 共價鍵結於芳香環上取代硼氧環得標幟產物 F-18-AV-133 類似物。

**結果：**首先，由於起始物 9-desmethyl-(+)DTBZ 相當昂貴，每 10 毫克要價七萬元，所以我們利用五個步驟，自行合成 9-desmethyl-(+)DTBZ，現已可製備出每批次公克級產物。再者，為了在未來比較核研所開發之 F-18-AV-133 類似物，與先前已開發之 F-18-AV-133 在標誌效率與不同模式動物實驗的結果，我們利用起始物 9-desmethyl-(+)DTBZ，除了合成硼氧芳香環 AV-133 類似物及非放射性標準品 F-19-AV-133 類似物，亦同時合成 AV-133 及非放射性標準品 F-19-AV-133。最後，兩組標誌前驅物及比對用非放射性標準品，分頭進行各自的標誌實驗，比較標誌效率與放化純度。

**結論：**本研究目的即繼 Tc-99m-TRODAT-1 後，開發新型 F-18 正子巴金森症診斷用核醫藥物 F-18-AV-133 系列物，核研所已可獨立合成並提供昂貴的起始物 9-desmethyl-(+)DTBZ，兩組標誌前驅物與非放射性標準品，應用於在 AV-133 結構的側鏈或芳香環上標誌 F-18，希望有機會能與核醫各界先進討論與合作相關標誌及不同模式動物實驗。

PB-025

## The User Experience of [18F]PSMA-1007 Produced by Multi-Modular and Cassette Synthesizer

Chun-Tse Hung, Geng-Ying Li, Chi-Wei Chang, Shih-Pei Chen,  
Wen-Yi Chang, Nan-Jing Peng

*Department of Nuclear Medicine, National PET/Cyclotron Center, Taipei Veterans General Hospital, Taiwan*

**Introduction:** [18F]PSMA-1007 was a radiotracer combined with the Prostate-Specific Membrane Antigen (PSMA). There had been two types of equipment that can be used for manufacturing [18F]PSMA1007 in our center. By comparing these two synthesizers, we could choose better production procedure for clinic.

**Methods:** [18F] nuclide ( $^{18}\text{O}(p,n)^{18}\text{F}$ ) produced by cyclotron was transferred to the Eckert & Ziegler Multi-Modular-Lab system and the ORA Neptis Mosaic RS cassette system. In the Eckert & Ziegler Multi-Modular-Lab system, PSMA-1007 precursor (1 mg) dissolved in DMSO (1 mL) was added to the [18F]TBAF complex, and heated at 80°C for 10 min. The final product was eluted with 30% ethanol (3 mL) and formulated with normal saline (9 mL). In the ORA Neptis Mosaic RS cassette system, precursor (1.6 mg) dissolved in DMSO (2 mL) was also added to the [18F]TBAF complex but heated at 100°C for 10 min. The final product was eluted with 30% ethanol (5 mL) and diluted with 0.9% saline (15 mL) which containing 100 mg sodium ascorbate.

**Results:** In the multi-modular synthesizer, [18F]PSMA-1007 was produced in 85 min with mean 15.3% EOS yield. In the cassette synthesizer, [18F]PSMA-1007 was produced in 45 min with mean 47.55% EOS yield.

**Conclusions:** Cassette type synthesizer had better EOS yield and shorter reaction time than multi-modular synthesizer. It could offer a stable and convenient way for the production of [18F]PSMA-1007.

PB-026

## 以可信賴專業活動原則為出發 進行放射實習生教學創新評量

謝沁彰 莊穎昌 楊士頤 李世昌

成大醫院影像醫學部核子醫學科

**教案背景：**可信賴專業活動 Entrustable Professional Activities (EPAs) 指學生(員)有足夠的專業核心能力得以被信賴而獨立操作之活動，依據各等級來分級其被信賴程度及其可進行之臨床工作。以此原則設計符合放射實習學生的教學活動，並應用在核醫單光子造影檢查 - 全身骨頭造影。

**教案目的：**可以階層區分放射實習學生學習程度情況，並使實習學生在學習後可達到一致的標準。

**教學及受測對象：**放射實習學生

**評量對象：**臨床醫事放射教師

**評量期間：**110 年

**評量方式：**以日常臨床作業型式規劃五個關卡循序漸進之方式以檢測實習學生學習程度情況。

第一關：使用線上影片課程預先學習全身骨骼造影臨床知識，並透過課後測驗了解實習學生學習前程度。

第二關：使用單光子造影檢查查核表，由臨床教師主動指導帶領實習學生臨床操作，能讓實習學生更明確的了解全身骨骼造影之步驟。

第三關：同樣使用第二關查核表，不同的是由實習學生操作，臨床教師在旁觀看並給予被動指導，使實習學生能了解到自己操作上的缺失及需要注意的問題。

第四關：使用原有的 DOPS 測驗，全程由實習學生獨立完成並以分數區分實習學生之間的臨床應對能力。

第五關：核醫實習結束前進行期末測驗，檢測實習學生對於核醫實習期間學習核醫相關知識之學習結果。

**結論：**將全身骨頭造影分成關卡式學習，能讓實習學生漸入佳境了解檢查的步驟、臨床知識及醫病溝通，利用分級的概念使老師更清楚實習學生的學習情況而能針對問題點給予回饋指導。不論是各學校、各階段程度的實習學生皆能達到相同等級的學習成果亦能於實習學生間分出成績。未來亦能將此教學方式應用於核醫各項檢查、正子造影及放射免疫檢驗或其他臨床專業課程，相信在教學上能得到更好的教學成果。

PB-027

## PET/CT 和 PET/MR 臨床合作 以提高病人服務並減少藥物浪費之臨床經驗分享

鍾紫柔 林立凡 陳穎柔 邱創新

三軍總醫院核子醫學部

**背景介紹：**三軍總醫院正子中心繼於 2014 年 11 月引進 PET/CT 正子電腦斷層複合式掃描儀後，又在 2020 年 1 月完成建置 PET/MR 正子磁振同步掃描整合系統提供病人多方位的服務；有鑑於 PET/CT 的臨床需求日益增多導致等候時間較長，所以我們結合本中心的 PET/CT 與 PET/MR 兩具儀器共同合作，以代檢的方式創造雙贏，核子醫學部能降低病人等候時間而放射診斷部能提高 PET/MR 的臨床經驗。

**方法：**以臨床診斷為食道癌、頭頸癌、甲狀腺癌的病人及放射部及核醫部兩科的主治醫師指定的病人為主要代檢的對象；先執行 PET/MR 及 MRI 檢查，PET/MR 造影完成後，再進行肺部及病灶區 PET/CT (如：食道癌病人，需從 OM LINE 至肝臟上緣)，若病人於 PET/MR 檢查期間，因為幽閉恐懼症及無法配合呼吸控制的病人，則改由 PET/CT 執行全身造影檢查。

**結果：**從 2021 年 1 月到從 2021 年 8 月共有 88 例順利完成檢查，其中有 4 位病人因有幽閉恐懼症及 1 位病人無法配合呼吸調控故無法執行 PET/MR 檢查，轉安排 PET/CT 後均順利完成檢查。

**結論：**結合核子醫學科的 PET/CT 與放射診斷科的 PET/MR 以代檢的方式共同合作，一方面幫助核子醫學部能降低病人等候時間而放射診斷部則能提高 PET/MR 的臨床經驗，除了創造雙贏的合作關係外，還能提高檢查的效率及完成率，提供更好的病人服務品質。

PB-028

## The SwiftScan Technology Using the ACR Phantom

Ing-Jou Chen, En-Shih Chen, Chuang-Hsin Chiu

*Department of Nuclear Medicine, Tri-Service General Hospital, National Defense Medical Center, Taipei, Taiwan*

**Introduction:** The SPECT SwiftScan technology (General Electric, GE) with low energy high resolution and sensitivity (LEHRS) collimator was a novel technology for improve image quality. The aim of this study was to compare the performances of this new technology using Jaszczak ACR phantom.

**Methods:** The cold rod dimensions in ACR phantom were 4.8 mm, 6.4 mm, 7.9 mm, 9.5 mm, 11.1 mm, and 12.7 mm. We used a NM/CT 870 scanner with LEHRS collimator. The planar scan of posterior view was acquired with  $140.5 \text{ keV} \pm 7.5\%$  of photo-peak window width,  $256 \times 256$  matrices, and 500K of total scan counts per second. Clarity 2D processing was applied to five planar blend ratio (0%, 20%, 40%, 60% and 80%). The scan count rate was applied to 500K counts/sec (100%), 375K counts/sec (75%) and 250K counts/sec (75%). The ROI was drawn on cold rod and background for contrast ratio (contrast ratio = count rate of cold spot / count rate of cold spot) calculation.

**Results:** The results showed the contrast ratio of cold spot 12.7 mm and 11.1 mm in five planar blending ratio and three count rate. The contrast ratio of clarity 100% show the higher performance, but the images were overcorrected. The clarity 20% and 40% were optimal for image quality.

**Conclusion:** In our preliminary study showed the clarity blending ratio of 20% and 40%, which were appropriate for clinical use.

PB-029

## The Difference of $^{18}\text{F}$ -FDG Manufacture and Quality Control between ORA Neptis Mosaic RS and Tracer-Lab MXFDG Coincidence Synthesizer

Chun-Tse Hung, Geng-Ying Li, Chi-Wei Chang,  
Shih-Pei Chen, Wen-Yi Chang, Nan-Jing Peng

*Department of Nuclear Medicine, National PET/Cyclotron Center, Veterans General Hospital, Taipei, Taiwan*

**Introduction:** National PET/Cyclotron Center, Veterans General Hospital, Taipei (VTGH) installed a new synthesizer ORA Neptis Mosaic RS and Perform in May 2021 to replace Tracer-Lab MXFDG Coincidence synthesizer for  $^{18}\text{F}$ -FDG synthesis which synthesis and quality control are approval by the US FDA.

$^{18}\text{F}$ -FDG is a widely used PET radiotracer so far.  $^{18}\text{F}$ -FDG is a good indicator of glucose uptake and cell viability, so it is important to clinical PET or commercial activity. Many companies develop the synthesizer and its consumables for  $^{18}\text{F}$ -FDG synthesis as well as the machine of quality control over the last 20 years.

**Methods:** Compare the new ORA Neptis Mosaic RS and Perform synthesizer with Tracer-Lab MXFDG Coincidence synthesizer, either can synthesis  $^{18}\text{F}$ -FDG with better quality. We used the same material to synthesize cassette (Roten), mannose triflate precursor (Huayi), and reagent package (Huayi). Recorded each batch of  $^{18}\text{F}$ -FDG quality control which is followed by the guidance of United States Pharmacopeia (USP) and Taiwan official guideline for the compounding of PET drug products. By Analyze quality control statistics, we aimed to figured out which synthesizer is more powerful.

**Results:** Neptis Mosaic RS and Perform synthesis time are faster than Tracer-Lab MX. Somehow, we should be more careful of the gas leakage when we install  $^{18}\text{F}$ -FDG cassette. We also observed the radiochemical yields and radiochemical purity of the final product  $^{18}\text{F}$ -FDG made by Neptis Mosaic RS are almost the same as which made by Tracer-Lab MX, while the residual solvent especially the residual acetonitrile are higher than Tracer-Lab MX.

**Conclusions:** Although the new synthesizers are faster, still they have some problems to solve that we had contacted the Neptis company to improve the system.



PB-030

## Evaluation of Human Biodosimetry

Tse-Zung Liao<sup>1</sup>, Fang-Yu Ou Yang<sup>1</sup>, Ying-Hsun Chang<sup>1</sup>, Kuan-Yin Chen<sup>1</sup>,  
Kang-Wei Chang<sup>2</sup>, Chih-Hsien Chang<sup>1</sup>, Ruth C. Wilkins<sup>3</sup>, Wan-Chi Lin<sup>1</sup>

<sup>1</sup>Isotope Application Division, Institute of Nuclear Energy Research (INER), Taiwan

<sup>2</sup>Taipei Medical University (TMU), Taiwan

<sup>3</sup>Consumer and Clinical Radiation Protection Bureau, Health Canada, Ottawa, Ontario, Canada

**Introduction:** There were approximately 50,000 radiation-related workers in various fields such as nuclear power plants, industry, hospitals and academic institutions in Taiwan. Once the radiation exposure accident occurred, evaluation the exposure dose of staff members by biodosimetry could be used as the reliable strategy for further medical care accordance. In the current investigation, we had established the biodosimetry technology and set-up the world-class biodosimetry laboratory. From 2012 to 2019, we generated two important issues including: the dose–response curves of dicentric chromosome assay and the database of 25 background samples. We also participated the international competence test organized by Health Canada.

**Methods:** The dicentric chromosome assay of lymphocyte isolated from personnel who were exposure to radiation. According to the well-established standard curve between the dose and the number of dicentric chromosomes, the body acceptance during radiation exposure could be easily estimated.

**Results:** Seven standard curves and their differences had been statistically calibrated in our laboratory. Those seven standard curves had been further merged to generate the binary quadratic equation to present as the local biodosimetry formula (Figure 4). In addition, a total of 28 background samples have been measured in recent years. According to our analysis, 22 dicentric chromosomes had been identified in 21 cells from totally 28,411 cells. The incidence of dicentric occurring is 0.77‰. There was no significantly difference between Taiwan and other countries (1‰).

**Conclusions:** Our laboratory completed the dose–response curves with cobalt-60 radiation exposure and 28 individual cases for background value. Our laboratory participated the international competence test and the results from the test conformed our lab with international standard.

PC-001

## The Relationships of TBS or TBS FRAX with Coronary Artery Calcification in Female Adults

Tzyy-Ling Chuang<sup>1,2</sup>, Yuh-Feng Wang<sup>1,2,3</sup>

<sup>1</sup>Department of Nuclear Medicine, Dalin Tzu Chi Hospital, Buddhist Tzu Chi Medical Foundation, Chiayi, Taiwan

<sup>2</sup>School of Medicine, Tzu Chi University, Hualien, Taiwan

<sup>3</sup>Center of Preventive Medicine, Dalin Tzu Chi Hospital, Buddhist Tzu Chi Medical Foundation, Chiayi, Taiwan

**Introduction:** To examine the association between trabecular bone score (TBS), fracture risk assessment tool (FRAX) scores, TBS-adjusted FRAX (TBS FRAX) and coronary artery calcification (CAC) score in female adults.

**Methods:** The medical records of 116 female adults who underwent both coronary computed tomography and bone mineral density (BMD) studies in a package during their health exams were reviewed at a regional hospital in Southern Taiwan. Data collected included health history, anthropomorphic characteristics, clinical laboratory results, BMD and T-score. TBS values, TBS T-score, TBS Z-score were retrospectively collected using spine DXA files from the database. Univariate and multivariate linear regression analysis were used to assess the association between CAC score and 10-year probability of major osteoporotic fracture (MOF) and hip fracture (HF) determined by FRAX and TBS FRAX.

**Results:** The mean age of the female participants was  $55.8 \pm 8.3$  years, and 24.1% were osteoporosis. Simple linear regression showed TBS and TBS T-score were significantly and inversely correlated with CAC score, but their relationship was attenuated in multiple linear regression. Univariate linear regression analysis also showed that increases in MOF and HF risks, as measured by FRAX and TBS-adjusted FRAX, were significantly and positively associated with CAC score. Multiple linear regression analysis adjusting for potential confounders showed that CAC score remained significantly associated with FRAX and TBS FRAX, including right MOF ( $r = 0.365$ ,  $p = 0.001$  and  $r = 0.350$ ,  $p = 0.002$ ), left MOF ( $r = 0.315$ ,  $p = 0.004$  and  $r = 0.298$ ,  $p = 0.006$ ), right HF ( $r = 0.233$ ,  $p = 0.014$  and  $r = 0.264$ ,  $p = 0.005$ ), and left HF ( $r = 0.204$ ,  $p = 0.027$  and  $r = 0.225$ ,  $p = 0.015$ ).

**Conclusions:** TBS and TBS T-score had no significant association with CAC after adjustment. Increased risks of MOF and HF as determined by FRAX and TBS-adjusted FRAX were significantly and independently associated with CAC score in females.

PC-002

## MUGA 檢查對於乳癌患者口服 Letrozole 造成 LVEF 下降的評估 - 案例報告

王苡安<sup>1,2</sup> 莊紫翎<sup>1,4</sup> 王昱豐<sup>1,3,4</sup> 廖建國<sup>1</sup> 林俊宏<sup>5,6\*</sup>

<sup>1</sup> 佛教慈濟醫療財團法人大林慈濟醫院核子醫學科

<sup>2</sup> 佛教慈濟醫療財團法人大林慈濟醫院護理部

<sup>3</sup> 佛教慈濟醫療財團法人大林慈濟醫院預防醫學中心

<sup>4</sup> 慈濟學校財團法人慈濟大學醫學院醫學系放射線學科

<sup>5</sup> 佛教慈濟醫療財團法人大林慈濟醫院一般外科

<sup>6</sup> 慈濟學校財團法人慈濟大學醫學院醫學系外科學科

**背景：**心臟搏出分率及心室壁活動 (MUGA) 測定檢查可評估左心室射出分率以及心室壁運動情形。此項檢查乃利用放射性同位素標誌紅血球，來觀察左心室收縮，藉由伽馬攝影來擷取影像。Letrozole 抗癌藥 (Femara) 復乳納 2.5 mg/tab 口服化療藥物副作用在心臟有高血壓、胸痛、心絞痛、心肌梗塞等等。本院臨床醫師將此檢查做為乳癌患者口服化療藥物前後心臟功能比較。近期發現此特殊案例，因此整理病人檢查相關資料，提出分享。

**案例：**一位 69 歲女性，有高血壓病史。2020 年 02 月在外院做了乳房切片檢查顯示為惡性。故來院徵求第二意見，本院進行 CT 檢查，結果顯示左側乳房腫塊分期為 cT1N0M0。全身骨骼掃描中，沒有顯示骨骼轉移的情形。因此，於 2020 年 03 月接受了左側全乳切除術並做乳房重建手術，手術前搭配核子醫學科前哨淋巴結檢查進行淋巴摘除。病人執行口服化療藥物前，醫師需要精確了解病患各種心臟功能參數，以掌握病人的臨床過程與藥物治療後的療效，故在治療前 2020 年 4 月安排第一次 MUGA 檢查，檢查後便開始進行口服 Letrozole (Femara) 治療，至今仍持續進行治療，在這其中共 4 次檢查，其中發現 2020 年 4 月 15 日治療前 LVEF 值為 81%，2020 年 7 月 16 日治療第一次 LVEF 值為 81%，2020 年 10 月 12 日治療第二次 LVEF 值為 76%，2021 年 5 月 7 日治療第三次 LVEF 值為 70%。顯示受檢者心臟功能降低 11%。MUGA 測定檢查最重要是可計算 LVEF 值，LVEF 正常為 > 50%。治療後，若 LVEF 比治療前減少 10%，則表示有輕微的心臟毒性。

**結論：**臨床上有賴於核醫 MUGA 測定檢查，讓醫師在口服化療藥前後知道病人心臟的變化，也證實藥物確實有副作用在，也因為這樣使得病患可以得到更好的照顧。

PC-003

## 二聯律 (Bigeminy) 在心肌灌注掃描之心電圖門控影像取像方式

蔡雅茹 楊承領

台北醫學大學附設醫院核子醫學科

**背景介紹：**我們報告一案例為二聯律 (bigeminy) 心律不整，即一個正常竇性心律配上一個心室早期收縮 (Premature Ventricular Contraction, PVC)，在心肌灌注掃描之心電圖門控影像 (ECG-gated imaging) 的取像時，排除 PVC 訊號，僅收取正常收縮的訊號重組左心室收縮影像。

**病例報告：**一名 74 歲女性長期有暈眩問題，為確認是否患有缺血性心臟病而轉介至核子醫學科進行心肌灌注掃描檢查。檢查開始後於 3-5 分鐘內靜脈注射心血管擴張劑 (Persantin)，接著靜脈注射 Tl-201 Chloride (2.0 mCi) 後，使用備有心電圖門控 (8-frame ECG-gated) 的半導體 (CZT) 儀器進行壓力態心臟成像，約 3-4 小時後使用與壓力態相同的成像條件進行休息態的檢查。照影像過程中因病人患有二聯律 (bigeminy) 使得影像訊號收集不易，故而變更心電圖門控影像 (ECG-gated imaging) 的收取範圍，將心室早期收縮 (PVC) 的訊號去除，僅收取正常收縮的訊號重組心電圖門控影像 (圖一)。該病人正常心臟收縮時間約為 460 mSec，PVC 所需時間約在 1000-1400 mSec 之間 (圖二) 且臨床觸診為無脈搏波。心臟掃描結果顯示該病人無明顯心肌缺血或梗塞，且去除 PVC 後的竇性心律無心肌運動異常 (圖三)。

**結論：**心律不整定義指的是心電不正常活動。正常的心電活動應是有節奏的竇性心律放電，但種種原因會造成其它部份的心肌細胞也自行產生放電活動，造成心律不整。心電圖門控影像是以心電圖 RR 間距作為信號，按設定的時間間隔連續採集每個心跳周期心肌灌注的影像，經專用軟體進行圖像處理和斷層重建，就可以獲得左心室在收縮期及舒張期的一系列心肌灌注斷層影像，與心室功能指標和室壁運動等信息。若是遇上心律不整，可能使成像不易。即便成功成像亦有心室功能分析錯誤之疑慮。因此遇到有一定規則的心律不整，如二聯律 (bigeminy)、三聯律 (trigeminy) 等等，可經由心電圖門控 (ECG-gated) 的設定，依心跳速度排除心律不整之波型，僅收取正常收縮的訊號重組影像。

PC-004

## 心臟類澱粉酶沉積症在 <sup>99m</sup>Tc-pyrophosphate 掃描的表現

許文齡 張淑敏 莊雅雯 張晉銓 許玉春 李岱恩

高雄醫學大學附設中和紀念醫院核子醫學部

**背景介紹：**類澱粉酶沉積症 (Amyloidosis) 為異常的蛋白質在細胞外沉積所引起的一種疾病，源自於錯誤摺疊的蛋白質並堆積，心臟類澱粉酶沉積為描述澱粉樣蛋白質異常積累於心臟。未經治療的心臟類澱粉酶沉積會造成病患心臟壁厚度增加，導致體內的積液過多，形成充血性心臟衰竭 (congestive heart failure)，常見症狀包括呼吸急促、腿部腹部腫脹，心臟超音波顯示心臟壁增厚，此外使用含釷造影劑的核磁共振也可用於診斷此疾病。核醫 <sup>99m</sup>Tc-pyrophosphat (<sup>99m</sup>Tc-PYP) 焦磷酸鹽造影原先使用於急性心肌梗塞造影，其機轉可能為急性心肌梗塞後，鈣離子進入病灶血液中獲得 <sup>99m</sup>Tc-PYP 而顯影。使用 <sup>99m</sup>Tc-PYP 量化類澱粉蛋白負荷 (amyloid burden) 自 1980 年代開始持續進行，直到近年來才被證明在區分心臟類澱粉酶沉積症 AL (light-chain) 及 ATTR (transthyretin cardiac amyloidosis) 具有高靈敏度及特異性。

### 案例報告：

案例一：一位 62 歲女性，有乳癌、血脂異常 (dyslipidemia) 病史，此次抱怨近兩年發生過兩次沒有前兆的暈厥伴隨著無力、心悸、胸悶等症狀，心臟超音波顯示左心室向心性肥大 (concentric hypertrophy) 伴隨著異常鬆弛 (relaxation) 而入院近一步接受檢查及治療。心肌梗塞 (myocardial infarct) 造影在給予 <sup>99m</sup>Tc-PYP 三小時後掃描中顯示，心肌攝取增加 (半定量視覺分級 3 級)。

案例二：一位 80 歲男性，有糖尿病 (diabetes mellitus)，慢性腎病 (chronic kidney disease)，心臟衰竭 (heart failure) 及腦血管病變 (cerebrovascular accident) 病史，此次因持續數天的勞累性呼吸困難而入院接受治療，胸部 X 光顯示心臟肥大伴隨肺靜脈鬱血 (pulmonary congestion)。在給予 <sup>99m</sup>Tc-PYP 三小時後影像中顯示，骨頭攝取正常，心肌攝取增加 (半定量視覺分級 3 級)。

**結論：**對於診斷心臟類澱粉酶沉積症目前黃金標準還是以心內膜心肌切片取樣 (endomyocardial biopsy)，結合免疫組織化學染色法 (immunohistochemistry) 或特定質譜法 (mass spectroscopy)。然而此診斷方法必須在專門的醫院中心執行，且不能提供足夠的訊息包含心臟類澱粉酶沉澱的程度或分佈、疾病的進展或對治療的反應，此外，對於相對年長的患者，執行侵入性檢查意願相對低，不利準確診斷。近年來使用 <sup>99m</sup>Tc-PYP 進行心臟類澱粉酶的研究趨於進步，此項檢查能提供臨床更多選擇及足夠的證據、訊息以利診斷。

PC-005

## Effect of CT- based Attenuation Correction on Myocardial Perfusion Imaging in Suspected CAD Patients

Sheng-Kai Chen<sup>1</sup>, Guang-Uei Hung<sup>2</sup><sup>1</sup>Department of Nuclear Medicine, Show Chwan Memorial Hospital, Changhua, Taiwan<sup>2</sup>Department of Nuclear Medicine, Chang Bing Show Chwan Memorial Hospital, Changhua, Taiwan

**Introduction:** Single-photon emission computed tomography combined with computed tomography (SPECT/CT) systems have been widely used in clinical routines of nuclear medicine departments, including myocardial perfusion imaging (MPI) for evaluation coronary artery disease (CAD). One of the major advantages of SPECT/CT for MPI is utilizing its CT images for attenuation correction (CTAC) of SPECT. The purpose of this study is to investigate the effect of CTAC on the calculations of perfusion scores and diagnostic accuracy in patients of suspected CAD.

**Methods:** Sixty-nine patients (36 males, mean age:  $69 \pm 11.8$ ) received both MPI with SPECT/CT (Siemens, Symbia T2) and invasive coronary angiography (CAG) within 6 months were retrospectively enrolled. CT protocols of SPECT/CT used a scan field of 50 cm, rotation time of 1.0s, temporal resolution of 400ms and spiral acquisition mode of  $2 \times 4$  mm. Perfusion scores were automatically generated by commercially available software (QPS, Cedars-Sinai). Comparison of summed stress scores (SSS) before and after CTAC was tested with paired t-test. Diameter stenosis  $\geq 70\%$  in at least one of three major coronary arteries on CAG was considered as the criteria of CAD. Receiver operating characteristic (ROC) curve analysis was used for comparing the accuracy of CAD diagnosis.

**Results:** Global SSS before and after CTAC were  $6.6 \pm 7.1$  and  $6.6 \pm 7.4$ , respectively ( $p = 0.93$ ). Territorial SSS before and after CTAC were  $2.3 \pm 3.4$  and  $2.6 \pm 3.9$  ( $p = 0.11$ ) for LAD,  $3.1 \pm 3.2$  and  $2.7 \pm 2.8$  ( $p = 0.037$ ) for LCX, and  $1.2 \pm 2.8$  and  $1.3 \pm 2.9$  ( $p = 0.33$ ), respectively. ROC analysis showed that the areas under the curve of global SSS before and after CTAC for CAD diagnosis were 0.627 and 0.668, respectively ( $p = 0.323$ ).

**Conclusion:** Our experience showed that CTAC generally did not significantly change the calculation of SSS, except for the territory SSS in LCX significantly decreased after CTAC. There was no significant improvement on the accuracy of CAD diagnosis after CTAC, either.

PC-006

## Persantin 對心肌灌注掃描檢查病人血壓影響之初探 — 以南部某醫院核醫科為例

張虹麗<sup>1</sup> 丁瑞玫<sup>2</sup> 梁育雅<sup>1</sup> 江佳諭<sup>1</sup> 鄭揚霖<sup>1</sup> 顏玉安<sup>1</sup> 李將瑄<sup>1</sup>

<sup>1</sup> 奇美醫療財團法人奇美醫院核子醫學科

<sup>2</sup> 中華醫事科技大學護理系

### 背景介紹：

心肌灌注掃描檢查 (Myocardial Perfusion Imaging, MPI)，是核子醫學科經常施行且主要的檢查之一。該檢查係利用靜脈注射放射性藥物來描繪出休息或壓力狀態下心肌血流的分佈情形，以評估病人的狀況。台灣目前以藥物介入法，形成病人心肌血流呈現壓力狀態最常使用的藥物之一即是 Persantin。由於 Persantin 是利用擴張冠狀動脈血管以增加血流量，因此可能導致檢查病人血壓下降，進而影響病人安全。因此靜脈注射 Persantin 後施行心肌灌注掃描檢查之血壓變化，頗值得探討。本文即以南部某醫院核醫科為例，探討 Persantin 對心肌灌注掃描檢查病人血壓影響之研究。

### 方法：

1. 收集南部某醫院核醫科，自 2021 年 8 月 12 日至 9 月 3 日止，共 120 位接受心肌灌注掃描檢查病人之血壓數據。
2. 以 Welch Allyn 牌 53N00 型電子血壓計，於每位病人靜脈注射 Persantin (劑量為體重 \*0.56) 前與後，分別測量其收縮及舒張血壓值共 4 筆資料並予記錄。
3. 共收集 120 位病人，每人 4 筆資料，合計 480 筆血壓資料。
4. 整理、統計前項數據，以提出結果及結論。

### 結果：

1. 注射 Persantin 前，病人之收縮壓，最高為 209 最低為 86，平均為 135，中位數為 133 mmHg。病人之舒張壓，最高為 111 最低為 47，平均為 77.4，中位數為 78 mmHg。
2. 靜脈注射 Persantin 後，病人之收縮壓，最高為 176 最低為 83，平均為 119.5，中位數為 117 mmHg。病人之舒張壓，最高為 104 最低為 41，平均為 68.6，中位數為 68 mmHg。
3. 注射 Persantin 前病人之收縮壓減注射後之收縮壓，最高為 37 最低為 -19，平均為 15.5，中位數為 14 mmHg。
4. 注射 Persantin 前病人之舒張壓減注射後之舒張壓，最高為 28 最低為 -17，平均為 8.7，中位數為 9 mmHg。
5. 注射 Persantin 後之收縮壓相較注射前之收縮壓，最高下降了 27.8% 最低為 -16.4%，平均下降了 11.3%，中位數則為 10.7%。
6. 注射 Persantin 後之舒張壓相較注射前之舒張壓，最高下降了 35% 最低為 -29.3%，平均下降為 11.3%，中位數則為 10.4%。

**結論：**

本研究發現，南部某醫院核醫科，接受心肌灌注掃描檢查病人：

1. 靜脈注射 Persantin 前之收縮壓、舒張壓相減注射後之收縮壓、舒張壓，收縮壓減收縮壓平均為 15.5 mmHg，中位數 14 mmHg，舒張壓減舒張壓平均為 8.7 mmHg，中位數為 9 mmHg。
2. 靜脈注射 Persantin 後之收縮壓相較注射前之收縮壓平均下降了 11.3%，中位數 10.7%，注射 Persantin 後之舒張壓相較注射前之舒張壓平均則下降了 10.9%，中位數為 10.4%。



PC-007

## eGFR 對 Tc99m-PYP scan H/CL ratio 之影響探討

吳忠順 胡璿 譚鴻遠

高雄榮民總醫院核醫科

**背景介紹：**臨床使用 Tc99m-PYP scan 診斷 Transthyretin Cardiac Amyloidosis，在造影時間方面，中華民國核醫學學會及中華民國心臟學會建議以施打 Tc99m-PYP 後 3 小時進行平面造影及 SPECT (或 SPECT/CT) 為主，另外可加選 1 小時造影，而美國心臟核醫學會 (ASNC) 2019 年的建議則以 1 小時平面造影及 SPECT (或 SPECT/CT) 為主，本研究目的在比較 1 小時及 3 小時平面造影 H/CL ratio 之差異及 eGFR 高低對 H/CL ratio 是否具有影響進行比較探討。

**材料方法：**使用 GE DR-870 搭配 LEHRS 準直儀，受檢者於施打 Tc99m-PYP 20 mCi 後分別於 1 小時及 3 小時進行平面及 SPECT/CT 造影。平面造影收集前後位影像，造影參數為收集 750k counts、放大倍率 1.45、矩陣 256 x 256。SPECT 造影參數收集 360 度影像，共收集 120 張，每張 20 秒。SPECT/CT 的目的為排除心血池放射積聚造成之偽陽性。執行 H/CL ratio 分析時於平面前位像之心臟位置圈選 ROI 後，再使用鏡像 (mirror) 將心臟 ROI (heart ROI) 複製到對側胸部 (contralateral lung)，圈選時避開胸骨，將 heart ROI 與 contralateral lung 之總計數 (total counts) 相除之後得 H/CL ratio。將檢查結果為陽性之受檢者排除之後，以 1 小時與 3 小時之 H/CL ratio 作統計分析比較，並依 eGFR 功能高低分成兩組之後，再進行 H/CL ratio 比較。

**結果：**本研究共收集 53 位受檢者，其中男性佔 60%，女性佔 40%，平均年齡 58.1 歲。1 小時與 3 小時 H/CL ratio 平均比值分別為 1.19 與 1.15，結果顯示 2 者並無差異。將 eGFR 小於 60 之受檢者分為 A 組，eGFR 大於 60 之受檢者分為 B 組，A 組之平均 eGFR 為 35.7，其 1 小時與 3 小時之 H/CL ratio 分別為 1.19 及 1.14，B 組之平均 eGFR 為 88.2，其 1 小時與 3 小時之 H/CL ratio 分別為 1.19 及 1.15。

**結論：**以 Tc99m-PYP scan 診斷 Transthyretin Cardiac Amyloidosis，檢查結果為陰性的受檢者其 1 小時與 3 小時 H/CL ratio 並無差異。eGFR 功能對 1 小時與 3 小時之 H/CL ratio 並無影響，eGFR 低下之受檢者並無明顯心血池積聚 Tc99m-PYP 的現象。但因本研究並非大數據分析，可收集更多數據做進一步驗證。

PC-008

## Evaluation of Coronary Blood flow and Coronary Flow Reserve in Heart Failure Patients by Dynamic SPECT/CT

Yi-Ling Wu<sup>1</sup>, Hung-Pin Chan<sup>2</sup>, Ming-Hui Yang<sup>3</sup>, Hueng-Yuan Shen<sup>2</sup>, Yu-Chang Tyan<sup>1</sup>

<sup>1</sup>Department of Medical Imaging and Radiological Sciences, Kaohsiung Medical University, Kaohsiung, Taiwan

<sup>2</sup>Department of Nuclear Medicine, Kaohsiung Veterans General Hospital, Kaohsiung, Taiwan

<sup>3</sup>Department of Medical Education and Research, Kaohsiung Veterans General Hospital, Kaohsiung, Taiwan

**Introduction:** Heart failure (HF) is a complex clinical syndrome that causes by structural or functional impairment of ventricular filling or decreased ejection fraction (EF) of left ventricle (LV). It causes high mortality and high hospitalization rate of patients. The factor of prognosis in HF patients is unclear. The goal of this study is to evaluate the correlation of coronary blood flow and coronary flow reserve and several cardiac parameters in HF patients.

**Methods:** A total of 23 patients, who were diagnosed non-ischemic or ischemic HF. The parameters were collected and compared that includes N-terminal pro-brain natriuretic peptide (NT proBNP) by blood sample, LVEF by echo and quantitative coronary blood flow data by Dynamic SPECT/CT. It was measured by <sup>99m</sup>Tc-Sestamibi (MIBI) Dynamic SPECT/CT by one day rest/dipyridamole-stress protocol. Statistical analysis was performed with commercially available soft ware (SPSS version 13) and P < 0.05 was considered statistically significant.

**Results:** Mean age of our patients is 56.8 years. Male dominant was noted in this study (male: female, 21:2). Five patients was diagnosed ischemic HF proved by PCI result. Eight patients was noted preserved coronary stress blood flow (SBF) and coronary flow reserve (CFR) on Dynamic SPECT/CT, but coexisted with ejection fraction impairment and elevated NT proBNP level (defined > 450 pg/mL). After three months follow-up, it showed good clinical status with increased EF (P < 0.05) and decreased NT proBNP level (P = 0.05). The negative correlation of follow-up NT proBNP level with follow-up EF revealed significant difference (P < 0.01).

**Conclusions:** We concluded preserved SBF and CFR in HF patients that might yielded restore EF after 3 months follow-up. Coronary blood flow and coronary flow reserve could be one of factor in HF patients' prognosis.

PC-009

## A Novel Method of Best Septal View Acquisition on Equilibrium Radionuclide Angiocardiography

Chien-Ying Lee<sup>1,2</sup>, Chi-Fen Lin<sup>1</sup>, Liang-Chi Wu<sup>1</sup>, Nan-Jing Peng<sup>1,2</sup>, Lien-Hsin Hu<sup>1,2</sup>

<sup>1</sup>Department of Nuclear Medicine, Taipei Veterans General Hospital, Taipei, Taiwan

<sup>2</sup>School of Medicine, National Yang Ming Chiao Tung University, Taiwan

**Introduction:** Equilibrium radionuclide angiocardiography (ERNA) is well established and provides a relatively simple and noninvasive method to assess ventricular function. The left anterior oblique (LAO) view is used to visualize the septum that allows the best separation of the right and left ventricles. However, the optimal angle of best septal view varies among individuals. We aim to evaluate the best septal view via different direction of images before proceeding acquisition.

**Methods:** Thirty-five patients who underwent ERNA studies in our department were included. A 90° non-circular orbit starting from anterior view to left lateral view with 15% windows centered on the 140-KeV photo peaks was used. Images were acquired in a 64 x 64 matrix with a zoom of 1.23, using 30 views at 5 sec per projection in step-and-shoot mode with the patient in the supine position. Then, the best septal views were chosen.

**Results:** All patients were examined smoothly. The mean and standard deviation (SD) of the best septal views among individuals were 41 ± 9, ranged from 21° to 60°. In patients with multiple ERNAs, the difference were 2 ± 2, ranged from 00 to 60.

**Conclusions:** The acquisition angles on ERNA varied among individuals, but similar in the same patients. We believe this novel method of choose the best septal view for ERNA increase the accuracy of ventricular function assessment and improve patient's follow-up.

PC-010

## 以簡易型個人劑量計 評估核醫 Tc-99m MIBI 心肌血流灌注檢查藥物滯留時間

周國堂<sup>1</sup> 潘榕光<sup>2</sup> 謝政道<sup>1,2</sup> 蔡世傳<sup>1,2</sup><sup>1</sup> 臺中榮民總醫院核子醫學科<sup>2</sup> 中臺科技大學醫學影像暨放射科學研究所

**背景介紹：**在冠狀動脈心臟病的診斷中，鎝-99m MIBI 心肌灌注掃描檢查屬於一種例行性且非侵入性的檢查，通常被用來協助區別正常或缺血的心肌狀態。由於鎝-99m MIBI 具有輻射，因此評估接受檢查病人的輻射劑量有其必要性。過去的文獻提供注射鎝-99m MIBI 後頭部、胸部及腳之輻射劑量，但相對於接受較大劑量之腹部並無量測數據可供參考。本研究以個人輻射劑量器量測受檢者注射藥物後之胸部腹部體外劑量，配合病患性別、年齡及體態進行分析，試圖建立該檢查之族群衰減數據資料庫。

**方法：**本次研究收集 66 例接受心臟血流灌注檢查病患數據，注射鎝-99m MIBI (休息態) 30 mCi 後，於 30、60、120、180 分鐘時，使用簡易型個人劑量計 (Hitachi PDM-122-SH, Japan) 量測病患胸部及腹部體表劑量，計算出休息態平均藥物滯留時間，並與病患性別、年齡、BMI 進行統計分析，以求得輻射劑量與其相關性。(本研究通過人體試驗委員會審查，編號 CE21138B)。

**結果：**透過劑量量測估算出平均藥物滯留時間，經過公式計算後可得到病人劑量代謝時間，經過統計檢定 t-test 得到性別、年齡、BMI 與平均藥物滯留時間之關係。胸部滯留時間：男性為 216.7 ± 82 分鐘，女性為 201.3 ± 60 分鐘；年齡 ≤ 64 為 203.4 ± 69 分鐘，年齡 > 65 為 215.0 ± 77 分鐘；BMI ≤ 24 為 209.7 ± 74 分鐘，BMI > 25 為 208.9 ± 73 分鐘。腹部滯留時間：男性為 249.9 ± 109 分鐘，女性腹部滯留時間為 260.5 ± 112 分鐘；年齡 ≤ 64 為 232.8 ± 104 分鐘，年齡 > 65 為 276.1 ± 112 分鐘；BMI ≤ 24 為 253.9 ± 108 分鐘，BMI > 25 為 255.5 ± 113 分鐘。

**結論：**本研究藉由預測平均藥物滯留時間可供工作人員輻射防護及對受檢者對於檢查時之相關劑量參考。

PC-011

## The Possible Causation of Prolonged Pulmonary Mean Transit Time in First Pass Radionuclide Angiography

Hsin-Ning Wang<sup>1</sup>, Lien-Hsin Hu<sup>1,2</sup>, Tse-Hao Lee<sup>1</sup>, Chi-Fen Lin<sup>1</sup>, Nan-Jing Peng<sup>1,2</sup>

<sup>1</sup>Department of Nuclear Medicine, Taipei Veteran General Hospital, Taipei, Taiwan

<sup>2</sup>School of medicine, National Yang Ming Chiao Tung University, Taiwan

**Introduction:** First pass radionuclide angiography (FPRA) provides a fast and accurate assessment of both the right and left ventricle ejection fraction, for pre-operation survey and heart function evaluation. However, some of them had prolonged pulmonary mean transit time (PMTT), which might lead to inaccurate result.

**Methods:** 5 cases of FPRA-associated prolong PMTT were reviewed, where each of their medical chart was examined, images reviewed, and cardiac function calculated. The normal range of PMTT was set at smaller than 8 seconds.

**Results:** Case 1: increased infiltrations in bilateral lungs by the chest X-ray; case 2: dilated main pulmonary artery by the echocardiograph; case 3: pulmonary stenosis; case 4: enlarged bilateral hilum via chest X-ray; case 5: moderate increased airway resistance assessed by the pulmonary function test.

**Conclusions:** All of cases exhibited some kind of abnormality of right heart function and/or pulmonary disease. Theoretically, PMTT represented the blood flow (the radionuclide) pass through lungs. As the pulmonary resistance increases, the flow rate decreases and the passing time increases, and that matches our clinical findings. Therefore, the abnormality of prolonged PMTT can be a reliable predictor for pulmonary function and pulmonary status, which may have future diagnostic significance.

PC-012

## Correlation between Cadmium Zinc Telluride SPECT for Myocardium Perfusion Imaging and Coronary Angiography

Hsin-Ning Wang, Lien-Hsin Hu, Tse-Hao Lee, Yao Shan-Fan, Peng Nan-Jing

*Department of Nuclear Medicine, Taipei Veteran General Hospital, Taipei, Taiwan*

**Introduction:** Previously, the parallel two-headed gamma camera was the choice for the SPECT machine for myocardium perfusion imaging. Cadmium Zinc Telluride (CZT) as the SPECT gamma camera for myocardium perfusion imaging has recently gained popularity, since CZT SPECT saved time and dosage for the radiation. Still, few studies had been conducted for the comparison between the new CZT SPECT camera and the traditional coronary angiography.

**Methods:** Cases were collected, on patients who underwent coronary angiography between January-June 2021, and also received myocardium perfusion imaging with CZT SPECT within 3 months. Cross-comparison of myocardium perfusion imaging and coronary angiography was conducted.

**Results:** Findings of the coronary angiography can be very different from those of the myocardium perfusion imaging. For those with positive myocardium perfusion imaging results might commonly have negative findings in coronary angiograph, and that made us wonder whether we myocardium perfusion imaging was over-interpreted.

**Conclusions:** The correlation between the findings from the myocardium perfusion imaging obtained by CZT SPECT and those by coronary angiography was mediocre, especially the positive predict value. However, the negative predict value was high. As a result, myocardium perfusion imaging might still serve as a gate keeper for ischemia heart disease. For diagnostic confirmation, we might need computed tomography for attenuation correction.

PC-013

## Myocardial Perfusion Imaging and Myocardial Blood Flow Quantification for the Detection of Microvascular Dysfunction: Correlation with Coronary Flow Reserve using Invasive Coronary Thermodilution Measurement

Ming-Tsung Wu<sup>1</sup>, Meng-Ying Lu<sup>2</sup>, Kuang-Te Wang<sup>2</sup>

<sup>1</sup>Department of Nuclear Medicine, Taitung MacKay Memorial Hospital, Taitung, Taiwan, Republic of China

<sup>2</sup>Division of Cardiology, Department of Internal Medicine, Taitung MacKay Memorial Hospital, Taitung, Taiwan, Republic of China

**Introduction:** Patients who underwent MPI and/or MBF with abnormal findings are believed to be indicative of coronary angiography for coronary artery disease (CAD). However, a significant proportion of such patients are found to have normal (false-positive MPI) or insignificant appearing coronary arteries called as non-obstructive coronary artery disease that may be expressed as coronary microvascular dysfunction (CMD) or microvascular angina. Coronary flow reserve (CFR) with intracoronary pressure guide wire is used as gold standard to diagnose microvascular dysfunction. We aim to assess the CMD ratio in patients with non-obstructive coronary artery disease.

**Methods:** This study prospectively enrolled 32 patients with abnormal findings in MBF quantification by dynamic SPECT or MPI, but normal FFR assisted coronary angiography. Coronary thermodilution CFR was measured in each participant by an intracoronary pressure wire.

**Results:** All participants finished the examinations and tolerated the procedure well. There were 20 men and 12 women included and the age was  $59.7 \pm 13.6$  years. From the coronary angiography (CAG), 20 of them presented patent or less than 30% diameter stenosis, and 12 of them presented 50~70% luminal stenosis in the major coronary arteries with fractional flow reserve  $> 0.80$ . All patients had resting and hyperemic physiology measurement. 16 (50%) were classified as having coronary microvascular dysfunction (CFR  $< 2.0$ ) and 16 (50%) had normal CFR.

**Conclusions:** With coronary thermodilution CFR measured by an intracoronary pressure wire in patients with abnormal MPI and/or MBF but normal or insignificant appearing coronary arteries in CAG, the CMD ratio of these patients is intermediate. MBF quantification by dynamic SPECT and MPI might be not accurate to detect coronary artery disease in some cases, but their predict value of CMD should be determined in further studies.

PC-014

## 以不同軟體分析 MBF 及 MFR 其結果一致性之評估

魏文祺 張嘉容 姚珊汎 彭南靖

臺北榮民總醫院核醫部

**背景介紹：**心肌血流灌注造影 (MPI) 是核子醫學檢測心肌缺血的主要方法，而以動態 SPECT 造影方式對心肌進行血流定量是評估心肌缺血的另一種新方法。本研究的目的是比較不同心肌血流定量軟體在 myocardial blood flow (MBF) 及 myocardial flow reserve (MFR) 的分析結果。

**方法：**11 位病人接受動態 SPECT 心肌血流定量檢查，Rest 及 Stress 分別注射 18 mCi 及 36 mCi 的 Tc99m-MIBI，先執行 Rest 造影，3 個小時後再執行 Stress 造影，另執行心臟電腦斷層掃描做心肌血流定量分析時之衰減校正。使用的造影設備為 GE NM530C 及 GE NM/CT 870。定量分析使用 MyoFlowQ 與 Corridor4DM，分析左心室的 myocardial blood flow (MBF) 與 myocardial flow reserve (MFR)。Corridor4DM 的血流模型採用 GE 530c Tc-99m ROI NetRet Leppo。統計分析軟體使用 MedCalc。連續變量以平均值 ± 標準差表示，一致性評價以 Bland-Altman 圖呈現。

**結果：**MyoFlowQ 與 Corridor4DM 有做衰減校正的 Stress MBF 分別為： $2.04 \pm 0.67$  ml/min/g 與  $1.00 \pm 0.31$  ml/min/g；Rest MBF:  $0.81 \pm 0.09$  ml/min/g 與  $0.60 \pm 0.38$  ml/min/g；MFR:  $2.38 \pm 0.74$  與  $1.60 \pm 0.40$ ；Corridor4DM 未做衰減校正的 Stress MBF 與 Rest MBF 分別為： $2.04 \pm 0.56$  ml/min/g 與  $0.86 \pm 0.35$  ml/min/g；MFR 為  $2.79 \pm 1.05$ 。以 Corridor4DM GE 530c Tc-99m ROI NetRet Leppo 血流模型分析經衰減校正所得到的 MBF 與 MFR 較 MyoFlowQ 的結果為低，而未做衰減校正會得到較高的 MBF 與 MFR，而與 MyoFlowQ 結果較為相近。一致性評價以圖一與圖二的 Bland-Altman 圖呈現。

**結論：**使用不同分析軟體會因其使用的血流模型參數及操作技術的不同而呈現一些差異，更多的樣本分析對本研究的結果會有正面的幫助。



PC-015

## Follow-up of Patients with Prolonged Pulmonary Mean Transit Time in First-pass Radionuclide Angiography

Chi-Fen Lin<sup>1</sup>, Chien-Ying Lee<sup>1</sup>, Liang-Chi Wu<sup>1</sup>, Nan-Jing Peng<sup>1,2</sup>, Lien-Hsin Hu<sup>1,2</sup>

<sup>1</sup>Department of Nuclear Medicine, Taipei Veterans General Hospital, Taipei, Taiwan

<sup>2</sup>School of Medicine, National Yang Ming Chiao Tung University, Taiwan

**Introduction:** First-pass radionuclide angiography (FPRA) is a classic examination to evaluate both left and right heart function in one study. With bolus injection of radiotracer, initial central circulation data was collected and analyzed. It is a safe and time efficient examination in which image acquisition takes only 40-60 seconds. However, some of them had prolonged pulmonary mean transit time (PMTT), which might lead to inaccurate result. The aim of this study is to further evaluation of these patients.

**Methods:** The normal range of PMTT was set at less than 8 seconds. Patients who had prolonged PMTT in FPRA from Jan. 2014 to Jun. 2021 were selected. The follow-up ejection fraction (EF) values of left and right ventricle in FPRA and/or equilibrium radionuclide angiocardigraphy (ERNA) examination were retrospectively analyzed.

**Results:** We found a poor linear correlation between LVEF values in FPRA of prolonged PMTT and repeated FPRA or ERNA in these patients, as compared with a strong positive linear relationship in controls with both FPRA and ERNA. The difference reached statistical significance ( $p < 0.01$ ).

**Conclusions:** The LVEF of FPRA and follow-up FPRA/ERNA shows a poor correlation in patients with prolonged PMTT. We suggested an alternative method of LVEF evaluation should be performed when a prolonged PMTT occur in FPRA.

PC-016

## Subconjunctival Hemorrhage After Dipyridamole-stress Myocardial Perfusion Imaging

Chien-Wei Kuo<sup>1,2</sup><sup>1</sup>*Department of Nuclear Medicine, Kaohsiung Veterans General Hospital, Kaohsiung, Taiwan*<sup>2</sup>*Department of Medical Imaging and Radiological Sciences, Kaohsiung Medical University, Kaohsiung, Taiwan*

**Introduction:** Although dipyridamole is an antiplatelet medicine, hemorrhage is not a common adverse effect of dipyridamole-stress myocardial perfusion imaging (MPI). Here we report an unusual event happened during our daily routine thallium scan.

**Case Report:** A 62-year-old woman who suffered from intermittent chest tightness, palpitation and dyspnea on exertion came for thallium-201 MPI. After dipyridamole-induced stress, she had no specific discomfort and then underwent first scan smoothly. However, her family noted that she had red eye on right side, just about 1-1.5 hour after dipyridamole infusion. She denied eye pain or blurred vision, but just complained about mild foreign body sensation. Subconjunctival hemorrhage was impressed, and she was suggested to keep observation on eye condition. In the next few days, red eye resolved spontaneously, and no visual impairment was noted.

**Conclusion:** To our knowledge, subconjunctival hemorrhage was not reported as an adverse effect of dipyridamole-stress MPI. The association of them should be further evaluated.

PC-017

## Use Gated Blood Pool SPECT QBS Software and Multiple Gated Blood Pool (MUGA) Diagnosis Results to Explore the Correlation with Echocardiography

Tzu-Chi Chang<sup>1,2</sup>, Yu-Sheng Hung<sup>1</sup>

<sup>1</sup>*Division of Nuclear Medicine, Chi Mei Medical Center, Liouying, Tainan, Taiwan*

<sup>2</sup>*Department of Medical Imaging and Radiological Sciences, Kaohsiung Medical University*

**Propose:** Use cardiac ultrasound as a reference standard for left ventricular ejection rate, and understand which of planar MUGA and gated blood pool SPECT is more accurate and better.

**Materials and Methods:** The patient does not need any preparation before the examination. The examination method is intravenous injection of pyrophosphate and Tc-99m pertechnetate, followed by an EKG gated scan. Use E.CAM gamma camera to take images, use e-soft software and QBS algorithm to calculate LVEF. Use SPSS statistical software and Excel for data integration and correlation analysis. Use dual correlation to analyze the results of GBPS, MUGA and cardiac ultrasound. Analyze the EF diagnosis results of GBPS and cardiac ultrasound, MUGA and cardiac ultrasound.

**Results:** The average LVEF values measured by GBPS, MUGA and cardiac ultrasound were  $45.2 \pm 21.2\%$ ,  $43.2 \pm 13.6\%$ ,  $47.4 \pm 14.1\%$  and  $45 \pm 13\%$ , respectively. The LVEF value derived from GBPS shows a high correlation with cardiac ultrasound and a statistically significant difference. The LVEF value obtained from MUGA also shows a high correlation and statistically significant difference with cardiac ultrasound. Compared with traditional MUGA, GBPS has a 1.13 times higher diagnostic power.

**Conclusion:** The accuracy of GBPS is higher than MUGA. At present, GBPS has been routinely used clinically as an examination method to assess ventricular function.

PC-018

## Evaluation of Gastroesophageal Reflux and Gastric Emptying in One Study

Ya-Ju Tsai, Tzu-Hua Lee

*Department of Nuclear Medicine, Taipei Medical University Hospital*

**Introduction:** We evaluated gastroesophageal reflux and gastric emptying in one combined study in a patient with prandial coughing and vomiting.

**Case reports:** 5-yr-old boy is a case of anaplastic astrocytoma of the cerebellum status post treatment with a nasogastric feeding tube. Post prandial coughing and vomiting were noted. A study to evaluate gastroesophageal reflux and gastric emptying consisted of dynamic imaging of chest and upper abdomen subsequent to the oral ingestion of 0.5 mCi of Tc-99m DTPA in 100 ml liquid formula. On supine position, imaging started immediately after the ingestion of the radiolabeled liquid with a frame rate of 10 sec/frame for 60 minutes, and imaging acquired in the anterior & posterior projections using a dual-head gamma camera. Gastroesophageal reflux evaluated by visual analysis of the dynamic images of chest showed no evidence of gastroesophageal reflux or aspiration in lungs. Gastric empty time calculated by drawing a region-of-interest (ROI) of stomach and using the geometric mean method revealed a borderline gastric empty time with half-time of gastric emptying (T1/2) at 88 minutes.

**Conclusions:** Combination of gastric emptying and gastroesophageal reflux studies is simple and feasible to evaluate both organs in one scan especially in children, because the field of view is usually large enough to cover chest to upper abdomen.

PC-019

## Relationship between the Metabolic Signals of the Brain FDG-PET and the Cognitive Function in Mesial Temporal Epilepsy

Syu-Jyun Peng<sup>1</sup>, Hsin Tung, MD<sup>2,3,4</sup>, Pu-Jung Huang<sup>5</sup>, Shih-Chuan Tsai<sup>5,6</sup>

<sup>1</sup>Professional Master Program in Artificial Intelligence in Medicine, College of Medicine, Taipei Medical University, Taipei, Taiwan

<sup>2</sup>Institute of Clinical Medicine, National Yang Ming Chiao Tung University, Taipei, Taiwan

<sup>3</sup>Center of faculty development, Taichung Veterans General Hospital, Taichung, Taiwan

<sup>4</sup>Division of Epilepsy, Neurological Institute, Taichung Veterans General Hospital, Taichung, Taiwan

<sup>5</sup>Department of Nuclear Medicine, Taichung Veterans General Hospital, Taichung, Taiwan

<sup>6</sup>Department of Medical Imaging and Radiological Technology, Institute of Radiological Science, Central Taiwan University of Science and Technology, Taichung, Taiwan

**Introduction:** Brain <sup>18</sup>F-labeled fluoro-2-deoxyglucose positron emission tomography (FDG-PET) presented metabolic images, commonly used for the dementia and epilepsy. In epilepsy, the regions had asymmetrically hypometabolic signals were thought as the possible. However, whether the metabolic signals of the epilepsy patients are different with the healthy controls and whether they had the relationship with the cognitive functions have not been identified.

**Methods:** We collected the brain FDG-PET imaging of the 26 mesial temporal lobe epilepsy (MTLE) patients (right-MTLE: 13, left-MTLE: 13) and 13 age and gender-matched controls in 2019 from neurological outpatients in Taichung Veteran General Hospital. The FDG-PET images were spatially normalized to the Montreal Neurological Institute (MNI) atlas using the software toolkit Statistical Parametric Mapping 12. The average standardized uptake values (SUV) of the pons were used as the reference, to normalize the SUV of the whole brain gray matters. Subsequently, we conducted spatial smoothing with an 8 mm full width at half maximum Gaussian kernel. The SUV values of the two MTLE groups were voxel-by-voxel compared with the values of the controls. Then, the voxel-based analysis was conducted to establish the relationship between the SUV and the individual seizure duration, intelligence quotients (full IQ, verbal IQ, performance IQ), working memory, and processing speed index. P value < 0.01 was thought as significance.

**Results:** Left-MTLE had more extensive low-SUV regions compared with the controls, involving bilateral cerebellar hemispheres, left mid-temporal, left inferior parietal lobule, left postcentral gyrus, right inferior orbitofrontal, right frontal opercular, right superior-medial frontal, and right angular regions (t score < -3). In contrast, right-MTLE showed relatively restricted area with low-SUV than the controls over the ipsilateral cerebellar hemisphere, temporal pole, thalamus, lingual gyrus, and cingulum gyrus (t score < -3). PIQ scores were the only prominent cognitive item correlated with the SUV in left-MTLE, which were positively related with the left superior temporal region SUV. In right-MTLE, working memory was the only significant item, which were negatively correlated with the SUV of the left thalamus. However, seizure duration did not have any relationship with the FDG-PET metabolism in both groups.

**Conclusions:** Left-MTLE had most extensively decreased glucose metabolism area than the right-MTLE did, suggesting they have different network topology. In addition to localization of the epileptogenic zone, the regional brain metabolism of the PET imaging might be related to the patients' cognitive functions, especially PIQ and working memory.

PC-020

## TRODAT SPECT 比較輸入影像中有無包含小腦對 Q-TRODAT 全腦 (Global) 背景數值的影響

李佩璇 楊朝瑋

澄清綜合醫院中港院區核子醫學科

**背景介紹：**臨床上以 TRODAT SPECT 造影做為多巴胺系統功能分析的重要依據。藉由大腦紋狀體區域之功能性影像缺損情況判別。目前臨床大都是以手動圈選進行半定量分析，缺點是低再現性與操作人為主觀因素影響影像圈選部位的大小位置等問題。Q-TRODAT (紋狀體自動化定量分析軟體) 帶入 SPECT Transverse plane 後，將自動選定紋狀體影像範圍，以降低手動圈選的問題。Q-TRODAT 在分析過程中，會將影像以標準腦模組化；本研究探討影像中是否包含小腦對背景數值的影響。

**方法：**本回溯性研究收集從 110 年 6 月至 110 年 8 月間，進行 TRODAT SPECT 造影共 37 人 (男性 16 位，女性 21 位)。使用 Siemens Symbia E 與 Siemens Symbia Evo Excel 搭配低能量高解析度準直儀，旋轉半徑約為 12-15 公分，影像矩陣大小為 128 x 128，採用 step and shoot 每 3 度取一張投影，每個角度收集 20 秒。影像重建採用濾波反投影 (filtered back projection)。衰減校正則使用 Chang's method，衰減校正係數 ( $\mu$ ) 為 0.12/cm。遵循以上方法將同一位病人的 SPECT Transverse plane 分為包含小腦及不包含小腦兩組，帶入 Q-TRODAT (Ver. 2.7) 中進行分析。利用配對樣本 T-檢定 (Paired Sample T-test) 進行相關係數與散佈圖觀察。

**結果：**本研究測量包含小腦及不包含小腦的全腦 (Global) 背景數值的平均數分別為  $48.62 \pm 11.62$  及  $46.75 \pm 11.14$ ， $p$ -value 為 0.000，相關係數 0.979。有統計學上顯著性差異且為高度正相關。

**結論：**Q-TRODAT (紋狀體自動化定量分析軟體) 可在臨床上減少人為因素的誤差，但輸入的影像仍會影響其結果。因此，在臨床使用上，建議使用統一標準，以避免影響。

PC-021

## Cerebral Perfusion SPECT Scan — A Case Report

張添信 陳慶元

佛教慈濟醫療財團法人台中慈濟醫院核子醫學科

**背景介紹：**內政部公布 109 年簡易生命表，國人的平均壽命為 81.3 歲，其中男性 78.1 歲、女性 84.7 歲，皆創歷年新高，隨著社會結構的高齡化導致人口急速老化，腦部相關疾病也與日俱增，根據國健署資料分析在腦血管疾病 (Cerebrovascular disease) 在 2020 年位居十大死因的第四位，核子醫學在這方面檢查優勢，功能性腦血流灌注檢查，利用放射性示蹤劑，可了解病患腦部血流分佈圖譜，臨床上可以用來協助腦血管病變、癲癇病灶、失智症等之診斷，再結合影像醫學科系資料 (MRI)，達到更全面化影像 (分子與功能性影像)，提高診斷效率與精準性，臨床上常見中風或腦傷患者，臨床醫師多半注重在患者肢體癱瘓或麻木等活動上的問題，對於神經系統病變，而引起的語言障礙經常忽略，本個案例為急性缺血性腦中風 (Acute ischemic stroke) 是指缺血性腦中風的成因，主要來自於腦血管動脈硬化、小動脈硬化 (俗稱腦梗塞) 或來自於心臟或大血管的血栓 (簡稱腦栓塞)，不論是梗塞或栓塞，皆會造成流向腦部血液的缺損而使影響範圍內的腦細胞死亡，約佔中風 (CVA) 總患者的八成為最常見病因；神經心理學檢查是一種大腦功能性的檢查，它的功用在於檢驗病人是否有大腦認知功能的缺損，它可以測量病人的智力功能，包含注意力，語言障礙，記憶功能，視覺空間功能與大腦高級認知功能。

**案例報告：**該案例為男性 (71 歲) 有高血壓及急性缺血性中風病史 (110.8) 此次住院原因，後續出現行動與失讀及記憶相關方面問題，經由神經心理學檢查鑑別有明顯語言及右側無力導致行動不便，尤其語言問題，表現在其難以命名物品 (Pure alexia) 及回應答案均無法順利，這類群體過去的報導多概述是受損部位在 Lt Parietal-Temporo-Occipital Lobe (PTO) 部分，該個案有施行核醫腦血流灌注檢查 (Cerebral Perfusion Scan ECD)、磁振造影 (MRI)，均發現在左側顳葉及枕葉部分有異常。

**結論：**利用核醫工作站 (Xeleris 3) 進行腦血流灌注分析 (Segmental Analysis)，與影像融合 (SPECT/MRI)，可以提高影像達到分子與功能性目的，進而提供臨床科系最佳診斷訊息，本案例經由融合後發現，腦血流灌注缺損與磁振造影發現異常部位極為一致，神經心理學檢查也經評估後推測可能是該部位受損。



PC-022

## 利用腦血流灌注檢查診斷失智症 並使用 eZIS 影像分析軟體輔助追蹤患者退化之情形

劉宛如 陳慶元

台中慈濟醫院

**背景介紹：**根據 WHO 全球十大死因統計，失智症已由 2000 年的第 14 名竄升至 2016 年第 5 名，衛生福利部依據 WHO 定義之失智症範圍進行統計 2017 年全民健保申報資料中，因失智症就醫者約 17 萬人，其中 65 歲以上約 16.8 萬人。隨著年齡增加，因失智症就診比例亦隨之增加。失智症是腦部疾病的其中一類，它的症狀除了導致思考能力和記憶力長期而逐漸的退化，還會影響到其他的認知功能，包括語言能力、空間感、判斷力…等各方面的功能，同時可能出現個性改變、妄想或幻覺等症狀，這些症狀會影響患者的人際關係與工作能力。輕度認知障礙 (Mild cognitive impairment) 簡稱 MCI，是一個介於正常認知功能與輕度失智症之間的一種過渡階段，雖然有少部分的患者會由 MCI 回復到正常的認知功能，但就大部分的患者而言，這是一個會退化到失智症的高危險群。輕度認知功能障礙 (MCI) 是指當記憶力測試顯示一個人的記憶問題比同齡人士的平均程度嚴重時，就是患有輕度認知功能障礙 (MCI)。輕度認知功能障礙病人在短期記憶力上有困難，但仍可以進行日常活動。使用 eZIS 分析 ECD 檢查之結果，可供臨床醫師分析患者情況評估時的參考依據。

**方法：**患者為一位 59 歲女性，因最近出現憂鬱、焦慮、失眠及忘東忘西的情況。因此至本院就診，因此醫師安排心理測試及磁振照影 (MRI)，經醫師評估後懷疑為抑鬱症及遺忘型 MCI，於是安排核醫腦部血流灌注掃描 (Cerebral perfusion scan) 檢查輔助診斷。先請患者在暗室休息 10 分鐘後，注射 25 mCi 的 ECD 藥物，經過 30 分鐘休息後，請患者至掃描室執行檢查，檢查使用 GE SPECT/CT 儀器搭配 fan beam collimator 執行 60 分鐘腦部掃描。

**結果：**磁振照影結果腦部血流灌注掃描結果無異常發現，因此醫師先給予憂鬱症藥物治療。一年後追蹤該患者之情況，而患者兩年來一直有持續更嚴重的認知功能症狀抱怨，情緒部份亦只有很非常輕微的焦慮與憂鬱，因此醫師一樣安排心理測試、磁振照影及腦部血流灌注掃描，心理測試結果正常，磁振照影結果腦部血流灌注掃描結果也無異常發現。於是我們將該患者去年掃描之影像及今年檢查之影像經由 eZIS 軟體分析發現患者的一年前的 Severity、Extent 和 Ratio 的 threshold 各為 0.83、2.27%、1.98，而今年檢查的結果為 Severity、Extent 和 Ratio 的 threshold 各為 1.33、11.61%、4.37，比去年的上升數值許多，因此醫師在評估 eZIS 分析結果後，考慮進行阿茲海默症之治療。

**結論：**因患有輕度認知功能障礙的病人患上阿茲海默症的機率較高。這意味著患有輕度認知功能障礙的病人，比沒有患輕度認知功能障礙者，有高 3 到 4 倍的機會患上阿茲海默症。因此若能夠早期發現這些患者，便可持續追蹤並於早期給予治療。雖然影像上並無明顯異常，不過經由 eZIS 影像分析可以清楚知到患者腦部變化之比較，輔助臨床醫師診斷之參考。

PC-023

## Supervised Machine Learning Algorithms using Automatic Semi-quantitative Parameters for Tc-99m TRODAT SPECT Image Interpretation

Chien-Chin Hsu<sup>1</sup>, Kuo-Wei Ho<sup>2</sup>, Yung-Cheng Huang<sup>1</sup>

<sup>1</sup>Department of Nuclear Medicine, Kaohsiung Chang Gung Memorial Hospital

<sup>2</sup>Department of Nuclear Medicine, Chiayi Chang Gung Memorial Hospital

**Introduction:** DaTQUANT (GE Healthcare) is an automatic software for semi-quantifying striatal specific binding ratios in dopamine transporter (DAT) single photon emission tomography (SPECT). The aim of this study is to assess the performance of supervised machine learning algorithms using automatic semi-quantitative parameters for Tc-99m TRODAT SPECT image interpretation.

**Methods:** From January 2017 to June 2019, 516 patients who underwent Tc-99m TRODAT SPECT were enrolled. Age and 12 parameters obtained from DaTQUANT, including: right striatum, left striatum, right anterior putamen, left anterior putamen, right posterior putamen, left posterior putamen, right caudate, left caudate, right putamen/caudate ratio, left putamen/caudate ratio, putamen asymmetry, and caudate asymmetry were used to develop machine learning model. We used six machine learning algorithms for supervised learning: K-nearest neighbor (KNN), logistic regression (LR), Naïve Bayes (NB), decision tree (DT), random forest (RF), and support vector machine (SVM). Tc-99m TRODAT SPECT images were labeled as normal and abnormal by consensus of three experienced nuclear medicine physicians. According to the sequence of imaging date, the dataset was split into 416 training data and 100 testing data.

**Results:** There were 211 normal and 205 abnormal images in the training data and 54 normal and 46 abnormal images in the testing data. The classification accuracies of KNN, LR, NB, DT, RF, SVM classifiers were 0.82, 0.85, 0.82, 0.92, 0.92, 0.88 in the training data, and 0.80, 0.82, 0.82, 0.86, 0.88, 0.87 in the testing data, respectively. All the supervised machine learning classifiers performed well on the training and testing data, and RF had highest accuracy.

**Conclusions:** Our results suggested that supervised machine learning algorithms could accurately interpret Tc-99m TRODAT SPECT using age and automatic semi-quantitative parameters obtained from DaTQUANT.

PC-025

## 探討無肝病成年人的 GOT/GPT 比率 與骨小樑指數之初步研究

蔡依良<sup>1,2</sup> 莊紫翎<sup>1,3</sup> 廖建國<sup>1</sup> 王昱豐<sup>1,3</sup>

<sup>1</sup> 佛教慈濟醫療財團法人大林慈濟醫院核子醫學科

<sup>2</sup> 佛教慈濟醫療財團法人大林慈濟醫院醫學研究部

<sup>3</sup> 慈濟學校財團法人慈濟大學醫學系

**背景介紹：**作者們過去曾探討腰椎和髖部的骨質密度 (BMD) 與 GOT/GPT 比率間存在著顯著的負相關。而骨骼是由皮質骨與骨小樑所構，骨小樑指數 (TBS) 可以作為骨骼微結構的替代品，評估腰椎的骨骼紋理，進而推測骨骼的強度。目前有許多研究指出肝臟疾病，如 B 型肝炎、C 型肝炎、喝酒及脂肪肝等，皆與骨質密度相關。GOT (Glutamic oxaloacetic transaminase) 及 GPT (Glutamic pyruvic transaminase) 為表示肝臟受損的指標之一，數值越高，受損的程度越嚴重。臨床上也常以 GOT/GPT 比率做為判定肝臟疾病的指標之一。本研究欲進一步透過骨小樑指數與 GOT/GPT 比率，初步探討肝臟健康與骨骼強度之間的相關性。

**方法：**回溯性收集本院預防醫學中心，2014 年 6 月至 2020 年 7 月接受健康檢查的受檢者。我們排除腰椎、髖骨有手術史的人，以及為了盡可能收集健康肝臟的人，我們剔除有 B 型肝炎、C 型肝炎、喝酒史和 GOT 或 GPT 數值大於 40 U/L 的患者。根據上述條件，總共收集 9,938 位的受檢者。統計方法以簡單線性回歸來分析骨質密度 (x) 與骨小樑指數 (y) 的相關性，及 GOT/GPT 比率 (x) 與骨小樑指數 (y) 的相關性。當  $p$  值小於 0.05 時，視為有統計上的意義。

**結果：**共收案 9,938 位平均年齡  $56.7 \pm 11.4$  歲、平均 GOT/GPT 比率為  $0.90 \pm 0.31$ ，平均骨小樑指數為  $1.351 \pm 0.106$  的受檢者。經簡單線性回歸分析發現，骨骼密度與強度的線性模型擬合度為 26.9 ~ 47.6%，其中以腰椎骨骼紋理做為評估的骨小樑指數，與腰椎骨骼密度的模型擬合度為當然最高 ( $r = 0.690$ )。模型中骨小樑指數與不同部位的骨骼密度皆呈現顯著的正相關。最後以簡單線性回歸分析初步探討骨骼強度與 GOT/GPT 比率，骨小樑指數與 GOT/GPT 比率呈現顯著的負相關 ( $p < 0.001$ )。當 GOT/GPT 比率愈高時，骨骼強度將隨之降低。

**結論：**初步研究結果顯示 GOT/GPT 比率與骨骼強度為負相關 ( $p < 0.001$ )。GOT/GPT 比率較高的病患，除了骨質密度外，骨骼強度也將隨之降低。因此肝臟受損的病患也需多加留意本身的骨骼健康。

PC-026

## 透過骨小樑指數 比較不同骨質疏鬆程度的患者之骨骼強度

蔡依良<sup>1,2</sup> 莊紫翎<sup>1,3</sup> 廖建國<sup>1</sup> 王昱豐<sup>1,3</sup><sup>1</sup> 佛教慈濟醫療財團法人大林慈濟醫院核子醫學科<sup>2</sup> 佛教慈濟醫療財團法人大林慈濟醫院醫學研究部<sup>3</sup> 慈濟學校財團法人慈濟大學醫學系

**背景介紹：**依據世界衛生組織 WHO 的定義，T 分數是與同性別健康年輕人的骨骼密度 (BMD) 平均值進行比較，計算有幾個標準差 (SD) 的差異。當腰椎、股骨頸或總髌骨任一個部位的 T 分數  $\leq -2.5$  個 SD 時，診斷為骨質疏鬆症；T 分數介於  $< -1.0$  至  $> -2.5$  個 SD 時，診斷為骨量減少；最後當 T 分數  $\geq -1.0$  個 SD 時，診斷為正常人。骨骼是由皮質骨與骨小樑所構，骨骼密度的減少不一定會真正的提高骨折風險。現今測量 BMD 的儀器 DXA 只能檢測出骨骼的「量」，尚不能直接檢測「質」。因此我們藉由 TBS iNsight 軟體評估腰椎的骨骼紋理，分析出骨小樑指數 (Trabecular bone score, TBS)，進而推測骨骼強度。本研究預計以 TBS 比較正常人、骨量減少及骨質疏鬆患者之間的骨骼強度有何不同。

**方法：**回溯性收集本院預防醫學中心，2014 年 6 月至 2020 年 7 月接受骨骼密度健康檢查的受檢者。我們排除腰椎或髌骨有手術史的人，總共收集 17,453 位受檢者。依據 WHO 對正常人、骨量減少及骨質疏鬆症的定義，分別將族群分成三個組別。統計方法採用 Chi-square 和 One way ANOVA 比較三組的差異，事後檢定則使用 Tuckey test 進行組別之間的兩兩比較。之後以正常人作為基準組別，進行多項式羅吉斯回歸分析，比較骨量減少和骨質疏鬆症患者 TBS 的勝算比 (Odds ratio)。並且進一步將年齡、性別和身體指數 (BMI) 等因子加入模型進行調整。當  $p$  值小於 0.05 時，視為有統計上的意義。

**結果：**本次收案的骨質疏鬆症患者中女性比例高達 85.0%；骨量減少的患者女性占 60.3%；而正常人中女性占 48.7% ( $p < 0.001$ )。此外結果顯示當骨骼流失的程度越嚴重時，年齡有越高，BMI 越低的趨勢。在 TBS 上也發現到，當骨骼流失的程度越嚴重時有越低的趨勢 ( $p < 0.001$ )。風險因子年齡、性別及 BMI 在多項式羅吉斯回歸分析中，皆具有統計上的意義。加入風險因子後的調整模型，組別骨量減少的 TBS 勝算比從未調整的 0.305 下降至 0.254，骨質疏鬆症的 TBS 勝算比則從未調整的 0.090 下降至 0.073 ( $p < 0.001$ )。

**結論：**當骨質疏鬆症的程度越嚴重時，骨骼除了「量」的下降外，「質」也將顯著的隨著流失嚴重度而下降。因此作者預計下一步將加入十年骨折風險率，對骨折進行更進一步的探討。

PC-027

## 初步探討停經婦女的骨骼強度 與鹼性磷酸酶之相關性

蔡依良<sup>1,2</sup> 莊紫翎<sup>1,3</sup> 廖建國<sup>1</sup> 王昱豐<sup>1,3</sup><sup>1</sup> 佛教慈濟醫療財團法人大林慈濟醫院核子醫學科<sup>2</sup> 佛教慈濟醫療財團法人大林慈濟醫院醫學研究部<sup>3</sup> 慈濟學校財團法人慈濟大學醫學系

**背景介紹：**鹼性磷酸酶 (Alkaline Phosphatase, ALP) 於正常情況下，成年人體內的水平介於 20 至 140 IU/L 間，並在肝臟的代謝和骨骼發育中扮演著重要角色。因此臨床上可透過 ALP 作為診斷病患是否罹患骨骼疾病或肝膽疾病的生化指標之一。骨骼是由皮質骨與骨小樑所構。骨小樑指數 (Trabecular bone score, TBS) 可以作為骨骼微結構的替代品，評估腰椎的骨骼紋理，進而推測骨骼的強度。目前已有許多研究探討過 ALP 與骨骼密度 (Bone mineral density, BMD) 之間的關聯性，但 BMD 只能檢測出骨骼的「量」，尚不能直接檢測「質」。加上停經後婦女因雌性激素的分泌量大幅降低，而導致骨質快速流失。因此本研究預計收集 51 歲以上的女性，視為停經後女性，探討其 ALP 與 TBS 的相關性。

**方法：**回溯性收集本院預防醫學中心，於 2014 年 6 月至 2020 年 7 月間接受健康檢查之 51 歲以上的婦女。我們排除腰椎、髖骨有手術史和癌症史的人，並將族群分成正常人、骨質流失和骨質疏鬆症三個組別，以正常人作為基準組別，使用多項式羅吉斯回歸來分析 ALP 和 TBS 分別於骨質流失組和骨質疏鬆組的勝算比 (Odds ratio)。以及使用簡單線性回歸來分析 ALP (x) 與不同部位的 BMD 和 TBS (y) 的相關性。

**結果：**共收案 7,202 位平均年齡  $61.3 \pm 7.0$  歲、平均 ALP 為  $80.6 \pm 23.3$  IU/L，平均 TBS 為  $1.301 \pm 0.095$  的女性受檢者。其中被診斷為骨質疏鬆的病患 2,634 位、骨質流失的病患 3,555 位，正常的人有 1,013 位；分別占總收案人口的 36.6%、49.4% 和 14.1%。以正常人作為基準組別，經多項式羅吉斯回歸分析後顯示骨質流失組的勝算比為 1.281；骨質疏鬆組的勝算比為 1.579，且都具有統計上的意義 ( $p < 0.001$ )。最後經簡單線性回歸分析，發現骨質強度與鹼性磷酸酶呈現顯著的負相關 ( $r = -0.105$ )。

**結論：**初步研究結果顯示在停經婦女中，鹼性磷酸酶與骨骼強度為負相關 ( $p < 0.001$ )。可能原因為骨骼重塑時，骨骼流失的速度愈快，骨骼合成的速度也跟著加快。因此與骨生成相關的鹼性磷酸酶，在本研究中呈現出負向關係的結果。

PC-028

## The Effect of BMD on Cases of BPH Combined with High PSA

Pao-Liang Chen<sup>1,2</sup>, Tzyy-Ling Chuang<sup>1,4</sup>, Jian-Guo Liao<sup>1</sup>, Yuh-Feng Wang<sup>1,3,4</sup>

<sup>1</sup>Department of Nuclear Medicine, Dalin Tzu Chi Hospital, Buddhist Tzu Chi Medical Foundation, Chiayi, Taiwan

<sup>2</sup>Department of Medical Research, Dalin Tzu Chi Hospital, Buddhist Tzu Chi Medical Foundation, Chiayi, Taiwan

<sup>3</sup>Center of Preventive Medicine, Dalin Tzu Chi Hospital, Buddhist Tzu Chi Medical Foundation, Chiayi, Taiwan

<sup>4</sup>Department of Radiology, School of Medicine, Tzu Chi University, Hualien, Taiwan

**Background:** According to the previous studies, we have separately explored the effects of benign prostatic hypertrophy (BPH) and prostate specific antigens (PSA) on bone mineral density (BMD). Therefore, this study will further analyze the combination of BPH and PSA, and divide subjects into. BPH with PSA greater than 4 ng/mL (disease group) and no BPH with normal PSA (less than 4 ng/mL) (normal group). We compare the two variables at the same time to find whether the factors have a comprehensive impact on BMD.

**Methods:** Total of 5,605 males who were examined in the preventive medical center of our hospital were collected for evaluation. Total hip replacement surgery, internal fixation in the lumbar spine or hip, lumbar vertebroplasty, or incomplete data were excluded. In the study, clinicians used ultrasound to confirm the diagnosis of BPH. The serum by chemiluminescence immunoassay is also used to determine whether the value of the PSA level is normal or not. PSA level greater than 4 ng/mL is considered abnormal. A dual-energy X-ray absorptiometer was used to measure the BMD of three parts (lumbar spine and bilateral hips).

**Results:** Of the 5,605 males, 5,323 (95%) were in the normal group and 282 (5%) in the disease group. The mean age of patients was  $53.85 \pm 12.10$  years in the normal group and  $68.46 \pm 7.72$  years in the disease group ( $p < 0.001$ ), with a significant difference. The diseased group having significantly increased BMD at the lumbar spine area, but significantly decreased BMD in the bilateral hips, as compared with the normal group.

**Conclusions:** In conclusion, the disease group had high lumbar spine BMD but lower BMD in the bilateral hips. These findings suggest that men diagnosed with BPH or high PSA should be considered at risk for hip fractures and need the evaluation for BMD.

PC-029

## BMD Result and Fracture Rate were Effected by Single-Site Fracture on DXA Study

Pao-Liang Chen<sup>1,2</sup>, Tzyy-Ling Chuang<sup>1,4</sup>, Jian-Guo Liao<sup>1</sup>, Yuh-Feng Wang<sup>1,3,4\*</sup>

<sup>1</sup>Department of Nuclear Medicine, Dalin Tzu Chi Hospital, Buddhist Tzu Chi Medical Foundation, Chiayi, Taiwan

<sup>2</sup>Department of Medical Research, Dalin Tzu Chi Hospital, Buddhist Tzu Chi Medical Foundation, Chiayi, Taiwan

<sup>3</sup>Department of Preventive Medical Center, Dalin Tzu Chi Hospital, Buddhist Tzu Chi Medical Foundation, Chiayi, Taiwan

<sup>4</sup>Department of Radiology, School of Medicine, Tzu Chi University, Hualien, Taiwan

**Background:** The purpose of this study is to compare that all three parts (including lumbar spine and bilateral hip) bone mineral density (BMD) can be analyzed and that a single part BMD can not be analyzed (any part of the lumbar spine and bilateral hip) due to surgery. Between the two groups, the difference in BMD of different parts, and the change of fracture rate in ten years is further evaluated.

**Method:** This is a retrospective study. Data was collected from November 2014 to March 2021, in a regional teaching hospital in southern Taiwan, including the subjects underwent an outpatient BMD exam. The subjects were divided into two groups: the control group (all three parts—the lumbar spine, left hip, and right hip can be analyzed), and the surgical group (one part of lumbar, left hip or right hip underwent surgery, and data was excluded if two parts underwent surgery). Base on the surgical history, the subjects were divided into two groups for analysis, including spinal surgery (open reduction and internal fixation, vertebroplasty or metal prosthesis), hip surgery (total hip replacement or internal fixation with steel nails).

**Results:** This study initially found that when using of BMD to detect three parts, if one part cannot be assessed after surgery, compared with all three parts, the BMD of the surgical patients is lower than that of the control group and the risk of fractures increases, because the surgical part affects the BMD assessment.

**Conclusion:** Therefore, this study concluded that, in the future, clinicians should regularly follow up changes in bone mineral density when metal implants are implanted to reduce re-fractures.

PC-030

## Intervention Threshold of FRAX<sup>®</sup> Should be Adjusted According to Specific Age in Elder People

Pao-Liang Chen<sup>1,2</sup>, Tzyy-Ling Chuang<sup>1,4</sup>, Yuh-Feng Wang<sup>1,3,4</sup>,  
Jian-Guo Liao<sup>1</sup>, Min-Hong Hsieh<sup>5,6,7\*</sup>

<sup>1</sup>Department of Nuclear Medicine, Dalin Tzu Chi Hospital, Buddhist Tzu Chi Medical Foundation, Chiayi, Taiwan

<sup>2</sup>Department of Medical Research, Dalin Tzu Chi Hospital, Buddhist Tzu Chi Medical Foundation, Chiayi, Taiwan

<sup>3</sup>Department of Preventive Medical Center, Dalin Tzu Chi Hospital, Buddhist Tzu Chi Medical Foundation, Chiayi, Taiwan

<sup>4</sup>Department of Radiology, School of Medicine, Tzu Chi University, Hualien, Taiwan

<sup>5</sup>Department of Orthopedics, Dalin Tzu Chi Hospital, Buddhist Tzu Chi Medical Foundation, Chiayi, Taiwan

<sup>6</sup>Division of osteoporosis center, department of Orthopedics, Dalin Tzu Chi Hospital, Buddhist Tzu Chi Medical Foundation, Chiayi, Taiwan

<sup>7</sup>Department of Orthopedics, School of Medicine, Tzu Chi University, Hualien, Taiwan

**Background:** In 2008, the World Health Organization developed an assessment tool which integrate relevant clinical risk factors and the bone mineral density of the femoral neck to estimate a patient's next 10-year fracture risk. It is recommended the patients whose major osteoporotic fracture > 20%, and the risk of hip fractures > 3%, they should be treated. However we noted that certain groups who had low fracture risk still have osteoporotic fractures. Therefore, the aim of this study was to analyze the relationship between fracture history and fracture risk of patients over 50 years old, and to clarify whether the fracture risk threshold of the elder people in Taiwan should be adjusted according to specific age.

**Method:** It was a retrospective study. The subjects who had undergone dual energy x-ray absorptiometry from November 2014 to March 2021 were enrolled. Exclusions are patients who can not be assessed in a single regional of the three parts (Included internal fixation or vertebroplasty surgery in lumbar spine area, unilateral or bilateral with hip joint internal fixation or total hip replacement surgery) or age younger than 50 years.

The basic data of 8,049 subjects were collected and there were 1,303 (16.2%) males and 6,746 (83.8%) females. Their age, anthropometry, past medical history, history of osteoporosis fractures, life style and 10-year fracture risk were analyzed.

**Results:** There were significant differences in anthropometry, including body height, body weight, body mass index, as well as past medical history, bone mineral density, and the ten year probability of fracture among the three ethnic groups. The probability of ten-year fracture increases with age among each group, and some of the age groups do not meet the recommended treatment standards, which may cause one or more fractures. Low bone density and high FRAX<sup>®</sup> were independent and significant factors in osteoporosis fracture.

**Conclusion:** This study showed that the BMD was significantly lower in the patients with previous fractures. It is the intervention threshold with FRAX<sup>®</sup> for osteoporosis treatment whether specific age groups in the elder people over 50 years old should be modified. It is recommended that the FRAX<sup>®</sup> threshold for treatment should be adjusted according to different age groups, which will help to make early recommendations for treatment and follow-up for patients with middle-to-high-risk osteoporosis.



PC-031

## 糖尿病與骨質密度增加研究分析

陳保良<sup>1,2</sup> 莊紫翎<sup>1,4</sup> 廖建國<sup>1</sup> 王昱豐<sup>1,3,4\*</sup>

<sup>1</sup> 佛教慈濟醫療財團法人大林慈濟醫院核子醫學科

<sup>2</sup> 佛教慈濟醫療財團法人大林慈濟醫院醫學研究部

<sup>3</sup> 佛教慈濟醫療財團法人大林慈濟醫院預防醫學中心

<sup>4</sup> 慈濟學校財團法人慈濟大學醫學院醫學系放射線學科

**簡介：**隨著人口老化與生活型態及飲食習慣改變，糖尿病的盛行率逐年上升顯示糖尿病對於人體是有一定的影響，本篇研究目的為探討糖尿病對於骨質密度之影響，我們將利用飯前血糖（短期）與糖化血色素（長期）異常，與正常的受檢者進行比較分析。

**材料方法：**我們利用本院預防醫學中心健康檢查受檢者之資料庫，利用雙能量 X 光測量儀量測腰椎與雙側髖部骨質密度測量結果進行分析研究，也收集相關病史（採問卷方式），另外飯前血糖正常值為  $\leq 100$  (mg/dL)，糖化血色素正常值為  $\leq 7$  (%)，將分成正常與異常組來進行研究。根據上述之條件收集 2014 年 6 月至 2021 年 04 月受檢者，共計收集 21416 位受檢者，男性 8018 位 (37.4%)，女性 13398 位 (62.6%)。

**結果：**第一部分我們分析性別間對於骨質密度有無差異，結果發現男性骨質密度高於女性其具有統計差異 ( $p < 0.001^*$ )。第二部分我們將糖化血色素分成正常  $\leq 7\%$  與異常  $> 7\%$  來進行比較，結果發現糖化血色素越高，骨質密度越好。第三部分我們將飯前血糖分成正常  $\leq 100$  mg/dL 與異常  $> 100$  mg/dL 來進行分析，結果發現與糖化血色素一樣，血糖越高骨質密度越好，這樣的結果主要原因與我們受檢者以第二型糖尿病居多較有相關。

**結論：**我們總覺得骨質密度增加是一件好的事情，但若因疾病或藥物所造成的異常增加，我們必須注意，以本篇研究糖尿病對於骨質密度高於正常組，就應該接受進一步治療找出原因。骨質密度增加或降低，將會根據罹患糖尿病的類型不同而有所變化。

PC-032

## 骨質密度評估區域骨折僅評估單一區域 造成骨密降低之研究分析

陳保良<sup>1,2</sup> 莊紫翎<sup>1,4</sup> 廖建國<sup>1</sup> 王昱豐<sup>1,3,4</sup>

<sup>1</sup> 佛教慈濟醫療財團法人大林慈濟醫院核子醫學科

<sup>2</sup> 佛教慈濟醫療財團法人大林慈濟醫院醫學研究部

<sup>3</sup> 佛教慈濟醫療財團法人大林慈濟醫院預防醫學中心

<sup>4</sup> 慈濟學校財團法人慈濟大學醫學院醫學系放射線學科

**目的：**本篇研究利用分析骨質密度檢測區域中（腰椎、雙側髖部）僅評估單一部位與三部位均能分析對骨質密度之差異研究。

**材料方法：**收集本院自 2014 年 11 月至 2021 年 03 月間，利用本院雙能量 X 光測量儀檢測骨質密度之受檢者數據，總共收集 9234 位受檢者，將分成二組，第一組控制組（三部位，腰椎與雙側髖部均能分析）收集 8928 位，第二組手術組（三個部位中，僅一個部位能分析）收集 306 位，我們將利用第一組與第二組來進行較。

**結果：**控制組 8928 位 (96.7%)，各區域手術佔比，腰椎與右側髖部 56 位 (0.6%)，腰椎與左側髖部 49 位 (0.5%)，雙側髖部 201 位 (2.2%)。年齡分布控制組 14-102 歲，手術組 26-102 歲。各組間相比骨質密度均顯著降低，且骨折率均增加。

**結論：**雙部位以上骨折相較於控制組會使骨質密度降低。此外腰椎加髖部手術相較於雙側髖部手術也是降低的。因此雙部位骨折術後要持續監測骨質密度降低之狀況。

PC-033

## 血清骨鈣素濃度與骨質密度之相關性探討

張素雲<sup>1</sup> 薛仔婕<sup>1</sup> 林淑靜<sup>1</sup> 廖建國<sup>1</sup> 王昱豐<sup>1,2</sup>

<sup>1</sup> 佛教大林慈濟醫院核子醫學科

<sup>2</sup> 慈濟大學醫學系

**背景：**骨鈣素 (Osteocalcin) 由骨芽母細胞 (Osteoblasts) 在 Vit.K 的介入及 Vit.D3 的刺激下合成。形成後，一部份進入骨細胞間質，另一部份則釋放到血清中。因此 Osteocalcin 在血中的濃度會和骨質形成速率或骨質替換速率成正比。單就 Osteocalcin 一項而言，濃度偏低可能意味著骨質生成速率過慢，濃度偏高代表骨質替換速率過快，二者皆是發生骨質疏鬆症 (Osteoporosis) 的徵兆。因此我們探討 Osteocalcin 濃度高低和 Osteoporosis 之間的相關性。

**方法：**收集 2020/07/01 至 2021/06/30 間，共收集 328 位病患，扣除 2 位男性和骨折打鋼材病患，實際人數為 164 位，同時接受骨質密度以及血清 Osteocalcin 之檢查，腰椎、髖關節和股骨近端的骨質密度使用骨質密度儀 (HOLOGIC Discovery Wi) 檢查，血清 Osteocalcin 濃度使用 ROCHE cobas e601 電子化學免疫分析法 (ECLIA) 測量，參考區間為 11-46 ng/mL，並將其結果分為 Osteocalcin < 11、11-46、> 46 三組，骨密分為 Normal、Low bone mass、Osteoporosis 分別進行統計，探討三組骨質密度之間的差異。統計分析採用卡方檢定和 One-way ANOVA 分析， $p < 0.05$  具統計上意義。

**結果：**結果顯示 Osteocalcin 血清 < 11 有 74 人，其中有 56 人 (75.7%) 為 Osteoporosis，Osteocalcin 血清 11-46 有 80 人，其中有 62 人 (77.5%) Osteoporosis，Osteocalcin 血清 > 46 有 10 人，其中有 10 人 (100%) Osteoporosis (表 1、2)，Osteocalcin 血清 3 組在腰椎 T-score 則不具有顯著性差異，Osteocalcin 血清 3 組和左右兩邊髖關節的骨質密度及 T score 均顯著差異 ( $p < 0.05$ ) (表 3)。

**結論：**Osteocalcin 是一種骨質生成速率 (formation rate) 的指標，可用來監控造骨功能，及評估骨質替換速率。本研究結果顯示患有骨質疏鬆症的病人其 Osteocalcin 濃度偏高的比率為 100%，Osteocalcin 偏低的比率為 75.7%，而濃度於參考區間的比率為 77.5%。Osteocalcin 特異性不高，但可作為臨床治療後評估指標，若同時檢驗 PTH-Intact 和 25-OH VitD 更能輔助其診斷。

PC-034

## The Bone Quantity and Quality Difference Between Vegetarian and Non-vegetarian Middle-aged and Elder Women

Yuh-Feng Wang<sup>1,2</sup>, Tzyy-Ling Chuang<sup>1,2</sup>, Malcolm Koo<sup>3</sup>

<sup>1</sup>Department of Nuclear Medicine, Dalin Tzu Chi Hospital, Buddhist Tzu Chi Medical Foundation, Chia-Yi, Taiwan

<sup>2</sup>School of Medicine, Tzu Chi University, Hualien, Taiwan

<sup>3</sup>Graduate Institute of Long-term Care, Tzu Chi University of Science and Technology, Hualien, Taiwan

**Introduction:** Remodeling of bones is a continuous and complex process. In assessing the combined effects of physical and nutritional factors on bone health in children and adolescents, physical activity and diet were found to be the most relevant factors affecting bone mineral density (BMD) and fracture risk. However, the effect of a vegetarian diet on bone health remains controversial.

**Material and Methods:** This is a retrospective medical record review. The changes in BMD and trabecular bone score (TBS) between vegetarian and non-vegetarian middle-aged and older women who underwent two general health examinations (T1 and T2) approximately 3 years apart were compared. Generalized estimating equations was used to compare the change in the lumbar spine and bilateral hip BMD and TBS over time.

**Results:** The mean age of the patients was 56.6 years at T1; the mean interval between T1 and T2 was 2.7 years. For women aged 40-55 years, a vegetarian diet was associated with a significantly greater decrease in lumbar spine BMD ( $p < 0.001$ ) and left hip femoral neck BMD ( $p = 0.015$ ) over time. However, in those aged  $> 56$  years, changes in BMD at any site were insignificant. Moreover, a vegetarian diet was not significantly associated with changes in TBS in women 40-55, 56-64, or 65-90 years. The changes in BMD and TBS over a 3-year interval did not differ significantly between vegetarian and non-vegetarian postmenopausal women.

**Conclusion:** In perimenopausal women, a vegetarian diet reduced bone quantity, as reflected by BMD, but not bone quality, as reflected by TBS.

PC-035

## Antacid and Sucralfate-Induced Osteomalacia Mimicking Skeletal Metastasis on Bone Scintigraphy

Ya-Wen Chuang, Chia-Yang Lin, Ying-Fong Huang,  
Chin-Chuan Chang, Hsiu-Lan Chu

*Department of Nuclear Medicine, Chia-Yi Chang-Gung Memorial Hospital, Chia-Yi,  
Taiwan Department of Nuclear Medicine, Kaohsiung Medical University Hospital, Kaohsiung, Taiwan*

**Introduction:** Hypophosphatemia (serum phosphorus concentration < 2.5 mg/dl, 0.8 mmol/l) is commonly observed in hospitalized patients and may be associated with drug therapy. The clinical manifestations are usually mild but might also be severe and potentially life-threatening. Bone scintigraphy of the disease has rarely been reported.

**Methods:** The case of a 78-year-old woman with multinodular type hepatocellular carcinoma (T2N0M0, stage II), presented with chest pain, without antecedent trauma, was referred from outside hospital for detecting bone metastasis.

**Results:** Multiple areas of increased uptake were accidentally found in the routine bone scintigraphy, causing confusion with malignant metastatic disease. The low serum level of phosphorus was noted in laboratory findings, and investigation disclosed hypophosphatemia after prolonged ingestion of antacids and sucralfate for upper gastrointestinal bleeding.

**Conclusions:** Hypophosphatemia frequently develops in the course of treatment with drugs commonly used in every-day clinical practice. A careful drug history is important, and careful interpretation is needed of the unusual uptake for cancer work up.

PC-036

## A Single Osteolytic Metastasis of Humerus Mimics A Primary Bone Tumor – A Case Report

Yi-Hsun Chen, Yu-Ling Hsu

*Department of Nuclear Medicine, Ditmanson Medical Foundation Chia-Yi Christian Hospital*

**Case report:** A 59-year-old man complained right shoulder pain with right upper arm soreness for more than 3 months. Without history of trauma, the pain was first suspected to be caused by sports injuries. MR imaging from other hospital showed mild hypertrophy of the right acromioclavicular joint. Increasing signal on proton density but not on T2WI indicated tendinitis; right humeral cyst with irregular margin suggesting bony metastasis therefore bone scan was performed for further evaluation.

Whole body bone scan showed focal increased Tc-99m MDP radioactivity only at right proximal humerus; primary malignant bone tumor, too, was reasonably suspected. After the serial survey accompanied with his symptoms of losing weight in half a month, further imaging such as CT was arranged. Chest CT showed left upper lung cancer with mediastinal invasion, encasement of left subcalvian artery. PET/CT later revealed suspicious malignancy at left upper lung lobe of lung with invasion to mediastinum with metastatic lymphadenopathy at right axillary and suspiciously para-aortic regions, also probable metastases at right proximal humerus and left adrenal gland. Histopathological examination confirmed the lesions at right humerus was metastatic adenocarcinoma.

**Discussion:** Advanced lung cancer is complicated by skeletal metastases either due to direct extension from adjacent primaries or, more commonly, due to haematogenous dissemination of neoplastic cells. Lung cancer with bone metastasis refers to the spread of cancer cells from the primary tumor to the bones through the bloodstream or lymphatic system. About 30% to 40% of patients with advanced lung cancer will be affected by bone metastases. In people with lung cancer, the bones are the third most common site for metastases after the liver and adrenal glands. However, atypical metastasis only to right humerus in bone scintigraphy, in this case, should always be kept in mind that it could still be metastasis from any occult malignancy, even though the imaging pattern suggests primary bone tumor.

PC-037

## Malignant Bone Tumor or Active Inflammation? A Case Experience with Bone Scintigraphy

Shih-Fu Wang, Yu-Ling Hsu

*Department of Nuclear Medicine, Ditmanson Medical Foundation Chia-Yi Christian Hospital*

**Introduction:** Simple and aneurysmal bone cysts (ABCs) are benign lytic bone lesions, usually encountered in children and adolescents. Simple bone cyst is a cystic, fluid-filled lesion, which may be unicameral (UBC) or partially separated. UBC can involve all bones, but usually the long bone metaphysis and otherwise primarily the proximal humerus and proximal femur. ABCs are metaphyseal, excentric, bulging, fluid-filled and multicameral, and may develop in all bones of the skeleton. Simple cysts can resolve in childhood; ABCs are potentially more aggressive.

**Case Report:** A 34-year-old young female patient was referred to our hospital because of left thigh pain for three months and left inner thigh dermatitis. A series of examinations were arranged. X ray revealed an ill-defined radiolucent lesion over left femoral metaphysis. MR imaging suspected metaphyseal lesion at the left proximal femur with periosteal and adjacent muscle enhancement. Differential diagnoses included: malignancy and inflammatory/infectious process. Whole body bone scan suggested mildly increased radioactivity at the left proximal femur which was likely to be a giant cell tumor, enchondroma, or other nature. Later on, the pathologic result was proved to be bone cyst rupture, either simple or aneurysmal, with active inflammation after biopsy.

**Conclusion:** In our case, the likely bone cysts has ruptured with active inflammation made it even more difficult to differentiate benign lesions from malignancies from imaging pattern. However, whole body bone scan did help to exclude the likelihood of bone metastases, at least. Although simple and aneurysmal bone cysts are benign lesions, bone fracture and destruction should still be carefully prevented if found early. The accurate diagnosis should be made according to patients symptoms/signs, imaging patterns, also finally tissue proof. Biopsy must be made to identify soft-tissue parts, as telangiectatic sarcoma can mimic ABC.

PC-038

## 全身骨骼掃描上發現之心外按摩導致的骨骼損傷

張秀瑛<sup>1</sup> 莊紫翎<sup>1,2</sup> 王昱豐<sup>1,2</sup><sup>1</sup> 佛教慈濟醫療財團法人大林慈濟醫院核子醫學科<sup>2</sup> 慈濟學校財團法人慈濟大學醫學系

**背景介紹：**心外按摩是心肺復甦術 (cardiopulmonary resuscitation, CPR) 的重要組成部分。雖然心肺復甦術可以挽救生命，但在它施行的過程中可能也會導致併發症，其中骨骼外傷，尤其是肋骨及胸骨的骨折即是在施行心肺復甦術的心外按摩時最常發生的併發症。在此，我們介紹一位因接受心肺復甦術的心外按摩而導致胸骨與肋骨骨折，且在全身骨骼掃描中呈現活性攝取異常增加的案例。

**影像報告：**一名 71 歲男性肺癌患者自 2020 年開始由外院轉入本院進行常規的治療及追蹤。在此期間除採胸部 X 光、胸部電腦斷層掃描及抽血等追蹤檢查之外，患者於 2021 年 6 月接受了在本院的首次全身骨骼掃描。掃描結果中發現在左側上頷竇、左側膝關節、雙側踝關節及雙側足部有活性增加的現象，除此之外在其雙側肋骨及胸骨也呈現了異常的活性攝取增加 (圖一)，且其影像表現方式疑似外傷所造成，經向患者詢問相關病史之後發現，該患者在數月前曾因肺炎所導致的心臟驟停接受過心肺復甦術的心外按摩，故其雙側肋骨及胸骨的異常活性攝取增加因是由心肺復甦術時胸部按壓所引發的骨折所致。

**結論：**全身骨骼掃描是核子醫學部門當中最常執行的檢查，除可評估骨骼的轉移性病變之外，它對骨骼損傷或骨折等也具有極高的靈敏度。放射師的角色非常重要，熟悉心肺復甦術造成的骨骼掃描型態和即時詳細的病史詢問，可以避免醫師錯誤診斷為多發性骨髓瘤或多發性的骨轉移。



PC-039

## 全身骨骼掃描出現手套現象一案例報告

林培堯<sup>1</sup> 謝婷娟<sup>1</sup> 郭諭燁<sup>3</sup> 黃奕琿<sup>2</sup> 鄭媚方<sup>2</sup> 柯冠吟<sup>1</sup>

<sup>1</sup> 國立臺灣大學醫學院附設醫院癌醫中心分院核子醫學部

<sup>2</sup> 國立臺灣大學醫學院附設醫院核子醫學部

<sup>3</sup> 新生醫護管理專科學校護理科

**背景介紹：**全身骨骼掃描是核子醫學用來追蹤癌症是否有骨骼轉移的檢查，具有高敏感度及早期偵測骨骼病灶的能力，Tc-99m MDP 是骨骼掃描的常用藥物，經由靜脈注射後隨血流運送到全身組織，靜脈注射後約 2~4 小時後進行全身造影，當偶然發生由動脈注射入藥物時，高濃度的藥物會造成該動脈供應的組織有較高之藥物吸收形成手套現象 (glove phenomenon)。

**病例報告：**本案例為一位 78 歲女性，因肺腺癌於 2021 年 3 月下旬進行全身骨骼掃描，在上午注射 Tc-99m MDP，下午掃描時，發現到左手手腕到手指有明顯的異常攝取，像是戴了一隻手套。起初醫師診斷可能是打漏、發炎、骨髓炎或是手套現象 (glove phenomenon)，詢問值班放射師，注射 Tc-99m MDP 時 (打針位置為左手手腕)，確認病人無不舒服的反應，後續追蹤病人於 4 月初接受 FDG 正子造影全身檢查 (打針位置為右小腿)，從 PET/CT 影像中，在左手相同位置處，無異常的 FDG 攝取，由此推測當時的全身骨骼掃描影像出現的手套現象是因為核醫藥物是從動脈注入造成的。

**結論：**Tc-99m MDP 的吸收機制是與骨骼上羥基磷灰石晶體的表面結合，若 Tc-99m MDP 由四肢的動脈注射，注射處的遠端骨頭直接曝露高濃度的藥物，造成攝取過度增加，本案例就是如此呈現。輻射工作人員在注射核醫藥物 Tc-99m MDP 時，通常會找四肢的周邊血管注射，可以從回血的狀況 (血液的顏色、流速)，確認此血管是否為靜脈，以減少出現手套現象 (glove phenomenon)。

PC-040

## SPECT/CT 定量技術於 下背痛患者骶髂關節定量檢查之應用

陳在揚 林立凡 高峻皓 許天睿 鄭澄意

三軍總醫院核子醫學部

壁報論文發表摘要·臨床組

**背景介紹：**近年來隨著電腦設備及影像演算法的進步，使得標準攝取值 (SUV) 定量技術，現亦可應用在單光子電腦斷層 (SPECT/CT) 中，而骨掃描因其優異的靈敏度與性價比，一直以來被臨床醫師廣泛運用在骨病變診斷上，新的 SPECT/CT 定量技術可提供更精準的診斷價值。

本研究起因於骶髂關節平面影像定量技術，在 1970 年代即被發表運用在診斷下背痛患者骶髂關節炎上，但因過去在技術條件限制下，難以鑑別特定骶髂關節炎，故希望藉由新技術的革新，以更精準的立體影像定量方式，提升下背痛患者醫療診斷品質。

**方法：**本研究回溯收納自 2018 年 4 月 10 日至 2018 年 8 月 30 日，復健部醫師因患者下背痛而開立全身骨掃描及 SPECT/CT，排除骨轉移及手術後，共 29 例，注射  $^{99m}\text{Tc}$  MDP 後 3 到 4 小時造影，使用 Xeleris 4 影像工作站比對其骶髂關節平面影像 (planar) 與 SPECT/CT 之定量數值，依相似方法學 SPECT/CT 亦區分左右側及上中下，共六處計算，且分別統計其  $\text{SUV}_{\text{max}}$ 、 $\text{SUV}_{\text{max}}$  SI/S、 $\text{SUV}_{\text{mean}}$ 、 $\text{SUV}_{\text{mean}}$  SI/S 數值。

**結果：**其定量數值統計概述 planar 整體平均為  $1.21 \pm 0.42$ 、 $\text{SUV}_{\text{max}}$  為  $11.51 \pm 8.26$ 、 $\text{SUV}_{\text{max}}$  SI/S 為  $1.29 \pm 0.61$ 、 $\text{SUV}_{\text{mean}}$  為  $4.39 \pm 2.10$ 、 $\text{SUV}_{\text{mean}}$  SI/S 為  $1.32 \pm 0.47$ ，在 32 例患者中，平面定量數值六處皆低於 1.25，但在 SPECT/CT 影像上發現病灶，計有 7 例，其中 1 例為疑似早期壓力性骨折，其餘疑似退化性關節炎，病灶處可見  $\text{SUV}_{\text{max}}$  SI/S 提升；此外影像診斷疑似腫瘤骨轉移 2 例，其病灶處  $\text{SUV}_{\text{max}}$  之平均分別為 52.7 與 92，顯著高於母體平均值；planar 及 SPECT/CT 影像無明顯異常，但其中 1 例  $\text{SUV}_{\text{max}}$  顯著偏低 ( $4.65 \pm 1.11$ )，可能和與骨質疏鬆有關。

**結論：**骨掃描的 SPECT/CT 定量技術近三年被大量發表在國際期刊上，但就我們所知，尚無針對骶髂關節定量新舊技術比較的文章，傳統的平面影像定量方式，基於 40 年前的技術條件限制，無法精準的鑑別特定關節炎，故本研究以 Q.Volumetrix MI 設計了模擬傳統的定量模式，統計數據雖尚未追蹤患者後續的醫療病歷，但 SUV 數值已近似國際研究在脊椎上之統計結果，後續尚須修正骶骨的取樣方式，以平衡骶髂關節上及下的數值差異，並增加正常人及患者的案例數量，期待將來藉由新技術的應用，精進骶髂關節疾病鑑別能力，提供臨床優質的醫療影像服務。

PC-041

## The Discrepancy between F-18 FDG PET and Tc-99m MDP Whole Body Bone Scan in Breast Cancer Post Treatment – A Case Report

Fang-Shin Liu<sup>1</sup>, Chun-Hung Lin<sup>2</sup>, Yuh-Feng Wang<sup>1</sup>

<sup>1</sup>Department of Nuclear Medicine, Dalin Tzu Chi Hospital, Buddhist Tzu Chi Medical Foundation, Chiayi, Taiwan

<sup>2</sup>Department of General Surgery, Dalin Tzu Chi Hospital, Buddhist Tzu Chi Medical Foundation, Chiayi, Taiwan

**Introduction:** We present a case of breast cancer with multiple bone metastases and discuss the discrepancy between F-18 FDG PET and Tc-99m MDP whole body bone scan.

**Case report:** The 43-year-old female was diagnosed with left breast cancer with nodal and bone metastases in 2020. The whole body bone scan done on 2020/03/03 revealed multiple bone metastases, at left parietal bone of skull, spinal vertebrae, sacrum, sternum, right clavicle, bilateral scapulae, bilateral ribs, bilateral proximal humeri, bilateral sacroiliac regions, bilateral pelvic bones and bilateral proximal femurs. The following bone scan after treatment showed great improvement of the prior lesions. However, because of elevated tumor markers (CA153: 2020/02/18: 79.37->2021/05/14: 167.64), further F-18 FDG PET was arranged and showed not only multiple bone metastases but also multiple organ involvement with intense hypermetabolism.

**Discussion:** Bone scan relies on an osteoblastic bone response to tumor, whereas FDG PET depends mainly on the glucose metabolic characteristics of a tissue for the diagnose of disease. Purely osteolytic lesions with bony destruction not associated with significant reactive changes and in patients with slow-growing lesions in which reactive bone is not detectable. In addition, assessment of glucose metabolic processes, other than just measurement of mineral turnover, might be a powerful tool to differentiate benign from malignant bone lesions. Therefore, FDG PET could more accurately detect bone metastases than Tc-99m MDP bone scan, especially at an early stage, perhaps when they are confined to the bone marrow. On the contrary, FDG PET has been reported to be less sensitive for detecting sclerotic metastases than Tc-99m MDP bone scan. It was considered because that some bone metastases sufficient to stimulate increased osseous uptake of Tc-99m MDP may not be glycolytically active and may be below the requisite tumor mass needed for FDG accumulation. Therefore Tc-99m MDP bone scan and F-18 FDG PET are complementary modalities.

PC-042

## 骨骼掃描意外發現乳房植入物消失之影像差異

朱秀蘭<sup>1</sup> 莊雅雯<sup>1</sup> 游慧貞<sup>2</sup><sup>1</sup> 高雄醫學大學附設中和紀念醫院核子醫學部<sup>2</sup> 高雄醫學大學附設中和紀念醫院影像醫學部

**背景介紹：**乳癌一直是台灣女性癌症的第一位，其發病的平均年齡較西方國家年輕 10 歲左右，而確診後的治療以乳房切除手術為主，可分為腫塊切除、部分乳房切除及乳房全切除。部分病患在切除乳房後，會因介意失去乳房而在心理產生的巨大衝擊，所以會進一步選擇進行乳房重建，找回自信以建立新的生活。

乳房重建手術可分為自體組織（脂肪）重建及植入物重建，雖然自體組織乳房重建能提供較滿意的效果，但較瘦的病患並沒有足夠的自體組織可提供重建，此時植入物乳房重建便成為首選。自體組織乳房重建的形狀較為自然，但手術的困難度較高，傷口也需要較長時間癒合，而植入物乳房重建的手術過程雖較短且簡單，但可能會發生乳房形狀較不自然、變形、感染、夾膜攣縮或植入物破裂等併發症。

乳房重建不會影響後續的放射治療或化學治療，也不會增加乳癌的復發率及降低存活率。

**病例報告：**一位 51 歲罹患右側乳房惡性腫瘤之女性病患，於右側乳房切除手術後進行植入物乳房重建。在 2016 年 2 月接受核醫全身骨骼掃描時發現位於右側乳房植入物處的肋骨影像因植入物遮擋而稍微模糊（圖一），側面胸部影像顯示位於右側乳房的周邊組織因植入物而隆起（圖二）。病患須定期間隔半年至一年，進行核醫全身骨骼掃描之追蹤，此間其影像與 2016 年 2 月影像相比並無變化，但於 2020 年 12 月再次接受核醫全身骨骼掃描追蹤時，發現位於右側乳房植入物處的肋骨影像與圖一相比較為清晰（圖三），且側面影像之周邊組織隆起已消失（圖四）。經了解，病患於 2019 年 8 月的胸部電腦斷層攝影影像中（圖五），病患的乳房植入物仍存在，但在 2020 年 8 月的影像中，發現右側乳房植入物已消失（圖六），因此可判斷應是植入物破裂後而造成此位置的影像變化。

**結論：**此病患所進行之植入物乳房重建是一個相較簡單之重建方式，手術時間也較短，位置為患側胸部的皮膚及肌肉下，植入物可分為鹽水或矽質植入物，但植入物可能會發生莢膜攣縮、移位、變硬或破裂等不良反應，若上述情形發生，需要手術換置或移除植入物。此病患是使用鹽水植入物，發生破裂情形主要是因為材質的退化引起，其分散的鹽溶液進入人體，並不會造成病患生命危險，只是需要回醫院更換新的鹽水袋即可。

PC-043

## FDG PET/CT 於乳癌骨轉移之評估 — 案例報告

李佩璇 楊朝瑋

澄清綜合醫院中港院區核子醫學科

**背景介紹：**骨骼是乳癌患者最容易發生遠處轉移的器官。臨床上評估是否有骨轉移最常用核醫骨骼掃描，是將「鎝 -99m 甲基雙磷酸鹽」(Tc-99m MDP) 經由靜脈注射至人體，骨骼修復較多的部位就會吸收較多的磷酸鹽。當癌細胞轉移至骨頭後，會破壞骨組織，骨組織被破壞之後，會刺激周圍的骨骼修復；修復的新生骨會吸收更高的鈣及磷酸鹽，而在骨骼掃描上呈現放射性增高的影像。然而當乳癌細胞入侵骨骼後，會刺激蝕骨細胞 (Osteoclast) 的生長，加速骨骼的分解並破壞骨骼結構，則可能在骨骼掃描影像上表現較不明顯。

**病例報告：**一名 48 歲女性，於 2018 年發現乳癌並施作乳房全切除手術併前哨淋巴結摘除手術及標準腋下淋巴廓清術。每隔三個月到一年定期做核醫骨骼掃描追蹤皆無骨轉移發生。2019 年 6 月發現 CA-153 升高，所以於 2019 年 7 月進行正子造影檢查，發現在左側鎖骨、胸骨、左側第 6 根肋骨、第 7 節胸椎、右邊肩胛骨、第 4 節腰椎、左右兩側骨盆、髌骨及左側股骨皆有氟 -18 去氧葡萄糖代謝增加，有多發骨轉移發生。

**討論：**骨骼掃描為平面影像容易因相對位置重疊且因蝕骨細胞 (Osteoclast) 的生長，骨頭吸收 Tc-99m MDP 較少在影像上表現不明顯而不易被發現。如鎖骨與肋骨、胸骨與胸椎、肩胛骨與肋骨等都易重疊。正子造影利用腫瘤細胞和正常細胞氟 -18 去氧葡萄糖之代謝差異來尋找腫瘤的位置，因此懷疑有遠端轉移時可提供有效的影像資訊來幫助轉移病灶的定位。

**結論：**正子造影對蝕骨性骨轉移診斷率較骨骼掃描高。因此，使用骨骼掃描未能找出蝕骨性骨轉移的部位，這時可考慮改用正子造影來協助診斷。

PC-044

## Incidental Superscan on $^{99m}\text{Tc}$ -MDP Bone Scintigraphy in A Male Hepatocellular Carcinoma: Case Report

Hsin-Chang Chen, Yen-Hsiang Chang

*Department of Nuclear Medicine, Kaohsiung Chang-Gung Memorial Hospital, Kaohsiung, Taiwan*

**Introduction:** Primary myelofibrosis (PMF) is an uncommon myeloproliferative disorder that is characterized by bone marrow fibrosis. Symptoms and signs include splenomegaly, hepatomegaly, fatigue, hypermetabolic state, and bone involvement. PMF may be manifested with superscan phenomenon on bone scintigraphy due to increased cortical bone blood flow.

**Case Report:** We described a 62-year-old male patient of hepatocellular carcinoma (HCC), complicating with cirrhosis, splenomegaly and anemia. Bone scintigraphy was performed for excluding bone metastasis and revealed diffusely increased radioactivity uptake in whole body skeleton, including axial and appendicular bones. There was only minute radioactivity of both kidneys. Laboratory tests demonstrated appearance of granulocyte precursors and nucleated red cells, elevations of serum lactate dehydrogenase, uric acid, and vitamin B12. A subsequent bone marrow biopsy confirmed the diagnosis of PMF, with positive JAK-2 V617F mutation.

**Conclusions:** There are many causes of superscan such as renal osteodystrophy, hyperparathyroidism, and diffuse bone metastases from prostate, breast, or lung origin. However, PMF may present a superscan pattern on bone scintigraphy, and the images thus need to be interpreted with caution.

PC-045

## Incidental Gallbladder Adenosquamous Carcinoma with High Volume Bone Metastases

Ya-Cing Hsu, Yu-Ling Hsu

*Department of Nuclear Medicine, Ditamanson Medical Foundation Chia-Yi Christian Hospital*

**Case:** A 65-year-old man went to emergency department because of tarry stool, coffee-ground vomit associated with abdominal pain. Therefore, abdominal CT was performed and suggested incidental finding of advanced tumor lesions over gallbladder and liver with obstruction over second portion of duodenum. Also osteoblastic pattern over bone structure was noted. Further survey started because of high likelihood of malignancy. Except abdominal echo that confirmed again the bulky tumor over hepatoduodenal region, the <sup>99m</sup>Tc-MDP bone scintigraphy also revealed high volume multiple bone metastases. The final pathological data proved that the tumor was a poorly differentiated adenosquamous carcinoma over gallbladder with liver metastasis.

**Discussion:** Adenosquamous/squamous cell carcinoma (AS/SCC) of the gall bladder are a rare histopathologic subtype and account for nearly 1 to 12% of all cases. The literature available is limited and suggests that these rare tumors are more aggressive in comparison to adenocarcinoma and often infiltrate the adjacent viscera. Adenosquamous cell carcinoma comprises of a mixture of glandular and squamous elements and is described as a tumor wherein the squamous component is between 25 and 99%.

Disseminated blood-borne metastases from carcinoma of the gall bladder are uncommon and usually occur late. Autopsy studies have reported around 64.8% incidence of distant metastasis. However, most of these metastases are in the liver and only 20% are in other sites. The most common site of extra-abdominal metastasis is the lung followed by the brain. Skeletal metastases in carcinoma of gall bladder are very rare.

Although bone scintigraphy may not be a routine survey regarding to gallbladder cancer, it is still considered important and can be very helpful encountering advanced gallbladder cancer with rare pathologic pattern, which was fully demonstrated in our case.

PC-046

## Assessment of $^{223}\text{Ra}$ Treatment Procedures and Implications for Metastatic Castration-Resistant Prostate Cancer

Ying-Hsuan Li, Fang-Chi Chang

*Department of Nuclear Medicine, Changhua Christian Hospital, Changhua, Taiwan*

**Introduction:** The global increase in the incidence of prostate cancer raises the demand for management of mCRPC. A multitude of agents are employed for this purpose, including but not limited to hormonal, steroidal, and immunotherapies. Radium-223, an alpha-emitting radionuclide, is a unique option among these, characteristically targeting bone metastases while sparing normal tissue. This isotope therapy has been well-tolerated and improves survival and quality of life.

**Methods:** A total of twelve patients (ages 71 to 95) were chosen to receive the therapy. The patients received bone scintigraphy or equivalent examinations for diagnosis of whole body bone metastasis without visceral involvement and have symptoms of pain.

Six doses of 55 kBq/kg via intravenous injection were given at one-month intervals. Blood tests were performed prior to injections to ensure WBC and platelet counts meet the standards for administration. The patients were observed for 30 minutes post-injection to monitor the occurrence of immediately adverse reactions. Bone scintigraphy scans were performed one month after the end of treatment to evaluate the patients' conditions.

**Results:** Of the twelve patients observed, nine were able to complete the course of six injections. One patient received four injections, with the fourth delayed due to decreased WBC counts after the third injection. Two patients expired soon after the first injection. The comparison of pre- and post-treatment whole body bone scans of patient No. 12 showed more prominent radioactivity in the axial bones after the  $^{223}\text{Ra}$  treatment, and the condition was less than ideal. At the time of writing, four patients have expired, three of which survived more than one year after completion of treatment. The remainder patients are still under observation.

**Conclusions:** This case analysis showed the therapeutic effects of  $^{223}\text{Ra}$  treatment in mCRPC patients, able to prolong life without significant discomfort of adverse effects. Some passed prior to completion of the course of treatment due to the progression of disease or other chronic conditions. Overall,  $^{223}\text{Ra}$  therapy still proves to be a safe and effective isotope drug in the setting of mCRPC.



PC-047

## 十五例攝護腺癌以鐳 -223 以及放射線治療緩解骨轉移疼痛病例分析

李政穎<sup>1</sup> 張桂蘭<sup>1</sup> 張晉銓<sup>1</sup> 黃昉儀<sup>2</sup> 顏維徵<sup>1</sup> 張淑敏<sup>1</sup>

<sup>1</sup> 高雄醫學大學附設中和紀念醫院核子醫學部

<sup>2</sup> 高雄醫學大學附設中和紀念醫院放射腫瘤部

**背景介紹：**攝護腺癌好發於 60 歲以上男性，六成以上病患在癌症晚期有骨轉移發生的情形，常見治療方法包括手術切除、賀爾蒙治療、化療藥物以及放射線治療等方式進行積極治癒或保守性治療緩解疼痛。在核醫學領域中，鐳 -223 可釋放高能量  $\alpha$  射線緩解病患骨轉移之疼痛，改善生活品質。

**方法：**回顧性研究完整注射六劑鐳 -223 的 15 位攝護腺癌患者，進行案例分析及討論，有 2 位患者先注射鐳 -223 再接受放射線治療骨轉移；8 位患者先接受放射線治療再進行鐳 -223 注射，其中有 3 位患者在後續又進行放射線治療緩解骨轉移疼痛；5 位患者注射鐳 -223 之前或之後皆未曾進行過放射線治療。

**結果：**以平均體重 70 公斤患者為例，每次注射約 3850 kBq 劑量，完整注射六劑鐳 -223 後骨骼細胞平均吸收劑量約 2650 cGy/6 次；放射線治療緩解骨疼痛處方劑量約為 3000 cGy/10fr。在接受單一種治療方式後仍持續有骨轉移疼痛的病患，其骨頭掃描檢查有部分緩解，但持續惡化或更加惡化，攝護腺特異抗原指數 (PSA) 亦有持續上升的趨勢，並由門診醫師轉介繼續接受其他治療。

**結論：**先後接受鐳 -223 注射或放射線治療的攝護腺癌骨轉移病患，不會超過骨頭生物耐受劑量，建議病患應持續進行骨頭掃描檢查及門診追蹤攝護腺特異性抗原等檢查，若骨轉移持續惡化或疼痛未能有所緩解，在病患體力可負荷之情況下，建議求助門診安排放射線治療療程，或與醫師討論進行接受鐳 -223 注射治療，以提升生活品質及延緩癌症進程。

PC-048

## 全身骨骼掃描之膀胱壓跡形狀與前列腺相關探討

陳薇璇<sup>1</sup> 許幼青<sup>1</sup> 張秀瑛<sup>1</sup> 莊紫翎<sup>1,2</sup> 王昱豐<sup>1,2,3</sup>

<sup>1</sup> 慈濟醫療財團法人大林慈濟醫院核子醫學科

<sup>2</sup> 慈濟學校財團法人慈濟大學醫學系放射線學科

<sup>3</sup> 慈濟學校財團法人大林慈濟醫院預防醫學中心

**目的：**全身骨骼掃描是一項可用來追蹤癌症是否轉移至骨骼的檢查，在臨床上已被廣泛被使用，膀胱活性攝取的形狀變化亦可進行討論。然而，核醫學醫師往往忽視這種徵象，因為他們與此檢查的目的較不相關。本研究的目的是對全身骨骼掃描中膀胱壓跡形狀與前列腺進行相關性的探討。

**材料方法：**本研究回溯 2010 年 1 月至 2018 年 12 月間，接受門診及住院之所有開立全身骨骼掃描檢查的男性患者。病因包括肺癌、前列腺癌、口腔癌等癌症。排除了泌尿道手術、置入尿路引流管和患有膀胱良、惡性腫瘤之病患。並由兩位核醫科醫師進行目視判讀膀胱有無壓跡或者是冷區的影像。全身骨骼掃描檢查排除掉重複的病患後，最後膀胱壓跡的病患共有 112 位。

**結果：**全身骨骼掃描檢查為膀胱壓跡的病患共有 112 位，前列腺癌的病患共有 43 位，良性前列腺增生有 28 位，其餘列為其他組共 41 位。

將血清前列腺特異抗原之數值與膀胱壓跡之病患進行分析，排除無資料後，共 78 筆，膀胱壓跡呈甜甜圈形狀有 4 位，由下往上將膀胱擠壓成兩邊有 5 位，由下往上呈凹陷狀有 69 位。利用 Receiver-operating-characteristic curve (ROC curve)，我們將膀胱壓跡呈甜甜圈形狀與由下往上將膀胱擠壓成兩邊設為 0，將由下往上呈凹陷狀設為 1，在 Cut-off point = 5.590 時，曲面下面積 AUC = 74.6% (SD = 0.08)，具可接受之鑑別力， $p = 0.017$ ，具有統計差異。95% CI = (0.589, 0.902)。靈敏度 = 0.609，特異性 = 0.889。可見當血清前列腺特異抗原數值高於 5.590 ng/ml，膀胱壓跡的形狀越有可能為由下往上呈凹陷狀的機率越高，此時可懷疑為前列腺癌或者良性前列腺增生的機率亦增高。

**結論：**在全身骨骼掃描檢查影像中，我們的數據顯示，膀胱壓跡與臨床前列腺增生之間的相關性，這可能是良性前列腺增生、前列腺癌或慢性前列腺炎。本研究發現在全身骨骼掃描時，膀胱壓跡具有臨床意義，尤其在臨床診斷為非前列腺癌的病人上，可協助醫師預判前列腺的相關症狀，也能為臨床提供更多有價值的訊息。

PC-049

## Comparison of Radiomic Features between Metastatic Lesions and Degenerative Lesions on Tc-99m MDP Bone Scan in Patients with Prostate Cancer

Sin-Di Lee<sup>1</sup>, Nan-Jing Peng<sup>2,3</sup>

<sup>1</sup>Department of Nuclear Medicine, Kaohsiung Veterans General Hospital, Kaohsiung, Taiwan

<sup>2</sup>Department of Nuclear Medicine, Taipei Veterans General Hospital, Taipei, Taiwan

<sup>3</sup>National Yang Ming University, Taipei, Taiwan

**Introduction:** Bone scan is widely used in surveillance of bone metastases for patients with prostate cancer. The aim of this study is to investigate the difference of the radiomic features based on Tc-99m MDP whole body bone scan in the metastatic bone lesions and degenerative change on vertebral bones.

**Methods:** We collected 7 metastatic lesions from 2 patients (M group) and 32 degenerative lesions from 8 patients (D group). ITK-SNAP was used for image segmentation; pyRadiomics v3.0.1 on Python v3.7.9 platform was used for radiomics features extraction. A total of 107 radiomic features were extracted for each lesion, which included 14 shape features, 18 first-order statistical features and 75 texture features. The texture feature included gray-level co-occurrence matrix (GLCM, n=24), gray-level dependence matrix (GLDM, n=14), gray-level run length matrix (GLRLM, n=16), gray-level size zone matrix (GLSZM, n=16), and neighborhood gray tone difference matrix (NGTDM, n=5). T-test was used to screen the useful features to distinguish two groups of lesions.

**Results:** Among the 107 radiomic features, 82 features were with statistically significant difference in the two groups of lesions. In all of the shape features, no significant difference was noted. In all of the first-order statistical features, the difference between two groups was statistically significant. There was significant difference in 64 of the 75 texture features, included 22 of GLCM features, 12 of GLDM features, 14 of GLRLM features, 13 of GLSZM features and 3 of NGTDM features.

**Conclusions:** Radiomics could be a feasible approach to classify the lesions on Tc-99m MDP bone scan in patients with prostate cancer.

PC-050

## Assessing the Internal Dose for Patients Undergone $^{99m}\text{Tc}$ -MDP Bone Scan Examination Using Personal Dosimeter and a Simplified Method

Shih-Tsung Lin<sup>1,2</sup>, Yun-Feng Wang<sup>1,3,4</sup>, Lung-Kwang Pan<sup>2\*</sup>

<sup>1</sup>Department of Nuclear Medicine, Dalin Tzu Chi Hospital, Buddhist Tzu Chi Medical Foundation, Chiayi, Taiwan

<sup>2</sup>Department of Medical Imaging Radiological Science, Central Taiwan University of Science and Technology, Taichung, Taiwan

<sup>3</sup>Center of Preventive Medicine, Dalin Tzu Chi Hospital, Buddhist Tzu Chi Medical Foundation, Chiayi, Taiwan

<sup>4</sup>Department of Radiology, School of Medicine, Tzu Chi University, Hualien, Taiwan

**Introduction:** Whole body bone scan is one of the common examinations in clinical nuclear medicine examination. Although it is known that the radiation dose is low, but the actual dose is rarely measured. This study used personal dosimeters to evaluate the absorbed doses of nuclear medical bone scan patients.

**Material and Method:** A total of 209 patients were collected from November 2020 to May 2021, of which 69 males and 140 females, aged between 24 and 92 years old. We use a personal dosimeter to measure the radiation dose at a distance of 30 cm away from the patient 30 minutes, 120 minutes and 180 minutes after the injection of  $^{99m}\text{Tc}$ -MDP. Then we use STATISTICA 7.0 software to evaluate the retention time and absorbed dose from the  $^{99m}\text{Tc}$ -MDP. A semi-empirical formula is obtained by adding five major factors from biological data.

**Result:** After calculation, the gender, age and BMI, retention (mean life) time in the body of the chest and abdomen, as well as the absorbed dose and surface dose of the body are obtained. Then, using SPSS software, mean life time has statistical significance ( $p < 0.05$ ) in gender group of chest and in age group of chest and abdomen. The mean life time and adsorbed dose matched well, the prediction reached 80% accuracy in the  $\pm 20\%$  uncertainty.

**Conclusion:** It is convenient for the viewpoint of public hygiene to take the five major biological data in predicting the absorbed dose of patient undergone  $^{99m}\text{Tc}$ -MDP examination in future. This information also provided to radiation technician for radiation protection.

PC-051

## 加贅之下的影像 – Co-57 的妙用

張秀瑛<sup>1</sup> 劉芳馨<sup>1</sup> 王昱豐<sup>1,2</sup>

<sup>1</sup> 佛教大林慈濟醫院核子醫學科

<sup>2</sup> 慈濟大學醫學系

**背景介紹：**前哨淋巴結的觀念最早已普遍地被運用在乳癌、黑色素瘤甚至於頭頸部癌症等，現行於臨床上最常見為乳癌且被廣泛使用，本院亦是以乳癌居多，肢端黑色素瘤次之，頭頸部癌症則較為少見。以往在執行頭頸部區域的前哨結淋巴檢查時，因身體輪廓較不明顯而導致影像不易判別，因此在掃描時常會以手持點射源的方式來描繪患者的身體輪廓，以利臨床醫師更易於判別影像，這次我們利用 Co-57 平面射源來嘗試可否更容易地呈現出患者的身體輪廓且可提供較佳的影像品質。

**病例報告：**一名 81 歲女性患者在 7 個月前於左眉長出一顆約米粒大小的腫塊，一開始不予理會，半年前有變大情形，故至診所求治，在歷經服用藥物、換藥治療，換藥約 1 個月傷口後並未改善，故又至本院求治，經切片檢查確診為鱗狀上皮細胞癌 (Squamous cell carcinoma, SCC)，因此外科醫師建議在術前利用前哨淋巴結檢查確定淋巴是否轉移。前哨淋巴結檢查是採常規的流程執行，於腫瘤的四周採用皮下注射打入總劑量約 2 mCi 的 Tc-99m Phytate (共 4 針)，分別收取前位、斜位相及側位等影像。在第一次收取影像時我們試著不描繪身體輪廓，卻發現整個影像因為對比太過強烈而無法有效地幫助判別，接下來採用常規手持點射源的方式描繪輪廓時，影像品質有些微的改善，最後利用 Co-57 平面射源來收取患者身體輪廓影像時，明顯地可看出在影像中患者的身體輪廓更為清晰也更為接近真實，對於操作者而言也更容易執行。

**結論：**在本院頭頸部前哨淋巴結檢查常因注射部位的影像對比太過強烈而導致影像不易判別，藉由手持點射源來描繪患者的身體輪廓可以幫助提升影像品質，但影像品質優劣又會因操作者而異而使得變異性太大，故我們此次藉由日常校正儀器所需的 Co-57 平面射源來更簡易地顯現患者身體輪廓，除可減輕操作者的壓力之外也可提升影像品質，利於診斷。除頭頸部之外，相信對於乳癌及肢端黑色素瘤等處的前哨淋巴結檢查也會有所幫助。

PC-052

## Bone Metastasis to Left 4th Proximal Phalanx of Hand Detected by FDG-PETCT

Ya-Ju Tsai

*Department of Nuclear Medicine, Taipei Medical University Hospital*

**Introduction:** Metastasis to the hand bone is rare with a reported incidence of about 0.1%. We reported a case of esophageal cancer with initial presentation as pathologic fracture of left 4<sup>th</sup> finger.

**Case report:** A 50-year-old male is a case of soft palate cancer status post wide excision and right supraomohyoid neck dissection last year (pT1N0, stage I). Left 4th finger swelling was noted since six months ago. X-ray imaging showed bone destruction at left 4th proximal phalanx of hand with soft tissue swelling, suspecting pathologic fracture (figure 1). Wide excision was performed and pathology reported metastatic squamous cell carcinoma. Endoscopy, chest CT and biopsy demonstrated esophageal cancer with mediastinal lymphadenopathies and right lung nodules. FDG-PETCT was arranged for complete staging and revealed esophageal cancer, with multiple bone metastases, lung metastases, regional & non-regional lymphadenopathies (figure 2). In addition to left 4th proximal phalanx (figure 3), the bone metastases also involve left scapula, left 1st rib, left ilium, right distal femur & left proximal tibia. The patient has been received concurrent chemo-radiotherapy to esophageal tumor followed by systemic chemotherapy.

**Discussion:** Bone is one of the most common sites of metastasis. Metastasis to the hand bone is rare with a reported incidence of about 0.1% in all metastatic lesions to skeleton. The small amount of red marrow and the lack of dense vascular channels and large sinusoids for tumor seeding account for low frequency of acral metastatic disease compared with the axial skeleton. It has been reported that the distal phalanx is the most common site of bone metastasis in hand, which can be explained by a greater vascularization as well as microtrauma. Acrometastasis might be associated with a poor prognosis and related to widespread disease. In our case, pathologic fracture of finger as an initial presentation of an occult cancer is extremely rare. Conclusions: Metastasis to the hand bone is rare and might related to an advanced disease. Acrometastasis should be kept in the differential diagnosis of a hand tumor.

PC-053

## Diagnosis Challenge: Breast Cancer with Synchronous Multiple Stomach, Colon and Bone Metastases on FDG PET/CT

Tzyy-Ling Chuang<sup>1,2</sup>, Yuh-Feng Wang<sup>1,2,3</sup>

<sup>1</sup>Department of Nuclear Medicine, Dalin Tzu Chi Hospital, Buddhist Tzu Chi Medical Foundation, Chiayi, Taiwan

<sup>2</sup>School of Medicine, Tzu Chi University, Hualien, Taiwan

<sup>3</sup>Center of Preventive Medicine, Dalin Tzu Chi Hospital, Buddhist Tzu Chi Medical Foundation, Chiayi, Taiwan

**Introduction:** We present a case with breast cancer with synchronous multiple stomach, colon and bone metastases on FDG PET/CT.

**Case report:** A 52-year-old woman had non-painful palpable hard mass about 5.5 x 6 x 1 cm for years, weight loss (80 to 62 kg), lower appetite, bilateral loin to low back pain, and loose stool passage in the antecedent two months. Mammography showed right breast stationary UOQ focal asymmetry and small round calcification, BIRADS category 2. FDG PET/CT was arranged for her unexplained weight loss and cancer origin investigation. It showed uptake to stomach, cecum, T-colon, right breast, right axillary lymph nodes, axial and appendicular skeletons. Bone marrow biopsy of right iliac crest showed metastatic carcinoma, compatible with invasive lobular carcinoma (ILC) of breast in origin. Panendoscopy showed two gastric polypoid lesions and colonoscopy showed edematous and subepithelial tumor-like appearance at cecum and T colon; biopsy of two gastric lesions, cecum and T-colon all showed metastatic poorly differentiated carcinoma, consistent with breast origin. Core needle biopsy of right lower lateral breast showed ILC.

**Discussion:** ILC of the breast accounts for 6% to 10% of all breast cancers. When comparing invasive ductal carcinoma, which tends to metastasize to lungs, liver, brain and bones, with ILC that frequently affects bones, gynecological organs, peritoneum, retroperitoneum, and GI tract. Differentiating GI metastasis from breast cancer from primary colon cancer may be challenging. Clinical presentations are diverse and nonspecific, such as abdominal pain, diarrhea, weight loss, GI bleeding, bowel obstruction, poor appetite, and nausea, mimicking other GI diseases. These add to the diagnostic challenge. Synchronous multiple stomach, colon and bone metastases from breast cancer diagnosed simultaneously, such as our case, is even rare. Although FDG PET is not as sensitive as IDC to detect ILC, metastases of ILC are FDG avid and that negative results correlate well with absence of metastatic disease. It also can be the tool to assist the diagnosis of GI metastases, in addition to CT and endoscopy.

PC-054

## Silicone Granulomas with Diffusely Increased FDG Uptake in a Breast Cancer Patient: A Case Report

Xuan-Ping Lu, Jui-Hung Weng, Pan-Fu Kao

*Department of Nuclear Medicine, Chung Shan Medical University Hospital, Taichung, Taiwan*

**Introduction:** Breast implant rupture is categorized as intracapsular and extracapsular. Extracapsular rupture is often associated with silicone migration. Leaked silicone may remain within the breast or migrate to axillary and sometimes internal mammary nodes. The leaked silicone may provoke the immune system to separate the foreign material, which results in a siliconoma.

**Methods:** We reported a breast cancer patient who had received right partial mastectomy one year prior to the scan and silicone augmentation years ago. FDG-PET scan was performed after fasting for 6 hours with a GE Discovery MI PET/CT scanner at 60 min after intravenous injection of F-18- FDG. The CT scan is low-dose without contrast enhancement. The scan area covers vertex to above knees. Images are reconstructed iteratively with attenuation correction.

**Results:** FDG-PET/CT scan demonstrated diffusely increased FDG uptake at bilateral breasts with scattered small calcifications. Breast MRI also demonstrated a speculated lesion about 1.5 cm in right axilla. The lesion was then excised and the pathology report showed prominent fibroblastic stroma with granulation tissue and multinucleated giant cells.

**Conclusions:** Breast cancer patients are often followed up with FDG-PET/CT to detect local recurrence and metastasis. Any abnormal uptake should be interpreted with caution as it may represent a malignancy and should be correlated with histopathologic findings.



PC-055

## Reactive Lymphadenopathies in Axilla Following COVID-19 Vaccination on Oncologic FDG PET: Characteristics and Clinical Implication

Jui-Hung Weng<sup>1,2</sup>, Pan-Fu Kao<sup>1,2</sup>

<sup>1</sup>Department of Nuclear Medicine, Chung Shan Medical University Hospital, Taichung, Taiwan

<sup>2</sup>School of Medicine, Chung Shan Medical University, Taichung, Taiwan

**Introduction:** In Taiwan, COVID-19 vaccines had been first available since Mar. 2021. Reactive lymphadenopathies in axilla on oncologic FDG PET studies in examinee who had received vaccination recently have been encountered in clinical practice. A retrospective analysis was conducted to this population to investigate the characteristics and clinical implication in this setting.

**Methods:** 283 consecutive examinee who underwent oncologic FDG PET/CT study by using a GE Discovery MI digital PET/CT scanner with a routine protocol during Jul. 01 to Aug. 25, 2021 were retrospectively enrolled in this study. History of if vaccinated recently and injection site were collected. SUVmax of visible axillary lymph node with higher uptake than mediastinum, either early only or both early and delay, were recorded. For visible LAPs, either reactive or metastatic in nature was determined by a board certified experienced nuclear medicine physician. Two sample t test was used to determine if the difference of average SUVmax early/delay and % SUVmax increment between the two groups are significant.

**Results:** 55 examinee (9.4%) had increased uptake in lymph nodes at least in unilateral axilla, with 9 bilateral, 10 right and 36 left. Among the 283 examinee, 67 of 161 people had recent vaccination. 29 of 67 people had lymph node(s) with increased uptake were probably resulted from recent vaccination, suggested an incidence of 47% (29/67) for reactive lymphadenopathies following vaccination. For reactive LAPs, The average SUVmax early of 25 was 3.89, SUVmax delay of 12 was 6.75, % increment of 12 was 107.7%. For metastatic LAPs, the average SUVmax early of 15 was 10.05, SUVmax delay of 8 was 8.89, and % increment% of 8 was 41.8%. The abovementioned parameters of each group were all significantly different between each other. Only 3.6% (2/55) visible LAPs seemed equivocal on FDG PET.

**Conclusions:** Vaccine-reactive and metastatic LAPs are distinguishable on FDG PET/CT scan. However, careful history review and avoiding FDG injection in ipsilateral limb with either prior vaccination, lymph node metastasis or surgical intervention are the mainstay of unequivocal FDG PET studies.

PC-056

## 口腔癌患者於正子電腦斷層造影 運用紗布作為輔助之可行性評估

藍瑋承 王婉麗 周易賢

國立臺灣大學醫學院附設醫院雲林分院核子醫學部

**背景介紹：**正子電腦斷層掃描 (PET/CT) 結合正子掃描 (PET) 及電腦斷層 (CT)，是目前臨床上廣泛應用於癌症診斷、評估分期、再分期與復發的實用影像工具，透過 CT 影像提供的衰減校正和解剖資訊，可確定腫瘤的位置與分期。然而，正子影像常常難以精確區分兩頰側組織與齒齦處，原因在於解剖構造上的接近。

因此本研究評估口腔癌患者在執行 PET/CT 時，使用紗布做為顏面口腔病灶與鄰近牙周組織的間隔物之可行性。

**方法：**考慮間隔物的材質不會使病患在長時間造影過程中感到不舒服而造成頭部移動。因此使用紗布作為輔助工具，且其質地柔軟、易塑形、能吸附口水、成本低亦不會影響影像品質。

造影前放射師將 4 英吋 × 4 英吋的紗布捲成棒狀，無論口腔病灶為單頰側或雙頰側，請病患自行於口腔兩側皆填塞紗布進行檢查。在開啓自動管電流調控之下進行頭頂至大腿中段電腦斷層掃描之後，正子影像使用在頭部段為 0.7 mm/s 速度進行影像蒐集，完成後請醫師判讀影像評估其可行性。

**結果：**比較同一位頭頸癌患者的影像，包含未使用紗布當作口腔間隔物以及使用紗布後將兩頰側肌肉與病灶組織間隔開來的頭部正子和電腦斷層影像。

後者在融合影像上能明顯區分出病灶位置及範圍，且使用紗布作為間隔材料在電腦斷層影像上並未造成假影，亦不會造成患者於造影過程的不適感，亦改善病灶感興趣區域圈選處的標準攝取值 (standard uptake value)。

**結論：**紗布適合做為口腔癌患者於顏面病灶與鄰近牙周組織的間隔物，讓醫師在口腔癌患者的診斷和分期評估上更加準確。

PC-057

## Improving Evaluation of Primary Gastric Malignancy by Dual Time-Point F-18 FDG PET/CT: A Case Report

Chao-Jung Chen<sup>1</sup>, Er-Jung Hsueh<sup>2</sup>, I-Tsou Tseng<sup>3</sup>

*Departments of<sup>1</sup>Nuclear Medicine,*

*<sup>2</sup>Haematology-Oncology, and*

*<sup>3</sup>General Surgery, Yuan's General Hospital, Kaohsiung, Taiwan*

**Introduction:** Gastric cancer is the fourth most commonly diagnosed cancer and the second most common cause of cancer-related death worldwide. The F-18 fluorodeoxyglucose positron emission tomography/computed tomography (F-18 FDG PET/CT) has proven to be useful in the diagnosis and evaluation of various malignancies. However, its value in staging gastric carcinomas is still controversial. We herein present a case of advanced gastric cancer with a hepatic metastatic lesion seen in the delayed images on a dual time-point F-18 FDG PET/CT.

**Case report:** A 72-year-old man was diagnosed as gastric cancer and the staging by contrast-enhanced abdominal CT is T3N1M0. F-18 FDG PET/CT was performed for a systemic survey. At the 1-hour post-injection F-18 FDG PET/CT image, it showed a hypermetabolic tumor in the gastric antrum with several locoregional lymph nodes which were the same in the abdominal CT. In addition, a suspicious hypermetabolic focus in the liver was also noted. Subsequent 1st and 2nd delayed images confirmed the hepatic lesion. Surgical intervention was done and the final pathological staging for the stomach cancer is pT4bN3aM1 with a confirmation of the hepatic metastasis.

**Discussion:** It is reported that there is a visually and statistically significant increase in the number of detected lesions seen in delayed images and dual time-point F-18 FDG PET/CT imaging seems useful in detecting primary and metastatic lesions in gastric cancer. In our case, the hepatic lesion is equivocal at the early image and it did present more apparent at the delayed images. F-18 FDG PET/CT was more sensitive than contrast-enhanced CT in detecting the hepatic metastasis in the patient, but abdominal magnetic resonance imaging (MRI) found more metastases in the liver. Nonetheless, F-18 FDG PET/CT provided more useful information than the abdominal CT and changed the treatment plan. The extra finding of the hepatic nodule warranted further evaluation such as abdominal MRI.

**Conclusion:** The presented case showed an equivocal hepatic nodule in the early study and became more evident in the delayed images. Dual time-point F-18 FDG PET/CT imaging seems helpful and necessary in detecting potential metastatic lesions in gastric cancer. It may provide more information than contrast-enhanced CT and lead to changes in the treatment strategy.

PC-058

## Prognostic Significance of Preoperative Evaluation with Positron Emission Tomography in Esophageal Cancer After Neoadjuvant Therapy: A Nationwide Population-Based Study

Hsi-Huei Lu<sup>1</sup>, Mu-Hung Tsai<sup>2</sup>, Nan-Ching Chiu<sup>1</sup>

<sup>1</sup>Department of Medical Imaging, National Cheng Kung University, Tainan, Taiwan

<sup>2</sup>Department of Radiation Oncology, National Cheng Kung University, Tainan, Taiwan

**Introduction:** <sup>18</sup>F-FDG PET/CT plays an important role in treatment response evaluation of esophageal cancer. Despite its limited ability to discriminate residual disease from post-treatment inflammation, early detection of disseminated disease remains crucial in preoperative survey. The purpose of this study is to evaluate the prognostic significance of preoperative PET in esophageal cancer following neoadjuvant therapy.

**Methods:** We utilized the Taiwan Cancer Registry (TCR) and National Health Insurance Research Database (NHIRD) to select newly diagnosed non-metastatic esophageal squamous cell carcinoma patients from 2009 to 2015 who were treated with neoadjuvant therapy and underwent subsequent operation. Preoperative PET was defined by the presence of PET between neoadjuvant therapy and operation. Overall survival was calculated from the first day of treatment to date of death, or censored on December 31, 2018 if a record of death could not be found. Survival curves between patients with and without preoperative PET were compared using the log-rank test.

**Results:** A total of 1459 patients were included in this study (451 with preoperative PET and 1008 without preoperative PET). The median follow-up time for patient with and without preoperative PET were 3.01 years and 2.22 years, respectively. After adjusting for sex, age, stage, tumor location and tumor grade, patients with preoperative PET had a lower risk of death compared with those without preoperative PET (hazard ratio = 0.85 [95% confidence interval: 0.73-0.98], p = 0.03).

**Conclusions:** The utilization of preoperative <sup>18</sup>F-FDG PET in esophageal squamous cell cancer after neoadjuvant therapy was associated with a lower risk of death, which may attribute to improved prediction of tumor response, detection of interval distant metastasis, or more precise operation modifications.

PC-059

## Polycystic liver 之肝臟轉移在 PETCT 之病例報告

沈淑禎<sup>2</sup> 姚維仁<sup>4</sup> 門朝陽<sup>1</sup> 曾柏銘<sup>1</sup> 呂建璋<sup>2</sup> 林雅婷<sup>2</sup> 蕭聿謙<sup>3</sup>

<sup>1</sup> 天主教中華聖母修女會醫療財團法人天主教聖馬爾定醫院正子造影中心

<sup>2</sup> 天主教中華聖母修女會醫療財團法人天主教聖馬爾定醫院核子醫學科

<sup>3</sup> 亞東紀念醫院核子醫學科

<sup>4</sup> 戴德森醫療財團法人嘉義基督教醫院核子醫學科

**前言：**Polycystic liver 在人口比率大約佔 5%，大多為良性，但在 polycystic liver 發生肝轉移的病例報告很少見，在診斷是一大挑戰，我們報告一個乳癌病人，在治療期間兩次 PET/CT 影像，發生肝臟轉移的影像變化。

**案例報告：**病人，38 歲女性，六年前兩邊乳房發現乳癌，經開刀後，在治療追蹤期間，發現癌症指數持續升高，CEA (105/05 為 2.5；110/05 為 7.7；110/07 為 17.9)，CA-153 (105/05 為 9.5；109/12 為 278；110/04 為 204；110/08 為 653)，第一次 PET/CT (109/12) 發現多處骨骼轉移，110/05 做了電腦斷層只顯示 Polycystic liver 並無明顯的肝轉移，110.08 做第二次 PET/CT 發現骨骼轉移惡化，肝臟部份發現多處 FDG 吸收增加，均在 cyst 的外圍組織，FDG uptake SUV 變化從原第一次 PET 檢查的 3.13 升至 16.24；2.09 升至 34.83，Spine T9 從 7.4 升至 10.72；L1 由 5.87 升至 11.29。

**討論：**PET/CT 用於診斷乳癌病人的肝轉移一般有高的敏感度。CT，MRI 也常用於肝轉移的診斷，在此病人的追蹤期間，電腦斷層並無發現肝臟轉移，因此病人併發有 Polycystic liver disease，因此在影像上的肝轉移比較複雜而不易偵測，此一病例在兩次的 PET/CT 影像可見明顯的 SUV 變化，且集中在 cystic lesion 周圍的肝組織，且臨床上 Tumor marker 急劇增加，及肝臟轉移之明顯惡化等臨床徵兆，因可推斷為肝臟轉移。

**結論：**大部份的肝臟轉移，影像上的表現多為一或多個 solid mass，CT，MRI 診斷的靈敏度均高，但複雜的病例如合併 Polycystic liver 則較不易診斷，利用 PET/CT FDG 吸收的不同，可以幫助臨床上做更早期的診斷。而進一步的做病理切片可得確認診斷。

PC-060

## 回溯性分析 [F-18]FLT 正子電腦斷層掃描 於頭頸癌患者之生理分布

王靖誼<sup>1,2</sup> 翁瑞鴻<sup>1</sup> 張白容<sup>1</sup> 高潘福<sup>1,3</sup> 陳健懿<sup>2</sup>

<sup>1</sup> 中山醫學大學附設醫院核子醫學科

<sup>2</sup> 中山醫學大學醫學影像暨放射科學系

<sup>3</sup> 中山醫學大學醫學系

**背景介紹：**目前臨床常用的正子藥物仍以 2-[F-18]Fluro-2-deoxy-D-glucose (<sup>18</sup>F-FDG) 為主，但其對感染、發炎等易造成偽陽性現象，且缺乏對腫瘤偵測之特異性而有所侷限。不受控制的細胞分裂是惡性腫瘤的特性，3-deoxy-3-[F-18]-fluorothymidine (<sup>18</sup>F-FLT) 已被證實與腫瘤增殖性有關。FLT 藥物自 1998 年發表第一篇研究報告以來，國內的相關研究甚少，本研究旨在於藉由回溯性的分析影像，建立器官參考值，以期提供核醫科醫師判讀影像之參考依據。

**方法：**病人注射 FLT 藥物後〈劑量約 0.1 mCi/kg〉休息 60 分鐘，透過 GE Discovery MI PET/CT System 擷取影像〈2 min/bed〉，利用後處理工作站 GE AW Server 3.2 進行 SUV mean 的量測。回溯性分析 60 位頭頸癌患者之影像，排除參考器官具有疾病之案例，分別於腦部、肺部、肝臟、血池（主動脈或內頸動脈）、脾臟、肌肉（腰大肌）、骨髓（腰椎第五節）、以及腎皮質處圈選感興趣區 (ROI)，量測體積直徑大小分別為 3、3、3、2、2、1.5、1.5 及 1 公分之球體。計算 SUV 於各器官之平均值及標準偏差。

**結果：**60 位患者平均注射劑量為  $6.48 \pm 1.12$  mCi，量測結果 SUV mean 為：腦部  $0.19 \pm 0.06$ 、肺部  $0.27 \pm 0.10$ 、肝臟  $5.11 \pm 1.41$ 、血池  $0.58 \pm 0.17$ 、脾臟  $2.29 \pm 1.03$ 、肌肉  $0.75 \pm 0.19$ 、骨髓  $8.44 \pm 2.07$  以及腎皮質  $3.72 \pm 1.42$ 。

**結論：**透過這些器官的量測，建立參考數值範圍，除了可了解 FLT 於正常器官吸收累積的情形，實際量化後的數據在未來 FLT PET/CT 檢查普及化後，亦可提供核醫科醫師在影像判讀上的參考。

PC-061

## The Efficacy of $^{18}\text{F}$ -FDG PET/CT and Physical Examination for Assessment of Neck Disease in Patients with Head and Neck Cancer

Bor-Tau Hung, Pei-Ing Lee, Yu-Yi Huang

*Department of nuclear medicine, Koo foundation Sun Yat-Sen Cancer Center*

**Purpose:** To compare the sensitivity, specificity, PPN, and NPV of PET/CT and physical exam (clinical nodal staging) in the preoperative prediction of the presence of neck disease in patients with head and neck cancer.

**Methods:** Patients with head and neck cancer were enrolled between January 2019 and October 2020 at Koo foundation Sun Yat-Sen cancer center. Patients with NPC or thyroid cancer were excluded. Among the remaining 223 cases who received  $^{18}\text{F}$ -FDG PET/CT for staging or restaging of head and neck cancer, 138 cases without neck dissection were also excluded. Finally, 85 reports of the PET/CT study were collected and images were selectively reviewed. The standard of reference for a positive node was the presence of tumor at histopathologic examination. The presence of tumor in any node defined that side of the neck as positive for disease.

**Results:** Of the 85 patients enrolled in the study, 54 had a clinically negative neck, 31 had a clinically positive neck. The overall sensitivity, specificity, PPN, and NPV was 96%, 53%, 71%, and 91%, respectively, for PET/CT identification of neck disease. The overall sensitivity, specificity, PPN, and NPV was 64%, 97%, 97%, and 69%, respectively, for clinical nodal staging. PET/CT was superior in sensitivity and NPV ( $p < 0.05$ ). On the contrary, clinical nodal staging was superior in specificity and PPV ( $p < 0.05$ ). In the subgroup of patients with a clinically negative neck, the sensitivity, specificity, PPN, and NPV was 88%, 54%, 44%, and 91%, respectively, for PET/CT identification of neck disease.

**Conclusions:** Imaging by PET/CT is complementary to the clinical exam for the staging and restaging of the neck lymph nodes. PET/CT evaluation results in frequent false-positive assessment of regional nodes. It is very sensitive, though not specific, for neck disease, even in patients with a clinically negative neck.

PC-062

## Evaluation of the Feasibility of 24-hr Discharge of Patients Treated with I-131

Chien-Hua Lu<sup>1</sup>, Chiang-Hsuan Lee<sup>2</sup> (Corresponding Author: Chiang-Hsuan Lee)

<sup>1</sup>*Division of Nuclear Medicine, Chi Mei Medical Center, Liouying, Tainan, Taiwan*

<sup>2</sup>*Division of Nuclear Medicine, Chi Mei Medical Center, Tainan, Taiwan*

**Purpose:** The hospital currently takes I-131 to treat inpatients with an average stay of 2 to 4 days. In response to the increasing number of inpatients taking I-131 treatment, to evaluate the shortening of the number of hospital stays in order to increase the number of hospitalizations.

**Methods:** If the patient's hospital stay cannot be accurately determined, it will affect the withdrawal and withdrawal of other treatment patients. The treatment time, according to the current domestic standards for the release of I-131 inpatients and discharges from the hospital, each hospital has different reference standards and documentary basis. If the average number of days of hospitalization is determined according to the standard and compared with the actual detected exposure dose rate, the time for patients to be admitted to the hospital can be effectively scheduled and the utilization rate of the ward can be improved. Therefore, statistics from 107.01.02. to 110.07.02. For patients receiving hospitalized I-131 80-200 mCi dose drug treatment, the radiation exposure dose rate at 1 m 24 hrs after taking the drug is used as a reference indicator to evaluate the hospitalization. The feasibility of 24-hr discharge, patients are given proper health education before hospitalization. In the process, the ATOMTEX AT1121 scintillation detector is used to detect the radiation exposure dose.

**Results:** A total of 303 person-times were counted. The radiation exposure rates were all between 3.3–72 mSv/hr, and the average dose rate was 27.84 mSv/hr, which were lower than those of patients. The standard of external release dose.

**Conclusion:** According to the external release standard, the radioactive intensity of the patient, the exposure rate at 1 m is less than 11 mR/hr within the release intensity range of this item, and some family members are under 45 yrs old. Under proper guidance and control, the patient can be released and discharged from the hospital. Based on the dose rate calculated in this assessment, the patient can be released from the hospital after taking the I-131 drug within 24 hrs.



PC-063

## The First Experience of Peptide Receptor Radionuclide Therapy with Lutetium-177 DOTATATE in Taipei Veterans General Hospital-A Patient with Neuroendocrine Tumor of Rectum

Tse-Hao Lee<sup>1</sup>, Chih-Yung Chang<sup>1</sup>, Shan-Fan Yao<sup>1</sup>, Bang-Hung Yang<sup>1</sup>,  
Wen-Yi Chang<sup>1</sup>, Chih-Hwa Chen<sup>1</sup>, Ming-Huang Chen<sup>2</sup>,  
Wen-Sheng Huang<sup>3</sup>, Nan-Jing Peng<sup>1</sup>

<sup>1</sup>Department of Nuclear Medicine, Taipei Veterans General Hospital, Taipei, Taiwan

<sup>2</sup>Department of Oncology, Division of Medical Oncology, Taipei Veterans General Hospital, Taipei, Taiwan

<sup>3</sup>Department of Nuclear Medicine, Taipei Medical University Hospital

**Introduction:** This is a 52 year-old woman who was diagnosed of neuroendocrine tumor of the rectum, which initially presented increased mucus discharge from anus for about 1 year, feeling of tenesmus and an episode of anal bleeding when defecation in. Colonoscope revealed a tumor at rectum and biopsy revealed neuroendocrine tumor. She received laparoscopic low anterior resection of rectum and the final pathological diagnosis was rectal neuroendocrine tumor, T2N0Mx. Four months later, she was then diagnosed of hepatic metastasis of neuroendocrine tumor, for which biopsy was done and the pathology report revealed strong expression for somatostatin receptor subtype 2A (SSTR2A). She received radiofrequency ablation (RFA) and trans-arterial embolization (TAE), respectively for hepatic metastasis and started octreotide therapy. However, follow-up MRI revealed progression of hepatic metastasis. Peptide Receptor Radionuclide Therapy (PRRT) with Lutetium-177 DOTATATE (<sup>177</sup>Lu- DOTATATE) was considered.

**Methods:** Laboratory data including complete blood count (CBC) with differential count (DC), renal function and liver function all revealed within normal range. She received pre-medication with anti-emetics and H2 blocker. Amino acid including Arginine and Lysine was intravenously administered to the patient for total four hours. At least 30 minutes after starting amino acid infusion, <sup>177</sup>Lu-DOTATATE was intravenously administrated to the patient for 40 minutes using gravity method.

**Results:** The whole course of <sup>177</sup>Lu-DOTATATE administration concomitant with amino acid administration was smooth. After finishing <sup>177</sup>Lu-DOTATATE infusion, we continued and completed four-hour course of amino acid administration. No acute or delayed nausea or vomiting was noted. There was no symptom or sign suspicious hormone crisis.

**Conclusions:** One day after PRRT therapy, she received planar scintigraphy of gamma ray emission from <sup>177</sup>Lu-DOTATATE. Due to the stable condition, she was discharged.

PC-064

## The Prognostic Value of $^{18}\text{F}$ -FDG PET in Patients with Advanced Small Cell Lung Cancer

Yu-Hung Chen<sup>1,2</sup>, Sung-Chao Chu<sup>3</sup>, Kun-Han Lue<sup>4</sup>,  
Sheng-Chieh Chan<sup>1,2</sup>, Shu-Hsin Liu<sup>1,4</sup>

<sup>1</sup>*Department of Nuclear Medicine, Hualien Tzu Chi Hospital, Buddhist Tzu Chi Medical Foundation,  
Hualien 97002, Taiwan*

<sup>2</sup>*School of Medicine, College of Medicine, Tzu Chi University, Hualien 97002, Taiwan*

<sup>3</sup>*Department of Hematology and Oncology, Hualien Tzu Chi Hospital, Buddhist Tzu Chi Medical Foundation,  
Hualien, Taiwan*

<sup>4</sup>*Department of Medical Imaging and Radiological Sciences, Tzu Chi University of Science and Technology,  
Hualien, Taiwan*

**Introduction:** Small cell lung cancer (SCLC) only accounts for 15% of all lung cancer cases, and the prognosis is less favorable than non-small cell lung cancers (NSCLC). Many studies have shown that the  $^{18}\text{F}$ -FDG PET features can predict survival outcomes in NSCLC. However, the prognostic value of  $^{18}\text{F}$ -FDG PET features is less studied in SCLC.

**Methods:** We retrospectively analyzed 44 patients with a diagnosis of stage III-IV SCLC. All patients underwent pre-treatment  $^{18}\text{F}$ -FDG PET. We extract image features including primary tumor  $\text{SUV}_{\text{max}}$ , MTV, TLG, SUV entropy, sum entropy (from gray-level co-occurrence matrix), and small area emphasis (SAE). We also recorded the pre-treatment staging status (using the 8th edition of the AJCC staging manual) for analysis. We analyzed the effect of study variables on the overall survival (OS) and progression-free survival (PFS) using Cox regression analysis (continuous variables were not dichotomized).

**Results:** Eighteen and 26 patients were initially diagnosed with stage III and stage IV status, respectively. The median follow-up period was 12.0 months (0.8-84.4 months). Among all 44 patients, 38 patients died during follow-up. The estimated median PFS and OS were 6.6 and 11.7 months, respectively. In the univariate and multivariate Cox regression analysis, only MTV was the significant and independent predictor of PFS (HR = 1.004, 0.022) and OS (HR = 1.005,  $p = 0.008$ ).

**Conclusions:** Our results showed that the MTV is predictive of survival outcomes in SCLC. The prognostic potential of  $^{18}\text{F}$ -FDG PET feature in patients with SCLC warrant to be explored in a larger prospective cohort.

PC-065

## The Glycolytic Features Extracted from $^{18}\text{F}$ -FDG PET are Correlated with Morphological Features of Surgical Pathology in Lung Adenocarcinoma

Yu-Hung Chen<sup>1,2</sup>, Yen-Chang Chen<sup>2,3</sup>, Ming-Hsun Li<sup>3</sup>,  
Sung-Chao Chu<sup>4</sup>, Kun-Han Lue<sup>5</sup>

<sup>1</sup>Department of Nuclear Medicine, Hualien Tzu Chi Hospital, Buddhist Tzu Chi Medical Foundation, Hualien 97002, Taiwan

<sup>2</sup>School of Medicine, College of Medicine, Tzu Chi University, Hualien 97002, Taiwan

<sup>3</sup>Department of Anatomical Pathology, Hualien Tzu Chi Hospital, Buddhist Tzu Chi Medical Foundation, Hualien

<sup>4</sup>Department of Hematology and Oncology, Hualien Tzu Chi Hospital, Buddhist Tzu Chi Medical Foundation, Hualien, Taiwan

<sup>5</sup>Department of Medical Imaging and Radiological Sciences, Tzu Chi University of Science and Technology, Hualien, Taiwan

**Introduction:**  $^{18}\text{F}$ -FDG PET is able to measure the glycolytic feature of lung adenocarcinoma, and the uptake intensity correlates with pathological grade. However, using novel radiomic  $^{18}\text{F}$ -FDG PET features to assess heterogeneity is currently hypothetical and has not been compared with other phenotypical studies.

**Methods:** We retrospectively analyzed 69 patients with lung adenocarcinoma underwent curative surgery. We extract pre-treatment  $^{18}\text{F}$ -FDG PET features, including primary tumor  $\text{SUV}_{\text{max}}$  and first-order entropy. We record the fraction of each pathological subtype (lepidic, acinar, papillary, micropapillary, and solid) and tumor grade from the surgical pathology. The heterogeneity index (HI) of pathology was calculated from the fraction of pathological subtypes of each tumor. The correlation between primary tumor entropy and HI of pathology was analyzed with Pearson's correlation. Also, we compare with image features between different pathological grades using t-test.

**Results:** The primary tumor entropy significantly correlated with pathological HI ( $r = 0.242$ ,  $p = 0.045$ ). Also, the entropy significantly differed between grades and showed ascending orders in grades 1 (2.3), 2 (3.0), and 3 (3.6). The mean primary tumor  $\text{SUV}_{\text{max}}$  also showed ascending orders in grades 1 (3.1), 2 (5.5), and 3 (9.2). The differences of  $\text{SUV}_{\text{max}}$  between grades were significant except for grade 2/3 ( $p = 0.073$ ).

**Conclusions:** The  $^{18}\text{F}$ -FDG PET entropy significantly correlates with morphological heterogeneity of pathology. Our study provides support for the use of entropy as a heterogeneity biomarker. Also, both entropy and  $\text{SUV}_{\text{max}}$  are related to differentiation. Further study on tumor genetics is warranted to decipher the connection between genotypical and different phenotypical heterogeneity features.

PC-066

## Diagnostic Performance of $^{18}\text{F}$ -FDG PET/CT for Assessing Mediastinal Lymph Node Metastasis in Lung Adenocarcinoma

Pei Ing Lee, Yu-Yi Huang, Bor-Tau Hung

*Department of Nuclear Medicine, Koo Foundation Sun Yat-Sen Cancer Center, Taipei, Taiwan*

**Introduction:** The aim of this study is to assess the efficacy of FDG PET/CT on mediastinal and hilar nodal staging of lung adenocarcinoma, and to investigate other variables that predict lymph node (LN) metastasis.

**Methods:** This retrospective study included all patients with lung adenocarcinoma who underwent pre-operative F-18 FDG PET/CT and lobectomy or segmentectomy with lymph node dissection between January 2017 and December 2018. Mediastinal or hilar LN stations were considered positive on FDG PET/CT if they exhibited focal and asymmetrical increased FDG uptake higher than mediastinal blood pool activity. They were considered negative if FDG uptake was lower than mediastinal blood pool activity, or if FDG uptake in mediastinum was symmetrical. Mediastinal and hilar nodal metastasis was pathologically defined and classified according to the 8th edition of International Association for the Study of Lung Cancer (IASLC) lymph node map.

Nodal-station based analysis was performed, comparing FDG PET/CT findings and other variables (tumor SUVmax, tumor size, serum CEA level) with histopathology results. The optimal cutoff value for each parameter was determined using receiver operator characteristic curve analysis.

**Results:** One hundred and two patients with a total of 401 nodal stations were included. Sixty-one patients had T1 disease, 31 had T2, 6 had T3 and 4 had T4 disease. Mediastinal or hilar LN metastasis was found in 23 patients (22.5%). Of 401 nodal stations resected, 43 LN stations (10.7%) were positive for metastasis. FDG PET/CT demonstrated 30.2% sensitivity, 96.2% specificity, 54.2% positive predictive value, 92.1% negative predictive value and 89.8% accuracy for detecting mediastinal or hilar LN metastasis. The combined use of all 3 variables (SUVmax cut-off of 9.6, tumor size of 3.4 cm, serum CEA level of 5 ng/ml) yielded 93% sensitivity, 60% specificity, 74% positive predictive value, 89% negative predictive value and 86% accuracy for predicting nodal metastasis.

**Conclusions:** Our results showed that FDG PET/CT has a low sensitivity but favorable specificity and accuracy for detecting mediastinal or hilar LN metastasis in lung adenocarcinoma. Patients with high tumor SUVmax, tumor size and serum CEA level pose greater risk for developing LN metastasis.

PC-067

## Tuberculosis Pericarditis in Lung Cancer Patient on FDG PET/CT

Szu-Han Chang<sup>1</sup>, Yu-Chuan Chang<sup>1,2</sup>

<sup>1</sup>*Department of Nuclear Medicine and Molecular Imaging Center, Chang Gung Memorial Hospital at Linkou,  
Taoyuan, Taiwan*

<sup>2</sup>*Department of Medical Imaging and Radiological Science, College of Medicine, Chang Gung University,  
Taoyuan, Taiwan*

**Introduction:** FDG PET/CT is useful in the initial non-small cell lung cancer (NSCLC) staging, identifying more patients with mediastinal and extrathoracic disease than conventional staging and reduces both the total number of thoracotomies and the number of futile thoracotomies. NCCN guidelines recommend the use of FDG PET/CT to differentiate true malignancy from benign conditions such as atelectasis, consolidations, and radiation fibrosis detected on standard CT. We describe a case of tuberculous pericarditis that showed markedly increased FDG uptake with history of NSCLC.

**Case report:** This 68-year-old male had history of left lung cancer large cell neuroendocrine carcinoma, staging T4N3M0 at 2018 with complete response after radiation therapy, fractionated dose of cisplatin and vinorelbine. This time, he suffered from productive cough with sputum and dyspnea. CT showed bilateral pleural effusion but cytology demonstrated negative for malignancy. FDG-PET was arranged in July, 2021, showing pericardial effusion with peripheral FDG uptake, and pleural effusion combine with nodules with FDG uptake. Besides, enlarge lymph nodes with FDG uptake was found at hilar, mediastinum, right supraclavicular, celiac and aortocaval regions, indicating recurrent lung cancer. He had cardiogenic shock and thoracoscopic pericardial window surgery was performed. Pericardium and pleural biopsy reports both revealed granulomatous inflammation. Although acid fast stain was all negative and no growth of sputum culture for TB, his condition improves after anti-TB therapy.

**Conclusions:** There were few case reports about tuberculous pericarditis in FDG PET. In this case, tuberculosis pericarditis was misinterpreted as recurrent malignancy in cancer patient with pericardial effusion with FDG uptake, tuberculous pericarditis should be taken into consideration.

PC-068

## Lymphoscintigraphy Guided Sentinel Lymph Node Biopsy in the Patients with Oral Cavity Squamous Cell Carcinoma

Yu-Li Chiu<sup>1,2</sup>, Ching-Chih Lee<sup>3</sup><sup>1</sup>*Department of Nuclear Medicine, Kaohsiung Veterans General Hospital, Kaohsiung, Taiwan*<sup>2</sup>*Department of Medical Imaging and Radiology, Shu-Zen Junior College of Medicine and Management, Kaohsiung, Taiwan*<sup>3</sup>*Department of Otolaryngology, Head and Neck Surgery, Kaohsiung Veterans General Hospital, Kaohsiung, Taiwan*

**Introduction:** Sentinel lymph node biopsy (SLNB) is well established and used widely in the treatment of breast cancers and melanomas of the skin, but it remains the subject of debate whether this procedure should be used routinely in clinically and radiologically N0 patients with oral cavity squamous cell carcinoma (OSCC). The aim of this study was to provide high-quality lymphatic mapping using lymphoscintigraphy and guide SLNB for the identification of occult neck metastasis in the patients with OSCC.

**Methods:** Lidocaine hydrochloride 10% spray or a high lingual nerve block (injection just below the mucosa behind the 3rd molar tooth, distant from the tumor site) was applied to reduce the pain of the injection and the risk of patient movement during the radiotracer injection. Tc-99m phytate was administered with four submucosal injections around the cancer at 3, 6, 9, and 12 o'clock. The total injected activity was 2 mCi in a total volume 0.4 ml of saline solution (0.1 ml each syringe). Dynamic images of the neck in anterior view was acquired within 5 minutes after radiotracer injection. Early static images in anterior and lateral views was acquired shortly after dynamic acquisition. Late static images was acquired at 60-120 minutes post-injection if there was no visualization of sentinel lymph nodes (SLNs) in early static images. SPECT/CT was performed immediately after static images if there was visualization of SLN(s) or equivocal finding of static images. Skin marking was done to guide the surgeon to search SLNs.

**Results:** Sixteen patients received 18 lymphoscintigraphy from December 2019 to March 2021. SLNs were detected in 11 patients (11/18, 61.1%) and 3 patients showed contralateral SLNs. Eight patients showed initial visualization of SLNs in dynamic and early static images, 2 in late static images, and 1 in SPECT/CT only. SLNs were not detected in 7 patients (7/18, 38.9%); higher rate of non-visualization of SLNs in the patients with ipsilateral or contralateral neck dissection before (4/7 vs. 3/11). Six patients received SLNB (1 used methylene blue), and 8 patients received SLNB and neck dissection (1 used methylene blue). Nodal status was upstaged in 4 patients; 3 by SLNB and 1 by neck dissection. No patients had nodal recurrence during follow-up (at least 4 months).

**Conclusions:** Dynamic images were useful to reconfirm the location of the first node in the subsequent static image. Late static images could identify SLNs that received a somewhat slower direct drainage from the tumors. SPECT/CT not only provided the exact nodal stations of SLNs but also identified additional LNs.

PC-069

## The Robust Value of FDG PETCT in Diagnosis and Stage of Esophageal Cancer with SCC—role of Central Necrotic Lymph Nodal Pattern

Yu-Wen Chen<sup>1,5</sup>, Yato Huang<sup>2</sup>, Yii-Cheng Wu<sup>3,5</sup>, Hsien-Pin Li<sup>4,5</sup>, Reu-Sheng Sheu<sup>2,5</sup>

<sup>1</sup>Department of Nuclear Medicine, <sup>2</sup>Department of Radiology, <sup>3</sup>Division of Gastroenterology, <sup>4</sup>Department of Medicine, Division of Thoracosurgery, <sup>5</sup>Department of Surgery, Kaohsiung Medial University Hospital; School of Medicine, Kaohsiung Medical University, Kaohsiung, Taiwan

Esophageal cancer (SCC) is common in south Taiwan, due to special epidemiology.

Exact imaging stage is essentially for treatment strategy (stage IIa/IIb). Therefore, FDG PETCT provides high sensitivity in detection of SCC metabolism, become promising imaging to revise traditional XCT diagnosis.

**Patients and Methods:** From past fifteen months (Nov, 2019 to March, 2021), we collected thirty two patients (31 male and one female; mean age 61 years old). Almost tissue diagnosis was SCC, except one adenocarcinoma after endoscope biopsy. Both XCT and FDG PETCT were diagnosed consequently. FDG PETCT was performed with standard procedure (MIDR, GE). Imaging interpretation was performed by two experienced radiology and nuclear medicine physicians.

**Results:** Almost of half patients are initial S/S with dysphagia and middle third esophageal cancer, therefore, directly adjacent left bronchus and aorta invasion should be interpreted carefully by traditional XCT. The distribution of high FDG avid mass (SUVm 15 above) provide direction of growth risk for T stage. In our cases, over half patients belong to T3 to T4b. FDG PETCT is helpful identified vocal cord palsy due to recurrent laryngeal nerve invasion (T4a). In our experience, FDG PETCT is also important to localize regional T3 on diffuse T2 patient by final EUS diagnosis. FDG PETCT is pivot role in N stage diagnosis, we have around 30% change of stage by dual imaging comparison. In here, we disclose central necrosis growth of metastasis lymph nodes with donut sign in FDG imaging should be added risk by oncologic metabolism.

Metastasis pulmonary nodules is always not FDG avidity, therefore, transitional XCT still plays promised role of diagnosis. In this study, less imaging evidence of bone metastasis by T99m MDP bone scan and XCT, however, heterogeneously increased FDG avid marrow metabolism (SUV m 4) is disclosed in advanced stage patients.

**Conclusion:** FDGPETCT with high resolution CT becomes a promised imaging modality. High sensitivity of FDG avid central necrotic lymph nodes (donut sign) provide risk of prognosis in the esophageal cancer with SCC.

PC-070

## Retroperitoneal Schwannoma Resembles Malignant Peripheral Nerve Sheath Tumor in FDG PET/CT

Yueh Lee, Chuang-Hsin Chiu, Cheng-Yi Cheng, Li-Fan Lin

*Department of Nuclear Medicine, Tri-Service General Hospital and National Defense Medical Center, Taipei, Taiwan*

**Introduction:** Schwannomas are the most common neural sheath tumors but rarely discovered in the retroperitoneal space with very low incidence of malignant transformation, which most often locates over roots of limbs. They are usually incidentally identified by cross-sectional imaging such as CT and MRI. In FDG PET/CT, they mostly present with low FDG uptake. In this case report, we present a case 68-year-old woman who underwent follow-up abdominal CT and MRI, which revealed a 9 cm intra-abdominal mass. FDG PET/CT scan showed high FDG avidity of the mass lesion and raised the concern of malignancy. However, pathologic results after excisional biopsy disclosed benign schwannoma.

**Case report:** A 68-year-old woman with past history of papillary thyroid carcinoma, which was diagnosed and treated 7 years ago in stable condition, presented an 9.7 cm intra-abdominal mass incidentally by contrast-enhanced abdominal CT ordered due to symptom of persistent back soreness. The mass displaced abdominal aorta to the left and showed arterial phase heterogeneous contrast enhancement with focal cystic hypodense area. Subsequent FDG PET/CT revealed maximum SUV of 8.5 of the tumor. Due to suspicion of malignancy raised by imaging findings, surgical resection of the retroperitoneal tumor was performed. The pathological report revealed spindle-like cells arranging in palisading pattern with dominant hypercellular Antoni A areas as the component of the well encapsulated tumor with diffuse expression of S100, as well as hypervascularity. The above results were compatible with benign schwannoma.

**Conclusions:** Functional imaging such as FDG PET might be helpful in the diagnosis of schwannoma. Though literatures implied that weaker FDG-avidity corresponds with lower probability of malignancy, the cutoff value between benign and malignant schwannoma lacks consensus. Benign schwannomas are uncommon in the retroperitoneal space and usually present with relatively low glucose metabolism. The rare presentation with very high SUVmax level like our case remained challenging for imaging diagnosis.



PC-071

## The Application of Dual-Phase Whole Body MIBI Scan and SPECT/CT in Recurrent Parathyroid Carcinoma

Tzyy-Ling Chuang<sup>1,2</sup>, Kuo-Wei Ho<sup>3</sup>, Yuh-Feng Wang<sup>1,2,4</sup>

<sup>1</sup>Department of Nuclear Medicine, Dalin Tzu Chi Hospital, Buddhist Tzu Chi Medical Foundation, Chiayi, Taiwan

<sup>2</sup>School of Medicine, Tzu Chi University, Hualien, Taiwan

<sup>3</sup>Department of Nuclear Medicine, Chiayi Chang Gung Memorial Hospital, Chiayi, Taiwan

<sup>4</sup>Center of Preventive Medicine, Dalin Tzu Chi Hospital, Buddhist Tzu Chi Medical Foundation, Chiayi, Taiwan

**Introduction:** We present a case with parathyroid carcinoma post surgery showed recurrence at dual-phase whole body MIBI scan and SPECT/CT.

**Case report:** A 79-year-old man had two parathyroid carcinoma of left inferior and left perithyroid, pT1(2) N0M0, s/p left thyroidectomy, parathyroidectomy and mediastinal tumor excision on 2017/12/18. Preoperatively, intact-PTH (iPTH) was 2728.2 pg/mL. One day after surgery, iPTH fell to 230.4 pg/mL. However, around 9 months after surgery, iPTH gradually elevated to 561.47 pg/mL. Under the suspicion of recurrence, dual-phase whole body scan 10 and 90 minutes after intravenous injection of 25 mCi Tc-99m MIBI was acquired. There was one abnormal focus with persistent accumulation of radiotracer in the upper mediastinum with no other prominent focus in the whole body survey. Routine neck and chest parathyroid scan showed right thyroid bed visualized in the initial planar image (10 minutes) and gradual washout in the delayed planar images (2 hours). Delayed SPECT/CT localized the persistent abnormal focus in supra-manubrial region. Ultrasound-guided biopsy of anterior neck soft tissue showed recurrent parathyroid carcinoma.

**Discussion:** The etiology of parathyroid carcinoma remains unclear, though a history of multiple endocrine neoplasia, neck radiation, parathyroid adenoma and thyroid cancer, can be its risk factors. Many patients have disease recurrence after resection, with reported rates of 50%-100%. The mean time to recurrence ranges from 2 to 23 years after resection, with frequently within 2-3 years, invading the surrounding tissue and spreading to contiguous structures in the neck. The mainstay of therapy is resection of amenable recurrent disease. Distant metastases may occur via hematogenous spread in 25% of patients, with lung, bone, and liver being the most common sites. Clues that the patient may have parathyroid carcinoma include severe hypercalcemia or extremely high serum PTH levels. SPECT/CT may help to localize the parathyroid carcinoma, while Tc-99m MIBI whole body scan is valuable for detecting metastasis. The diagnosis of parathyroid cancer is quite problematic. A thorough examination to rule-out metastatic disorder may include whole body MRI, CT, bone scan and possibly FDG-PET/CT. We provide a protocol of dual-phase Tc-99m MIBI whole body scan with routine parathyroid scan and delayed SPECT/CT to survey suspicious recurrent parathyroid carcinoma.

PC-072

## Technetium-99m Sestamibi Scintigraphy and SPECT/CT for the Localization of Ectopic Parathyroid Tissue in Superior Mediastinum: A Case Report

Yu-Chien Shiau, Po-Wei Li, Ya-Huang Chen, Chia-Wen Lai, Che-Wei Chang, Chao-Chun Huang, Yen-Wen Wu, Shan-Ying Wang

*Division of Nuclear Medicine, Far Eastern Memorial Hospital, New Taipei, Taiwan*

**Introduction:** Ectopic parathyroid tissue is a relatively rare condition and not so many reports were found in the literature. Their detection is mostly done by CT and some by technetium-99m sestamibi scintigraphy, 18F-fluorocholine PET/CT, or 11C-methionine PET. We report a case of ectopic parathyroid tissue in superior mediastinum detected by technetium-99m sestamibi scintigraphy and SPECT/CT, which may elucidate the clinical usefulness.

**Case report:** The 62 year-old male suffered from skin pruritus and arthralgia for 1 year. He had past history of end stage renal disease, s/p subtotal parathyroidectomy, valvular heart disease, coronary atherosclerosis, hypertension, diabetes mellitus, type 2, paroxysmal atrial fibrillation, gouty arthritis, and duodenal ulcer. Previously, the patient had under PD at FEMH. Two years ago he had renal hyperparathyroidism with iPTH 1334.0 pg/ml and Ca 11.7 mg/dL. Technetium-99m sestamibi scintigraphy and SPECT/CT was done and showed parathyroid adenoma at left superior parathyroid gland and suspected ectopic parathyroid adenoma at right superior mediastinal region. He received subtotal parathyroidectomy. After the surgery, the iPTH level did not dropped, and during regular follow-up, elevated iPTH level 2542 pg/mL was noted. Technetium-99m sestamibi scintigraphy and SPECT/CT was done again and showed a hot nodule with tracer retention, ectopic and located in upper paratracheal region, suspecting ectopic parathyroid adenoma. Neck CT scan revealed a 2.2\* 1.4 cm oval, well-circumscribed nodule in the superior mediastinum. The patient was referred for another surgical intervention of partial sternotomy for anterior mediastinal tumor excision. Pathology showed ectopic parathyroid gland tissue. After surgery the patient was follow-up in OPD.

**Conclusions:** Renal hyperparathyroidism is commonly seen in end stage renal disease and patients with hemodialysis. We present a case whose technetium-99m sestamibi scintigraphy and SPECT/CT was useful in the initial detection of parathyroid adenoma and subsequent localization of ectopic parathyroid tissue in superior mediastinum.

PC-073

## FDG-PETCT Detecting Bone Metastases in a Case of Newly Diagnosed Prostate Cancer with a Negative Bone Scan

Ya-Ju Tsai

*Department of Nuclear Medicine, Taipei Medical University Hospital*

**Introduction:** FDG-PET is less sensitive but more specific than bone scan for bone metastasis in prostate cancer. We reported a case of newly diagnosed prostate cancer with bone metastases detected by FDG-PETCT but Tc-99m MDP bone scan was normal.

**Case report:** A 65-year-old male is a case of newly diagnosed prostate cancer (Gleason score: 4 +3; PSA: 18 ng/ml) with a negative Tc-99m MDP bone scan (figure 1). Chest CT showed bilateral lung nodules. FDG-PETCT was further arranged and revealed FDG-avid prostate tumor, bilateral lung metastases and bone metastases in T10 vertebral body & bilateral acetabula (figure 2). In addition, mild-FDG avid, normal-sized metastatic lymphadenopathies in bilateral pelvic sidewall, exertional iliac & inguinal regions were suspected. The bone metastatic lesions on FDG-PETCT were not detected by bone scan.

**Discussion:** FDG-PETCT is an unsatisfactory imaging modality for prostate cancer due to low FDG avidity of most prostate tumors and interfering urine activity in prostate bed. For detecting bone metastasis in prostate cancer, FDG-PETCT is less sensitive although more specific than bone scan according to previous literatures. But bone scan could be insensitive in bone metastasis limited in bone marrow, small lesions or lesions masking by overlying normal skeletal structures. Some studies showed that FDG-PETCT may be useful in evaluation of advanced primary tumors (Gleason score greater than 7) and metastatic extent in high-risk patients because FDG uptake tended to increase in more aggressive prostate cancer.

**Conclusions:** FDG-PETCT maybe a complementary study to conventional imaging for overall assessment for metastatic disease in high risk prostate cancer.

PC-074

## 奧攝敏正子電腦斷層掃描 在生化復發攝護腺癌之應用 – 病例報告

王雅萍<sup>1</sup> 曾能泉<sup>1</sup> 歐宴泉<sup>2</sup>

<sup>1</sup> 童綜合醫療社團法人童綜合醫院核子醫學科

<sup>2</sup> 童綜合醫療社團法人童綜合醫院泌尿腫瘤中心

**簡介：**攝護腺癌是男性最常見的惡性腫瘤之一，在初次治療後會觀察血清中之特異抗原 (prostate specific antigen, PSA) 數值上升來判斷是否有復發。依據 NCCN Guideline 定義生化復發 (biochemical recurrence, BCR) 為術後 PSA 數值連續兩次上升超過 0.2 ng/mL，或放療後以最低 PSA 數值較最低值上升超過 2 ng/mL，即可以奧攝敏正子電腦斷層造影評估腫瘤全身分布。其示蹤劑是合成的胺基酸正子藥物 (<sup>18</sup>F -Fluciclovine)，在癌細胞復發及轉移病灶可見胺基酸轉運體被攝護腺癌細胞攝取增加而呈現明顯表現。且此藥物優點是它由尿液排出的劑量只有微量甚至無排出，因此不易忽略掉攝護腺床及骨盆腔膀胱周圍的病灶。適用於評估生化復發，並具疫調整後續治療計畫。

**病例報告：**本病例是 73 歲男性攝護腺癌的患者，接受達文西機器人輔助攝護腺癌根治術摘除腫瘤，因術後定期回診追蹤抽血檢測為 PSA: 1.0 ng/mL，2 個月後再回診抽血檢測為 PSA: 2.280 ng/mL，4 個月後再回診抽血檢測為 PSA: 4.263 ng/mL，因連續 2 次以上攝護腺 PSA 濃度上升而懷疑攝護腺癌生化復發，且其他影像檢查沒有發現明顯異狀，因此安排奧攝敏正子電腦斷層掃描，掃描結果為攝護腺切除並無復發，但在右側骨盆腔區域數顆淋巴結 (SUVmax：4.69、7.33、10.62、16.49) 及左側恥骨 (SUVmax：6.70) 有明顯吸收，奧攝敏示蹤劑對此有高度攝取顯示，由這些發現，高度懷疑攝護腺癌已有骨盆腔淋巴結惡性轉移與左側恥骨骨轉移的可能。後續安排患者接受完整放射治療，PSA 指數已降為 1.05 ng/mL。

**結論：**當有攝護腺癌生化性復發，奧攝敏正子電腦斷層掃描能有效協助診斷。所使用的奧攝敏正子示蹤劑，其成分為胺基酸，因此過敏機率極低，藉由攝護腺癌細胞表面大量增加的胺基酸通道被癌細胞吸收代謝，不容易受到尿液活性影響判讀，能呈現更好的影像品質，可以在早期的患者復發階段即確認病灶的部位，輔助臨床醫師據此調整治療計畫。但其造影流程與廣泛使用之正子葡萄糖掃描有顯著不同，需要特別注意。

PC-075

## 利用奧攝敏正子造影 偵測攝護腺癌病人之全身轉移 – 病例報告

蔡沛君<sup>1</sup> 曾能泉<sup>1</sup> 歐宴泉<sup>2</sup><sup>1</sup> 童綜合醫療社團法人童綜合醫院核子醫學科<sup>2</sup> 童綜合醫療社團法人童綜合醫院泌尿腫瘤中心

**簡介：**根據衛福部統計，攝護腺癌為 109 年十大癌症死因死亡率之第五名，每年攝護腺癌新增人數約為 6644 人，其中復發率約為 37.2%，推算復發人數約為 2471 人，其發生率與死亡率有逐年上升之趨勢。攝護腺癌常復發轉移的部位包含攝護腺床、骨骼、肝臟、肺部等。依據美國泌尿學會 (AUA) 及歐洲泌尿學會 (EAU) 的定義，當兩次血中攝護腺特異抗原 (prostate specific antigen, PSA) 皆超過 0.2 ng/ml，或是相較於最低點，PSA 上升超過 2 ng/ml 時，即稱作生化性復發 (Biochemical recurrence, BCR)。奧攝敏正子造影 (<sup>18</sup>F-Fluciclovine PET/CT scan)，適用於先前接受治療後因 PSA 濃度上升而懷疑攝護腺癌復發之病患，以協助診斷攝護腺癌之復發。

**病例報告：**病患為 47 歲攝護腺癌男性，於抽血發現 PSA 數值高達 161 ng/ml，全身骨頭掃描發現右側薦腸關節疑似骨轉移，新輔助荷爾蒙治療半年後於核磁共振檢查發現攝護腫瘤縮小，遂安排達文西機器手臂攝護腺根除手術 (RARP)，治療後 PSA 恢復正常值為 0.029 ng/ml。但相隔不到半年 PSA 又數值上升至 7.642 ng/ml，故接受奧攝敏正子造影檢查。病患空腹 4 小時，於右手注射 <sup>18</sup>F-Fluciclovine，劑量 10 mCi，正子造影掃描儀型號為 GE Discovery MI，注射完畢 4 分鐘後立即進行造影。造影範圍為骨盆至頭頂，正子造影部分第 1~2 床段每段 5 分鐘、第 3~6 床段每段 3 分鐘、第 7~9 床段每段 2 分鐘。

**結論：**造影結果發現攝護腺、左骨盆腔淋巴、雙側肺部、右側坐骨與右下薦腸關節皆有藥物聚集，因此判定除了攝護腺有腫瘤，同時還轉移到了淋巴、肺部與骨盆骨，隨即安排影像導引放射治療 (Image-guide Radiotherapy)，經治療後 PAS 下降至 0.414 ng/ml，並持續追蹤。利用奧攝敏正子造影檢查影像可清楚顯示攝護腺床及其他各處攝取，精準判別病灶位置，單一檢查就能顯示全身各處復發、轉移，提供臨床醫師及病患完整訊息，並及早調整後續治療計畫。

PC-076

## 鐳治骨 (鐳 223) 對全身骨轉移 攝護腺癌病患的治療效果 – 病例報告

張佳琪<sup>1</sup> 曾能泉<sup>2</sup> 歐宴泉<sup>2</sup>

<sup>1</sup> 童綜合醫療社團法人童綜合醫院核子醫學科

<sup>2</sup> 童綜合醫療社團法人童綜合醫院泌尿腫瘤中心

**背景介紹：**台灣的攝護腺癌發生率近幾年快速上升，目前已是男性國人的第五大癌症，而幾乎一半以上的攝護腺癌病患會發生轉移到骨頭的情形，若經荷爾蒙治療無效後，就稱為去勢抗性攝護腺癌；而鐳 223 可用於治療攝護腺癌的骨轉移，就目前研究顯示其對於去勢抗性攝護腺癌，擴散到骨頭，有骨頭疼痛的症狀，但無已知內臟轉移的病人有治療效益，但於治療中追蹤骨掃描時，部份患者會發現有假性進展 (pseudoprogression) 增多跡象，此次報告的病例觀察運用鐳 223 治療骨轉移的攝護腺癌病患，於治療前治療中及治療後的骨轉移變化，病例為一 79 歲男性，於 2021 年 2 月、3 月、4 月、5 月、6 月、7 月共進行 1 個療程 6 次治療，分別於 2020 年 12 月、2021 年 5 月、2021 年 7 月進行全身骨頭掃描。

**病例報告：**此病例為一 79 歲男性，患攝護腺癌有發現 2 處以上骨轉移，臨床科醫師為其安排 1 個鐳 223 治療療程，共計 6 次靜脈注射治療；分別於 2021 年 2 月、3 月、4 月、5 月、6 月、7 月進行 6 次靜脈注射治療，另外也於 2020 年 12 月、2021 年 5 月、2021 年 7 月安排全身骨頭掃描追蹤；比較三次之全身骨頭掃描影像，可發現多發性骨轉移，在進行三次鐳 223 治療後，骨轉移處放射性活度有明顯之降低及減少，在進行六次鐳 223 治療後，骨轉移處放射性活度降低及減少得更明顯。

**結論：**經由比較三次全身骨頭掃描影像，發現雖然研究指出在鐳 223 治療過程中部份患者會有假性進展 (pseudoprogression)，但在此案例中卻發現一有趣現象，進行三次鐳 223 治療後，在全身骨頭掃描影像中發現有多處骨轉移有明顯之改善，且於 6 次治療後的全身骨頭掃描影像，更可觀察到某些骨轉移處放射性活度降低及減少得更明顯。目前此病例持續追蹤中，由此病例之影像結果可知在三次治療後多發性骨亦可得到明顯的治療效果，我們也會持續觀察此現象，是否也會在其他病例中發現，以幫助更多前列腺癌患者。

PC-077

## 改良式 Ra-223 注射方法 – 個案報告

許幼青<sup>1</sup> 廖建國<sup>1</sup> 陳薇璇<sup>1</sup> 莊紫翎<sup>1,2</sup> 王昱豐<sup>1,2,3</sup><sup>1</sup> 佛教慈濟醫療財團法人大林慈濟醫院核子醫學科<sup>2</sup> 慈濟學校財團法人慈濟大學醫學系<sup>3</sup> 佛教慈濟醫療財團法人大林慈濟醫院預防醫學中心

**背景介紹：**Ra-223 藥物可以運用於治療前列腺癌骨骼轉移的患者身上，其藥物本身會釋放出阿法粒子，所以可短距離及高能量的治療標的器官，但在注射藥物過程中若發生滲漏會出現無法挽救的情形，於本科治療幾位案例中，有一位病人採用原本注射方式進行療程，反而出現需要一直重新施打靜脈留置針，造成治療過程不順利，故想知道如何可以減少施打靜脈留置針的方式，同時又可以很確定藥物進入到身體內，減少藥物滲漏的可能性。

**個案報告：**一名罹患前列腺癌的 79 歲男性，沒有其他器官轉移只有骨骼轉移，患者定期使用骨骼掃描追蹤檢查，臨床醫師通過事審安排 Ra-223 治療方案。原本每次療程前先靜脈注射留置針，施打 Ra-223 前先給予 1 mCi 的 Free Tc，並用 10 c.c. N/S 沖洗，注射後進行造影，使用中能量的準直儀，能峰設定 140 keV (10%)，但這位患者血管很特殊，施打 1 mCi 的 Free Tc 注射後造影，每次在影像上都出現殘留的情形，故重新施打靜脈留置針共有三次，團隊討論後，決定改用接上點滴同時造影，殘留的情形才消失，注射部位無藥物堆積無滲漏的現象，才敢從三路活塞處之一路施打 Ra-223 藥物，藥物施打後接續針筒反覆沖洗後，另一邊點滴滴著同時造影，使用中能量的準直儀，能峰設定 82 keV (20%)、154 keV (15%)、270 keV (10%)，影像上如同 Free Tc 之影像，表示在注射部位無藥物堆積無滲漏 (圖一)。

**結論：**Ra-223 治療中若藥物滲漏嚴重的話會有組織壞死的狀況，所以有無滲漏是一件非常值得討論的事情，本科一開始先給予 1 mCi 的 Free Tc 注射後進行造影，若無藥物殘留則給予 Ra-223 治療，但有位患者則效果不彰，故用此改良式注射方式，給予 1 mCi 的 Free Tc 注射同時給予點滴和造影，意外發現效果非常好，此做法可避免患者因藥物滲漏引發不必要的傷害，且可減少護理人員的心理壓力。

PC-078

## PET/CT 手臂蓄積放射活性之改善 — 案例報告

吳麗君 李將瑄\*

奇美醫療財團法人奇美醫院

**簡介:**靜脈回流會受到外力如肌肉收縮的擠壓作用、呼吸運動、重力作用等等的影響，施行全身氟-18 去氧氟化葡萄糖正子放射斷層 / 電腦斷層 (18F-FDG PET/CT, PET) 時，需以體積 2-3 ml FDG 注射後，再以 100 ml 生理食鹽水點滴滴入，可減少 FDG 蓄積注射位置 (如手背或手肘等)，亦可減少工作人員輻射暴露。此二案例為淋巴瘤病人在 PET/CT 的 CT 影像手上臂部有 FDG 蓄積攝取，認為此現象與靜脈回流有關，請病人在同側注射的手臂按摩抓捏 5 分鐘後照延遲影像，FDG 蓄積減弱，排除肌肉轉移，故特此提出。

**病例報告:**兩位分別為 34 歲和 58 歲女性，皆為淋巴瘤患者，施行 18F-FDG PET/CT 全身檢查，最初掃描影像時雙手放下，在手上臂有 FDG 蓄積攝取，而延遲像時，讓病人在蓄積 FDG 的手臂部位按摩 (抓捏 5 分鐘)，FDG 蓄積減弱 (SUV max 5.6 vs. 3.5) 和 (SUV max 19.5 vs. 5.5)，所以認為此現象為靜脈回流在病人手臂，非肌肉轉移。

**結論:**當全身 PET/CT 時手放下，若有看到同側注射處的上臂有 18F-FDG 活性蓄積攝取，建議可按按摩抓捏 5 分鐘後照延遲影像，可能的話讓他舉手來回運動，可以排除肌肉轉移的可能性。



PC-079

## A Hypermetabolic Lesion in the Adrenal Gland Confirmed as Ganglioneuroma

Po-Ling Chang, Lien-Yen Wang

*Department of Nuclear Medicine Changhua Christian Hospital*

**Introduction:** FDG PET is very sensitive to detect distant metastasis of non-small cell lung cancer. However, false-positive results may prevent the patient with non-small cell lung cancer from receiving curble surgery. We present a case of lung cancer with a hypermetabolic lesion in the left adrenal gland.

**Methods:** The 61 year-old female patient received a chest X-ray because of fever and a nodule was noted in the right lung. The followed chest CT scan revealed a 3.1 cm mass in the right middle lobe and a 1cm nodule in the left adrenal gland. There was no obvious enlarged lymph node in the CT scan. She was diagnosed with adenocarcinoma in the right middle lobe of lung by EBUS biopsy. A FDG PET/CT scan was arranged for cancer staging. The FDG FDG PET/CT scan revealed hypermetabolic lesions in the right middle lobe and left adrenal gland. There was no focal FDG uptake in the mediastinum and bilateral hila. A laparoscopic adrenalectomy was arranged to differentiate benign or malignant.

**Results:** A lesion with increased FDG uptake was noted in the left adrenal gland and SUV was increased in the delayed study (from 3.4 to 4.1) and it was measured as 1cm on the CT scan. The pathology result of laparoscopic adrenalectomy was ganglioneuroma. Because there was no obvious distant metastasis. The patient received an operation for cancer treatment. The pathology stage was T2aN0M0.

**Conclusions:** Hypermetabolic lesions noted in the FDG PET scan will affect the choice of treatment of lung cancer. A pathology study to distinguish benign or malignant can preserve the possibility of surgical treatment for the patient.

PC-080

## Comparison of Post-therapy Yttrium-90 PET Images Using Different Reconstruction Algorithms

Lan-Yi Chiu, Ju-Ling Cheng, Chien-Chin Hsu

*Department of Nuclear Medicine, Kaohsiung Chang Gung Memorial Hospital*

**Introduction:** Selective internal radiation therapy (SIRT) with Yttrium-90 (Y-90) loaded microspheres has been widely used as a locoregional therapy for liver tumors. After SIRT, imaging is performed to verify microspheres delivery and detect any significant extrahepatic activity. However, images are usually poor due to low count statistics and noise. Q.Clear (GE Healthcare) is a new Bayesian penalized likelihood reconstruction algorithm that suppresses noise by a penalization factor (termed  $\beta$ ). The aim of this study is to compare Y-90 positron emission tomography (PET) images using different reconstruction algorithms and to optimize the penalization factor of Q.Clear for post-SIRT imaging.

**Methods:** From July 2019 to August 2020, 13 patients with 30 liver tumors were enrolled. A total of 12 reconstruction methods were used, including: ordered subset expectation maximization (OSEM), OSEM with point spread function (PSF), OSEM with time of flight (TOF), OSEM with PSF and TOF, Q.Clear with  $\beta$  values of 500, 1000, 2000, 3000, 4000, 5000, 6000, and 8000. Quantitative image analysis of contrast, noise, and signal to noise ratio (SNR) were calculated for comparison.

**Results:** Applying PSF resulted in significantly higher contrast and SNR (both  $P < 0.001$ ). There was no significant difference in contrast, noise, or SNR with and without TOF. In Q.Clear, increasing the value of  $\beta$  led to a decline in noise, thereby improving SNR. In comparison to OSEM with PSF and TOF, Q.Clear with  $\beta$  values above 2000 had significantly lower noise (all  $P < 0.001$ ) and higher SNR (all  $P < 0.001$ ).

**Conclusions:** Our results indicate that Q.Clear with  $\beta$  values above 2000 reduces the image noise and improves SNR in post-SIRT Y-90 PET images.

PC-081

## <sup>18</sup>F-Fluciclovine PET/CT Between Low-grade and High-grade Gliomas: Case Reports

Chin-Ho Tsao<sup>1,3,5</sup>, Ting-Chi Yeh<sup>2</sup>, Ren-Shyan Liu<sup>4,5</sup>

<sup>1</sup>Department of Nuclear Medicine, Mackay Memorial Hospital Taipei, Taiwan

<sup>2</sup>Department of Pediatrics, Mackay Memorial Hospital Taipei, Taiwan

<sup>3</sup>Department of Medicine, Mackay Medical College, New Taipei City, Taiwan

<sup>4</sup>Department of Nuclear Medicine, Cheng-Hsin General Hospital Taipei, Taiwan

<sup>5</sup>Institute of Clinical Medicine, School of Medicine, National Yang Ming Chiao Tung University Taipei, Taiwan

**Introduction:** <sup>18</sup>F-Fluciclovine is a radiolabeled amino acid analog that the amino acid transport is upregulated in several types of cancers. However, its potential role in glioma is not yet well investigated despite promising results. Here, we showed <sup>18</sup>F-Fluciclovine PET/CT imaging in three separate cases from low-grade to high-grade glioma.

**Case reports:** The first patient is a 13 years old male with low-grade glioma in the left cerebellum (ganglioglioma, WHO grade II). He had received partial excision of his brain tumor on 2020/08/26. Adjuvant chemotherapy and radiotherapy were completed in 2020/10. Follow-up MRI after completion of radiotherapy revealed presence of residual tumor with slightly enlarged of tumor size. <sup>18</sup>F-Fluciclovine PET/CT confirmed local recurrence in the left cerebellum and left pons, with an SUVmax of 8.86.

The second patient is an 8 years old female with high-grade glioma in the pons. She had received radiotherapy (30 times) from 2020/10/29-2020/12/09, and adjuvant chemotherapy. Disease progression was noted at MRI in 2021/02 and she continued to receive adjuvant chemotherapy. <sup>18</sup>F-Fluciclovine PET/CT in 2021/05 showed rim-shaped local recurrence in the left pons, with an SUVmax of 1.37.

The third patient is a 19 years old female with secondary high-grade glioma (glioblastoma multiforme) in the periventricular region. She underwent craniotomy, concurrent chemoradiation therapy and adjuvant chemotherapy. Local recurrence is suspected at MRI in 2021/05. <sup>18</sup>F-Fluciclovine PET/CT showed no definite evidence of recurrence. In contrast, <sup>18</sup>F-FDG PET/CT revealed local recurrence in the right periventricular region, with an SUVmax of 14.77.

**Conclusions:** <sup>18</sup>F-Fluciclovine PET/CT is useful for detecting recurrent gliomas, and the SUVmax seems to have a downward trend from low-grade to high-grade. For aggressive high-grade glioma, <sup>18</sup>F-Fluciclovine PET/CT may be less helpful, while <sup>18</sup>F-FDG PET/CT may play a complementary role in detecting its recurrence.

PC-082

## MUGA 檢查之乳癌病人多針注射一個案報告

王苡安<sup>1,2</sup> 陳保良<sup>1,3</sup> 廖建國<sup>1</sup> 王昱豐<sup>1,4,5\*</sup>

<sup>1</sup> 佛教慈濟醫療財團法人大林慈濟醫院核子醫學科

<sup>2</sup> 佛教慈濟醫療財團法人大林慈濟醫院護理部

<sup>3</sup> 佛教慈濟醫療財團法人大林慈濟醫院醫學研究部

<sup>4</sup> 佛教慈濟醫療財團法人大林慈濟醫院預防醫學中心

<sup>5</sup> 慈濟學校財團法人慈濟大學醫學院醫學系放射線學科

**背景：**心臟搏出分率及心室壁活動 (MUGA) 測定檢查方式都以靜脈注射為主，因此注射品質極為重要，為造影前作業中扮演非常重要的角色。本個案報告特別介紹此多針注射之案例，並探討靜脈注射失敗常見原因。

**病例報告：**74 歲女性有高血壓和糖尿病史。20201207 右乳癌全乳切除，病理顯示惡性，癌別等級為 T4bN1M0，stage IIIB。臨床上右手禁止注射、量血壓、提重物相關動作，故只剩左手及雙下肢可施打。病人執行化療前，醫師需要精確了解病患各種心臟功能參數，以掌握病人的臨床病程與藥物治療後的療效，故在治療中安排了 MUGA 檢查。檢查流程如下：第一次會由靜脈注射 2 c.c. PYP，過 15 分鐘後再由靜脈留置軟針，如果遇到困難不好施打者則不留靜脈留置軟針，改打頭皮針。在注射時患者告知護理人員，血管不易找尋，施打時正如患者所陳述，確實找不到明顯可見之血管，此次共動員本科三位醫療人員協助找尋血管，最後施打位置為左手腕處，該患者共計施打 11 針，總共 24G 安全留置軟針 2 針、非安全頭皮針 23G x 19 mm 5 針、非安全頭皮針 25G x 19 mm 4 針。

**討論：**一般執行靜脈注射時應選擇粗直、彈性好、不易滑動的靜脈，常用的有肘窩的貴要靜脈、正中靜脈、頭靜脈，或手背、足背、踝部等處。科內目前大多使用 24G (0.6 x 19 x 305 mm) 安全針具及 24 安全留置軟針，不得已情況下使用非安全頭皮針 23G x 19 mm、25G x 19 mm。一般常見注射失敗的原因包括 (1) 針頭刺入較深或淺，有回血情形，但推藥時溢出至皮下導致皮膚有隆起現象，表示針頭一部份於組織內，一部分於血管內。(2) 止血帶綁太鬆，導致血管浮現不明顯，且血管彈性不好，故沒打到血管。(3) 一開始病患握拳握很緊，打上後突然放鬆了，導致血管位置移動進而漏針。若病患是長期洗腎、化學治療、淋巴水腫和長期服用類固醇製劑及止痛劑等，大多數血管都較深沉或是血管管徑較細及血管管壁彈性、張力較差等情形。因此就本科之經驗，遇到不好施打的病人，臨床上執行靜脈注射上限為兩針，如果已達兩針依然打不上，則會進一步請求其他醫療人員之協助支援。

**結論：**臨床上常見血管較難施打的病人，影響病人及醫護同仁的心情，除了依賴護理師之專業技術外，醫護同仁間的互相支援，期望病人也能體諒，才能順利完成臨床檢查。個人方面平時應加強學理知識及技術上練習，以利持續提升注射品質。

PC-083

## COVID-19 疫情下之教學配套措施

邱祖廷<sup>1</sup> 方雅潔<sup>1</sup> 余景陽<sup>1</sup> 韓璞<sup>1</sup> 陳芄嘉<sup>1</sup> 林慶齡<sup>1,2</sup>

<sup>1</sup> 國泰綜合醫院放射免疫實驗室

<sup>2</sup> 國泰綜合醫院內分泌新陳代謝科

**背景介紹：**COVID-19 自 2019 年 12 月以來全球疫情逐漸升溫，反觀台灣疫情控制得宜，全球有目共睹，疫情並未對台灣人民生活造成太大影響；然而作為醫學中心之實驗室，面對疫情需保有未雨綢繆之想法。每年初來乍到的實習生正轉換著生活模式，從學生生活逐漸踏入職場中，身為醫學中心臨床教師的我們期待將臨床知識竭盡所能傳遞給實習生們。倘若疫情嚴重至實習生們無法進入醫院實習，在仍須排定實習生教學課程的情況下，如何兼顧實習生之安全與教學目的之達成？為此次探討之主題。

**方法：**受疫情之影響，為保護實習生們安全，本實驗室認為不該侷限於實際現場教學，因而多方研究遠距教學，除了普遍的線上教學課程外，也攝製實驗室教學影片，讓實習生們能更有臨場感，也透過影像加深實習生對於整體實驗室工作環境的空間感及儀器原理的熟悉程度。

**結果：**為了進一步了解線上教學課程及實驗室教學影片是否達到教學目的，我們製作了放射免疫室考題提供給實習生做課前與課後測驗，結果顯示經教學過後大大提升了實習生們對於放射免疫室的了解。除了考題測驗外，透過課後回饋，得知實習生們對於實驗室環境熟悉程度高於儀器原理及整體實驗室運作，讓我們能夠在遠距教學不足的方面多加著墨，並以每位實習生都能更加了解放射免疫室作為本實驗室在教學方面不斷努力及學習的目標。

**結論：**不受 COVID-19 疫情之干擾，本實驗室提前安排教學的配套措施。透過開發一套遠距的替代教學方案，同時達成實習生的教學與測驗等優異的系統性教學成果。此次疫情雖帶來諸多限制，但也提升了實驗室對於意外的應變能力以及造就了我們的教學多樣性。

PC-084

## 實驗室如何兼顧防止 COVID-19 疫情 及儀器準確度？

邱祖廷<sup>1</sup> 方雅潔<sup>1</sup> 余景陽<sup>1</sup> 韓璞<sup>1</sup> 陳芄嘉<sup>1</sup> 林慶齡<sup>1,2</sup>

<sup>1</sup> 國泰綜合醫院放射免疫實驗室

<sup>2</sup> 國泰綜合醫院內分泌新陳代謝科

**背景介紹：**在 2021 年 5 月中旬，台灣 COVID-19 疫情爆發，中央疫情指揮中心宣布自 2021 年 5 月 19 日起提升全國疫情警戒至第三級，本實驗室進行實驗室人員分流上班，也對於儀器廠商、試劑廠商…等外部人員進出實施嚴格管制：非必要禁止進出實驗室。然而作為醫學中心下之 TAF 認證實驗室，仍須確保儀器準確度，但如何在這波疫情下達成？為本次探討之主題。

**方法：**本實驗室品質文件規定一年一次將儀器設備委託 TAF 認可之校正實驗室施行遊校，而三級警戒期間恰逢實驗室兩台離心機(桌上型離心機、落地型高速冷凍離心機)、一台迴轉震盪器及四台冰箱(輻射藥品冷藏櫃 -A、輻射藥品冷藏櫃 -B、輻射藥品冷藏櫃 -C、冷藏冷凍櫃 -B) 等儀器設備需遊校，而校正廠商無法前來，因此本實驗室擬出自行內校的配套措施：一、實驗室自行購買標準溫度計及轉速計於外校後，進行儀器內校。二、向其他經認證實驗室借已校正完成之溫度計及轉速計。由於時間緊迫，無法及時購買溫度計及轉速計，並完成外校，因而此次內校皆使用其他實驗室校正完成之溫度計及轉速計。

**結果：**本實驗室校正儀器之器差值允收標準為：離心機  $\pm 30$  rpm、迴轉式震盪器  $\pm 10$  rpm、冷藏冰箱  $\pm 2^{\circ}\text{C}$  及冷凍冰箱  $\pm 3^{\circ}\text{C}$ 。內校結果顯示，兩台離心機：桌上型離心機、落地型高速冷凍離心機之器差值分別為 1 rpm 及 0 rpm，符合允收；迴轉震盪器之器差值為 0.5 rpm，符合允收；四台冰箱：輻射藥品冷藏櫃 -A、輻射藥品冷藏櫃 -B、輻射藥品冷藏櫃 -C、冷藏冷凍櫃 -B 校正點為  $4^{\circ}\text{C}$ ，器差值皆符合允收。但冷藏冷凍櫃 -B 校正點為  $-20^{\circ}\text{C}$ ，其器差值  $-3.5^{\circ}\text{C}$  不符合允收標準，故調整為僅供已做檢體存放，待實驗室新購之玻璃溫度計完成外校後，使用其監控冷凍櫃。

**結論：**在 COVID-19 疫情衝擊下，本實驗室仍堅守 TAF 規範，如期完成實驗室儀器設備的校正及允收，針對不符合允收標準之儀器也有其應變措施，此次的疫情雖帶來諸多限制，但也提升了實驗室對於突發狀況的解決能力。

PC-085

## The COVID-19 Vaccine-Related Reactive FDG Avidity of Axillary Lymph Nodes on PET/CT

Hsin-Wei Huang<sup>1</sup>, Yu-Ting Wang<sup>1</sup>, Meng-Fang Tsai<sup>1</sup>, Song-Han Yang<sup>1</sup>,  
Po-Nien Ho<sup>2</sup>, Guang-Uei Hung<sup>1</sup>

<sup>1</sup>Department of Nuclear Medicine, Chang Bing Show Chwan Memorial Hospital, Changhua, Taiwan

<sup>2</sup>Department of Nuclear Medicine, Show Chwan Memorial Hospital, Changhua, Taiwan

**Objectives:** Since the novel human coronavirus disease 2019 (COVID-19) global pandemics in 2020, there were the total number of 15,983 cases confirmed and 834 deaths in Taiwan. The vaccine plays an important role to protect and against the COVID-19. Taiwanese government provides 3 different types of injectable vaccine products, including Moderna, AstraZeneca and MVC. The positron emission tomography scanner with low-dose CT (PET/CT) using the 18F-2-fluoro-2-deoxyglucose (FDG) is useful to detect various malignancies, infection and inflammation. Recently, the vaccine-related lymphadenopathy and FDG uptakes in the axillary, cervical or supraclavicular lymph nodes after injection have been reported. The aim of this study was to investigate the incidence and duration of vaccine-related FDG-avidity in axillary lymph nodes after administration of Moderna and AstraZeneca.

**Method:** A total 114 patients (female 54, male 60) after first vaccination of Moderna or AstraZeneca undergoing the FDG-PET/CT scan were included in this study from July to August, 2021. The vaccination type, injection site and date were recorded. The images data were reviewed by two experienced nuclear medicine physicians for assessment of vaccine-related FDG uptakes in axillary lymph nodes .

**Results:** The overall incidences of FDG-avid lymphadenopathy were 23% (12/52) for AstraZeneca and 38% (23/61) for Moderna, respectively. The incidences within 2 weeks of vaccination were 22% (2/9) and 31% (5/16), 25% (5/20) and 33% (5/15) for 2 to 4 weeks, 25% (2/8) and 48% (11/23) for 4 to 6 weeks, and 20% (3/15) and 14% (1/7) after 6 weeks, respectively.

**Conclusion:** The occurrence of vaccine-related FDG-avidity in axillary lymph nodes were not uncommon and may persist for more than 6 weeks after vaccination. Special caution on history taking is very important for avoiding mis-interpretation of these reactive FDG-avidity as metastasis.

PC-086

## Preliminary Study on Left Axillary Lymph Node Hypermetabolism of F-18 FDG PET/CT in Health Examination Clients and Patients with COVID-19 Vaccination

Yu-Chien Shiau, Yu-Chuan Lee, Shu-Min Chen, Chu-Chien Fan,  
Chine-Yu Chu, Yen-Wen Wu, Shan-Ying Wang

*Division of Nuclear Medicine, Far Eastern Memorial Hospital, New Taipei, Taiwan*

**Introduction:** During recent practice of 18F-FDG PET/CT studies, we have noticed some cases with FDG hypermetabolism in their left axillary lymph nodes, both in health examination clients and some oncology patients. In reviewing literatures, there had been several reports concerning 18F-FDG PET/CT hypermetabolism in left axillary lymph nodes in patients with COVID-19 vaccination. Because the phenomena are new to Taiwanese nuclear physicians, we conducted a preliminary study on left axillary lymph node hypermetabolism of 18F-FDG PET/CT both in health examination clients and oncology patients.

**Methods:** Thirty four health examination clients and patients referred for F-18 FDG PET/CT studies during October and September 2021, both with and without COVID-19 vaccination were retrospectively included. Patients with breast cancers, lung cancers, or lymphoma were excluded. SUVmax of left axillary lymph nodes or left axillary region were measured and compared to show FDG-avidity. Time of elapse between vaccination and PET/CT study was analyzed. Vaccinations with AZ and Moderna were also analyzed and compared separately.

**Results:** F-18 FDG PET/CT showed FDG-avid in left axillary lymph nodes to COVID-19 vaccine injection in 13/17 (76.5%) health examination clients with a mean SUVmax of 1.8 (range 1.0 – 4.3). No obvious F-18 FDG-avidity was noted in left axillary lymph nodes in 18/18 (100%) health examination clients and patients without vaccine injection. FDG-avid lymph nodes were noted in patients vaccinated with AZ (8/11 [72.7%]) and Moderna (4/5 [80.0%]) cases. The mean SUVmax is 1.94 (range 1.0 – 4.3) for AZ vaccine, and 1.53 (range 1.2 – 2.2) for Moderna vaccine.

**Conclusions:** Both AZ and Moderna of COVID-19 vaccination can induce some F-18 FDG hypermetabolism in left axillary lymph nodes. The phenomena had been noted and studied in several groups of investigators, and can influence the interpretation of PET/CT in both health examination clients and patients with cancers. We hope the phenomena could be noticed in clinical practice, and we hope that we can gather more cases in the future study or multicenter study could be organized.



PC-087

## COVID-19 住院患者血清 Ferritin 濃度 與疾病嚴重程度相關性之探討

薛仔婕<sup>1</sup> 張素雲<sup>1</sup> 林淑靜<sup>1</sup> 廖建國<sup>1</sup> 王昱豐<sup>1,2</sup>

<sup>1</sup> 佛教慈濟醫療財團法人大林慈濟醫院核子醫學科

<sup>2</sup> 慈濟學校財團法人慈濟大學醫學系

**背景：**由嚴重急性呼吸道症候群冠狀病毒 2 型 (SARS-CoV-2) 導致的嚴重特殊傳染性肺炎 (COVID-19) 所引發的全球疫情的大流行，症狀通常以呼吸道症狀為主，部分個案可能出現嚴重的肺炎與呼吸衰竭以及多重器官衰竭，或進展至死亡。當感染病菌時，身體適度的發炎反應可有利身體去除病原菌，但過度的發炎反應會引發大量細胞激素的產生 (細胞激素風暴 cytokine storm)，往往造成器官的損傷及衰竭，從免疫反應的角度來看，血清炎症標誌物包括 Ferritin 在內的急性期反應物的分析可能與疾病嚴重程度有關。因此我們探討 COVID-19 住院患者血清 Ferritin 濃度與疾病嚴重程度之間的相關性。

**方法：**回溯性收集由 2020 年 11 月至 2021 年 8 月於本院住院之 COVID-19 病人，共 42 名。病患於入院時皆採血檢測血清 Ferritin 濃度，檢驗方法為使用 Beckman Coulter 試劑 (FERRITIN IRMA KIT) 測量，參考值為男性：38-457 ng/mL、女性：7.4-165 ng/mL，並將病人依其疾病嚴重程度分為輕度及嚴重兩組，分組方式為：輕度組為病人無併發症之輕症，或病人胸部 X 光異常但不需氧氣設備輔助之病人。嚴重組為病人胸部 X 光異常且出現肺炎之臨床症狀，需使用非侵襲性或侵襲性呼吸器輔助呼吸之病人。將兩組別進行統計分析，比較血清 Ferritin 濃度之差異。

**結果：**共 42 名 COVID-19 住院病人，平均年齡為  $48.5 \pm 20.0$  歲，統計使用 T-test 進行分析，結果顯示如表 1，嚴重組 (共 15 名) 的血清 Ferritin 含量平均值為  $867.59 \pm 498.22$  ng/mL，顯著高於輕度組 (共 27 名) 的  $180.76 \pm 187.01$  ng/mL ( $p < 0.001$ )，此結果顯示血清 Ferritin 濃度與疾病嚴重程度具相關性，且嚴重組病人年齡顯著高於輕度組 ( $p < 0.001$ )，疾病嚴重程度與年齡也存在相關性。

**結論：**研究發現 COVID-19 病人血清中 Ferritin 濃度與疾病嚴重程度之間有顯著相關性 ( $p < 0.001$ )，因此當病人入院時檢測血清 Ferritin 濃度，對於用來預測 COVID-19 患者疾病的嚴重程度可能是有幫助的。

PC-088

## 比較診斷準確度 Tl-201 與 $^{99m}\text{Tc}$ -MIBI 在心肌血流灌注影像上之分析

林娜宜 陳慶元

佛教慈濟醫療財團法人台中慈濟醫院

壁報論文發表摘要·臨床組

**背景介紹：**在冠狀動脈心臟病的診斷方法中，除了臨床病史為最重要的診斷依據以外，會以非侵入性的檢查為優先選擇，包括有靜態或運動心電圖、超音波、以及核醫心肌灌注掃描，一般核醫心肌灌注掃描的核藥有  $^{99m}\text{Tc}$ -MIBI 與 Tl-201 兩種選擇， $^{99m}\text{Tc}$ -MIBI 與 Tl-201 檢查流程不同， $^{99m}\text{Tc}$ -MIBI 檢查前可以吃東西，藥物在靜態跟動態皆須打藥，Tl-201 檢查前要空腹 4 小時，藥物只要在動態打藥。 $^{99m}\text{Tc}$ -MIBI 與 Tl-201 有文獻查證論述  $^{99m}\text{Tc}$ -MIBI 的影像較為清晰，有的文獻則說並無差異，因為新冠肺炎疫情影響飛機航班，所以原本心肌灌注掃描使用的 Tl-201 核藥供應缺乏，故換成  $^{99m}\text{Tc}$ -MIBI 交替使用，因此藉由此次機會來比較一下兩者影像上的診斷準確度差異性。

**方法：**為了因應線上排程病人能在時間內做完檢查及回診看報告，故使用替代核藥  $^{99m}\text{Tc}$ -MIBI 替代使用，藉此分析兩種核藥在檢查後對冠種動脈狹窄的敏感度，最終以做心導管數據做為參考依據，回朔收集 3 月 1 日到和 4 月 31 日，兩種核藥交替次數較頻繁的期間，一共收集 307 位患者使用 Tl-201 有 248 位患者與  $^{99m}\text{Tc}$ -MIBI 有 59 位患者。

**結果：**其中 Tl-201 有施行心導管為 36 例，在核醫心肌灌注掃描的檢查後對冠狀動脈狹窄有意義為 19 例，與  $^{99m}\text{Tc}$ -MIBI 有施行心導管為 6 例，在核醫心肌灌注掃描的檢查後對冠狀動脈狹窄有意義為 3 例。兩種核藥在統計後分析陽性命中率為 100%，在陽性預測值約在 5 成 5 區間。

**結論：**分析結果顯示心肌灌注掃描的核藥  $^{99m}\text{Tc}$ -MIBI 與 Tl-201 這兩種，醫師在兩者影像上的判讀無太大差異，在影像上敏感度皆相似，因  $^{99m}\text{Tc}$ -MIBI 與 Tl-201 這兩種核藥檢查流程有所不同，考量經營成本問題，區域教學醫院的核醫科人力成本來，所以看各家醫院對哪一種檢查流程便利性及順暢度。

PC-089

## Incidental Abdominal Aortic Aneurysm (AAA) on Gastrointestinal Tract Bleeding Scan Imaging – A Case Report

Shu-mei Lu, Yu-Ling Hsu

*Department of Nuclear Medicine, Ditmanson Medical Foundation Chia-Yi Christian Hospital, Chia-yi, Taiwan*

**Case:** Here we report a 92 year-old female who has type 2 diabetes mellitus, dementia, anal squamous cell carcinoma status post operation with colostomy. This time, she was admitted for tarry stool for 5 days. PES was done and showed gastric erosion. Colonoscopy was also performed but no bleeding sign was noted. After admission, RBC scan was arranged for bleeding survey. There was abnormal radioaccumulation over abdomen which we did not expect. (Fig. 1) Therefore we trace back her history and found that there was abdominal aortic aneurysm around 5 cm noted a couple of years ago, as shown in Fig. 2. CVS was consulted at that time, but her family refused operation. This time, her family want to know the risk and management of AAA, and CVS was consulted again. Optimal treatment will be discussed and determined accordingly.

**Discussion:** Abdominal aortic aneurysm (AAA), which is an abnormal focal dilation of the abdominal aorta, is relatively common and has the potential for significant morbidity and mortality. A diagnosis of AAA generally requires imaging confirmation that an aneurysm is present, which is most often accomplished using abdominal ultrasound and computed tomography.

Gastrointestinal bleeding (GIB) is a life-threatening problem that requires a multidisciplinary approach for successful treatment. The Tc-99m RBC scan imaging can capture any abnormal lesions related to red blood cell distribution. In our case, the imaging pattern was compatible with incidental abdominal aortic aneurysm, which showcase the capability of detecting extra lesions of Tc-99m RBC scan.

PC-090

## 核醫腸胃道出血掃描案例分享

黃信慈 陳慶元

佛教慈濟醫療財團法人台中慈濟醫院

**背景介紹：**消化道出血 (hemorrhage of digestive tract) 是來自食道、胃、腸以及膽道、胰管等部位的出血。其中，屈氏 (Treitz) 韌帶以上的食道、胃、十二指腸以及膽道、胰管等部位的出血為上消化道出血，屈氏韌帶以下的空腸、回腸、結腸、直腸等部位的出血為下消化道出血。老年人消化道出血發病率高，死亡率也高，易被心血管病等其他疾病所掩蓋，又常成為腫瘤等其他疾病的診斷線索。臨床上常須兼顧止血治療、病發症治療、原發病治療以及心血管病等伴隨病變的治療。

**案例報告：**該案例為女性 (88 歲) 跌倒後有 T12 壓迫性骨折疾病史，因鮮紅色血便一週，開始低血容量性休克 (Hypovolemic Shock)，由急診進入加護病房觀察治療。優先安排 S 狀結腸纖維鏡檢查 Sigmoidoscopy，後發現直腸有粘膜下層腫瘤、乙狀結腸潰瘍，疑似缺血性結腸炎。血管攝影發現 SMA (Superior mesenteric artery) 區域沒有活動性出血、僅注意到升結腸和脾曲結腸部分節段的局部性充血，可能是炎症過程；IMA (Inferior mesenteric artery) 顯示管口嚴重狹窄，無法診斷是否出血。因此須藉由核醫腸胃道出血掃描找到出血時機及位置。

**結果：**本科臨床使用 Tc-99m 標記紅血球為體內標幟法 (In Vivo Method)。靜脈注射 Technescan PYP (20 mg/2cc.) 藥物，其後 20-30 分鐘再注射 20 mCi Tc-99m TcO<sub>4</sub><sup>-</sup> 追蹤劑；注射後 10 分鐘發現左上腹部和右上象限的放射性增加，在 15、30、45 和 60 分鐘的後續圖像上可以看到放射性追蹤劑的擴散，未見其他部位異常放射性。報告懷疑腸道間歇性 / 活動性胃腸道出血 (IMA 區域，可能來自結腸脾曲)。隔日立即安排外科腹腔鏡手術切除截掉出血部位，術後休復狀況良好，轉出一般病房後順利出院休養。

**結論：**消化道出血是腸胃道疾病中一種常見的表徵，核子醫學造影在腸胃道出血也扮演一個很重要角色，尤其對於間歇性出血或小量出血的靈敏度相當高；診斷和定位正確率在 75~85% 以上，具有準確性、簡便性、非侵襲性等優點。

PC-091

## 唾液腺檢查數據自動判讀之機器學習方法比較

林昶仲<sup>1</sup> 蘇詩琪<sup>1</sup> 譚鴻遠<sup>1</sup> 林欣名<sup>2</sup><sup>1</sup>高雄榮民總醫院核子醫學科<sup>2</sup>國立臺南藝術大學高階藝術管理碩士在職學位學程

### 背景介紹：

透過人工智慧領域中的多種機器學習演算法，以分類和預測兩種任務來自動判讀唾液腺檢查數據。比較不同的機器學習方法，探索進一步應用的可能性。

### 方法：

以 Orange Data Mining 自由軟體進行實驗，選取數種機器學習的方法，包括 Tree、Random Forest、kNN、SVM、Neural Network、Linear Regression、Logistic Regression、Naïve Bayes。訓練(含驗證)用資料集；2018 年至 2020 年間 561 個樣本；測試用資料集：2021 年一月至三月間 42 個樣本。首先針對訓練用資料集的 561 個樣本，除了病歷號忽略不計之外，以檢查分數或嚴重程度作為目標值，其餘數據皆作為樣本特徵。經由 5 折 (5-fold) 分層交叉驗證 (stratified cross validation) 方法分析結果之後，發現僅選取四項 EF (排出率) 特徵方可在分類與預測任務達到較佳表現。接著，再以該批全部 561 個樣本，分別訓練不同的機器學習模型，然後另外將測試用資料集的 42 個樣本作為自動判讀標的，比較兩種任務的表現。

### 結果：

1. 將 scores 當成 13 個類別進行分類任務。依 F1 優劣分數 (0.796~0.203) 排列，依序為 Tree、Random Forest、kNN、SVM、Neural Network、Naïve Bayes、Logistic Regression。
2. 將 scores 當成 13 個數值，進行預測任務。依 R2 優劣分數 (0.989~0.910) 排列，依序為 Random Forest、kNN、Tree、SVM、Neural Network、Linear Regression。
3. 將 types 當成 04 個類別，進行分類任務。依 F1 優劣分數 (0.976~0.881) 排列，分數依序為 Random Forest、Neural Network、Logistic Regression、Tree、Naïve Bayes、SVM、kNN。
4. 將 types 當成 04 個數值，進行預測任務。依 R2 優劣分數 (0.963~0.809) 排列，分數依序為 Tree、Random Forest、kNN、Neural Network、Linear Regression、SVM。

### 結論：

在 scores 方面，無論是分類或預測任務，Random Forest、Tree、kNN 這三種機器學習方法表現最佳；最低分的則是 Regression。在 types 方面，兩種任務中，Random Forest 皆有較佳的表現；SVM 則表現較差。

PC-092

## 腸胃道出血檢查分析與探討

張添信 陳慶元

佛教慈濟醫療財團法人台中慈濟醫院核子醫學科

**背景介紹：**腸胃道出血掃描 (Gastrointestinal bleeding Scintigraphy、GIBS) 在 1977 年首次被 Alavi 等人提出此檢查方法，後續經過幾次改良才有現今的標誌紅血球掃描，在歐洲與美國核醫學會均有制訂作業標準準則提供參考，檢查的目的是在確定患者是否有活動性出血，定位出血腸段，並估計失血量，偵測出血率為 0.05~0.2 ml/min，GIBS 在中下胃腸道中表現最佳，下消化道出血的常見原因包括血管發育不良、憩室病、良性和惡性腸腫瘤、腺瘤性息肉、炎症性腸病和感染性腸病等問題，好發於中老年人致死率約為 10~30%。

**方法：**以回溯性研究方式分析 2018.1 至 2021.8 年內單位執行腸胃道出血掃描共 85 例 (男/女：38/62%)，平均年齡 74 ± 13.79 歲，皆有黑便或暗紅或鮮紅色血便相關疾病史，執行腸胃道出血掃描前會先照會腸胃科執行上或下消化道內視鏡檢查，若無相關病程發現則轉會施行核醫腸胃道出血檢查，蔽單位為使用體內標記法 (in Vivo) 施行 GIBS，先給予氯化亞錫後 20-30 分再注射核醫示蹤劑 (TcO4-)，立即開始造影並在 1 小時後，確認甲狀腺是否攝取核醫藥物確認紅血球結合率效率。

**結果：**在 85 例 GIBS 中陽性預測值為 88.2% (75/85) 根據核醫專科醫師報告指出有異常出血，75 例陽性中在平均 14.68 ± 9.11 小時發現下腸胃道藥物不正常聚集，在 85 例中可以看到甲狀腺形狀外觀為核醫藥物紅血球標誌率不佳的有 27%，利用 SPSS 進行相關敘述統計交叉資料表分析，在 85 例中甲狀腺攝取藥物有 23 例，在 23 例中與陽性或陰性結果比較無顯著表現 (3 例為陰性 20 例為陽性)，平均年紀與甲狀腺攝取經過 SPSS 獨立樣本 T 檢定後也無顯著意義，甲狀腺有攝取平均在 73.35 ± 13.9 歲，甲狀腺未攝取為 75.29 ± 13.81 歲，標誌率優寡與年紀無正相關。

**結論：**考量經營成本問題，區域教學醫院的核醫科人力本來就是精簡的，不像醫學中心人力設置規模，使用體內標記法雖然較為簡便在人力有限的核醫科似乎是可行的，雖然不如其他兩種標誌法來得效率好，但根據此 85 例 GIBS 統計分析其臨床診斷表現甚佳，可以提供一線單位有用的臨床訊息幫助。

PC-093

## Role of SPECT/CT Images in Gallium-67: Hiatus Hernia with Gastric Volvulus Mimicking Pneumonia

Yu-Yu Lu, Jing-Uei Hou, Hsin-Yi Wang, Yi-Ching Lin, Shih-Chuan Tsai

*Department of Nuclear Medicine, Taichung Veterans General Hospital, Taichung, Taiwan*

**Introduction:** Gallium-67 scintigraphy has been reported of value in the evaluation of infection or inflammation. Compared with conventional planar images, co-registered fused single photon emission computed tomography/computed tomography (SPECT/CT) provides more information and improves the accuracy. We presented a case of hiatus hernia with gastric volvulus mimicking pneumonia in gallium-67 scan with SPECT/CT images.

**Case Report:** A case of an 84-year-old woman was referred to our department for unknown fever evaluation by gallium-67 scintigraphy. (A) Anterior and posterior planar images showed increased gallium uptake in the right lower lung field. Pneumonia is highly suspected (arrow) because anatomical information is limited. However, (B) co-registered fused SPECT/CT images showed the increased gallium uptake in the hiatus hernia with gastric volvulus. Gastric volvulus is a rare clinical entity characterized by rotation of the stomach along its long or short axis leading to variable degrees of gastric outlet obstruction. Primary and secondary forms of gastric volvulus are catalogued according to the etiology. Primary (idiopathic) gastric volvulus arises due to abnormalities of the gastric ligaments. The secondary subtype may occur as a result of the disorder of gastric function or gastric anatomy, or the abnormality of adjacent organs such as the diaphragm or spleen. Once it is diagnosed, surgical repair is advised. However, the successful results have been reported with a conservative treatment too. The SPECT/CT result had an impact on management of this patient.

**Conclusions:** We emphasize that role of co-registered fused SPECT/CT improves localization and gives more information necessary in planning of further treatment. As far as we know, this is the first case of hiatus hernia with gastric volvulus demonstrated on Gallium-67 SPECT/CT images.

PC-094

## 利用單光子斷層掃描儀執行淚腺攝影 診斷乾眼症患者－中部某區域教學醫院核醫科為例

洪睿言 鄭孝義

衛生福利部臺中醫院核子醫學科

**背景介紹：**乾眼症是現代人常見一種眼疾，隨著科技發達現民眾長期使用各類 3C 產品，此外多數人長時間使用隱形眼鏡以及在冷氣房內工作，造成乾眼症的病患日漸年輕化。本病歷討論該病患為 41 歲女性，主訴表示因準備考試長每日使用電腦閱讀長達 10 小時並維持 7 年之久，並在近兩年感到眼睛乾澀、但否認有口乾、口腔潰瘍、皮疹、關節痛等症狀，經臨床醫師判斷疑似 sjogren's syndrome，因此開立淚腺閃爍攝影檢查。本院採用單光子斷層掃描 (SPECT) 進行淚腺閃爍攝影進行影像診斷。

**方法：**檢查前準備：眼科下巴額頭支架乙支，調整好病患高度，並固定臉部防止病患在檢查期間移動造成影像假影。放射性藥物：使用兩支 Tc-99m Sodium Pertechnetate 劑量為 0.1 mCi (3.7 MBq)、體積：0.1 mL (使用 1 mL 空針裝載放射性藥物)。影像數據：使用動態影像連續照影共 30 分鐘、30 秒 / 張共連續收 60 張影像，使用 LEHR 的 collimator、Matrix Size: 64 x 64，影像放大 2.19 x (27.3) cm。影像執行流程：在固定好病患頭部與下巴後，從兩側眼角滴入放射性藥隨後立即開始攝影，病患可眨眼但不能將眼睛完全閉住，確認影像後就能讓病患離開。

**結果：**在淚腺閃爍攝影影像顯示，病患在兩側滴入放射性藥物後雙側淚液從眼部區域流向淚管有明顯延遲情形發生。在經影像後處理分析後，殘留指數 (RI) 和淚液清除半衰期分別為 73.66% 和 133 分鐘，大於正常範圍。(正常範圍：RI 12~16%，T1/2：3~5 分鐘)

**結論：**核醫淚腺閃爍攝影能提供臨床實用且非侵入性診斷方法，利用半定量的方式分析淚液殘留指數以及淚液清除半衰期，提供臨床上在診斷乾眼症時有更多選擇。



PC-095

## 應用手勢教導呼吸技巧於肺通氣檢查一個案報告

邱禹臻<sup>1</sup> 許幼青<sup>1</sup> 陳薇璇<sup>1</sup> 廖建國<sup>1</sup> 王昱豐<sup>1,2,3</sup>

<sup>1</sup> 佛教大林慈濟醫院核子醫學科

<sup>2</sup> 慈濟大學醫學系

<sup>3</sup> 佛教大林慈濟醫院預防醫學中心

**背景：**肺臟主要功能是供給養氣及呼出二氧化碳，完成這項功能需要有健康的呼吸道及肺血管系統充分的配合；肺通氣是指外界環境與肺部的肺泡之間氣體交換過程，當中包括吸氣和吐氣兩個部分。核醫肺臟掃描分為灌注 (perfusion) 與通氣 (ventilation) 掃描兩種，而通氣造影有很多種方式，我們是利用放射性物質霧化的方式經由面罩及密閉呼吸裝置進入病人肺部並進行造影，過程大約 6 分鐘，事前無需任何特別準備，可以正常飲食及服用藥物。由於病患無法確實執行吸氣及吐氣的動作會影響通氣掃描檢查結果，因此期望藉由本案例之分享，提供進行肺通氣檢查之衛教參考。

**個案報告：**81 歲男性病患，主要診斷為術後右側乳腺癌，次要診斷為慢性阻塞性肺病，有高血壓、良性前列腺肥大、聽力障礙等病史。每個月定期回診，常規 X 光檢查顯示肺部腫塊，正子造影檢查顯示左上肺 17.0 毫米結節及右肺有兩個結節，放射腫瘤科醫師開立肺臟掃描檢查，病患目前無胸悶、呼吸困難等不適症狀。病患本身重聽已十多年，未配戴助聽器，排檢時家屬表示病患嚴重聽力障礙，擔心檢查無法順利執行，故於排檢時護理師先用書寫方式與病患溝通，教導家屬及病患配合護理師手勢進行吸氣及吐氣動作，並要求病患依護理師手勢進行檢查。病患平躺於檢查台上，開始檢查時病患依照護理師手勢方向，當手勢往上時病患用力吸飽氣，護理師手勢往下時病患慢慢吐氣到底，整個通氣掃描過程中病患配合護理師手勢確實執行吸氣及吐氣的動作，順利完成通氣掃描。

**結論：**一般肺臟通氣掃描檢查是用口號的方式和病患搭配檢查，但此案例是一位嚴重聽力障礙的病患，若採用原本方式進行檢查會發現效果不彰，護理師思考改變檢查時病人配合的方式，教導病患配合手勢確實執行呼吸技巧，如此不但可幫助順利完成檢查，也能提供清楚的影像協助醫師發現病灶，提升醫療品質。

PC-096

## Suspicious Cutaneous T-cell Lymphoma On $^{18}\text{F}$ -FDG Imaging of Left Buccal Mucosa Squamous Cell Carcinoma Mucosa

Juang-Wei Hsieh, Yu-Ling Hsu

*Department of Nuclear Medicine, Ditmanson Medical Foundation Chia-Yi Christian Hospital*

**Case:** The patient is a 38-year-old male who was hospitalized because of left cheek mass lesion. The pathological diagnosis confirmed as squamous cell carcinoma, staging cT4aN0M0. After chemotherapy, he came to the nuclear medicine department for re-staging evaluation with  $^{18}\text{F}$ -FDG positron emission tomography.

**Results:** After  $^{18}\text{F}$ -FDG positron imaging, there was high FDG uptake in the nasopharynx, which could not be ruled out as a hidden malignant tumor. Also high FDG uptake in the upper left gingival area noted, which was presumed to be residual tumor tissue. Yet another abnormal  $^{18}\text{F}$ -FDG uptake was found in the epidermis of the patient's bilateral buttock regions and lower abdomen, and the amount of abnormal  $^{18}\text{F}$ -FDG uptake was relatively large. After asking the patient, we confirm that there were indeed abnormal palpable lesions on both buttock regions and lower abdomen. Revealed as very itchy skin rash, the lesions have been lasting for 5 or 6 years already. Oral medication and ointment treatment were not effective.

**Discussion:** There are many differential diagnoses regarding what the skin rash lesions could be, including benign and malignant causes. One of the hypotheses is cutaneous T-cell lymphoma, which progresses and grows very slowly. There are two main phenotypes: one is mycosis fungoides (MF), which is characterized by a lot of asymmetric rashes on the skin of the patient, accompanied by scaling, redness and other symptoms; the other type is called Sezary Syndrome, which is characterized by the skin redness of the patient's body, accompanied by lympho-cells entering the surrounding blood. The symptoms of our case are quite similar to those of mycosis fungoides cutaneous T-cell lymphoma: itching skin rash appeared on the affected area, and the general dermatological drug treatment does not work. Therefore, further biopsy is recommended. We will also keep following the results.

PC-097

## Gallium-67 Scintigraphy with SPECT/CT for CNS Infection: A Case Report

Tsu-Kang Chen, Chien-Chin Hsu

*Department of Nuclear Medicine, Kaohsiung Chang Gung Memorial Hospital, Kaohsiung, Taiwan*

**Introduction:** Central nervous system (CNS) infection is a potentially life-threatening disease, and identifying and evaluating the infection is essential for proper management. Apart from computed tomography (CT) and magnetic resonance imaging (MRI), gallium-67 (Ga-67) scintigraphy with single-photon emission computed tomography/computed tomography (SPECT/CT) provides critical information in confirming and locating ongoing inflammation.

**Case Report:** A 12-year-old boy with a history of autism presented with fever, altered consciousness, and slurred speech. Brain MRI revealed a left temporal brain abscess with rupture into the ventricle. The patient underwent emergent stereotactic aspiration for the brain abscess and received antibiotic treatment for four weeks. Follow-up brain MRI showed suspected residual abscess, and Ga-67 SPECT/CT of the brain confirmed inflammation in the left temporal region. The patient experienced a second operation of open craniotomy for removal of the brain abscess. Two weeks later, however, another episode of spiking fever occurred. Brain MRI unveiled suspected progression of ventriculitis. Ga-67 SPECT/CT of the brain demonstrated a new lesion in the posterior horn of the left lateral ventricle, while the previous left temporal lesion was in resolution. The patient underwent a third operation of keyhole aspiration craniotomy via occipital approach for the left posterior horn abscess aspiration. After three operations and a 10-week course of antibiotics, his clinical condition improved significantly. Follow-up Ga-67 SPECT/CT of the brain demonstrated resolution of the left lateral ventricle lesion. The patient was discharged home with complete recovery.

**Conclusions:** Ga-67 scintigraphy with SPECT/CT is a helpful tool for identifying and locating CNS infection and is crucial for clinical decision-making.

PC-098

## Ectopic Parathyroid Incidentaloma in Lungs

Yao-Kuang Tsai<sup>1</sup>, Chi-Jung Tsai<sup>2</sup><sup>1</sup>*Department of Nuclear Medicine, Tri-Service General Hospital and National Defense*<sup>2</sup>*Medical Center, Taipei, Taiwan*

**Introduction:** <sup>99m</sup>Tc-methoxy isobutyl isonitrile (MIBI) scintigraphy is widely used in diagnosis of a variety of malignant and benign diseases. It is usually considered for patients with hyperparathyroidism for pre-operative evaluation because it can identify abnormal parathyroid glands. However, malignancy can be also detected because of the characteristics that MIBI can be passively accumulated within the mitochondria of the tumor cells which are metabolically active.

**Case:** We presented a rare case of a 50-year-old woman with chronic renal failure and tertiary hyperparathyroidism. She underwent parathyroidectomy ten years ago but still presented with recurrent hyperparathyroidism. She accepted <sup>99m</sup>Tc-MIBI scan for further survey. The images showed no specific lesion in the neck, but multiple pulmonary nodules were incidentally found and two of them showed MIBI-uptake that were suspicious of malignancy. She underwent resection of the nodules, and the pathology revealed benign parathyroid glands.

**Discussion:** We suggested ectopic parathyroid incidentaloma might be considered for a patient with chronic renal failure and recurrent hyperparathyroidism after parathyroidectomy presenting multiple pulmonary nodules showing MIBI-uptake, which might be a diagnostic pitfall of malignancy.

PC-099

## 攝護腺癌骨轉移治療鐳 -223 注射治療劑量準確度分析

張桂蘭 李岱恩 顏維徵 張淑敏 張晉銓

高雄醫學大學附設中和紀念醫院核醫部

**目的：**去勢抵抗性前列腺癌 (CRPC) 患者發生骨轉移且尚未臟器轉移，使用鐳 -223 治療與其發病率和改善生活品質及提升生存率。Xoigo 是一種發射  $\alpha$  粒子的放射治療劑量方案為每千克體重 55 kBq (1.35 微居里) 間隔 4 周，共注射靜脈 6 劑。因為療程中可能產生的副作用病情因血液變化惡化甚至輸血；噁心食慾不振造成血球數量的不足等，因此注射治療劑量的準確度很重要。

首先將放射劑量測定儀校正好鐳 -223 的設定，注射劑量以 kBq 為單位；量測病人體重；確認放射藥品到貨日期之自然衰變之校正因子 (reference date)；確認藥品基本資料、計算給藥劑量、測量給藥前後之瓶內劑量；量測注射針前後之劑量。核對記錄這些數據；如此鐳 -223 注射的治療劑量的詳細量測，方可達到治療的準確性，以保護患者治療的安全。

**研究方法：**患者於注射前必須先行至門診抽血評估是否合適進行鐳 -223 的治療程序；核醫專科醫師再了解評估病患的臨床症狀及給予治療劑量。注射前依據患者的體重決定施打的劑量。事先將放射劑量測定儀校測定鐳 -223 的設定，依據治療劑量的換算：注射體積 (ml) = 體重 (Kg) \* 放射活性 (55 kBq/Kg 體重) / Dk 因子 \* 1100 KBq/ml 給予施打注射治療。

過程中特別要注意的是，到藥劑量 1100 kBq/ml，而每瓶內是 66 MBq/m 共 6 ml。記錄放射藥品到達日期即有效日期，確定使用時間的衰變因子，先行量測藥劑瓶內的劑量 (kBq)；準確量測注射針抽取毫升內劑量 (kBq)；量測瓶內剩餘劑量 (kBq)；再量測注射針殘餘剩餘量。記錄這些劑量數據可以確實計算出患者注射入體內治療劑量。注射體積小於 6 mL，以超過 1 分鐘時間緩慢注射，小心不可漏針。

**結論：**鐳 -223 經注射後至骨轉移處釋放  $\alpha$  射線將殺死癌細胞，抑制癌細胞纖維增生及減緩骨轉移之疼痛。放射藥師及注射護理師在執行上要別小心，以求達到標準注射劑量  $\pm 10\%$  以內，所以必須加強治療注射劑量的準確度，致力保護患者的安全與健康。

PC-100

## 運用 Power Bi 提升正子造影作業分析效率 —經驗分享

許幼青<sup>1</sup> 廖建國<sup>1</sup> 陳薇璇<sup>1</sup> 莊紫翎<sup>1,2</sup> 王昱豐<sup>1,2,3</sup>

<sup>1</sup> 佛教慈濟醫療財團法人大林慈濟醫院核子醫學科

<sup>2</sup> 慈濟學校財團法人慈濟大學醫學系

<sup>3</sup> 佛教慈濟醫療財團法人大林慈濟醫院預防醫學中心

**背景介紹：**Power BI 是一種數據分析，可以簡單的將數據轉成圖表，也可以連結其他資料庫直接進行分析，除此之外可將不同資料間轉換成相關性，並能用視覺化的方式檢視及分析資料內容，甚至於可以與任何人共用該資料。本科要提升醫品病安及價值管理成效，及確保本其餘細滿足永續發展，所以培育運用管理工具促進品質改善，期望可以簡化流程和減少人力，所以使用 Power BI 輸入正子造影檢查資料 (疾病別、開單醫師、科別等) 進行數據分析，主要目的了解科別、醫師之作業量的變化。

**Power BI 分析：**收集從 2018 年至 2021 年 6 月每月正子造影檢查患者之疾病、開單科別及開單醫師資料將資料輸入至 excel，從 Power BI 軟體導入 excel 資料進行分析。一、欲知道每年開單醫師的起伏狀況分析資料如下：選擇樹狀圖，群組選「科別」，值選「開單醫師計數」可以得到各科醫師的開單量 (圖一)。選擇群組直條圖，軸選「年分」、圖例選「科別」、值選「開單醫師計數」可以得到每年份各科醫師開單量 (圖二)。二、知道了每年開單醫師前三大排行榜，想針對前三大排行榜的科別，了解其作業量之間的差異，分別將各科醫師設定群組，分析資料如下：選擇折線與群組直條圖，共同軸選「年分」、直條圖數列「開單醫師」、直條圖值「開單醫師 (群組) 的計數」、折線圖值「開單醫師的計數」、鑽研處將想要科別勾選科別，可得到各科醫師的開單量情形 (圖三)。除此之外想得知這些醫師們的前三大排行榜，則可按右鍵點選「分析」，點選找出此分佈的不同之處，就可以進一步得知這些醫師中變化量最大的醫師。三、想進一步分析原因，故從其他資料庫去擷取各科醫師看診量來討論是否有相關性。1、先擷取醫師看診量資料庫，將資料載入後和原資料至模型處，將兩個不同資料庫編輯關聯性，則可結合兩個資料庫內容。2、選擇折線與群組直條圖，共同軸選「開單醫師」、直條圖數列「年分」、直條圖值「人數」、折線圖值「開單醫師 (群組) 的計數」、小倍數「年分」 (圖四)，可以得知醫師開單量和看診量之間的相關性。

**結論：**Power BI 是一個非常好的視覺化軟體，每個月做出來 excel 檔案直接放入原資料夾內，就可以更新當月的資料，所以可以讓使用者原本每個月可能花費 20 小時，降低成 10 分鐘，整整減少 10 倍以上，除此之外，主管可以在自己的電腦了解科室的作業量情形，對科室人力物力上都是很有幫助的軟體。

PC-101

## 核醫造影排檢指定個案之迴溯性分析

<sup>1</sup> 廖建國 許幼青<sup>1</sup> 莊紫翎<sup>1,2</sup> 王昱豐<sup>1,2</sup>

<sup>1</sup> 佛教大林慈濟醫院核子醫學科

<sup>2</sup> 慈濟大學醫學系

**背景：**核醫造影例行排檢作業中，病人由於個別因素而指定檢查日期之個案並不少見，本科今年開始嘗試努力，期望將排檢指定個案盡量減少，以提升檢查之效率。本研究目的即為迴溯性分析今年以來之排檢指定個案，以了解排檢指定比率及檢查完成天數之變化情形，以作為持續改善的參考。

**方法：**收集 2021 年 1 月至 2021 年 6 月本科核醫造影檢查之排檢紀錄資料，統計每月排檢指定個案中排檢天數大於 7 天之件數，並進一步分析各項目排檢指定比率及指定個案檢查完成天數，以比較排檢指定比率及檢查完成天數之變化情形。

**結果：**整理結果發現，2021 年 (1-6 月) 本科核醫造影之平均排檢指定比率為 36.77%，其中比率最高的月份為 3 月 (45.63%)，而最低為 5 月 (28.87%)，顯示排檢指定比率大多維持在 3-4 成左右。再觀察每月的變化，發現第 2 季的指定比率明顯較第 1 季低，顯示排檢指定比率有逐步下降的趨勢。進一步分析各項目的排檢比率，發現心肌灌注檢查之比率為 20.15%，骨骼掃描為 48.27%、正子造影為 17.75%、其他項為 24.90%，其中以骨骼掃描的比率最高；正子造影的比率最低，顯示骨骼掃描為指定個案的主要項目，而第 2 季較第 1 季比率減少主要也是因為骨骼掃描的指定個案大幅減少所致。另外，分析指定個案的檢查完成天數，發現 30 天內完成的比率佔 90.5%、30-89 天完成的比率佔 6.3%，而超過 90 天才完成的比率僅佔 3.1%，顯示絕大多數指定排檢日期的病人皆可在 1 個月內完成。

**結論：**分析結果顯示，本科核醫造影之平均排檢指定比率為 36.77%，其中以骨骼掃描的比率最高，其他項目則相對較少。因此，未來可優先針對骨骼掃描之檢查，透過排檢時的說明及溝通，請病人配合儘量於 7 日內完成檢查，以持續降低病人指定個案，進而提升整體檢查效率。

PC-102

## 核醫新進造影儀器之 TAF 異動申請—經驗分享

廖建國<sup>1</sup> 許幼青<sup>1</sup> 莊紫翎<sup>1,2</sup> 王昱豐<sup>1,2</sup><sup>1</sup> 佛教大林慈濟醫院核子醫學科<sup>2</sup> 慈濟大學醫學系

**背景：**2020年10月本科參加全國認證基金會(TAF)舉辦之年度實驗室主管訓練，課程中說明有關TAF常見處置案例、權利義務規章以及管理階層的要求等新的規定，其中TAF常見處置案例中包括「未依要求期限提出異動申請」之處置，這是根據TAF權利義務規章(TAF-AR-10)第4.10條之規定，申請人若有設備異動(含新增儀器/已裝機完成測試)，至遲應於異動發生之日起15日(日曆天)內提出申請。本科因正好於2020年10月新進1台SEPCT/CT(NM/CT 860)，因此立即向TAF申請異動，經現場評鑑通過後，取得認證核決。本文目的即為整理本科申請異動之過程，提出經驗分享。

**申請程序：**(1)由TAF資訊系統進行申請，填寫異動設備之儀器名稱、型號、異動日期以及所影響之檢查項目等資料，並上傳儀器操作作業標準、儀器安全測試紀錄與儀器登記證明文件，送TAF審核。(2)TAF審核通過後，安排現場評鑑事宜，待排定日期後通知申請單位。(3)申請單位針對TAF安排之日期，回覆是否可配合辦理。

**準備事項：**因新增1台儀器，造影室應優先制定儀器操作之作業標準，並針對新增儀器所影響的相關文件及表單進行變更修訂(例如各項檢查作業標準中使用儀器的說明、檢查作業品保作業程序中有關儀器品管作業的說明、各項造影檢查紀錄表中儀器選項的變更等)。另外，新增之造影儀器雖原檢查流程及步驟(操作方法)不變，但部份項目之儀器造影條件須增加新機之內容，因此我們也針對作業較大可順利配合試作驗收的項目，進行新機影像品質的確認，並備妥相關紀錄，以提供評鑑佐證使用。

**現場評鑑：**2021年12月16日接受TAF現場評鑑，訪查重點包括確認下列事項1.新購設備依據採購或驗收等程序所完成之紀錄2.依據造影室程序使用前應完成的評估作業3.因異動所涉及相關程序的審查或修訂4.因異動所涉及對應使用設備或操作程序之人員再訓練與考核5.因異動所涉及報告數值或報告內容變更之審查6.對應異動所涉及病人準備內容之修訂與對外的公告事項。

**結論：**設備異動申請之要求為TAF權利義務規章之規定，參加TAF認證的單位應清楚了解。此外，依TAF的最新規定，經TAF認可之服務範圍與項目的運作，除應遵照品質管理系統之規範外，也應符合TAF權利義務規章及監督要求，包括異動關鍵事項之辦理時機、認證標誌使用、資料保存期限、違反權利義務規章之處置規則、後續如涉及處置規則之重新申請或恢復之相關要求等。



PC-103

## 正子造影病人血糖值異常之分析及探討

廖建國<sup>1</sup> 許幼青<sup>1</sup> 莊紫翎<sup>1,2</sup> 王昱豐<sup>1,2</sup><sup>1</sup> 佛教大林慈濟醫院核子醫學科<sup>2</sup> 慈濟大學醫學系

**背景：**正子造影例行排檢及衛教時，會要求糖尿病患者檢查當日停用降血糖藥物，並盡量控制空腹血糖值於 150 mg/dL 以內，以確保影像品質。本研究目的即為分析近半年正子造影受檢者之血糖值監測情形，以了解造影前血糖值管控情形以及受檢者中有糖尿病史的比率，並探討糖尿病照護的議題。

**方法：**收集 2021 年 1 月至 6 月本科正子造影之檢查相關紀錄，逐一檢視各受檢者之血糖監測值、糖尿病史以及受檢者是否可自行活動與是否有家人陪同等狀況，分別依初次血糖值 < 70、> 150、> 200、> 350 mg/dL 計算各受檢者血糖值異常比率之分佈，並依受檢者有、無糖尿病史進行分析比較，再進一步比較兩者受檢狀況及家人陪同情形，以探討糖尿病人在正子造影檢查時的照護問題。

**結果：**整理結果發現，本科近半年正子造影受檢者中有糖尿病史者佔 21.69%；無糖尿病史者佔 78.31%。造影前血糖監測結果，血糖值 > 150 mg/dL 者佔 8.43%、> 200 mg/dL 者佔 3.61%；而 < 70 及 > 350 之比率皆為 0%。顯示大多數的受檢者於檢查前之血糖值管控良好，並無極端偏高 (> 350) 或偏低 (< 70) 之個案，惟仍有部份受檢者之初次血糖值 > 150 或 > 200，不過這些個案也在注射點滴或胰島素之處置後，順利完成檢查，也未影響造影品質，其中有糖尿病史之比率高於無糖尿病史者，與預期一致。另外，比較受檢者受檢狀況及其家人陪同情形，發現無法自行活動者佔 12.05%、無人陪同者佔 28.92%、無法自行活動且無人陪同者佔 0.6%，其中無法自行活動者有無糖尿病史並無明顯差異，無人陪同者中有糖尿病史之比率 (4.22%) 則明顯低於無糖尿病史者 (24.70%)，而無法自行活動且無人陪同者，僅有 1 例，此為非糖尿病患者。顯示正子造影檢查時，大多數的受檢者均可自行活動且有人陪同，並未發現糖尿病患者無法自行活動且無人陪同者

**結論：**本科近半年正子造影受檢者之血糖管控良好，初次血糖值 > 150 mg/dL 者僅佔 8.43%，其中有糖尿病史之比率明顯高於無糖尿病史者，經進一步處置後均未影響影像品質。此外，糖尿病人中無法自行活動者，均有人陪同前來檢查，檢查過程中若發生血糖過高或過低之症狀時，本科醫護同仁也會依本院糖尿病照護指引給予即時且適當的處置，以確保造影檢查時的病人安全及照護品質。

PC-104

## 運用風險管理持續改善 RIA 報告品質之成效分析

廖建國<sup>1</sup> 張素雲<sup>1</sup> 莊紫翎<sup>1,2</sup> 王昱豐<sup>1,2</sup>

<sup>1</sup> 佛教大林慈濟醫院核子醫學科

<sup>2</sup> 慈濟大學醫學系

**背景：**本科於 2020 年起建置風險管理機制，每發生 1 件不符合事件即評估其發生頻率及嚴重程度，並依據危害指數決定是否進行矯正措施。RIA 實驗室報告誤發之不符合事件，並不少見。本研究目的即為分析導入風險管理後報告品質之持續改善情形。

**方法：**收集 2020 年至 2021 年 (1-6 月) 報告誤發之不符合事件，分別統計各年度每月報告核發之總件數、報告更正件數及其誤發原因，並進一步比較各年度之報告更改率以及更改原因之件數變化，以了解導入風險管理後報告品質之改善成效。風險管理運作中危害指數之計算為發生頻率乘以嚴重程度，而發生頻率及嚴重程度各分為 4 個等級。危害指數  $\geq 8$  之不符合事件，屬於高風險應實施矯正措施。

**結果：**收集報告核發案例，總計 107523 件，包括 2020 年 77373 件；2021 年 (1-6 月) 30150 件。不符合事件總計 12 件，包括 2020 年 8 件；2021 年 (1-6 月) 4 件。比較導入風險管理後報告更改率變化情形，可了解 2021 年之報告更改率 (0.018%) 較 2020 年 (0.02%) 略為降低，顯示實驗室報告實施風險管理後已有進步的成果。進一步分析報告誤發之各項原因及其件數，發現近 2 年報告誤發的主要原因為未回乘稀釋倍數、後一筆數據蓋過前一筆、其餘原因相對較少。進一步比較近 2 年的表現，發現 2021 年未回乘稀釋倍數之件數，已由 2020 年 3 件降至 2 件；後一筆數據蓋過前一筆之件數，則由 2020 年 2 件降至 1 件。至於 2020 年未依最小靈敏度發報告、數值輸入錯誤、誤發未作之檢體等報告疏失，則 2021 年至今均未發生，惟清單順序錯誤是 2020 年未發生的項目，實驗室應特別注意監控改善，以避免再次發生異常。

**結論：**本科 RIA 實驗室運用風險管理之策略，針對每件報告不符合事件進行風險管控，分析比較近 2 年的報告品質，可了解 2021 年報告更改之比率已降至 0.018%，不符合事件也較 2020 年大幅減少，顯示透過風險管理的策略，的確可以達成持續改善的目的。

PC-105

## 利用影像後處理技術來觀察影像品質及 SUV 之變化

曾柏銘<sup>2</sup> 劉奇芝<sup>1</sup> 呂建璋<sup>3</sup> 沈淑禎<sup>3</sup> 門朝陽<sup>2</sup> 林雅婷<sup>3</sup> 蕭聿謙<sup>4</sup>

<sup>1</sup> 天主教中華聖母修女會醫療財團法人天主教聖馬爾定醫院影像醫學部

<sup>2</sup> 天主教中華聖母修女會醫療財團法人天主教聖馬爾定醫院正子造影中心

<sup>3</sup> 天主教中華聖母修女會醫療財團法人天主教聖馬爾定醫院核子醫學科

<sup>4</sup> 亞東紀念醫院核子醫學科

**背景介紹：**PET/CT 在病患的醫療過程中，為守護病患的一項重要檢查利器。PET/CT 有著影像功能性、解析學以及具全身掃描的混合影像，比起單獨的使用 PET 或 CT 具有更高的診斷能力。在 PET/CT 的造影過程中，FDG 的影像分佈及 SUV 的變化皆會影響醫師的診斷，故如何呈現良好的影像品質為每位醫事放射師需不斷努力的工作。

**方法：**我們使用了 Siemens Biograph 16 PET/CT 來做試驗，收集 40 位病人（男 / 女各 20 位），在 Early phase 時採用了 1 個 bed 兩分鐘的收集方式（intrinsic: 4，subset: 8，image size: 168，FWHM = 5），Delay phase 時在病患胸腔部同時收集 1 個 bed 2 分鐘（2 min/bed）與 3 分鐘（3 min/bed）的影像，VOI 圈選於左邊肺門部並排除因肺癌或轉移造成的肺門顯影個案，圈選之後我們分別去比對 delay/early phase、3min/bed /2min/bed 之 SUV 比值，以及調整 image size 168 x 168 與 336 x 336；intrinsic 4 與 8 之各項差異。

**討論：**在 VOI 的選定中，我們發現若將 VOI 圈選定於腫瘤處進行比對，則 Early 及 Delay phase 的 SUV 差異比例會加大，在經討論後我們將 VOI 選定於非轉移造成顯影的肺門處。試驗過程我們也發現 Early 及 Delay phase 在正常的掃描下並非呈線性關係。在 3 min/bed 與 2 min/bed 的掃描下，其 3 min/bed 大約會比 2 min/bed 增加 1-5% 的 SUV，但也有幾位呈現下降情況。我們認為此情況與病人本身的代謝效率（藥物有效半衰期）有關係；在影像處理部分，我們發現在腫瘤聚集之區域，如將疊代次數（intrinsic）增加，則更易將原聚集之腫瘤分開，但 SUV 也相對增加（intrinsic 4 與 8 約增加了 20%）。

**結論：**經由上述實驗我們發現在更動參數後，SUV 也隨之改變。故我們認為，SUV 需與影像品質分開處理，意即在掃描前參數皆不做任何改變，醫師於判圖中如需更銳利（或更平順）之影像則再重新進行組像，但重新組像後之 SUV 則較不具診斷意義。

PC-106

## 討論並分析在正子造影所造成的留置針藥物殘留原因

曾柏銘<sup>1</sup> 呂建璋<sup>2</sup> 沈淑禎<sup>2</sup> 門朝陽<sup>1</sup> 林雅婷<sup>2</sup> 蕭聿謙<sup>3</sup>

<sup>1</sup>天主教中華聖母修女會醫療財團法人天主教聖馬爾定醫院正子造影中心

<sup>2</sup>天主教中華聖母修女會醫療財團法人天主教聖馬爾定醫院核子醫學科

<sup>3</sup>亞東紀念醫院核子醫學科

**背景介紹：**FDG 是結合了去氧葡萄糖與放射性同位素 F-18 的診斷型核醫藥物。將 FDG 打進身體後可探討葡萄糖在人體的新陳代謝過程。在進行正子造影檢查過程，由於會擔心發生藥物過敏狀況，故留置針會在檢查結束後才予以拔除，而留置針的設置也會導致堆積正子藥物的狀況，由於前年我們利用 PDCA 手法成功解決因注射 Tc-99m MDP 造成的核醫藥物堆積，去年開始我們想要藉由此經驗來分析正子藥物 (18F-fluorodeoxyglucose, FDG) 造成藥物堆積之原因並予以解決。

**方法：**我們收集 2020 年 10 月 -2021 年 04 月曾經進行正子造影檢查之病人 (共 231 位，男 94 位，女 137 位)，分別以年齡、性別、不同種類之留置針 (Lock & T-connect)、以及生理食鹽水沖洗量 (10 cc & 20 cc)，來檢視造成正子造影藥物堆積的原因。

**討論：**依據去年的統計結果，我們發現生理食鹽水的沖洗量似乎可以降低留置針的藥物堆積情況，於是今年又針對生理食鹽水的沖洗量連續觀察七個月，在統計分析後卻發現並沒有太多異差性。在此次的統計分析中，我們觀察到造成留置針堆積的原因與性別 ( $P = 0.012$ )、留置針類型 ( $P = 0.004$ ) 與外在原因 ( $P = 0.000$ ，外在原因意即非本科護理師安裝之留置針或在注射過程護理師或病人感覺有異狀) 有顯著差異。而本科護理師只進行 lock 施打，T-connect 則由其它科室抽血完後順帶過來，在綜合判斷後，我們認為護理師的技術純熟度決定了留置針的殘留狀況。

**結論：**此次的實驗結果我們得知護理師的技術純熟度決定了留置針的藥物殘留比例，但在其它科室安裝好留置針後，除留置針塞住外，一般是不會再去重新安裝一個新的留置針。故如何消除由其它科室安裝之留置針產生的藥物堆積，就成了我們的觀察重點。我們仍會持續努力，並將留置針藥物堆積的比例降至最低。

PC-107

## 降低核醫造影藥物施打之滲漏率

張志維 林宜瀟 顏羽蓁 侯景維 楊郁茹 蔡世傳\*

臺中榮總醫院核子醫學科

**背景介紹：**核醫檢查注射造影藥物漏針會影響影像品質，為使檢查續行，有時會再次注射藥物，倘若可能影響影像後續分析數值時，甚至須讓受檢者擇日再行檢查。藥物滲漏會造成病患輻射暴露風險增加，也影響影像判讀；本研究嘗試利用品管手法，統計解析造成漏針的各項原因並擬定介入之改善措施，期望降低藥物施打之滲漏率。

**方法：**本研究收集 106 年 1 月至 3 月間骨骼掃描病患受檢資料，統計漏針與受檢總量之比率，透過品管手法找出並統計造成漏針時的可能原因，解析各項原因後擬定介入之改善措施，再統計使用改善措施後漏針的次數及該次原因，評估是否有效改善藥劑滲漏率。

**結果：**統計發現藥劑滲漏率在各檢查為 14.92% 至 19.44%，其中以骨頭掃描滲漏率最高 (19.44%，其中病人因素為 14.48%，針具因素為 2.38%，其它因素共佔 2.58%)。因此決定以骨頭掃描執行改善措施。針對病人因素及針具因素介入改善措施後，總藥劑滲漏率升為 21.31%，其中病人因素為 10.10%，針具因素為 7.51%。討論後應是改善措施落實度不佳，於檢討後更徹底確實落實改善措施後，總藥劑滲漏率仍有 20.58%，但病人因素下降至 7.46%，針具因素則上升為 8.59%。

**結論：**透過品管手法介入後，病人因素導致藥物滲漏比例大幅下降，表示針對病人因素的改善措施是有效的，但針具因素並無法有效下降，導因可能為使用留置針之受檢者，幾乎為住院病人，身上留置針狀況較難掌握，即使施打藥劑前後皆使用生理食鹽水沖洗多次，仍無法有效顯著改善藥物滯留於留置針的情形。

PC-108

## 建立「正子造影電子表單」， 提升醫療檢查品質資訊化

楊士頤 曾旭吟 周珉臻 盧淑婷 李世昌

國立成功大學醫學院附設醫院影像醫學部核子醫學科

**背景介紹：**正子造影檢查須確認受檢者相關過去病史、治療（包含服用或施打化療藥物、放射線治療）、近期有無手術、過敏史及是否懷孕等資料。傳統記錄依賴護理師手寫或列印表單方式提供資訊，不但耗時、耗紙、病歷保存空間且有可能出錯，更無法達到即時性。因此結合醫院資訊化政策，於正子造影中心推動正子造影電子表單，以 HIS 系統建立整合複雜且能完整保存呈現資訊，去除病歷紙本的產生並於系統上提供臨床醫師檢查時之相關資訊。

**方法：**2019 年初起收集護理師、醫師、放射師使用之表單進行統整，列出三張紙本表單 - 「受檢者基本資料單」、「藥物醫囑單」、「正子造影中心受檢流程 - 生理監控指數、正子藥物施打劑量、造影時間及輻射參數」。整合表單細節使用性分門別類及列出需病歷簽章之表單，再結合病歷室電子化設立在院內 HIS 系統即可編寫存檔、開立藥物醫囑、護理師簽署執行、放射師執行檢查等資訊，以上資訊皆能提供各臨床醫師於 HIS 系統查詢，了解病人當日檢查狀況。

**結果：**2019 年 11 月於院內 HIS 系統正式上線，實施此線上作業程序後，能即時性給予醫生目前病人狀況。如醫生須給病人藥物也無須到正子中心寫立紙本醫囑，只要有電腦安裝 HIS 系統登入帳密，即可於系統上點選藥物醫囑，並口頭告知護理師，再由護理師於系統確認醫囑，立即線上簽屬執行給藥，不耽誤病人檢查診斷時間。

**結論：**從 2019 年 11 月起至今，藉由結合院方 HIS 系統所發展之電子表單流程與傳統紙本記錄相比，充分改善醫師、護理師及放射師之間的溝通，以確保正子造影檢查之執行與品質，並降低檢查過程中錯誤風險的產生，達到以下成效：1. 具即時性，病人資訊能電子保存並藉由電子認證把關確保資料不被竄改。2. 去除紙本醫囑無法辨識或筆誤之情況而導致給藥錯誤。3. 減少紙本傳送遺失與紙張浪費。

PC-109

## 以 FMEA 手法提升核醫品質系統， 減輕風險造成之危害

楊士頤 莊穎昌 吳佩珊

國立成功大學醫學院附設醫院影像醫學部核子醫學科

### 背景介紹：

臨床風險狀況百百種，建立風險管理分析來降低風險事件發生的可能性或有系統地檢討分析來預防臨床流程、儀器設備、人為、藥品耗材所造成的淺在失效。

藉由 TAF ISO15189 認證條文之規定導入核子醫學影像，設立風險管理已是醫學實驗室認證重點之一，從檢查前、中、後不同的情境層面上，來監控各項危險因子，降低風險事件發生所造成的成本及損傷，在最低成本效率下，對風險進行監控、最小化或消除之管理。

### 方法：

1. 使用的風險管理手法：失效模式與效應分析 Failure Mode and Effect Analysis (FMEA)。是預應式風險管理的作法，有種防患於未然的方式，建立保護屏障，降低損失傷害。即使風險依然存在，但也是可容許度低的風險。
2. 設立傳統核醫造影檢查四大失效來源步驟：檢查前、檢查中、排檢失效、檢查後。
3. 找出四個可能發生之失效事件：同位素藥物施打錯誤、病人管路滑脫、設備故障時無零件更換、不良影像影響判讀。
4. 實施四組矯正行動：藥損數量及原因統計、管路執行率、排檢時間 > 14 天閾值、影像品質不良數。

### 結果：

自 110 年 3 月開始執行 FMEA 風險管理監控，在每月的科內品質管理會議上進行表格式的追蹤。統計至 8 月為止，失效事件件數為 0 件，各項控制行動執行率 100%。利用此手法顯著地降低不符合事件的發生，系統性避免可能產生的風險因子。

### 結論：

以傳統核醫造影檢查為核心，成員包含有醫師、護理師、藥師、放射師、櫃台行政人員等與整個醫療檢查照護流程有關為主，降低可能造成病人的傷害，使病人安全達至高品質。

PC-110

## 使用客觀結構式臨床測驗評量於核醫技術學之應用： 以臨床正子造影技術為例

楊士頤 曾旭吟 謝沁苙 李世昌

國立成功大學醫學院附設醫院影像醫學部核子醫學科

**背景介紹：**客觀性結構式臨床技能測驗 (objective structured clinical examination；簡稱 OSCE) 用來評量醫事放射實習學生在臨床教育上是否會正確的做 / 表現能力，以及在真正照顧病人時的實際行為 / 臨床表現。

**方法：**以 109 年 24 名醫事放射實習學生為對象，正子造影檢查為主題，制定正子檢查教案 (標準化病人指引、醫病情境劇本、考官指引、實作評估量表、雙向回饋)，透過情境模擬臨床病人狀況呈現，考驗學生是否能正確表現能力及靈機應變的回答病人提出的問題。依據檢查前、中、後，三大層面設計觀看項目，共 15 項，測驗 10 分鐘，滿分 30 分。

**結果：**經測驗結果，24 名學生皆通過 OSCE 考核，雙向回饋滿意度結果 (滿分五級分)：1. 考試內容來自平日實習所學內容為 4.8 級分，2. 試場標示及路線規劃為 4.8 級分，3. 試題指引內容清楚為 4.8 級分，4. 標準病人的演出像真實病人為 4.8 級分，5. 考試時間長短適當為 4.8 級分，6. 考試難易度為 4.8 級分，7. 運作流程紀律為 4.8 級分，8. 考官客觀評分為 4.9 級分，9. 對自己的測驗結果為 4.5 級分，整體滿意度平均皆達 4 級分以上。

**結論：**測驗過程中會有疏失或遺漏等情形發生，導致學生對自己的測驗結果滿意度偏低，期望值跟實際結果不同，但這就是臨床上會有突發的表現，能處變不驚，順利完成一個病人檢查過程，才是我們所要訓練的。未來在藍圖設計上，會再應用於傳統核醫造影、放射免疫分析、骨質密度等情境設計。



PC-111

## 放射免疫分析室之放射性廢棄物 與廢水產出關係之研究 – 以南部某醫院核醫科為例

張朝鈞 卓世傑 顏吉龍 張淑芬 曾宜玲 段淑薰 李將瑄

奇美醫療財團法人奇美醫院核子醫學科

### 背景介紹：

放射免疫分析室產出之放射性廢棄物與廢水由於會造成輻射暴露，基於安全與法規規定，是放射免疫分析室必須且經常需處理的事項之一。而放射性廢水與廢棄物的產量多寡，將會直接影響到後續儲存與外釋的許多問題。直覺的情形下，放射性廢水與廢棄物的產出量應有一定之關係。不過，究竟是否如此，則似欠缺類似的研究可供參考。因此擴增此方面之研究，實有必要。本文即為探討放射免疫分析室之放射性廢棄物與廢水產出關係之研究。

### 方法：

1. 紀錄南部某醫院核醫科放射免疫分析室，每次放射性廢水桶(定量 300 公升)開始儲存及滿桶之日期，據以計算扣除六、日之每桶實際工作日。
2. 紀錄南部某醫院核醫科放射免疫分析，每次放射性廢水桶啓用次日至滿桶當日止，每次包裝儲存放射性廢棄物(多為混合試管)之重量與日期。
3. 整理、統計，前兩項廢水與廢棄物等相關數據，以提出結果。

### 結果：

1. 共收集自 2018 年 2 月 27 日至 2021 年 5 月 2 日止，共計 15 筆，最多為 94、最少為 17 日，合計 833 日，平均每桶工作日約 55.5 日之放射性廢水儲放紀錄資料。
2. 共收集自 2018 年 3 月 9 日至 2021 年 4 月 27 日止，共計 408 筆，合計 2039.5 Kg，再依照廢水桶之 15 個工作日，分為 15 個區段，最高為 233、最少為 52 Kg，平均每區段約 136 Kg 之放射性廢棄物儲放紀錄資料。
3. 經相關性統計結果，發現放射性廢水桶每區段工作日數與相應之每區段放射性廢棄物產出量有 0.77 之相關性。
4. 經迴歸統計結果，發現放射性廢棄物每區段工作日產出量與放射性廢水桶工作日數相應之線性迴歸關係式為  $f(x) = 0.29 + 16.15$ 。

### 結論：

本研究發現，南部某醫院核醫科放射免疫分析室：

1. 南部某醫院核醫科放射免疫分析室之放射性廢水與廢棄物的產出量確實有高度之正相關，其係數為 0.77。
2. 放射性廢棄物每區段工作日產出量與放射性廢水桶工作日數相應之線性迴歸關係式大約為下式：廢棄物產出重量  $*0.29 + 16.15$  日 = 放射性廢水桶工作日。

PC-112

## 核子醫學檢查住院病人尿布核種統計之研究 — 以南部某醫院為例

卓世傑 陳懿貞 鄭揚霖 梁育雅 張虹麗 顏玉安 李將瑄

奇美醫療財團法人奇美醫院核子醫學科

### 背景介紹：

台灣各醫院對核子醫學科檢查住院病人，尿布之收集已行之有年。不過，有關尿布核種之分布研究，卻較為缺乏。實際上，由於不同的核種在輻射劑量率與儲存時間方面，都有極大之差異。因此探究尿布核種之分布情形，對於醫院公共安全與輻射風險的管制規劃皆有相當高的參考意義。本研究即是以南部某醫院核子醫學科住院病人為例，探究尿布核種分布之研究。

### 方法：

1. 收集南部某醫院 2018、2019 及 2020 年，共 3 年，每年各 100、130、148 人次（每人一次一件），合計 378 筆，接受核子醫學檢查住院病人之尿布資料。
2. 將上述資料，分別以年為單位將各病人尿布之核種，重量，分別歸類整理。
3. 統計與分析上述資料，並整理成結果，再據以提出結論。

### 結果：

1. 尿布件數雖然每年穩定上升，但每件均重部份（總重量 / 總包數）變化不大，自 2018 至 2020 年分別是 1062、1148 及 1100 g。
2. 自 2018 至 2020 年之尿布核種件數比率皆以 Tc-99m 最高，Ga-67 次之，且該 2 類核種件數合計即佔約 90%，其他核種尿布件數比率僅約佔 10% 左右。
3. 自 2018 至 2020 年之尿布核種重量比率亦皆以 Tc-99m 最多，其次為 Ga-67，且該 2 類核種重量合計亦佔約 90%，其他核種尿布重量比率僅佔約 10% 附近。
4. 含 Tc-99m 與 Ga-67 核種尿布中，Tc-99m 之件數與重量比率都呈逐次下降之趨勢，自 2018 至 2020 年分別為 78、67、64% 與 72、66、56%；相反的 Ga-67 之件數及重量比率則快速上升，比率為 14、22、24% 以及 17、25、34%。

### 結論：

依南部某醫院自 2018 至 2020 年，接受子醫學檢查住院病人之尿布資料顯示：

1. 每件尿布均重約 1100g 左右。
2. 不論是件數或重量，含 Tc-99m 或 Ga-67 核種合計之比率佔約 90%，其他核種僅約佔 10%。
3. 尿布之核種主要以 Tc-99m 為主，其件數與重量比率分別為 78、67、64% 與 72、66、56%。
4. 含 Ga-67 核種尿布之件數及重量比率，快速上升，分別是 14、22、24% 和 17、25、34%。
5. 若對尿布進行核種分類，因 Tc-99m 之存放時間較短，應可大幅減少尿布儲存空間。

PC-113

## 鈷 90 放射性廢棄物不同偵檢器偵測劑量率之比較研究

卓世傑 陳興隆 林凡珍 張南雄 鄭揚霖 顏玉安 李將瑄

奇美醫療財團法人奇美醫院核子醫學科

### 背景介紹：

鈷 -90 為純  $\beta$  輻射源，半衰期 64.2 小時，在台灣多使用於鈷 90 體內放射治療 (Yttrium 90 SIR Spheres Therapy) 作業。鈷 -90 治療作業需在導管室以導管注入直徑約 20 至 40 微米之鈷 -90 微球體進入人體，因此接觸之器具與人員衣物皆可能沾染鈷 -90，而成爲放射性廢棄物。由於放射性廢棄物之儲放與外釋作業均需以偵檢器進行劑量偵測，但核醫科經常使用之偵檢器又有閃爍式偵檢器或蓋格式偵檢器兩種，究竟此兩種偵檢器對純  $\beta$  射源之鈷 -90 的劑量偵測結果有無差異，頗值得探討。本文即爲探究此兩種偵檢器於偵測鈷 -90 放射性廢棄物有無差異之研究。

### 方法：

1. 分別以校正後之 ATOMTEX 公司生產之 AT1121 型閃爍式偵檢器及 S.E. International 公司生產之 Inspector 型蓋格式偵檢器，於以下 2. 之條件，測量相同之鈷 90 放射性廢棄物。
2. 於距離鈷 90 放射性廢棄物 100、30 及 5 cm 之位置，分別於高度 30 及 60 cm 處，將偵檢器依序放置在一個寬 30 cm 平板之最左、中間及最右側 (5 cm 位置無偵測左、右兩邊)，各別偵測其劑量值並予以紀錄。
3. 整理、統計前 2 項數據，以提出結果。

### 結果：

1. AT1121 型閃爍式偵檢器及 Inspector 型蓋格式偵檢器，含背景值各有 13 筆資料，共 26 筆資料 (詳見下表一)。
2. 相同偵測位置之 13 組比較資料中，測得之輻射劑量率數值差距自 -46.9 至 148.6 nSv/h 不等，平均爲 33.1 nSv/h，比率則由 -27.5% 到 60.6%，平均則爲 16%。
3. 若以左、中、右側各組輻射偵測劑量資料比較，則可發現 AT1121 型閃爍式偵檢器之偵測數值，相比 Inspector 型蓋格式偵檢器較爲穩定與線性。
4. 對相同之鈷 90 放射性廢棄物各種距離、高度及位置之偵測數值，Inspector 型蓋格式偵檢器，除一處外，均高於 AT1121 型閃爍式偵檢器。

### 結論：

本研究發現：

1. AT1121 型閃爍式偵檢器與 Inspector 型蓋格式偵檢器針對相同之鈷 90 放射性廢棄物，其測得之輻射劑量率數值差距自 -46.9 至 148.6 nSv/h 不等，平均爲 33.1 nSv/h，比率則由 -27.5% 到 60.6%，平均則爲 16%。
2. 相比 Inspector 型蓋格式偵檢器，AT1121 型閃爍式偵檢器對鈷 90 放射性廢棄物之偵測數值較爲穩定與線性。
3. 對相同之鈷 90 放射性廢棄物，各種距離、高度及位置之偵測數值，Inspector 型蓋格式偵檢器，大多高於 AT1121 型閃爍式偵檢器。

PC-114

## 未注射鐳 223 藥劑輻射劑量率之偵測研究 — 以南部某醫院核醫科為例

卓世傑 張南雄 陳興隆 林凡珍 江佳諭 顏玉安 李將瑄

奇美醫療財團法人奇美醫院核子醫學科

### 背景介紹：

核子醫學科使用之鐳 223 (Radium-223) 治療藥劑，近幾年之使用量不斷增加。因此其相關之輻射防護問題，亦逐漸引起相關從業同仁之重視。一般來說，歸屬於  $\alpha$  射源的鐳 223 著重的是防止誤食、吸入或傷口侵入等體內輻射的防護，較少關注僅皮膚或紙即可阻擋之  $\alpha$  粒子所造成之體外輻射防護。但是，半衰期 11.4 天的鐳 223，在衰減至穩定的鉛 207 之前，也會產生少量的  $\beta$  粒子及  $\gamma$  射線 (發射能量比例： $\alpha$  為 95.3%， $\beta$  是 3.6%， $\gamma$  約 1.1%)。所以鐳 223 輻射劑量率之多少，尤其是尚未注射之鐳 223 治療藥劑，是頗值得探究的問題。本文即為，探討未注射鐳 223 藥劑輻射劑量率之偵測研究。

### 方法：

1. 收集南部某醫院核醫科，每次到貨未注射之鐳 223 藥劑之輻射劑量率偵測紀錄。
2. 以 Inspector 型蓋格式偵檢器，測偵尚未拆封的含鐳 223 藥劑之正方形紙箱，其正面 (有輻射標籤)，上方與下方，分別於距離 5 cm 處及距離正面 100 cm 處，共四項含背景值之輻射劑量率並記錄。
3. 整理、統計尚未拆封含鐳 223 藥劑之正方形紙箱，其正面，上方與下方各距離 5 cm 處以及距離正面 100 cm 處，等四項數據，以提出結果。

### 結果：

1. 共收集自 2020 年 8 月 3 日至 2020 年 12 月 7 日止，共計 23 劑尚未注射之鐳 223 藥劑之正面、上方、下方與距離 100 cm 處，各 23 筆含背景值，合計 92 筆輻射劑量率資料。
2. 距離正面 5 cm 之輻射劑量率最高與最低分別為 3.15 及 1.47  $\mu\text{Sv/h}$ ，平均為 2.12  $\mu\text{Sv/h}$ 。
3. 距離上面 5 cm 之輻射劑量率最高與最低分別為 1.24 及 2.70  $\mu\text{Sv/h}$ ，平均為 1.89  $\mu\text{Sv/h}$ 。
4. 距離下面 5 cm 之輻射劑量率最高與最低分別為 3.76 及 1.68  $\mu\text{Sv/h}$ ，平均為 2.63  $\mu\text{Sv/h}$ 。
5. 距離正面 100 cm 處之輻射劑量率最高與最低分別為 0.30 及 0.09  $\mu\text{Sv/h}$ ，平均為 0.14  $\mu\text{Sv/h}$ 。
6. 以正面之輻射劑量率偵測值分別與上方、下方及 100 cm 處之偵測值，進行相關性統計，其相關係數分別為 0.559、0.077 及 0.058，顯示僅上方與正面之輻射劑量率偵測值較有相關性。

### 結論：

本研究發現：

1. 未注射鐳 223 藥劑之正面、上方與下方輻射偵測值紀錄，平均分別為 2.12、1.89 及 2.63  $\mu\text{Sv/h}$ ，最高紀錄值出現於下方之 3.76  $\mu\text{Sv/h}$ ，最低則為上面出現之 1.24  $\mu\text{Sv/h}$ 。
2. 未注射之鐳 223 藥劑，距離正面 100 cm 處之輻射劑量率最高與最低分別為 0.30 及 0.09  $\mu\text{Sv/h}$ ，平均為 0.14  $\mu\text{Sv/h}$ 。
3. 正面之輻射劑量率偵測值與上方、下方及 100 cm 處之偵測值，其相關係數分別為 0.559、0.077 及 0.058，顯示僅上方與正面之輻射劑量率偵測值較有相關性。

PC-115

## 鐳 223 治療病人體重與輻射劑量率關係之研究 — 以南部某醫院核醫科為例

卓世傑 鄭揚霖 江佳諭 梁育雅 陳懿貞 顏玉安 李將瑄

奇美醫療財團法人奇美醫院核子醫學科

### 背景介紹：

鐳 223 (Radium-223) 是近來引進核子醫學科用以治療，去勢抗性攝護腺癌 (castration-resistant prostate cancer, CRPC) 病人的放射性同位素藥物。鐳 223 主要是  $\alpha$  射源，半衰期 11.4 天，最後的產物是穩定的鉛 207。但衰減過程中，除了  $\alpha$  粒子亦會產生少量的  $\beta$  粒子及  $\gamma$  射線，發射的能量中， $\alpha$  粒子佔了 95.3% (能量範圍為 5.0-7.5 MeV， $\beta$  粒子的部分為 3.6% (平均能量為 0.445 MeV 和 0.492 MeV)， $\gamma$  射線的比例為 1.1% (能量範圍為 0.01-1.27 MeV)。雖然接受鐳 223 治療病人產生的  $\alpha$  射源，不需特別之體外輻射防護 (僅皮膚或紙即可阻擋)，不過其  $\beta$  及  $\gamma$  產生之輻射劑量究為多少，則頗值得探討。再由於鐳 223 治療係以病人體重，依照 1Kg/50Bq 之比例，施打治療用之鐳 223 活度。所以病人體重與其產生之輻射劑量，應有一定之關係。本文即以南部某醫院核醫科為例，探討鐳 223 治療病人體重與輻射劑量率關係之研究。

### 方法：

1. 收集南部某醫院核醫科，每次鐳 223 治療病人之體重資料。
2. 以 Inspector 型蓋格式偵檢器，於每位病人注射鐳 223 完畢後，測偵距背部 5 cm 之輻射劑量率並記錄。
3. 共收集自 2020 年 8 月 3 日至 2021 年 7 月 26 日止，接受鐳 223 治療之病人共 91 人次之體重與輻射劑量率資料。
4. 整理、統計前 2 項數據，以提出結果。

### 結果：

1. 91 人次中體重最輕與最重各為 42 與 93 Kg，平均及中位數則分別為 68.6 與 68.5 Kg。
2. 91 人次中含背景值之輻射劑量率，最低及最高分別為 2.1 及 5.1 uSv/h，平均及中位數則均為 3.6 uSv/h。
3. 以 91 人次之體重與輻射劑量率資料進行直線迴歸統計發現兩者之關係略呈正比之線型，其迴歸方程式大約為  $f(x) = 0.0182x + 2.3462$ 。

### 結論：

本研究發現：

1. 南部某醫院核醫科，鐳 223 治療病人之體重與輻射劑量率之關係經直線迴歸統計的結果，為略呈正比之線型，其輻射劑量率大約是病人體重乘以  $0.0182 + 2.3462$  uSv/h。
2. 南部某醫院核醫科，鐳 223 治療病人之體重最輕與最重各為 42 及 93 Kg，平均為 68.6 Kg。
3. 南部某醫院核醫科，鐳 223 治療病人含背景值之輻射劑量率，最低及最高分別為 2.1 和 5.1 uSv/h，平均為 3.6 uSv/h。

PC-116

## 人員劑量佩章管理實務 — 以高雄榮民總醫院的經驗為例

張春梅

高雄榮民總醫院核子醫學科

**背景介紹：**依「游離輻射防護安全標準」第十五條第一項及游離輻射防護法施行細則第7條規定，對輻射工作人員實施個別劑量監測，應記錄每一輻射工作人員之職業曝露歷史紀錄，並依規定定期及逐年記錄每一輻射工作人員之職業曝露紀錄。前項紀錄，雇主應自輻射工作人員離職或停止參與輻射工作之日起，至少保存三十年，並至輻射工作人員年齡超過七十五歲。輻射工作人員離職時，雇主應向其提供第一項之紀錄。

**方法：**劑量報告紀錄設定每月及每年監測值，資訊室每月更新，除了紙本、電子檔案外，還可以藉由“輻射管理平台”作監測，逐步增加輻射工作人員之健康檢查、教育訓練及劑量佩章使用狀況。為了防止離職人員未繳回佩章，增設“離職核覆”管制點，離職者須至輻射安全室填寫“空白信封及回執聯”，未完成者不核覆其離職之申請。提醒離職者關於職業曝露歷史紀錄之規定，須將回執聯寄回，以供查證。劑量計佩章因契約到期，承作廠商異動，申請佩章試用名額及試用期二個月，比較二家廠商計讀之效益。

**結果：**輻射管理平台，有助於管理全院輻射工作人員之劑量紀錄、健康檢查及教育訓練，降低人工監測的錯誤。設置“離職核覆”管制點，輻射安全室提醒離職輻射工作人員須配合的措施，職業曝露歷史紀錄之收執及回覆率確實提升不少。比較二家廠商 TLD 計讀效益，統計數據結果並無差異。

**結論：**醫事人力整併，加上佩章領用人異動工作單位頻繁，佩章管理更加困難。輻射管理平台的建置，確實有利於人員劑量佩章管理業務的推展。

PC-117

## 探討鉛屏蔽擺放的位置 對於看護者接受的輻射曝露之影響 — 以 F-18 FDG 正子全身造影為例

林培堯<sup>1</sup> 戴偉哲<sup>1</sup> 呂惠敏<sup>2</sup> 陳建榮<sup>2</sup> 徐中信<sup>3</sup> 劉高郎<sup>3</sup> 柯冠吟<sup>1</sup>

<sup>1</sup> 國立臺灣大學醫學院附設醫院癌醫中心分院核子醫學部

<sup>2</sup> 國立臺灣大學醫學院附設醫院核子醫學部

<sup>3</sup> 國立臺灣大學醫學院附設醫院癌醫中心分院影像醫學部

**背景介紹：**在 F-18 FDG 正子全身造影檢查中，常規的做法是病人在注射室打藥、休息約 60 分鐘後，再到檢查室照相，然而面對無法行走、必須由看護者協助的病人，通常會直接讓病人躺在正子檢查室內的檢查床上，注射正子藥物 F-18 FDG，其看護者照護前方正在等待吸收藥物的病人，需在檢查室內保持一定的距離，基於輻射防護之合理抑低 (ALARA, as low as reasonably achievable) 原則下，提供看護者前方一台鉛屏風屏蔽；本研究針對在病人和看護者之間放置的鉛屏蔽，在不同位置，評估看護者所接受到之輻射曝露。

**方法：**病人進入正子檢查室前，須先進行解尿，接著在檢查床上注射正子藥物 F-18 FDG，劑量活度約為 10 mCi，並在檢查室中的檢查床安靜休息 60 分鐘後，再次解尿後進行造影。我們將輻射個人劑量計 (PD, Personal Dosimeters) 放置在檢查室內的看護者的位置，使用鉛屏蔽為 20 mm 鉛當量，分別放置在看護者正前方 (A 組)、病人檢查床旁邊 (B 組)，計讀時間約為 55~60 分鐘。

**結果：**在 29 位病人中，A 組總共有 13 位，平均注射劑量為 10.46 mCi，平均累計時間為 56.69 分鐘，平均累計劑量為 0.508  $\mu$ Sv；B 組總共有 16 位，平均注射劑量為 10.34 mCi，平均累計時間為 56.31 分鐘，平均累計劑量為 2.28  $\mu$ Sv。從結果了解，注射正子藥物 F-18 FDG 後的躺平病人可視為一長形的輻射源，而鉛屏風的寬度約為 50 cm，故在屏風正後方的屏蔽效果是最多的。

**結論：**輻射防護基於時間 (減少人們受到照射的時間)、距離 (增加人員與輻射源之間的距離以減少照射) 和屏蔽 (在人員與輻射源之間使用鉛或混凝土等屏障) 的原則，以保護工作場所的人員。因此在臨床上面對大床或是無法自理的病人，進行核醫檢查，看護者需在場陪伴時，將鉛屏風放置靠近在看護者前方，所接受到的曝露是較低的，而看護者若在這兩組實驗設計下，所接受到的輻射曝露不會超過國際放射防護委員會 (ICRP) 的一般人建議之限值。

PC-118

## 同位素治療病房周圍環境和清床作業之輻射監控 —以北部某醫院為例

林培堯<sup>1</sup> 呂惠敏<sup>2</sup> 黃奕琿<sup>2</sup> 徐中信<sup>3</sup> 劉高郎<sup>3</sup> 柯冠吟<sup>1</sup>

<sup>1</sup> 國立臺灣大學醫學院附設醫院癌醫中心分院核子醫學部

<sup>2</sup> 國立臺灣大學醫學院附設醫院核子醫學部

<sup>3</sup> 國立臺灣大學醫學院附設醫院癌醫中心分院影像醫學部

**背景介紹：**非密封作業場所的使用必須符合行政院原子能委員會的審查，本院同位素治療病房總共有三間病室，比鄰其他部門，為使工作同仁更加安心，於周圍環境和清床作業設置環境監測劑量計，監測數個月，測量是否有超過輻射安全劑量的疑慮。也針對清床作業後，病室內各個區域進行環境偵測。

**方法：**本院病房於 109 年 8 月 10 日啓用，針對住院病人離院的路線和鄰近部門，使用清華大學 OSLD 劑量佩章，佈置於同位素治療病房周圍，啓用前三個月以資訊室的計讀數值為參考點，在啓用後於增加小護理站、清床作業和陽光會客室。且紀錄每個月的住院人數、每個月的平均累積劑量。在清床作業後，輻防師使用輻射偵測器 ATOMTEX AT1121，在病室內各個區域(病床、窗台、淋浴間、洗手檯、馬桶和嘔吐槽)進行環境偵測。

**結果：**從 109 年 8 月初至 110 年 6 月底，同位素治療病房總共治療 151 位碘-131 病人，服用藥物劑量為 100~200 mCi，清華大學平均背景參考值：0.08 mSv/m，核子醫學部平均背景參考值：0.115 mSv/m，資訊室累積劑量為 0.1~0.14 mSv/m，小護理站累積劑量為 0.09~0.14 mSv/m，清床作業累積劑量為 0.09~0.14 mSv/m，陽光會客室累積劑量為 0.09~0.12 mSv/m。在清床作業後，病室各區的偵測，病床和窗台平均曝露為 0.2 μSv/h，淋浴間、洗手檯、馬桶和嘔吐槽的平均曝露都超過 0.5 uSv/h，尤其是馬桶最高曝露為 2.22 μSv/h。

**結論：**同位素治療病房的外部環境(資訊室和陽光會客室)計讀的結果顯示，皆無異常讀值，故無超過輻射安全劑量的疑慮，病人皆有遵守衛教內容，依照指定動線離開醫院。同位素治療病房的內部環境，在清床後的偵測，雖然在浴廁區域數值偏高，仍符合評估報告的範圍，無污染之疑慮，但提醒工作人員進入病室時，在浴廁可以周圍不要停留太久，以減少輻射曝露。



PC-119

## 病人接受放射性藥物 (LUTATHERA<sup>®</sup>) 治療， 所產生廢棄物和廢水之管理

林培堯<sup>1</sup> 呂惠敏<sup>2</sup> 徐中信<sup>3</sup> 劉高郎<sup>3</sup> 鄭媚方<sup>2</sup> 柯冠吟<sup>1</sup>

<sup>1</sup> 國立臺灣大學醫學院附設醫院癌醫中心分院核子醫學部

<sup>2</sup> 國立臺灣大學醫學院附設醫院核子醫學部

<sup>3</sup> 國立臺灣大學醫學院附設醫院癌醫中心分院影像醫學部

**背景介紹：**LUTATHERA<sup>®</sup> 是一種用來治療神經內分泌瘤的放射性藥物，有別於甲狀腺癌治療是讓病人口服碘 131 膠囊，LUTATHERA<sup>®</sup> 以靜脈輸液 (infusion) 的方式給予病人高劑量的放射性藥物，輸注放射性藥物需要 30 至 40 分鐘，為了保護腎臟，會額外輸注 1000 ml 的胺基酸 (amino acid)，給藥程序大約需要 5 個小時後，病人在住院期間還會大量攝取水份，將多餘的放射性藥物透過尿液排出體外；LUTATHERA<sup>®</sup> 之放射性同位素為 Lu-177，半衰期為 6.65 天，但是因產源的不同，含有非需要的 Lu-177m，半衰期為 160.4 天較 Lu-177 長，且難以分離，其 Lu-177m / Lu-177 比值約為 0.02%，所以病人在住院時間所產生的廢棄物和廢水，需做對應的輻防考量。

**方法：**在實施 LUTATHERA<sup>®</sup> 輸液作業前，我們會在病床旁的地面、馬桶周圍，用看護墊貼牢，也會在病人注射位置處鋪上吸水墊，並且衛教病人坐姿如廁、嘔吐要吐在嘔吐槽，住院期間的廢棄物，都分別放入院方專用收集桶，待治療在病人離院後，利用輻射偵檢器 Thermo Scientific RadEye B20，進行輻射曝露之量測，最終暫存在放射性廢棄物暫存室，裡面有專屬的冰箱，依照標籤順序來存放。放射性廢水核衰槽，主要收集同位素治療病房專用廁所排放的含放射性 I-131、Lu-177、Lu-177m 放射性廢水，並透過監控系統了解放射性廢水的暫存狀況。

**結果：**從量測各專用收集桶表面最高曝露的結果：注射過程中產生之針筒和管線及棉球為 38.4  $\mu\text{Sv/h}$ 、執行靜脈輸液之防水隔離衣和手套為 0.23  $\mu\text{Sv/h}$ 、病室地面的看護墊為 0.54  $\mu\text{Sv/h}$ 、病患食用過之餐具和剩餘食物或嘔吐物等的廢棄物為 2.64  $\mu\text{Sv/h}$ 。住院期間的放射性廢水，將與本院其他同位素治療病房的廢水一起暫存於放射性廢水槽暫存室的核衰槽內。

**結論：**放射性廢棄物暫存室內，各冰箱依序編號，能方便清潔人員按照順序放入病房所產生的放射性廢棄物收集桶，也可讓輻射工作人員快速的取出量測收集桶表面，減少人員的曝露，預計暫存多日後，直到該收集桶表面低於背景值 (0.5  $\mu\text{Sv/h}$ ) 以下，才會移出暫存室當作一般醫療廢棄物處理。放射性廢水槽暫存室，監控系統可以自動化設定，核衰槽滿水後自動關閉，當廢水槽廢液取樣後核種分析，取樣結果低於法規限值 (游離輻射防護安全標準附表四之二規定)，將紀錄排放日期，才排入污水處理槽。

PC-120

## 探討同位素治療— 用針筒法注射放射性藥物 (LUTATHERA<sup>®</sup>) 時， 工作人員之輻射防護

林培堯<sup>1</sup> 謝婷娟<sup>1</sup> 呂惠敏<sup>2</sup> 黃奕琿<sup>2</sup> 鄭媚方<sup>2</sup> 柯冠吟<sup>1</sup>

<sup>1</sup> 國立臺灣大學醫學院附設醫院癌醫中心分院核子醫學部

<sup>2</sup> 國立臺灣大學醫學院附設醫院核子醫學部

**背景介紹：**LUTATHERA<sup>®</sup> 是一種胜肽受體放射性藥物，用於治療胃腸胰神經內分泌腫瘤，是用靜脈輸液的方式，於 30 分鐘內注射 200 mCi 的劑量，其成份為 Lu-177 標誌體抑素類似物 DOTATATE，而 Lu-177 半衰期為 6.65 天，β 能量為 498 KeV (78.6%)、177 KeV (12.2%)、γ 能量為 208 KeV (11%)、113 KeV (6.4%)。此治療有很多種的靜脈輸液的方法，故本研究探討用針筒法 (syringe method) 時，工作人員執行 LUTATHERA<sup>®</sup> 抽藥、輸液注射之輻射防護。

**方法：**針筒法 (syringe method)，藥師是將鉛藥罐的 LUTATHERA<sup>®</sup>，配合自製 6 mmPb 鉛針套在 30 ml 的針筒外，於 10 mmPb 的 L-Block 後進行 LUTATHERA<sup>®</sup> 抽藥，而護理師於 20 mmPb 的鉛屏風後利用針筒幫浦靜脈輸液入病人體內，放射師也在病室協助護理師，當開始 LUTATHERA<sup>®</sup> 注入至病患體內，這段期間護理師和放射師站在 20 mmPb 的鉛屏風後注意病人的生理狀況。相關人員穿著鉛衣 (相當於 0.5 mmPb) 的內外皆配戴輻射個人劑量計 (PD, Personal Dosimeters) Polimaster PM1610A，計讀累積時間和曝露。

**結果：**藥師執行抽藥業務 (計讀時間為 60 分鐘，LUTATHERA<sup>®</sup> 抽藥行為花費時間為 3 分鐘)，計讀出鉛衣內外之數值分別為 0.236 μSv、0.458 μSv，表示輻射劑量衰減 48.8%；護理師在病室內進行 LUTATHERA<sup>®</sup> 輸液注射和病人監控 (計讀時間為 68 分鐘，處理 LUTATHERA<sup>®</sup> 業務花費為 30 分鐘)，計讀出鉛衣內外之數值分別為 2.565 μSv、9.15 μSv，表示出輻射劑量衰減 73%；放射師在病室協助護理師 (計讀時間為 65 分鐘，處理 LUTATHERA<sup>®</sup> 業務花費為 30 分鐘)，計讀出鉛衣內外之數值分別為 2.137 μSv、2.735 μSv，表示輻射劑量衰減 21.9%。

**結論：**LUTATHERA<sup>®</sup> 為放射性治療藥物，在三位輻射工作人員所接受到的曝露，藥師進行抽藥作業時，使用原廠的鉛罐、鉛屏風和自製鉛針套，雖然有明顯的輻射劑量衰減，但是從花費之時間、累計之曝露數值，可考慮不用穿著鉛衣鉛頸；但是護理師或是放射師因為要操作針筒輸液幫浦注射 LUTATHERA<sup>®</sup>，雖然人員有在鉛屏風後方，但是要時觀測病人狀況，又可能會遇到需要貼近病人施作額外醫療行為，依循 ALARA 之原則，建議同仁穿鉛衣進行 LUTATHERA<sup>®</sup> 業務。

PC-121

## 放射免疫實驗室藉改善實驗流程品質提升工作效率

陳芄嘉<sup>1</sup> 方雅潔<sup>1</sup> 余景陽<sup>1</sup> 韓璞<sup>1</sup> 邱祖廷<sup>1</sup> 林慶齡<sup>1,2</sup>

<sup>1</sup> 國泰綜合醫院放射免疫實驗室

<sup>2</sup> 國泰綜合醫院內分泌新陳代謝科

**背景介紹：**Radioimmunoassay (RIA) 的實驗步驟包括了將檢體和含有碘 -125 液體加入附著有特異性抗體的試管中、經一定時間及環境條件下培育、清洗、進入  $\gamma$ -counter 計讀。在培育及清洗過程中，會將試管放置在覆有彈性塑膠片之塑膠架中，其目的為固定試管，防止試管在培育、清洗過程中因搖晃導致試管噴出。但隨著使用次數增加及個人使用習慣不同，彈性塑膠片會隨著時間脆化斷裂，無法固定試管。因製造覆有彈性塑膠片的塑膠架工廠已經停產，實驗室無法直接汰舊換新。彈性塑膠片脆化斷裂的問題，造成每個實驗所需使用的塑膠架數量增多，導致震盪器有限的擺放空間超過負荷及手動清洗時間增加。實驗室積極尋找其他塑膠架廠商，目前能提供的款式所能放置試管的數量較少，摩擦力大不易放入試管外，因底部具海綿結構無法放入水浴槽，不能滿足部分項目的培育條件，且該塑膠架狹長固定不利，擺放在震盪器上容易搖晃，因此使用頻率極低。為符合實驗室人員的使用習慣，決定改善舊款塑膠架的品質，使它用起來更為方便，讓實驗流程更加流暢同時提升工作效率。

**方法：**第一版的改良使用 PVC 材質的透明墊板，裁取適當大小覆上塑膠架後，以橡皮筋固定，並對應塑膠架的孔洞位置進行切割挖洞。之後根據使用情況進行第二版的改良，使用網狀防滑墊，裁取適當大小夾入彈性塑膠片和塑膠架之間的空隙中，再對應塑膠架的孔洞位置進行切割挖洞。

**結果：**第一版 PVC 材質透明墊板產生的摩擦力過大，導致實驗試管不易置入塑膠架亦不易拔取，實驗室人員使用意願低。經大家討論認為改善方向可行，尋求合適材質應可改善摩擦力問題。進行第二版改良，使用網狀防滑墊夾入彈性塑膠片和塑膠架之間，能有效固定試管且解決不易置入、不易拔取的問題，大大提升了使用意願。

**結論：**經過第二次改良，加裝網狀防滑墊大大增加了塑膠架的使用效率與減少一個實驗所需使用的塑膠架量，有助於提高作業效率，減輕了震盪器有限擺放空間的負荷。雖然只是一個小改變，但這個微小的變化不僅激發實驗室同仁們的向心力，同時也帶動了良好的工作氣氛，增強工作效率提升實驗室的服務品質，相信有了這樣的小轉變，實驗室同仁們也會願意付出更多心力促使實驗室更進步。

PC-122

## 針對顧客對報告數據提出疑問建立完整處理流程

方雅潔<sup>1</sup> 余景陽<sup>1</sup> 韓璞<sup>1</sup> 邱祖廷<sup>1</sup> 陳芄嘉<sup>1</sup> 林慶齡<sup>1,2</sup>

<sup>1</sup> 國泰綜合醫院放射免疫實驗室

<sup>2</sup> 國泰綜合醫院內分泌新陳代謝科

**背景介紹：**甲狀腺切除病患接受 Thyroxine 藥物治療，預期 Thyroid-stimulating hormone (TSH) 應逐漸下降，然而檢驗數據顯示不降反升。臨床醫師致電實驗室要求再次檢驗，實驗室將此事件列為不符合事件中的「顧客抱怨」並進行調查。

**方法：**顧客抱怨事件依「不符合事件管制作業程序」執行，實驗室主管指定承辦人負責辦理並進行原因分析。實驗室針對臨床醫師提出之疑問的報告數據，查核檢驗前是否有不正確檢體，檢驗中是否有隨機誤差、當日品管有無系統性誤差，檢驗後報告數據與原始數據是否符合。進行對先前結果的影響分析，同仁共同討論結果與立即措施，並與臨床醫師進行討論後回覆顧客，是否有進行風險評估之必要？是否進行矯正措施杜絕下次再發生？最後將所有紀錄表及原始資料歸檔保存。

**結果：**病患為住院病人，掃描手圈列印條碼，檢體原管上機，檢體試管種類使用無誤，排除不正確檢體。當日品管無系統性及隨機性誤差，進行再次檢驗，兩次數據之 Bias% 小於 Reference Change Value (RCV)，無檢驗數據隨機誤差及其他數據錯誤之疑慮。報告數據與原始資料相符。調查結果顯示實驗室核發之數據並無問題，實驗室端無法解釋此個案數據的變化。實驗室主動向臨床醫師進行溝通，臨床醫師回饋：「得到實驗室品管一切檢視都合格的訊息後，改變思考方向透過文獻搜尋、臨床病情檢討、用藥順序的比對，懷疑造成檢驗結果異常的原因是併用促進腸胃蠕動的藥物。為了印證這一個推論，進一步請實驗室加作 Prolactin 的檢測，檢測結果與預期一樣偏高，停藥後也如預期的出現下降，因此可確認病患 TSH 上升，為多巴胺拮抗劑藥物造成」。此事件經調查與追蹤可明確顯示病患數據異常，非本實驗室品管造成。

**結論：**實驗室建立顧客對實驗室檢驗數據提出疑問之探討標準流程，能快速、準確找出問題進而執行立即措施、矯正措施、預防措施，降低問題再發生率。當實驗室無法解釋時，主動與臨床醫師溝通、討論能增加找出問題的可能性，亦可加強醫檢師對臨床醫療的了解，提升臨床諮詢之能力，以逐漸提升實驗室之服務品質。

PC-123

## 量測不確定應用於試劑查驗

莊雅晴 郭珮怡 李世昌 邱南津

國立成功大學醫學院附設醫院核子醫學科

**背景介紹：**量測不確定度用來表示受測數值的合理離散程度，檢驗過程中涉及各步驟都具有潛在變異產生不確定性而使檢驗數值產生誤差影響最終結果，包含受測樣本特性、操作人員、試劑或儀器等，實驗室檢驗通常期望能得到待測物的真值，但每一次的量測值因受到操作流程中各種不確定性影響量測結果，藉由不確定度的評估可以用來描述量測範圍的分佈狀況，並檢視量測結果的品質。在放射免疫分析實驗室最常見的潛在變異來源是試劑批號之間的差異，本實驗室將量測不確定度運用於試劑轉換批號時的平行測試，以擴充不確定度作為評估試劑的允收標準。

**方法：**(1) 估算量測不確定度：收集 2020/1/1~2020/12/30 同一批號品管液 (Bio-rad 40360) 之各檢驗項目品管數據，統計出各檢驗項目組合不確定度並審查品管表現是否符合目標不確定度。(2) 建立試劑允收試算表，以各檢驗項目之擴充不確定度作為新舊批號試劑之平行測試允收標準。

**結果：**統計去年同批號品管液數據，大部份檢驗項目之擴充不確定度小於 10%，僅少部份低濃度品管液不確定度較高，各檢驗項目品管結果仍皆符合所訂定的目標不確定度 (0.75 CV<sub>i</sub> 或 1/3 TE<sub>a</sub>)。

**結論：**臨床上量測不確定度常應用於協助檢驗報告的判讀，提供檢驗報告使用者 95% 信賴水準下量測真值的區間資訊，本實驗室運用此概念以擴充不確定度作為試劑平行測試允收標準，相較於過去的允收標準 10% (不分品管濃度與檢驗項目)，更能適當且完整評估新舊批號試劑的變異。

PC-124

## RIA 試劑庫存管理改善成效分析

廖建國<sup>1</sup> 張素雲<sup>1</sup> 莊紫翎<sup>1,2</sup> 王昱豐<sup>1,2</sup>

<sup>1</sup> 佛教大林慈濟醫院核子醫學科

<sup>2</sup> 慈濟大學醫學系

**背景：**試劑庫存管理為實驗室運作與品質的重要項目之一，良好的庫存管理可確保試劑品質、減少浪費、控制成本，並避免試劑短缺造成報告逾時。由於 RIA 試劑之效期較短，庫存過高可能造成試劑過期，而庫存過低則可能導致試劑短缺而影響正常作業。今年以來，本科持續針對庫存管理進行檢討與改善。本研究目的即為分析近兩年試劑庫存之資料，以了解目前之改善成效，並作為持續改善的參考。

**方法：**收集 2020 年至 2021 年 (1-6 月) 間，每月試劑庫存與進出量之資料，分別統計每月各項目庫存過高以及庫存過低之件數及比率，並進一步分析年度平均庫存 / 消耗比 ( 庫存量 / 消耗量之比值 )，以比較不同年度與項目之庫存狀況及其合理性。庫存合理性之判定，以庫存 / 消耗比低於 0.25 ( 低於安全庫存 ) 判定為過低，高於 1.25 ( 高於最高合理庫存 ) 判定為過高。

**結果：**整理結果發現，2020 年庫存過高之件數為 22 件 (12.22%)，2021 年降至 8 件 (8.89%); 而 2020 年庫存過低的件數為 29 件 (16.11%)，2021 年則降至 10 件 (11.11%)。顯示今年以來本科試劑的管控已有不錯的成效。進一步分析各項目之庫存過高或過低之比率，發現異常率較高的項目中居前 3 位者分別為 Ferritin (5.56%)、prolactin (5.0%)、free T4 (5.0%)；而異常率較低的項目，則有 CA 125 (0.56%)、CEA (1.11%)、Thyroglobulin (1.11%) 等項目。若再比較近 2 年試劑之年度平均庫存 / 消耗比，可發現 2020 年有 2 項 (T4 及 prolactin) 庫存過高；而 2021 年則降為 1 項 (prolactin)。顯示若以近 2 年度的平均值來看，prolactin 之試劑庫存量相對較高，應優先進行改善。

**結論：**分析結果顯示，2021 年本科實驗室之試劑庫存異常比率與 2020 年比較，大幅下降 27%。顯示庫存管理的改善已有明顯的成果，未來仍可依據近 2 年的分析資料，針對曾有異常的項目加強管控，以持續提升庫存品質。

PC-125

## RIA 實驗室能力試驗表現之回顧與比較

廖建國<sup>1</sup> 張素雲<sup>1</sup> 莊紫翎<sup>1,2</sup> 王昱豐<sup>1,2</sup><sup>1</sup> 佛教大林慈濟醫院核子醫學科<sup>2</sup> 慈濟大學醫學系

**背景：**能力試驗（外部品管）為實驗室重要的品質活動，透過參與能力試驗可以了解實驗室操作的精準度，能力試驗的優良表現也是證明實驗室檢驗品質的方式之一。本研究目的即為回顧分析本科實驗室近 5 年之能力試驗表現，以作為持續改善的參考。

**方法：**收集 2017 年至 2021 年 (1-6 月) 間，本科參與能力試驗之回覆結果與品質指標（能力試驗不合格率）監測結果，分別依不同年度分析能力試驗不合格率、不合格項目及件數，以比較各年度、各項目之能力試驗表現情形。本實驗室參與之能力試驗系統為 RANDOX (RIQAS) 能力試驗機構，參加項目計 15 項，每月進行測試 1 次。能力試驗不合格之認定，依 RIQAS 之判定標準執行（當  $SDI > \pm 2$ 、Target score  $< 50$  且偏差大於允收值時）。能力試驗不合格率之計算，以不合格項數（分子）除以總項數（分母）而得。

**結果：**整理結果發現，近 5 年平均能力試驗不合格率為 0.78%，亦即本科參與外部品管的平均正確率高達 99.22%。比較各年度的表現，以 2020 年表現最好（不合格率 0%），2017 年表現最差（不合格率 1.16%）。進一步比較不同年度能力試驗不合格的項目，發現 2017、2018、2019 年每年皆各有 2 件能力試驗不合格，項目包括 T4、TSH、cortisol 及 PTH-i 等項；而 2020 年表現最好，無不合格項目；至於 2021 年 (1-6 月)，則有 1 件不合格項目 (PTH-i)，顯示近 2 年本科實驗室的能力試驗表現仍有持續的進步。另外，也顯示參加能力試驗的 15 個項目中，有 11 項 (T3、free-T4、AFP、CEA、CA 19-9、CA 15-3、CA 125、PSA、prolactin、ferritin、thyroglobulin) 在最近 5 年的正確率高達 100%。回顧檢討這些不合格事件，皆為隨機誤差所致。因此，如何再持續提升檢驗的精準度仍是我們努力的目標。

**結論：**本科實驗室近 5 年參與能力試驗的平均正確率高達 99.22%，表現值得肯定，但追求正確率 100% 仍是我們努力的目標。因此，未來可針對曾發生不合格的項目，再加強其精準度，以持續提升檢驗品質。

PC-126

## 高鐵蛋白血症患者與疾病診斷之相關研究

林淑靜<sup>1</sup> 廖建國<sup>1</sup> 張素雲<sup>1</sup> 薛仔婕<sup>1</sup> 王昱豐<sup>1,2</sup><sup>1</sup> 佛教慈濟醫療財團法人大林慈濟醫院核子醫學科<sup>2</sup> 慈濟學校財團法人慈濟大學醫學系放射線學系

**背景：**血清鐵蛋白 (Ferritin) 是體內重要的儲鐵蛋白，由脫鐵蛋白 (Apoferritin) 和  $Fe^{3+}$  形成的複合物。血清鐵蛋白是一個大的蛋白質，分子量 474 kDa，儲存於網狀內皮系統的細胞中。因生理特性不同，男女性的血清鐵蛋白濃度也會有所不同。血清鐵蛋白在急性發炎時期會升高，也是一種急性反應蛋白 (Acute-phase-protein)，在感染、發炎、溶血、肝病、惡性腫瘤時升高。此篇研究主要探討極端高鐵蛋白血症 (鐵蛋白 > 2000 ng/mL) 不同程度與臨床診斷之間的關聯性，提供臨床診治的方向。

**方法：**收集南部某教學醫院 2019-2020 年接受血清鐵蛋白檢查的患者進行回顧性研究，對象為年紀 18 歲以上，血清鐵蛋白 > 2000 ng/mL 之成年人，共有 86 例，進行極端值血清鐵蛋白與疾病之間的關係探討。依濃度不同分為兩大類，並和臨床實驗室的血液及生化結果進行分析，為求得完整的數據，在此部分的研究，共計 30 例。

**結果：**86 例中，平均年齡 62.87 歲，男性 57 位 (66.28%)，女性 29 位 (33.72%)。最常見的診斷是惡性腫瘤 23 例 (26.7%)，其次為肝臟疾病 21 例 (24.4%)，腎臟疾病 17 例 (19.8%)，貧血 14 例 (16.3%)，急性骨髓細胞性白血病 (Acute myeloid leukemia, AML) 有 5 例，成人史迪爾氏症候群 (Adult onset Still's disease, AOSD) 有 4 例，感染發炎有 2 例。成人史迪爾氏症候群 Ferritin 濃度最高，平均值高達 9473.3 ng/mL，肝臟疾病 6055.7 ng/mL，急性骨髓細胞性白血病 5941.5 ng/mL (Table 1)，三者濃度都 > 5000 ng/mL，顯示極端值的血清鐵蛋白在這三類疾病是具有診斷意義的。將血清鐵蛋白濃度分為兩組：2001-5000 ng/mL 及 > 5000 ng/mL，在血液常規及生化檢查數據中，RBC、Hb、GOT 及 TIBC 在兩組中具有差異性， $p < 0.05$  (Table 2)。其中 RBC、Hb 沒有因血清鐵蛋白越高而呈現越低的情況；數據顯示濃度越高的血清鐵蛋白，在 GOT 及 GPT 的數值中也越高，可能因發炎現象活化免疫細胞，刺激肝臟合成鐵蛋白，也減少釋放鐵離子，雙重作用使血清鐵蛋白濃度上升。

**結論：**引起高鐵血症的原因很多，臨床上應多加利用重複檢驗血清鐵蛋白，以區分是因為腫瘤或發炎引起，或是因輸血造成的鐵過載現象。其他研究顯示，血清鐵蛋白可以做為身體發炎的指標，同時也是一種腫瘤標誌，當血清鐵蛋白濃度異常過高時，除了發炎以外，也要謹慎思考惡性腫瘤的可能性，在臨床上若能同時與其他癌症指標如肝癌之  $\alpha$ -fetoprotein 及大腸直腸癌 CEA 合併檢查，則惡性腫瘤之診斷率可大為提升。



PC-127

## 評估完整型副甲狀腺激素 (Intact Parathyroid Hormone; I-PTH) 試劑 在 Rapid 和 Regular 方法學測試結果之適用性

林秋美 陳宜伶 陳素英 古琴鳳 蕭莉茹  
曾翠芬 陳怡如 劉怡慶 林家揚 張晉銓

高雄醫學大學附設中和紀念醫院核醫部

**目的：**完整型副甲狀腺激素 (Intact Parathyroid Hormone; I-PTH) 主要是檢測生活性型為 84 個胺基酸的多胜肽，其功能可以調節血液中鈣、磷的濃度也是左右人體血鈣代謝的重要因素。I-PTH 和鈣離子配合測定可用來區別高、低血鈣症亦可作為原發性或繼發性副甲狀腺亢進之診斷價值。本研究目的：因臨床甲狀腺、副甲狀腺切除手術所引發低血鈣症，急需儘速給予 I-PTH 報告以利臨床判讀及處方用藥的使用，故希望藉由評估試劑在血清中以 rapid 法和 regular 法比較其測試結果之探討，以期儘快提供檢測數據供臨床醫師儘早確立可靠的失調診斷及用藥。

**材料和方法：**本研究檢體採用血清共收集了 100 個樣本數，樣本數分成二管，分別進行反應時間為 Rapid (30 分鐘)、Regular (18 ± 2 小時) 等方法進行檢測。操作方法大致一樣，唯 Rapid 方法不測標準液 1 (標準液濃度從 S<sub>0</sub>~S<sub>5</sub>)，其他流程均相同只是反映時間不同。ELSA-PTH 測試原理為 Two-site Sandwich 免疫放射測定法 (Immunoradiometric assay)，即檢體中的 PTH 濃度與結合 ELSA 上的放射性濃度成正比進行樣本檢測。試劑採用 ELSA-PTH，Cisbio Bioassays。

**結果：**I-PTH 血清濃度 (平均值 ± 標準誤差) 於 Rapid、Regular 檢測結果分別為 145.02 ± 33.54 (pg/ml)、125.07 ± 30.02 (pg/ml)。本研究統計方法採用 Paired sample *t*-test。*T* 檢定值為 4.366，顯著性 *P* 值 < 0.05。其結果顯示反應時間長短其值差異性是可接受的。Rapid vs. Regular 相關性檢定其相關係數值 R = 0.991；y = 0.8865x。總結結果 Rapid 方法可適用於臨床快速報告的提供。

**結論：**本研究分析了 Rapid、Regular 不同時間反應測試結果，其數據顯示二者之間的差異度是不明顯且彼此間相關性強。故 Rapid 方法是可被選擇作為術中或急需報告時的提供。但缺點是相對成本也提高了。

PC-128

## 因應連假延長甲狀腺球蛋白 (Thyroglobulin) 血液分析反應時間之論證

曾翠芬<sup>1</sup> 楊雅晴<sup>2</sup> 劉怡慶<sup>1</sup> 古琴鳳<sup>1</sup> 林秋美<sup>1</sup> 林家揚<sup>1,3</sup> 張晉銓<sup>1,3</sup>

<sup>1</sup> 高雄醫學大學附設中和紀念醫院核醫部放射免疫分析組

<sup>2</sup> 高雄醫學大學附設中和紀念醫院核醫部閃爍攝影組

<sup>3</sup> 高雄醫學大學附設中和紀念醫院核醫部

**背景介紹：**甲狀腺球蛋白 (Thyroglobulin) 是由甲狀腺濾泡細胞合成之分子量 660,000 Da 的醣蛋白，為 T4、T3 的前驅蛋白。Thyroglobulin 全由甲狀腺細胞獨自完成因此構成了甲狀腺的特異標記，可用來做為甲狀腺癌的病人術後追蹤，且為臨床甲狀腺功能檢驗項目之一。本放射免疫分析實驗室所使用 Thyroglobulin 血液分析試劑反應時間二天，為了不因連假而延遲臨床發報告時間，所以本實驗將反應時間延長到三天視其結果是否仍可允收。

**方法：**隨機取 20 支未測檢體和 2 支已測過檢體 (inter-run)，以上 22 支檢體、標準液 (CAL1-CAL7) 和品管血清 (Low、High) 等各準備 2 套 coated tube，將 2 套分成 2 組 (A、B)，分析方法和試劑 Thyroglobuline IRMA (cisbio) 為固相的免疫放射三明治測定法，A 組是參照說明書上正常的反應時間，B 組則將步驟二的 incubate 16-20 hrs 再延長約 22 hrs，使用 2470 Automatic Gamma counter (Wizard<sup>2</sup>)，統計軟體 Microsoft Office Excel 2007，參考值 < 50 ng/mL。

**結果：**標準液 A 組 ED-20、50、80 分別為 345.3、197.5、82.23，B 組 ED-20、50、80 分別為 355.7、213.4、89.82，低和高濃度品管血清 A 組為 13.34、47.8，B 組 14.68、47.26 (單位：ng/mL)，檢體檢驗結果其 A、B 二組之  $R^2 = 0.995$  (P-value 0.894)  $Y = 1.0454x + 0.4681$ ，且 CV% 皆小於 10 (0.57-9.98)。

**結論：**本實驗室部分檢驗項目反應時間需要 20 小時左右，甲狀腺球蛋白 (Thyroglobulin) 為其中之一，但在連假期間為了不影響臨床報告送達且不另外增加工作時間和費用支出 (假日加班)，所以本實驗的設計是驗證反應時間延長的可行性，根據結果來看其二組的品管血清皆落在 L:  $15.9 \pm 3.2$ 、H:  $44 \pm 8.8$ ，二組病人檢體報告相關性很高且沒有顯著的差異，CV% 皆在本實驗室允收範圍內 (20%)，就以上統計結果將其檢驗分析反應時間延長至第三天是可行的。

PC-129

## Case Report: Thymic Rebound Hyperplasia

Jui-Hung Weng, Li-Jen Huang

*Department of Nuclear Medicine, Chung-Shan Medical University Hospital, Taichung, Taiwan*

**Introduction:** A 12 year-11 month-old boy with a history of osteosarcoma of right knee with lung metastasis, S/P chemotherapy treatment. The patient was admitted for PET scan and MRI/CT scan. The patient underwent multiple PET/CT, CT and bone scan in order to evaluate osteosarcoma for initial staging and subsequent recurrence. The patient was suspected of thymic rebound hyperplasia during image study due to chemotherapy history. Further follow up by using PET/CT also supported the findings of thymic rebound hyperplasia due to uptake pattern and the timeframe, rather than the more common causes of substernal mass such as thymoma, teratoma, thyroid, lymphoma. Subsequent related articles regarding thymic rebound hyperplasia were reviewed.

**Methods:** The study reviewed 535 consecutive PET/CT studies in 161 patients (F 75, M 86), aged 3-40y, with a diagnosis of lymphoma (n = 104), sarcoma (n = 11) and other malignancies (n = 46) were retrospectively reviewed.

**Results:** There were 116 T+ studies in 47 patients, for an overall incidence of 21%, with an equal gender distribution (F 25, M 22).

**Conclusion:** Physiologic thymic FDG uptake was found in 21% of studies in 29% of children and young adults with cancer. T+ studies were more frequent during FU after treatment. Intensity of thymic uptake was relatively high and showed a slight increase in relationship to time from treatment. Although as a group the T+ population was significantly younger, thymic uptake was found in 9% of patients in the 4th decade of life. Benign thymic hyperplasia should also be considered in the differential diagnosis of residual masses in young adults that are demonstrated by gallium scanning. These affected patients may need to have a biopsy of the mass prior to consideration of further treatment options.

PC-130

## Discussion on the Quantity Change of Nuclear Medicine Scan when Manpower Shortage

Chia-Hao Chang<sup>1</sup>, Yu-Sheng Hung<sup>1</sup>, Chiang-Hsuan Lee<sup>2\*</sup>

<sup>1</sup>*Division of Nuclear Medicine, Department of Medical Imaging, Chi Mei Medical Center, Liouying, Tainan, Taiwan*

<sup>2</sup>*Division of Nuclear Medicine, Department of Medical Imaging, Chi Mei Medical Center, Tainan, Taiwan*

**Introduction:** There are physicians, pharmacists, medical radiation technologists and nurses in nuclear medicine department usually. Medical radiation technologists are important manpower to perform nuclear medicine scan. The quantity of nuclear medicine scan will be affected if they ask for leave or resigned. This article will explore their correlation by actual situation we faced.

**Methods:** There are one SPECT scanner, one SPECT-CT scanner and one PET-CT scanner in our division with three medical radiation technologists. Because of staff resignation, paternity leave, sick leave, COVID-19 childcare leave, only one medical radiation technologist to perform nuclear medicine scan from May 31 to June 25 in 2021. We analyze the quantity of nuclear medicine scan in this period with the same period in 2020 to find the difference.

**Results:** 17 working days from May 31 to June 25 in 2021, compared to 19 working days from June 1 to June 26 in 2020, daily average quantity of PET-CT whole body scan decreased 10.3%; daily average quantity of whole body bone scan drop 28.6%; daily average quantity of myocardial perfusion scan fell 64.7%.

**Conclusions:** Radiological examinations are performed by medical radiation technologists majorly. The quantity of examination decreased when they ask for leave or resigned. This situation might be more obvious in nuclear medicine division with fewer medical radiation technologists. On the other hand, the arrangement for all kinds of scan needs to be considered and discussed when manpower shortage. PET-CT whole body scan plays a very important role when staging and treatment cancer, we put PET-CT scan on the first place when arrangement. So, compare with other scans, daily average quantity of PET-CT whole body scan decreased much lesser.

PC-131

## 探討數位式 PET/CT 進行快速掃描的可能性

宋慶琳<sup>1,2</sup> 陳詩媽<sup>1,2</sup> 詹勝傑<sup>3</sup> 劉淑馨<sup>1,4</sup> 呂坤翰<sup>4</sup><sup>1</sup> 佛教慈濟醫療財團法人花蓮慈濟醫院核子醫學科<sup>2</sup> 花蓮縣醫事放射師公會<sup>3</sup> 慈濟大學醫學院<sup>4</sup> 慈濟科技大學醫學影像暨放射科學系

**背景：**<sup>18</sup>F-FDG 正子造影檢查是透過 PET/CT 成像系統，偵測葡萄糖在人體內的細胞代謝情形，常用於惡性腫瘤診斷、分期、治療與預後追蹤以及偵測體內發炎。隨著時代的進步，新型數位式 PET/CT 使用 SiPM 探測器取代傳統的光電倍增管，重組技術也不斷進步，使得影像品質大幅提升。過去使用類比式 PET/CT 遇到躁動的病患時，往往無法提供正確影像給臨床醫師做出診斷，雖然數位式 PET/CT 有更好的技術可以縮短造影時間，但如何使這些病患接受快速掃描又能確保影像品質，現今仍沒有確切的證據證明。

**目的：**利用假體掃描，測試數位式 PET/CT 不同掃描時間及影像重組方式，對影像品質和活度參數的影響。

**材料與方法：**首先在球型假體 (Hollow Sphere Set (6)TM) 中注入三種不同濃度 (濃度為 20 kBq/mL、30 kBq/mL 及 40 kBq/mL) <sup>18</sup>F-FDG 的藥物，再以 GE Discovery MI，分別進行 List-mode 掃描。再根據不同掃描時間 (60 秒、90 秒、120 秒及 150 秒) 和不同 Q. clear 的  $\beta$  值 (550、450、350、250) 進行影像重組。影像品質則是依據肉眼觀測影像來評分，包含影像解析度與細緻度 (採五分制度，最低 1 分、最高 5 分；達 3 分以上是可接受之影像品質)。另外我們利用 Pmod 來計算活度參數。

**結果：**實驗結果發現掃描時間 150 秒，Q. clear 的  $\beta$  值為 550、450、350、250 時，其影像品質分數為 4-5 分 (平均為 4.25 分)；掃描時間 120 秒，分數則為 3-5 分 (平均為 4.25 分)；掃描時間 90 秒，分數則為 3-5 分 (平均為 3.5 分)；掃描時間 60 秒，分數則為 2-4 分 (平均為 3.25 分)。掃描時間越短，影像品質分數越低。掃描時間 60 秒時如果使用  $\beta$  值設為 550，進行影像重組，影像品質分數會上升至 4 分。不同掃描時間及  $\beta$  值所得活度參數皆約為 1.6 kBq/mL。

**結論：**這試驗發現利用數位式 PET/CT 進行快速掃描是可行的，當掃描時間縮短為 60 秒時，如果 Q. clear 的  $\beta$  值設定在 550，可以達到不錯的影像品質。

PC-132

## 正子造影檢查之糖尿病病患飲食控制成效 – 個案報告

邱禹臻<sup>1</sup> 許幼青<sup>1</sup> 陳薇璇<sup>1</sup> 廖建國<sup>1</sup> 王昱豐<sup>1,2,3</sup>

<sup>1</sup> 佛教大林慈濟醫院核子醫學科

<sup>2</sup> 慈濟大學醫學系

<sup>3</sup> 佛教大林慈濟醫院預防醫學中心

**前言：**正子造影檢查是藉由放射核種行正子衰變來產生影像的一種造影檢查，氟-18 氟化去氧葡萄糖 (F-18 fluorodeoxyglucose; FDG) 是將葡萄糖的結構去掉一個氧再加上一個 F-18，FDG 與葡萄糖的攝取會受到細胞表面的葡萄糖運輸蛋白 (glucose transporter; GLUT) 表現影響，血糖與胰島素數值也會影響影像品質；糖尿病患者可接受正子造影檢查，但如果是以氟化葡萄糖造影時，檢查前血糖控制是很重要的，建議控制空腹血糖低於 150 mg/dL 為佳。但因糖尿病受檢者檢查當日須停用降血糖藥物，導致檢查前血糖控制往往較不理想，而血糖太高會影響檢查結果，因此期望藉由本案例之分享，提供糖尿病受檢者進行正子造影檢查之衛教參考。

**個案報告：**83 歲女性病患，主要診斷為淋巴瘤，罹患高血壓、糖尿病已十多年，在住家附近診所看診拿藥，口服糖尿病藥物一天三次，平日無飲食控制，在診所測得血糖值約 180-250 mg/dL 之間，糖化血色素介於 6.0-8.0% 之間，檢查前 5 天開始電話給予飲食衛教，教導監測血糖值並記錄，並且每日電話追蹤其血糖值與飲食控制，檢查當日血糖值降為 115 mg/dL。

**討論：**病患與兒子、媳婦同住，三代同堂，家中三餐大多由媳婦掌廚，經常外食；主訴平日喜愛吃麵包、麵食類，飯後點心會吃芒果、鳳梨，荔枝等水果。

2021/06/29 電訪表示當日空腹血糖值為 180 mg/dL，早餐吃一個波羅麵包和一杯豆漿，午餐吃一碗魷魚羹麵，下午點心吃一顆芒果；2021/06/30 電訪表示當日空腹血糖值為 206 mg/dL，前一天晚餐吃約 10 顆水餃和 5 顆荔枝，當日早餐吃一份三明治和一杯豆漿，午餐吃一碗白米飯，配菜有滷豬腳、空心菜、鮭魚、大黃瓜排骨湯，下午點心為一顆奇異果，由於血糖一直沒有降下來，故正子護理師在電話特別給予飲食衛教看血糖是否會有下降情形。於 2021/07/01 電訪中當日空腹血糖值為 170 mg/dL，早餐吃一份吐司夾蛋和一杯無糖豆漿，午餐吃一碗什錦粥，下午點心吃 1/4 顆芭樂，再次加強給予飲食衛教。終於在 2021/07/02 當日空腹血糖值為下降為 136 mg/dL，早餐吃一份燕麥鮮奶，昨日晚餐及當日午餐吃 2/3 碗白米糙米飯 (比例 1:1)，配菜有涼拌小黃瓜、地瓜葉、吳郭魚、番茄豆腐湯，下午點心吃聖女蕃茄，病患知道自己血糖有控制下來感到非常開心，表示會持續飲食控制。直到 2021/07/05 電訪表示當日空腹血糖值為 126 mg/dL，以及 2021/07/06 檢查日空腹血糖值為 115 mg/dL，在正子護理師細心指導之下病人血糖控制非常好，此舉可提高正子造影檢查的影像品質，對於病患來說也是非常重要的。

**結論：**正子造影檢查對腫瘤偵測、腫瘤分期與治療評估有很大的幫助。在高血糖情況下，血中葡萄糖與 FDG 會相互競爭，造成腫瘤細胞對 FDG 攝取量減少，FDG 散佈於血液中，導致背景值升高、影像品質下降，容易造成診斷上誤判。透過每日電話追蹤其血糖值並給予飲食衛教，可有效控制糖尿病患者注射前的血糖，確保影像品質，如此才能有清楚的影像協助醫師發現癌症病灶，提升醫療品質。

PC-133

## 探討 PET/CT 影像中的部份體積效應

劉奇芝<sup>1</sup> 曾柏銘<sup>2</sup> 呂建璋<sup>3</sup> 沈淑禎<sup>3</sup> 門朝陽<sup>2</sup> 林雅婷<sup>3</sup> 蕭聿謙<sup>4</sup>

<sup>1</sup> 天主教中華聖母修女會醫療財團法人天主教聖馬爾定醫院影像醫學部

<sup>2</sup> 天主教中華聖母修女會醫療財團法人天主教聖馬爾定醫院正子造影中心

<sup>3</sup> 天主教中華聖母修女會醫療財團法人天主教聖馬爾定醫院核子醫學科

<sup>4</sup> 亞東紀念醫院核子醫學科

**背景介紹：**PET/CT 在核醫中具有定量的功能，能準確的測量 FDG 的濃度。其定量數值 SUV (Standard Uptake Value) 在臨床上也常常被用來檢視是否為惡性腫瘤的指標之一。雖然 PET/CT 可透過 SUV 來量測身體部份器官或組織的濃度，但 SUV 數值受影響的因素也非常多，其中一部份就是部份體積效應 (Partial Volume Effect, PVE)。部份體積效應在臨床上常常被忽略，且此效應造成的 SUV 的差異也極大，而造成部份體積效應的原因，有晶體 (Crystal) 的排列方式，腫瘤的形狀、VOI 圈選的大小，以後處理的方式，故我們今天想來探討減少部份體積效應的方法。

**方法：**我們使用了 Siemens Biograph 16 PET/CT 來做試驗，使用不同劑量的 FDG (1, 1.5, 2.5 mCi)，分別倒入燒杯中攪拌，均勻攪拌後將水倒入 ACR Phantom 及上面五個的小孔徑 (9.5 mm, 12.7 mm, 15.9 mm 及 31.8 mm) 中，使用 routine 的 protocol 進行 2 min 與 3 min 的掃描，並觀察其 SUVmax 之變化。

**討論：**我們在實驗中曾嘗試使用不同劑量，試圖找出 PVE 之修正值，但實驗結果並未得到太線性的規律，原因可能為實驗過程不夠嚴謹所致，故如何找出修正值乃是我們努力的方向之一；最小孔徑 (9.5 mm) 與最大孔徑 (31.8 mm)，SUVmax 差異約在 1.35-1.71 倍，而 15.9 mm / 12.7 mm 孔徑差異比值約為 1.01-1.35，15.9 mm / 12.7 mm 則約為 1.01-1.32；另外我們也發現實驗中假體孔徑在大於 12.7 mm 之後，其 SUVmax 的差異不明顯。在延長掃描時間中，SUVmax 亦呈現緩緩上升趨勢，但變化幅度皆不如部份體積效應結果來的大。

**結論：**SUV 會隨著 PVE、晶體排列、造影時間，以及各種參數所影響。但對於直徑較小的腫瘤而言，PVE 的影響更大。故在面對小腫瘤或需利用 SUV 來評估治療後的情形時應謹慎評估。

PC-134

## Ga-67 SPECT/CT 診斷心包炎之病例報告

曾柏銘<sup>1</sup> 沈淑禎<sup>2</sup> 姚維仁<sup>4</sup> 門朝陽<sup>1</sup> 呂建璋<sup>2</sup> 林雅婷<sup>2</sup> 蕭聿謙<sup>3</sup>

<sup>1</sup> 天主教中華聖母修女會醫療財團法人天主教聖馬爾定醫院正子造影中心

<sup>2</sup> 天主教中華聖母修女會醫療財團法人天主教聖馬爾定醫院核子醫學科

<sup>3</sup> 亞東紀念醫院核子醫學科

<sup>4</sup> 戴德森醫療財團法人嘉義基督教醫院核子醫學科

**前言：**心包炎或心肌炎的診斷通常由臨床症狀、心電圖，抽血檢驗、超音波及放射科影像，Ga-67 掃描可偵測發炎的區域，但 Ga-67 SPECT/CT 用於診斷心肌炎的病例報告並不多，此一病人因發燒住院，臨床上懷疑為心肌炎，做了一系列檢查，在此篇報告中，有 MRI 與 Ga-67 SPECT/CT 之影像比較。

**案例報告：**23 歲男性病人，因發燒、呼吸微喘住院，於 10 天前打過 AZ 疫苗，在急診室中，發燒至 39.3°C，心跳加快，白血球增加，Troponin T 升高至 126 ng/L，肌酸激酶 (CK: 58U/L) 升高而收住院。心電圖顯示心跳加快，具有非特性異的 ST-T change，心臟超音波顯示 mild anteroseptal hypokinesia, borderline LVEF, mild pericardial effusion，臨床上懷疑是感染引起的心肌炎。但與施打疫苗的相關性無法排除。MRI 影像顯示，於 myocardium 有不正常之顯影，診斷為心肌炎。Ga-67 SPECT/CT 檢查 IV 注射 3 mCi，24 小時做全身性掃描，加作心臟部位之 SPECT/CT，影像顯示在心臟周圍有中度 Ga-67 吸收增加。

**討論：**Ga-67 閃爍攝影用於診斷心包炎的文獻報告並不多，通常同位素聚集於心臟的輪廓周圍，此病例加作了 SPECT/CT，對照 CT 解剖位置，可見 Ga-67 的吸收集於 Pericardial region，若為心肌炎再 Ga-67 顯影區域則較偏重於 myocardium。有些文獻報告對於心肌炎或心包炎的診斷，有時亦需延遲 48 小時或 72 小時的照影才有比較好的影像品質，加作 SPECT/CT 亦可提高影像的靈敏度及確認病灶的解剖位置。

**結論：**Ga-67 SPECT/CT 為非侵入性檢查，對於心包炎可提供有用的診斷工具。加做 SPECT/CT 可以更明確的區分發炎部位，也可有效的把肝臟及橫膈的活性區分，以減少偽陽性，做出更準確的診斷。



## 大會組織

**主辦單位：中華民國核醫學學會**

**協辦單位：台中榮民總醫院**

**行政院原子能委員會核能研究所**

**經濟部技術處**

**會長 蔡世傳 會長**

**指導委員**（依姓氏筆畫順序，尊稱省略）

王安美、王昱豐、李將瑄、杜高瑩、林立凡、周大凱、邱南津、邱創新  
吳東信、吳彥雯、陳宜伶、陳輝墉、翁瑞鴻、許幼青、曹勤和、黃文盛  
黃英峰、黃奕琿、黃淑華、黃雅瑤、彭南靖、程紹智、詹勝傑、張智勇  
楊邦宏、廖炎智、廖建國、鄭媚方、蔡世傳、樊裕明、顏若芳、謝德鈞

**法律顧問** 蔡雅琴

**論文評選組**（依姓氏筆畫順序，尊稱省略）

**召集人** 王昱豐

**執行秘書** 陳保良

**壁報臨床組** 吳彥雯、林立凡、邱創新、許幼青、陳宜伶、彭南靖、黃玉儀、  
楊士頤、楊邦宏、蔡名峰

**壁報基礎組** 田育彰、吳東信、張志賢、鍾相彬

**口頭臨床組** 王安美、王昱豐、林宜瀨、林明賢、程紹智、黃奕琿

**口頭基礎組** 黃雅瑤、黃詠暉

**秘書處**（依姓氏筆畫順序，尊稱省略）

**秘書長** 路景竹

**執行秘書** 柯冠吟、莊佩儒、陳建榮

**秘書** 楊月桂、吳璉廷

# TAF認證分子影像暨放射藥理技術平台

## 核研所放射技術平台(概述)

- ◆ 核研所為我國唯一原子能專業研究機構，放射藥毒理與分子影像核心技術具國際競爭優勢
- ◆ 建置多項國際認證等級之放射技術平台，執行超過140件委託服務，協助新藥IND/NDA

## TAF認證分子影像暨放射藥理技術平台

### 試驗項目



藥物標誌 / 細胞結合試驗 / 活體分子影像 / 藥物生物體分布 / 藥物動力學分析

ISO 17025申請準備中

ISO 17025試驗項目

疾病動物模式建立/藥物療效評估/自體放射顯影技術/藥物排除試驗

### 時間



依實驗設計，預估為國外廠商1/3

### 效益



台灣首例TAF認證分子影像暨放射藥理技術平台,提供:

- 精準確認藥物體內分布及變化
- 快速評估新藥前期開發潛力
- 提昇研發策略決策可靠度
- IND/NDA之重要佐證資料數據
- 衍伸效益: 有助縮短藥物臨床試驗時程與花費，並降低機會成本。  
另協助試驗過程中之核醫產物，開發為核醫伴隨式診斷產品。



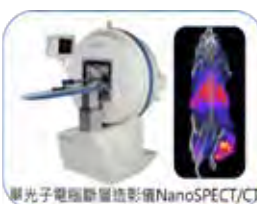
## 放射毒理技術平台核心設施儀器設備



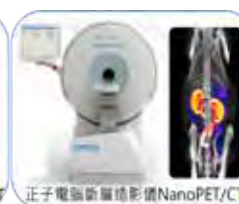
SPF動物房及試驗操作室



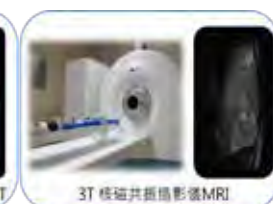
臨床病理分析室



單光子電腦斷層造影NanoSPECT/CT



正子電腦斷層造影NanoPET/CT



3T 核磁共振攝影MRI



光學造影Xtreme



電腦電動式冷凍切片機



超音波影像分析系統

## GLP放射毒理實驗室品質認證



TFDA GLP證書



## 協助藥物獲准進入人體臨床試驗

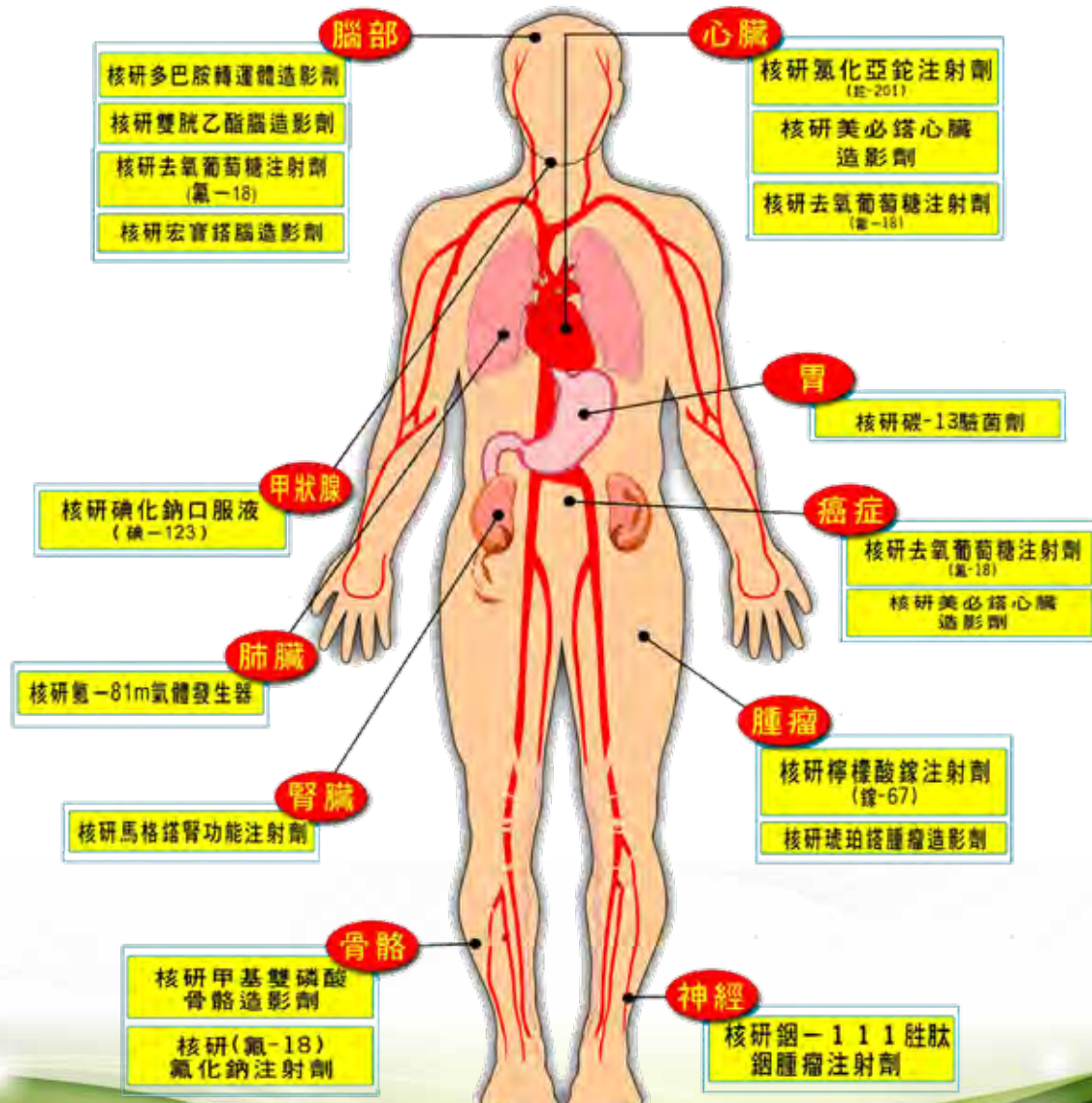
- 案例一：核研銻-188微脂體注射劑
- 案例二：核研銻必妥注射劑
- 國內多家廠商委託進行--動物BioD及分子影像試驗，協助新藥申請美國臨床試驗

# 核醫藥物供應與推廣

核能研究所積極應用原子能科技，陸續開發出國內迫切需求或不易進口的短半衰期的核醫藥物。在衛福部藥品PIC/S GMP及輻射防護等法規與制度下，生產Tl-201、Ga-67等放射性藥物，及MAG<sub>3</sub>、MIBI、ECD等凍晶藥物，每年提供國內約十幾萬人次之造影檢查，造福國人健康福祉。同時協助國內建立核醫藥物產業及精進生產技術滿足客戶需求，並於(1)107.05.04通過衛福部PIC/S GDP查核 (2)109.09.02通過衛福部PIC/S GMP後續查核，以更高的規格提供優良核醫藥物予國人使用。

產品名稱	藥品許可證 (衛署藥製字)	架儲期	適應症	核種 製造途徑
核研氯化亞鉈 (鉈-201)注射劑	R00012號	校正期後3天	心肌灌注造影(用以診斷冠狀動脈疾病、急性心肌梗塞和冠狀動脈繞道移植的手術後評估)	加速器
核研檸檬酸鎵 (鎵-67)注射劑	R00014號	校正期後5天	霍金氏病、淋巴瘤、支氣管性腫瘤等惡性腫瘤之助診	加速器
核研馬格諾腎功能造影劑	R00017號	9個月	腎功能造影診斷	核反應器
核研美必鎊心臟造影劑	R00025號	9個月	心肌功能及乳癌造影診斷	核反應器
核研雙肱乙酯腦血流造影劑	R00031號	6個月	局部腦血流灌注狀況	核反應器

配合市場需求提供各器官  
合法之核醫藥物且每週例行供應中



# 碳-14藥物代謝分析平台

## 簡介

### 碳-14藥物代謝分析平台

#### 試驗項目 (一般)

1. 藥物動力學
2. 藥物排除試驗
3. 生物體中藥物分布試驗
4. 呼氣中藥物含量分析試驗
5. 全鼠切片影像(QWBA)
6. 代謝物定性分析試驗

#### 試驗項目 (增加)

7. 個別代謝物之藥物動力學
8. 個別代謝物之生物體中藥物分布試驗
9. 個別代謝物之排除試驗
10. 呼氣中個別代謝物之含量分析試驗

#### 費用

- 項次1-6(一般試驗)都是以總量，意即藥物與代謝物一起計算  
若發現個別代謝物有藥效或毒性，依規定需要再進行項次7-10(增加試驗)
- 委託內容依廠商需求，可以逐步試驗
- 依據碳十四藥物合成困難度，碳十四藥物費用差異甚大，該費用與國外相近
- 除上述碳十四藥物費用以外，委託費用預估為國外廠商1/2-1/3

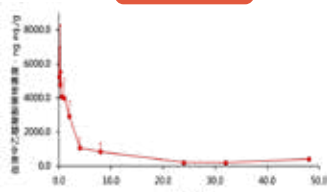
## 碳十四藥物代謝分析應用範圍(概述)

### 碳-14藥物代謝相關技術應用

#### 碳-14藥物純度分析



#### 藥物動力學



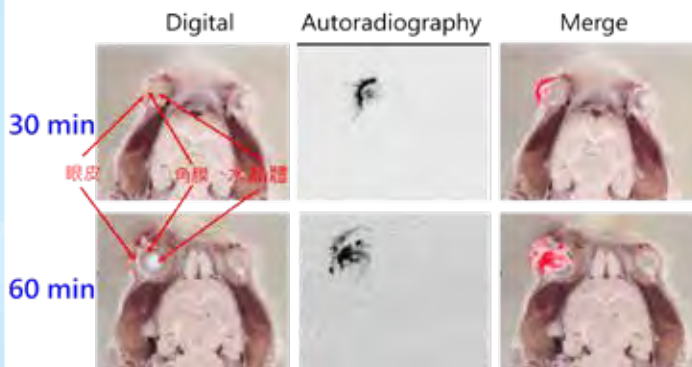
#### 排除試驗

Matrixes	Interval (Hours)	% Administered Dose - Recovered				
		#1	#2	#3	Absorb	SD
Urine	0-8	65.89	66.76	31.02	61.89	9.52
	8-24	15.13	15.98	32.64	23.26	9.87
	24-48	1.67	0.68	0.27	0.91	0.68
	48-72	0.45	0.26	0.23	0.31	0.12
Subtotal:		83.15	86.68	64.26	84.37	6.26
Feces	0-24	2.63	1.79	1.98	1.87	2.22
	24-48	0.25	0.19	0.09	0.16	0.08
	48-72	0.05	0.04	0.04	0.04	0.01
	Subtotal:	2.93	1.96	6.33	3.07	2.17
Metabolite in cage		0.72	0.96	4.05	4.23	1.83
Total:		87.84	93.69	84.58	91.20	3.80

#### 代謝物分析



### 碳-14藥物之全身自動放射顯影術造影圖



- 本平台協助委託單位進行眼藥傳遞路徑，本所以直觀且可信之碳-14標誌姿測藥物生物分布影像，證明藥物傳遞路徑可到達患部

#### 效益

- 產出之試驗數據可做為IND/NDA 重要佐證資料
- 大幅降低過往需委託國外廠商進行碳-14相關試驗之研發延宕與成本並有助於下游廠商承接與應用

- 以碳-14標誌乙醯胺酚(C14-Acetaminophen)藥物為參考標準品，進行平台代謝分析技術能力測試
- 能力測試成果與文獻相符，確認平台技術可靠性
- 碳-14藥物代謝分析平台重要性受美國醫藥公司、經濟部技術處與計畫審查委員肯定



## 贊助廠商

元新儀器有限公司

台灣拜耳股份有限公司

台灣飛利浦股份有限公司

台灣諾華股份有限公司

西門子醫療設備股份有限公司

貝克西弗股份有限公司

奇異亞洲醫療設備股份有限公司

昶洋貿易股份有限公司

恩典科研股份有限公司

泰歷藥品儀器股份有限公司

現代儀器股份有限公司

臺灣新吉美碩股份有限公司

輝瑞大藥廠股份有限公司

(依筆畫順序排列)

Xofigo<sup>®</sup> 鐳治骨 用於治療去勢抗性攝護腺癌病患，  
其合併有症狀的骨轉移且尚未有臟器轉移者



# Xofigo<sup>®</sup> 鐳治骨

## 健保給付生效！

### EXTEND SURVIVAL WITH XOFIGO<sup>®</sup>



健保給付規定：Radium-223 (如Xofigo)  
限用於治療去勢抗性攝護腺癌[castration-resistant prostate cancer]病患，其合併有症狀的骨轉移且尚未有臟器轉移者等，且病患需符合下列三項條件：

1. 患者須合併有症狀之骨轉移且骨轉移≥2處
2. 每位患者最高使用六個療程
3. 須經事前審核核准後使用，申請時需檢附：
  - (1) 用藥紀錄(證明為有症狀的骨轉移、需常規使用止痛藥物)
  - (2) 三個月內影像報告證明骨轉移≥2處
  - (3) 三個月內影像報告證明無臟器轉移
4. 不得合併使用abiraterone、enzalutamide及其他治療因惡性腫瘤伴隨骨骼事件之藥品，如denosumab、bisphosphonates等。

# 3

**3個月內  
影像報告**

# 2

**2處以上  
骨轉移**

# 1

**1種常規  
使用止痛藥物**

# 0

**0處  
器官轉移**

鐳治骨® (注射劑) Xofigo<sup>®</sup> solution for injection  
 批發商藥字號H000291號 承准藥品醫療使用

Xofigo<sup>®</sup> 鐳治骨 用於治療去勢抗性攝護腺癌[castration-resistant prostate cancer]病患，其合併有症狀的骨轉移且尚未有臟器轉移者。 鐳治骨治療方式 Xofigo<sup>®</sup> 的劑量使用為每日兩次給予 24 MBq 的放射劑量，每兩週給予一次。 此項研究對於 Xofigo<sup>®</sup> 治療的安全性與療效進行研究。 Xofigo<sup>®</sup> 與對照劑(安慰劑)對照，治療以標準化(通常為1分鐘)的方式給藥。 Xofigo<sup>®</sup> 屬於合併有症狀的骨轉移且尚未有臟器轉移的病患。 患者接受 Xofigo<sup>®</sup> 的治療是通過口服的藥丸。 藥物會與體內鈣結合，隨後會與骨骼中的鈣結合，以治療骨轉移。 當患者接受 Xofigo<sup>®</sup> 治療時，Xofigo<sup>®</sup> 會與骨骼中的鈣結合，以治療骨轉移。 Xofigo<sup>®</sup> 治療後，患者會感到骨痛減輕，且能減少止痛藥物的使用。 Xofigo<sup>®</sup> 治療後，患者會感到骨痛減輕，且能減少止痛藥物的使用。 Xofigo<sup>®</sup> 治療後，患者會感到骨痛減輕，且能減少止痛藥物的使用。 Xofigo<sup>®</sup> 治療後，患者會感到骨痛減輕，且能減少止痛藥物的使用。

詳細藥品說明書請參考下列網址之藥品說明書。 品名: Xofigo / CD05 / US PI / TW / Jun 2019  
 MA-XOP-TW-0029-07-2019  
 北市街藥學字第109060018號

鐳治骨<sup>®</sup>  
**Xofigo<sup>®</sup>**  
 radium Ra 223 dichloride  
 INJECTION

# PHILIPS

Vereos Digital PET/CT



## Proven accuracy inspires confidence

In the transition from volume- to value-based care, accurate treatment pathways are essential. Philips Vereos Digital PET/CT is the world's first and only fully digital PET/CT solution—and its accuracy is supported by rigorous clinical evidence measured in years, not months. There is always a way to make life better.

innovation  you



# LUTATHERA®

鐳癌平®注射液370百萬貝克/毫升  
0.37 GBq/ml solution for infusion

用於治療成人無法手術切除或轉移性，  
分化良好 (G1及G2) 且經體抑素類似物  
(Somatostatin analogue)  
治療無效之體抑素受體(Somatostatin receptor)  
陽性的胃腸道胰腺神經內分泌腫瘤  
(Gastroenteropancreatic neuroendocrine  
tumors, GEP-NETs)



#### 處方資訊摘要

[本藥須由醫師處方使用]

產品名稱：鐳癌平®注射液 LUTATHERA® (衛部藥輸字第R00104號)

主成分：Lutetium Lu 177 dotatate 適應症：LUTATHERA用於治療成人無法手術切除或轉移性，分化良好(G1及G2)且經體抑素類似物(somatostatin analogue)治療無效之體抑素受體(somatostatin receptor)陽性的胃腸道胰腺神經內分泌腫瘤 用法/用量：LUTATHERA建議劑量為7.4 GBq (200 mCi)，每8週一次共4劑。LUTATHERA不良反應的建議劑量調整請參考詳細仿單。禁忌：本品為具放射線藥品，確定或疑似懷孕，或尚未排除懷孕的情況下請勿使用。警語：1. 放射線暴露風險 LUTATHERA會增加病人長期整體放射線暴露量。長期累積放射線暴露量則會增加罹患癌症的風險。LUTATHERA投藥後可於尿液內偵測到放射線最長30天。依醫院良好放射線安全性規範、病人處置程序、行政院原子能委員會輻射防護規範，以及病人居家追蹤放射線保護說明，於LUTATHERA治療期間與治療後使病人、醫療人員以及家庭接觸者能盡量減少放射線暴露量。2. 骨髓抑制 監測血球細胞計數。依骨髓抑制嚴重程度暫停投藥、降低劑量或永久停用[請參考詳細仿單]。不建議於Lutathera治療之前對基準點血液功能嚴重受損的病人開始進行治療(例如Hb < 4.9 mmol/L或8 g/dL，血小板 < 75 x 10<sup>9</sup>/L或75 x 10<sup>3</sup>/mm<sup>3</sup>或白血球 < 2 x 10<sup>9</sup>/L或2000/mm<sup>3</sup>)。3. 繼發性骨髓增生不良症候群及白血病 在NETTER-1中，追蹤時間中位數為24個月，2.7%接受LUTATHERA加上長效octreotide的病人通報發生骨髓增生不良症候群(MDS)，相較之下接受高劑量長效octreotide則無病人發生MDS。4. 腎毒性 監測血清肌酸酐並計算肌酸酐廓清率。依腎臟毒性嚴重程度暫停投藥、降低劑量或永久停用LUTATHERA。5. 肝臟毒性 於治療期間監測轉胺酶、膽紅素與血清白蛋白。依肝功能不全嚴重程度暫停投藥、降低劑量或永久停用LUTATHERA。6. 神經內分泌荷爾蒙危象 監測病人是否出現潮紅、腹瀉、低血壓、支氣管收縮或其他腫瘤相關荷爾蒙分泌徵兆及症狀。視情況靜脈投予體抑素類似物、液體、皮質類固醇以及電解質。7. 胚胎-胎兒毒性 所有放射性藥物(包括LUTATHERA)都可能對胎兒造成傷害。使用LUTATHERA前請先確認具生育能力女性的懷孕狀態。應向具生育能力女性病人告知，在LUTATHERA治療期間與最後一劑後7個月內應使用有效的避孕方式。若男性病人的女性伴侶具生育能力，應向男性病人告知，在接受治療期間以及最後一劑藥物後4個月內應使用有效的避孕方式。8. 不孕風險 LUTATHERA可能導致男性和女性不孕。9. 與胺基酸溶液相關的高血鉀症 由於可能出現與容量過度負荷相關的臨床併發症，因此，在NYHA分類(美國紐約心臟協會)定義為第III級或第IV級的嚴重心臟衰竭病人，應謹慎使用精胺酸和離胺酸。10. 與胺基酸溶液相關的心臟衰竭 於酸中毒的形成可能與血鉀的迅速增加有關。副作用：最常見的不良反應(發生率30%以上)為噁心、嘔吐、疲倦。最常見第3至第4級不良反應(發生率2%以上)為噁心、嘔吐、腹痛、腹瀉、高血壓、背痛、腎衰竭。最常見實驗室數值異常(發生率50%以上)為淋巴球減少症、貧血、白血球減少症、血小板減少症、肌酸酐增加、高血糖、GGT增加、鹼性磷酸酶升高、AST增加。最常見第3/4級的實驗室數值異常(發生率3%以上)為淋巴球減少、嗜中性白血球減少症、高血糖、高尿酸血症、低血鉀症、GGT增加、鹼性磷酸酶升高、AST增加、ALT增加。

[衛福部食藥署網站]<http://www.fda.gov.tw> [簡仿版本] TW2105259737

詳細資訊請參閱完整仿單

 **NOVARTIS**  
台灣諾華股份有限公司

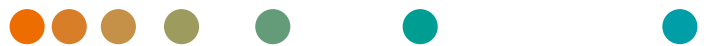
10480台北市中山區民生東路三段2號8樓  
電話：(02)2322-7777 傳真：(02)2322-7328  
免費諮詢專線：0800-880-870  
<http://www.novartis.com.tw>

北市衛藥廣字第110090139號  
北市衛食藥字第1103062438號

使用前請詳閱說明書警語以及注意事項



# PET/CT Biograph



Answering to clinical needs in oncology, neurology, cardiology, and radiology, Siemens Healthineers Molecular Imaging systems provide PET/CT Biograph solutions to help clinicians diagnose, treat, and monitor diseases more confidently.

<https://www.siemens-healthineers.com>

**SIEMENS**  
Healthineers

## GE Healthcare

是業界唯一可提供從同位素，核醫及正子藥物  
生產合成到影像設備整體解決方案的公司



### Tomorrow.....

Leveraging the power of AI/DL/ML to help solve critical challenges in image quality, assisted reading and precision medicine, enable your system to always have the latest capabilities and deliver One MI applications across all care areas



醫用迴旋加速器



正子藥物開發系統



Signa PET/MR  
PET/MR系統



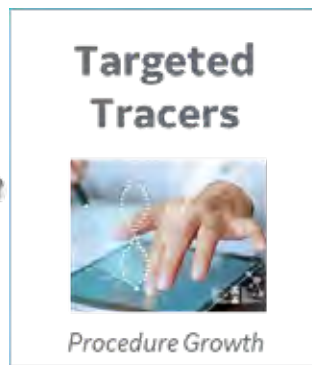
Discovery MI  
PET/CT系統



Discovery IQ  
PET/CT系統



NM/CT 850  
SPECT/CT系統



NM 830  
SPECT系統



SPECT CZT Detector



PET SiPM module

# 核醫診療標靶藥物中心



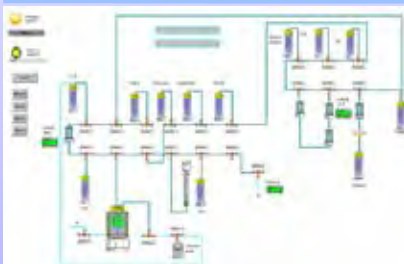
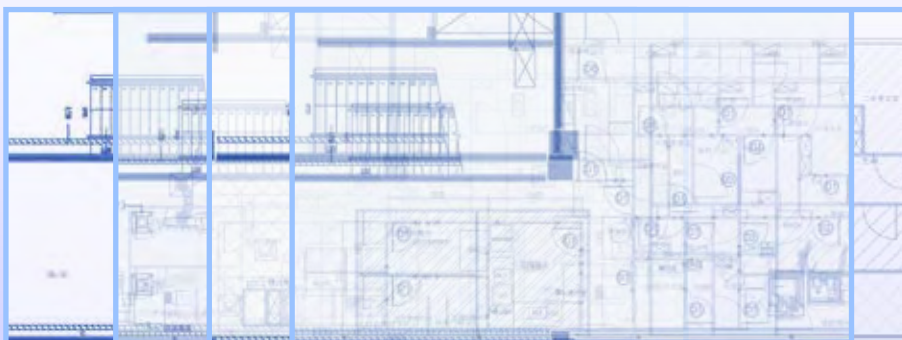
醫療財團法人辜公亮基金會和信治癌中心醫院  
Koo Foundation Sun Yat-Sen Cancer Center

2022年與您相見！

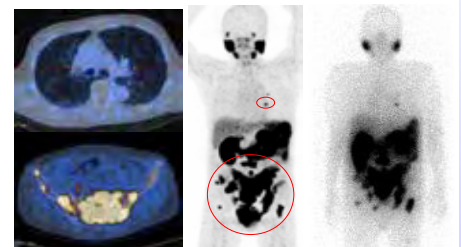
創新精巧的正子製藥設置計畫

打開核醫診療藥物無限可能

實現臨床、研究、教學各種任務



*Theranostics - PSMA*



# “肯門斯” 放射性藥物校準分裝系統

FEBO syringes dispensing system

- 符合GMP規範
- 內建劑量校準器
- 可分裝標誌18-F，90-Y，177-Lu，68-Ga的藥物。
- 可安裝於各式 laminar flow, isolators, hoods.



**FEBO-NM (核醫藥物)**  
用於核子醫學部門：  
裝備單次性使用套件管線和預定注射器的屏蔽，適合在核醫部門進行分裝操作。

**FEBO-RP (放射性藥物)**  
用於生產放射性藥物部門：  
裝備使用在線滅菌過濾器，在分裝到預定注射器前，將放射性藥物滅菌。



衛部醫器輸字第 033797號

泰歷藥品儀器股份有限公司  
Taiwan Life Support Systems, Inc.

0 8 0 0 - 0 5 0 1 5 8  
( 0 2 ) 2 5 5 5 - 9 7 0 0  
w w w . t l s s . c o m . t w  
北市衛器廣字第109110075號

## 自動化正子FDG/NaF輸液系統

### ■ 減少臨床人員輻射劑量

- 大瓶裝設計不需分藥作業
- 減少50%體部劑量
- 減少90%手部劑量

### ■ 給予病患安全與精準輸液

- 以體重自動計算劑量
- 依所設定的劑量做注射
- 兩種流速以及saline test

### ■ 提高工作效率

- 靈活的排程安排
- 無線輸出輸液記錄和輻射劑量到PACS



全球45個國家400台以上設備



超過3.5百萬次以上累計輸液



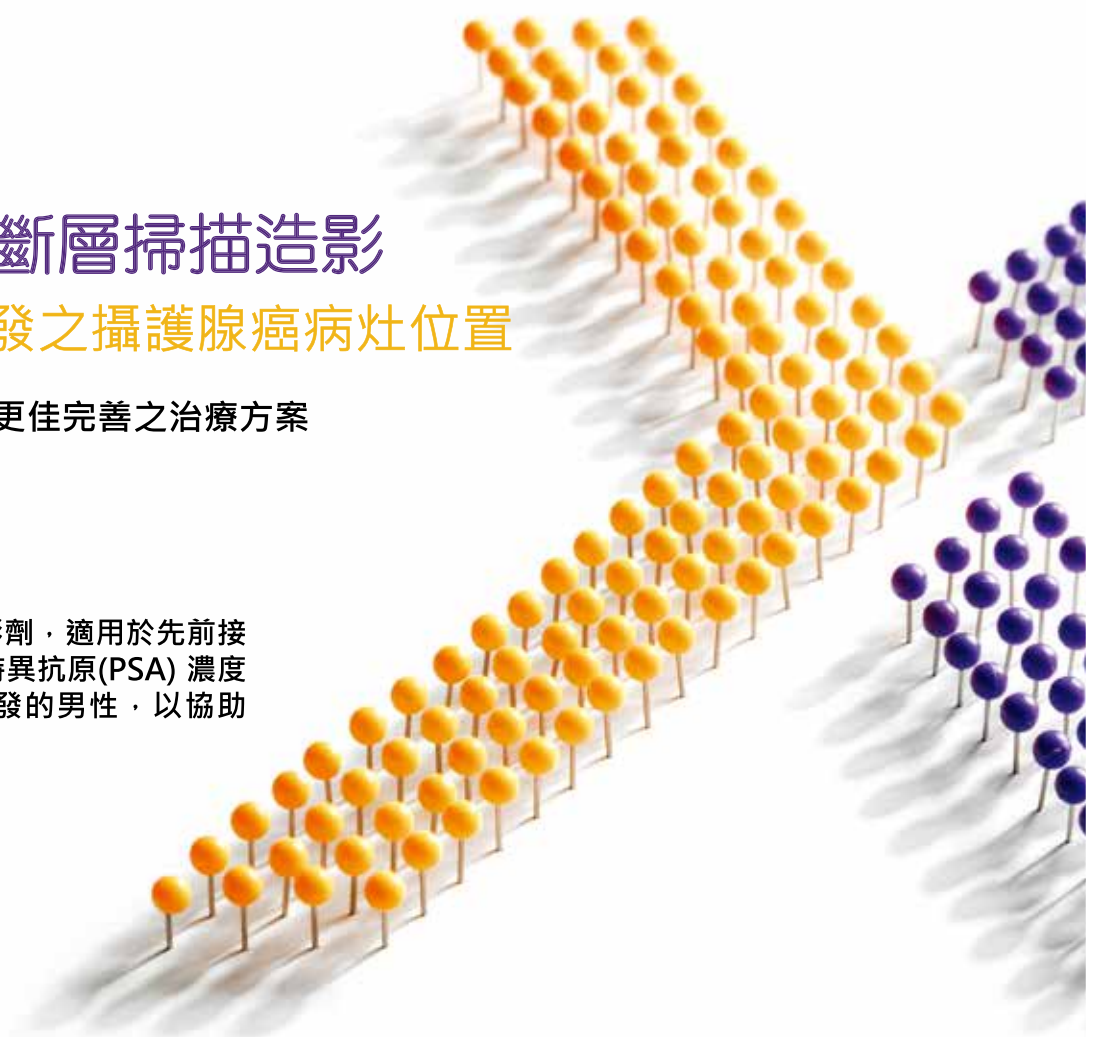
輸液過程即時活性輸出曲線圖

## 奧攝敏正子斷層掃描造影 偵測及標定復發之攝護腺癌病灶位置

協助醫師為患者擬定更佳完善之治療方案

### 適應症

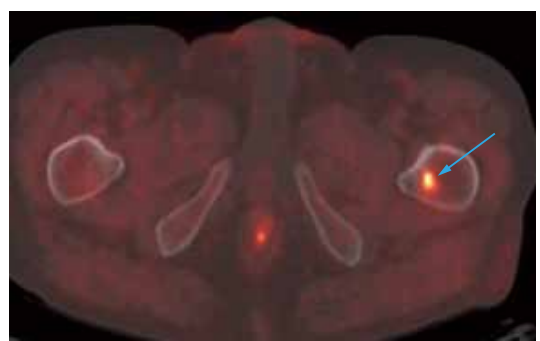
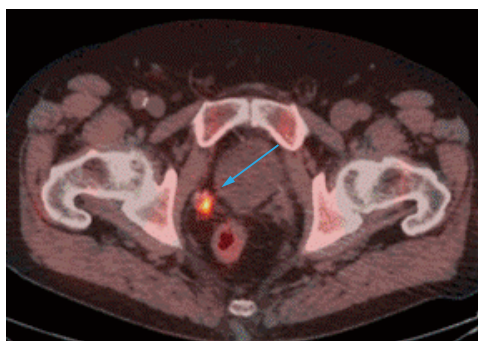
正子斷層掃描(PET) 造影劑，適用於先前接受治療後因血中攝護腺特異抗原(PSA) 濃度上升而懷疑攝護腺癌復發的男性，以協助診斷攝護腺癌之復發。



PET



PET/CT



# ATTR-CM (transthyretin amyloid cardiomyopathy)

## 是一種威脅生命的疾病

# Vyndamax™

(*tafamidis*)  
61 mg capsules

## 延長患者存活率 降低心血管疾病相關住院次數<sup>1</sup>

VYNDAMAX™ 是第一個、也是目前唯一的藥物\*，可降低 ATTR-CM 引起的全死因死亡率及心血管疾病相關住院次數。現在，您的患者有機會活得更久、過得更好<sup>1</sup>。



衛生福利部 109 年 7 月 31 日核發許可證

ATTR-CM 轉甲狀腺素蛋白類澱粉沉着症造成之心肌病變

維萬心軟膠囊 61 毫克 Vyndamax soft capsules 61 mg 處方資訊摘要

處方說明

【成分】每類軟膠囊內含 61 毫克微粒化 tafamidis。有關賦形劑的完整列表，請參閱完整仿單 6.1 節。【適應症】用於治療成人野生型或遺傳性的轉甲狀腺素蛋白類澱粉沉着症造成之心肌病變 (transthyretin-mediated amyloid cardiomyopathy)，以降低總死亡率和心血管住院率。【用法用量】建議劑量為 Vyndamax 61 毫克（類含 61 毫克 tafamidis 的膠囊）口服每日一次。Vyndamax (tafamidis) 61 毫克對應於 tafamidis meglumine 80 毫克。但兩者間每毫克無法等值互換。膠囊應該整顆吞嚥，不可以壓碎或切開。Vyndamax 可與食物併服，亦可不與食物併服。如果漏服劑量，請指示病人在記得時盡早服用該劑量，或者跳過此次漏服的劑量並在下次規定的時間服用，之後按時服用。請勿服用加倍的劑量（服用藥物）。【特殊族群】老年病人 (>65 歲) 無須調整劑量。腎功能不全或輕度至中度肝功能不全的病人不需調整劑量。重度腎功能不全病人 (肌酸酐廓清率低於或等於 30 毫升/分鐘) 的相關資料十分有限。未曾對重度肝功能不全病人使用 tafamidis 進行研究，建議謹慎使用。Tafamidis 並非針對兒童族群，無相關使用資料。【禁忌症】針對活性成分或完整仿單第 6.1 節所列的任何賦型劑過敏者。【特殊警語及使用注意事項】有生育能力的女性在使用 tafamidis 期間應採用適當避孕方式，並持續使用適當避孕方式直到停止 tafamidis 治療後 1 個月。Tafamidis 應增加到轉甲狀腺素蛋白類澱粉沉着症病人的標準治療中。醫師應監測病人，並持續評估是否需要其他治療，包括作為標準治療之一的器官移植。由於目前並無在器官移植情況下使用 tafamidis 的相關資料，因此進行器官移植之病人應停用 tafamidis。可能發生肝功能指數增加或甲狀腺素減少。本藥品的每類膠囊內含 44 毫克山梨醇。使用 tafamidis 時應考量到同時投予其他含山梨醇 (或果糖) 產品，以及飲食攝取山梨醇 (或果糖) 所造成的加乘作用。口服藥品的山梨醇成分可能會影響其他同時投予的口服藥品之生體可用率。懷孕：目前尚無 tafamidis 使用於懷孕婦女的資料。動物試驗已顯示發育毒性。不建議在懷孕期間使用 tafamidis，亦不建議用於有生育能力但未懷孕的女性。哺乳：動物試驗顯示 tafamidis 會分泌至乳汁中。無法排除對新生兒/嬰兒有害的風險。不應在哺乳期間使用 tafamidis。【不良作用】不良事件的評估，來自使用 tafamidis meglumine 的 ATTR-CM 各臨床試驗，主要為一項為期 30 個月、具安慰劑對照之試驗。接受 20 毫克或 80 毫克 (以 4 x 20 毫克方式投予) tafamidis meglumine 治療的病人出現不良事件的頻率與安慰劑組近似或相當。在一項為期 30 個月、具安慰劑對照之試驗中，接受 tafamidis meglumine 治療的病人因不良事件而停止治療的比例與安慰劑組近似，接受 80 毫克 tafamidis meglumine (以 4 x 20 毫克方式投予)、20 毫克 tafamidis meglumine 和安慰劑組病人因不良事件而停止治療比例分別為 12 (7%)、5 (6%) 和 11 (6%)。

仿單版本：SPC 20190107-4

此為處方資訊摘要，完整處方資訊請詳閱仿單



台北總公司  
台北市 110 信義區松仁路 100 號 42 樓  
TEL: (02) 5575-2000  
FAX: (02) 5575-2890

台中辦事處  
台中市 408 公益路二段 51 號 10 樓 A 室  
TEL: (04) 2328-2818  
FAX: (04) 2320-5438

高雄辦事處  
高雄市 802 苓雅區四維三路 6 號 16 樓 A 室  
TEL: (07) 535-7979  
FAX: (07) 535-7676

北市衛藥廣字第 110020076 號  
PP-VDM-TWN-0028-20101